NUREG/CR-5772
SAND91-1766/1
Vol. 1

Aging, Condition Monitoring, and Loss-of-Coolant Accident (LOCA) Tests of Class 1E Electrical Cables

Crosslinked Polyolefin Cables

Prepared by
M. J. Jacobus

Sandia National Laboratories
Operated by
Sandia Corporation

Prepared for
U.S. Nuclear Regulatory Commission

AVAILABILITY NOTICE

Availability of Reference Materials Cited in NRC Publications

Most documents cited in NRC publications will be available from one of the following sources:

1. The NRC Public Document Room, 2120 L Street, NW., Lower Level, Washington, DC 20555

2. The Superintendent of Documents, U.S. Government Printing Office, P.O. Box 37082, Washington, DC 20013-7082

3. The National Technical Information Service, Springfield, VA 22161

Although the listing that follows represents the majority of documents cited in NRC publications, it is not intended to be exhaustive.

Referenced documents available for inspection and copying for a fee from the NRC Public Document Room include NRC correspondence and internal NRC memoranda; NRC bulletins, circulars, information notices, inspection and investigation notices; licensee event reports; vendor reports and correspondence; Commission papers; and applicant and licensee documents and correspondence.

The following documents in the NUREG series are available for purchase from the GPO Sales Program: formal NRC staff and contractor reports, NRC-sponsored conference proceedings, international agreement reports, grant publications, and NRC booklets and brochures. Also available are regulatory guides, NRC regulations in the *Code of Federal Regulations*, and *Nuclear Regulatory Commission Issuances*.

Documents available from the National Technical Information Service include NUREG-series reports and technical reports prepared by other Federal agencies and reports prepared by the Atomic Energy Commission, forerunner agency to the Nuclear Regulatory Commission.

Documents available from public and special technical libraries include all open literature items, such as books, journal articles, and transactions. *Federal Register* notices, Federal and State legislation, and congressional reports can usually be obtained from these libraries.

Documents such as theses, dissertations, foreign reports and translations, and non-NRC conference proceedings are available for purchase from the organization sponsoring the publication cited.

Single copies of NRC draft reports are available free, to the extent of supply, upon written request to the Office of Administration, Distribution and Mail Services Section, U.S. Nuclear Regulatory Commission, Washington, DC 20555.

Copies of industry codes and standards used in a substantive manner in the NRC regulatory process are maintained at the NRC Library, 7920 Norfolk Avenue, Bethesda, Maryland, for use by the public. Codes and standards are usually copyrighted and may be purchased from the originating organization or, if they are American National Standards, from the American National Standards Institute, 1430 Broadway, New York, NY 10018.

DISCLAIMER NOTICE

This report was prepared as an account of work sponsored by an agency of the United States Government. Neither the United States Government nor any agency thereof, or any of their employees, makes any warranty, expressed or implied, or assumes any legal liability of responsibility for any third party's use, or the results of such use, of any information, apparatus, product or process disclosed in this report, or represents that its use by such third party would not infringe privately owned rights.

NUREG/CR-5772
SAND91-1766/1
Vol. 1

Aging, Condition Monitoring, and Loss-of-Coolant Accident (LOCA) Tests of Class 1E Electrical Cables

Crosslinked Polyolefin Cables

Prepared by
M. J. Jacobus

Sandia National Laboratories
Operated by
Sandia Corporation

Prepared for
U.S. Nuclear Regulatory Commission

AVAILABILITY NOTICE

Availability of Reference Materials Cited in NRC Publications

Most documents cited in NRC publications will be available from one of the following sources:

1. The NRC Public Document Room, 2120 L Street, NW., Lower Level, Washington, DC 20555

2. The Superintendent of Documents, U.S. Government Printing Office, P.O. Box 37082, Washington, DC 20013-7082

3. The National Technical Information Service, Springfield, VA 22161

Although the listing that follows represents the majority of documents cited in NRC publications, it is not intended to be exhaustive.

Referenced documents available for inspection and copying for a fee from the NRC Public Document Room include NRC correspondence and internal NRC memoranda; NRC bulletins, circulars, information notices, inspection and investigation notices; licensee event reports, vendor reports and correspondence; Commission papers; and applicant and licensee documents and correspondence.

The following documents in the NUREG series are available for purchase from the GPO Sales Program: formal NRC staff and contractor reports, NRC-sponsored conference proceedings, international agreement reports, grant publications, and NRC booklets and brochures. Also available are regulatory guides, NRC regulations in the *Code of Federal Regulations*, and *Nuclear Regulatory Commission Issuances*.

Documents available from the National Technical Information Service include NUREG-series reports and technical reports prepared by other Federal agencies and reports prepared by the Atomic Energy Commission, forerunner agency to the Nuclear Regulatory Commission.

Documents available from public and special technical libraries include all open literature items, such as books, journal articles, and transactions. *Federal Register* notices, Federal and State legislation, and congressional reports can usually be obtained from these libraries.

Documents such as theses, dissertations, foreign reports and translations, and non-NRC conference proceedings are available for purchase from the organization sponsoring the publication cited.

Single copies of NRC draft reports are available free, to the extent of supply, upon written request to the Office of Administration, Distribution and Mail Services Section, U.S. Nuclear Regulatory Commission, Washington, DC 20555.

Copies of industry codes and standards used in a substantive manner in the NRC regulatory process are maintained at the NRC Library, 7920 Norfolk Avenue, Bethesda, Maryland, for use by the public. Codes and standards are usually copyrighted and may be purchased from the originating organization or, if they are American National Standards, from the American National Standards Institute, 1430 Broadway, New York, NY 10018.

DISCLAIMER NOTICE

This report was prepared as an account of work sponsored by an agency of the United States Government. Neither the United States Government nor any agency thereof, or any of their employees, makes any warranty, expressed or implied, or assumes any legal liability of responsibility for any third party's use, or the results of such use, of any information, apparatus, product or process disclosed in this report, or represents that its use by such third party would not infringe privately owned rights.

NUREG/CR-5772
SAND91-1766/1
Vol. 1
RV

Aging, Condition Monitoring, and Loss-of-Coolant Accident (LOCA) Tests of Class 1E Electrical Cables

Crosslinked Polyolefin Cables

Manuscript Completed: August 1992
Date Published: August 1992

Prepared by
M. J. Jacobus

Sandia National Laboratories
Albuquerque, NM 87185

Prepared for
Division of Engineering
Office of Nuclear Regulatory Research
U.S. Nuclear Regulatory Commission
Washington, DC 20555
NRC FIN A1818

Abstract

This report describes the results of aging, condition monitoring, and accident testing of cross-linked polyolefin (XLPO) cables. Three sets of cables were aged for up to 9 months under simultaneous thermal (≈100° C) and radiation (≈0.10 kGy/hr) conditions. A sequential accident consisting of high dose rate irradiation (≈6 kGy/hr) and high temperature steam followed the aging. The test results indicate that most properly installed XLPO cables should be able to survive an accident after 60 years for total aging doses up to 400 kGy and for moderate ambient temperatures on the order of 50-55°C (potentially higher or lower, depending on material specific activation energies). Mechanical measurements (primarily elongation, modulus, and density) were more effective than electrical measurements for monitoring age-related degradation.

Table of Contents

Table of Contents (cont.)

List of Figures

List of Figures (cont.)

List of Figures (cont.)

List of Figures (cont.)

List of Figures (cont.)

List of Tables

Nomenclature

Unaged chamber	Refers to the test chamber associated with the cables that were not aged
3-month chamber	Refers to the test chamber associated with the cables that were aged for 3 months
6-month chamber	Refers to the test chamber associated with the cables that were aged for 6 months
9-month chamber	Refers to the test chamber associated with the cables that were aged for 9 months
AT0	Refers to the accident (steam) test performed on the unaged cables
AT3	Refers to the accident (steam) test performed on the cables aged for 3 months
AT6	Refers to the accident (steam) test performed on the cables aged for 6 months
AT9	Refers to the accident (steam) test performed on the cables aged for 9 months
LOCA	Loss-of-Coolant Accident; a hypothesized design basis event for nuclear power plants
IR	Insulation Resistance
PI	Polarization Index; the ratio of IRs at two different times
DF	Dissipation Factor
Keithley IR	IR measured using the Keithley electrometer apparatus
Continuous IRs	IRs measured at intervals ranging from 10 seconds to 5 minutes during the accident exposures
XLPO	Crosslinked polyolefin
XLPE	Crosslinked polyethylene, a specific type of XLPO
CSPE	Chlorosulfonated polyethylene
AWG	American Wire Gauge
/C	number of conductors
FR-EP	Flame retardant ethylene propylene
CPE	Chlorinated polyethylene
EPR	Ethylene propylene rubber

EPDM	Ethylene propylene diene monomer
TSP	Twisted shielded pair
FR	Flame retardant
BIW	Boston Insulated Wire
EPRI	Electric Power Research Institute
NRC	Nuclear Regulatory Commission
EQ	Equipment Qualification
e	Absolute elongation, the % elongation at break of test sample(s); $(l_{break} - l_{initial}) / l_{initial} * 100\%$
e_0	Absolute elongation of unaged samples
e/e_0	Elongation at break relative to unaged sample; relative elongation
T	Tensile strength of test sample(s)
T_0	Tensile strength of unaged samples
T/T_0	Tensile strength relative to unaged sample
H	Hardness
H_0	Hardness of unaged samples
H/H_0	Hardness relative to unaged sample
M	Indenter modulus
M_0	Indenter modulus of unaged sample
M/M_0	Indenter modulus relative to unaged sample
D	Density; Cable outside diameter
D_0	Density of unaged samples
D/D_0	Density relative to unaged sample
LICA	Low Intensity Cobalt Array, a facility for performing thermal/irradiation exposures

Acknowledgements

My appreciation is extended to a!l who contributed to this research effort. Ed Baynes, Mike Ramirez, Tim Gilmore, and Bob Padilla all contributed to setting up and running the tests. Gary Fuehrer performed the elongation and some of the dielectric measurements, Ray Vigil performed the density measurements, Mike Ramirez performed the hardness and indenter measurements, and Ed Baynes did the modulus profiling. Gary Fuehrer was responsible for coding many of the data reduction programs. Most of the individuals named above also helped perform the many electrical measurements during the aging and accident exposures. Special thanks goes to Bill Farmer of the NRC for his support and guidance throughout this program.

EXECUTIVE SUMMARY

This report describes the results of aging, condition monitoring, and accident testing of crosslinked polyolefin (XLPO) cables. The cable products tested are representative of typical XLPO cables used inside containments of U.S. light water reactors. Some manufacturer's specify a cable material of crosslinked polyethylene (XLPE); in this report, the more generic term XLPO will be used to represent all XLPE and XLPO cables. The test specimens included multiple samples of XLPO cable products from Brand Rex, Rockbestos, Raychem, and Samuel Moore. The Raychem product was purchased and tested in a single conductor unjacketed configuration. The remaining test samples were multiconductor jacketed cables. This report is the first of three volumes describing the results of the testing. Volume 2 will discuss ethylene propylene rubber (EPR) cable products and Volume 3 will discuss miscellaneous cable products.

Many types of cable are used throughout nuclear power plants in a wide variety of applications. Cable qualification typically includes sequential thermal and radiation aging intended to put the cable in its end-of-life condition. The radiation dose is normally applied at fairly high dose rates (1-10 kGy/hr) with Arrhenius methods used to establish accelerated aging times and temperatures. Generally, the radiation and thermal aging are applied to the specimens sequentially. These qualification efforts assume that sequential application of aging stressors approximates simultaneous thermal and radiation aging conditions. Because of the high dose rates and high temperatures that are typically employed, cable materials can experience oxygen diffusion effects that result in non-uniform aging. Consequently, it is of interest to determine the extent to which these factors might have affected previous testing. Typical qualification programs also provide very little information that is useful for establishing effective condition monitoring programs that can assess a cable's ability to survive an accident environment. The experimental program described in this report utilized considerably less accelerated, simultaneous thermal and radiation aging conditions and employed condition monitoring measurements during aging. In addition, similar accident tests were performed on cables aged to three different nominal lifetimes to compare their accident performance.

The primary objectives of the testing were to determine the long term aging degradation behavior of popular cable products used in nuclear power plants and to determine the potential for using condition monitoring (CM) for residual life assessment. More specific objectives were to assess the accident performance of cables aged more slowly (e.g., at lower temperatures and radiation dose rates) than in typical industry tests and under simultaneous conditions; to assess the conservatism associated with the IEEE 383-1974 post-accident mandrel bend and high potential testing; and to assess what additional qualification requirements might be needed as cables age beyond their current qualified life.

The experimental program consisted of two phases, both using the same XLPO test specimens. Phase I was a simultaneous thermal (≈100° C) and radiation aging (≈0.10 kGy/hr) exposure, and Phase II was a sequential accident exposure consisting of 1100 kGy of high dose rate irradiation (≈6 kGy/hr) followed by a simulated loss-of-coolant accident (LOCA) steam exposure. The test program generally followed the guidance of IEEE 323-1974 and IEEE 383-1974.

XLPO cable products (total of 18 cables comprising 40 individual conductors) were included in three different test chambers, with the cables in each chamber aged to a

different extent prior to accident testing. Cables were aged for 3 months in the first chamber, 6 months in the second chamber, and 9 months in the third chamber. The accelerated aging temperature was determined by equating the 6-month exposure to a 40-year life and assuming an activation energy of 1.15 eV and a plant ambient temperature of 55° C. Consistent with past Sandia testing, the accelerated radiation aging dose rate was determined by assuming a 40-year radiation dose of 400 kGy and the total accident radiation dose was 1100 kGy.

During the aging exposure, various electrical and mechanical condition monitoring measurements were performed on the cables. The electrical measurements were performed on long lengths of cable, while the mechanical measurements were performed on small samples removed from the test chambers during aging. The parameters measured included insulation resistance and polarization index at three different voltages, capacitance and dissipation factor over a wide range of frequencies, tensile strength and elongation at failure, modulus profiles, cable indenter modulus tests (using a cable indenter developed at Franklin Research Center under Electric Power Research Institute (EPRI) funding), hardness, and bulk density. During the accident exposure, the insulation resistance of the cables was monitored on essentially a continuous basis.

The conclusions of this experimental effort with regard to both the broad and specific objectives of the program are addressed below:

Objective: To determine the long term aging degradation behavior of popular cable products used in nuclear power plants.

Conclusion: The test results indicate that most properly installed XLPO cables should be able to survive an accident after 60 years for total aging doses up to 400 kGy and for moderate ambient temperatures on the order of 50-55°C (potentially higher or lower, depending on material specific activation energies).

Objective: To determine the potential of condition monitoring (CM) for residual life assessment.

Conclusion: Of the measurements tested, elongation is the best condition monitoring method. Although a quantitative generic acceptance criterion is difficult to establish based on these tests, a reasonable range (that is likely to be fairly conservative) would be about 50-100% absolute elongation remaining. Compressive modulus and density could also be somewhat effective for monitoring residual life, although acceptance criteria would be much more difficult to establish for these measurements because extensive testing has not been performed to demonstrate that modulus and density respond consistently for varied test conditions. The electrical measurements were not effective for monitoring residual life.

Objective: To assess the accident performance of cables aged more slowly (e.g., at lower temperatures and radiation dose rates) than in typical industry tests and under simultaneous conditions.

Conclusion: The accident performance (in terms of electrical properties) of the XLPO cables did not differ substantially from the accident performance of cables aged at more highly accelerated (both sequential and simultaneous) conditions in past Sandia tests, as well as in industry tests. However, it must be noted that this conclusion only applies up to the limits of the aging conditions simulated in this test program since the

testing does not prove or disprove whether highly accelerated tests to much higher total exposure conditions would produce the same results if the acceleration were greatly reduced.

Objective: To assess the conservatism associated with the IEEE 383-1974 post-accident mandrel bend and high potential testing.

Conclusion: The IEEE 383-1974 post-LOCA mandrel bend test on the cables that had been aged for 9 months induced cracking of three conductors of one cable type. The high potential test did not induce any cable failures (assuming the cable did not crack during the mandrel bend), even after bends significantly more severe than the IEEE requirement. Thus, for XLPO cables, the most severe part of the post-accident exposure appears to be the bend test.

Objective: To assess what additional qualification requirements might be needed as cables age beyond their current nominal 40-year qualified life.

Conclusion: The accident performance of cables aged to the three different lifetimes was not significantly different. Thus, for XLPO cables exposed to environments less severe than those simulated in this test program, these tests do not indicate the need for additional qualification requirements as cables age beyond their current qualified life. This conclusion is based on the technical finding that the cables tested did not fail (with only one exception) when exposed to the environments defined in this test program. It does not prove or disprove the adequacy of current qualification practices and requirements.

1.0 INTRODUCTION

1.1 Background

Many types of cable are used throughout nuclear power plants in a wide variety of applications. Cable qualification to IEEE 323-1974 [1] and IEEE 383-1974 [2] typically includes sequential thermal and radiation aging intended to put the cable in its end-of-life condition. The radiation dose is typically applied at fairly high dose rates (1-10 kGy/hr) with Arrhenius methods used to establish artificial aging times and temperatures. Generally, the radiation and thermal aging are applied to the specimens sequentially. These qualification efforts assume that sequential application of aging stressors approximates simultaneous thermal and radiation aging conditions. Some (primarily research) programs have applied the environments simultaneously [3-6]. However, because of the high dose rates and high temperatures that are typically employed, cable materials can still experience oxygen diffusion effects that result in non-uniform aging. Consequently, it is of interest to determine the extent to which these factors might have affected previous testing. Typical qualification programs also provide very little information that is useful for establishing effective condition monitoring programs that can assess a cable's ability to survive an accident environment. The current experimental program went beyond previous efforts [3-6] by employing considerably less accelerated, simultaneous thermal and radiation aging conditions; by employing many more condition monitoring measurements during aging; and by performing similar accident tests on cables aged to three different nominal lifetimes.

This report describes the results of aging, condition monitoring, and accident testing of crosslinked polyolefin (XLPO) cables. The cable products tested are representative of typical XLPO cables used inside containments of U.S. light water reactors. Some manufacturer's specify a cable material of crosslinked polyethylene (XLPE); in this report, the more generic term XLPO will be used to represent all XLPE and XLPO cables. This report is the first of three volumes describing the results of the testing. Volume 2 will discuss ethylene propylene rubber (EPR) cable products and Volume 3 will discuss miscellaneous cable products.

1.2 Objectives

The broad objectives of this experimental program were twofold:

a. to determine the long term aging degradation behavior of popular cable products used in nuclear power plants and

b. to determine the potential for using condition monitoring (CM) for residual life assessment.

More specific objectives were as follows:

a. to assess the accident performance of cables aged more slowly (e.g., at lower temperatures and radiation dose rates) than in typical industry tests and under simultaneous conditions;

b. to assess the conservatism associated with the IEEE 383-1974 [2] post-accident mandrel bend and high potential testing; and

c. to assess what additional qualification requirements might be needed as cables age beyond their current nominal 40-year qualified life.

1.3 Approach

To accomplish these objectives, an experimental program consisting of two phases was undertaken, both using the same test specimens. Phase I was a simultaneous thermal (≈100° C) and radiation aging (≈0.10 kGy/hr) exposure. Phase II was a sequential accident exposure consisting of 1100 kGy of high dose rate irradiation (≈6 kGy/hr) followed by a simulated loss-of-coolant accident (LOCA) steam exposure. The test program generally followed the guidance of IEEE 323-1974 [1] and IEEE 383-1974 [2].

Four separate test chambers were included in the program. Cables were aged for 3 months in the first chamber, 6 months in the second chamber, and 9 months in the third chamber. A fourth chamber contained unaged cables. Accident testing utilized the same test chambers as the aging. The accelerated aging temperature was determined by equating the 6-month exposure to a 40-year life and assuming an activation energy of 1.15 eV and a plant ambient temperature of 55°C. The accelerated radiation aging dose rate was determined by assuming a 40-year radiation dose of 400 kGy and the total accident radiation dose was 1100 kGy. It should be noted that typical generic industry qualification testing uses an aging dose of 500 kGy and an accident dose of 1500 kGy.

A complete list of the cables included in this program is given in Table 1. This report only describes the results for the XLPO cables, which are the first four entries in Table 1. Results for the other cables, which were concurrently tested in the same chambers as the XLPO cables, are in separate volumes of this report. Because of the generally good performance of the aged XLPO cables, no XLPO cables were included in the unaged cable test (although baseline electrical and mechanical properties tests of unaged cables were performed). Therefore, the testing of unaged cables will not be discussed further in this volume of this report.

Table 1 Cable Products Included in the Test Program
Note: Cables discussed in this volume are shown in boldface.

	Supplier	Description
1.	**Brand Rex**	30 mil XLPE Insulation, 60 mil CSPE Jacket, 12 AWG, 3/C, 600 V
2.	**Rockbestos**	Firewall III, 30 mil Irradiation XLPE, 45 mil Neoprene Jacket, 12 AWG, 3/C, 600 V
3.	**Raychem**	Flamtrol, 30 mil XLPE Insulation, 12 AWG, 1/C, 600 V
4.	**Samuel Moore**	Dekoron Polyset, 30 mil XLPO Insulation, 45 mil CSPE Jacket, 12 AWG, 3/C and Drain, 600 V
5.	Anaconda	Anaconda Y Flame-Guard FR-EP, 30 mil EPR Insulation, 45 mil CPE Jacket, 12 AWG, 3/C, 600 V
5a.	Anaconda *	Anaconda Flame-Guard EP, 30 mil EPR Insulation, 15 mil Individual CSPE Jackets, 45 mil Overall CSPE Jacket, 12 AWG, 2/C, 1000 V
6.	Okonite	Okonite Okolon, 30 mil EPR Insulation, 15 mil CSPE Jacket, 12 AWG, 1/C, 600 V
7.	Samuel Moore	Dekoron Dekorad Type 1952, 20 mil EPDM Insulation, 10 mil Individual CSPE Jackets, 45 mil Overall CSPE Jacket, 16 AWG, 2/C TSP, 600 V
8.	Kerite	Kerite 1977, 70 mil FR Insulation, 40 mil FR Jacket, 12 AWG, 1/C, 600 V
8a.	Kerite	Kerite 1977, 50 mil FR Insulation, 60 FR Jacket, 12 AWG, 1/C, 600 V
9.	Rockbestos	RSS-6-104/LE Coaxial Cable, 22 AWG, 1/C Shielded
10.	Rockbestos	30 mil Firewall Silicone Rubber Insulation, Fiberglass Braided Jacket, 16 AWG, 1/C, 600 V
11.	Champlain	5 mil Polyimide (Kapton) Insulation, Unjacketed, 12 AWG, 1/C
12.	BIW	Bostrad 7E, 30 mil EPR Insulation, 15 mil Individual CSPE Jackets, 60 mil Overall CSPE Jacket, 16 AWG, 2/C TSP, 600 V

* This cable was only used for the multiconductor samples in the 3-month chamber.

Note: See nomenclature section for abbreviations.

2.0 EXPERIMENTAL ARRANGEMENT

2.1 Test Strategy

2.1.1 Phase I--Simultaneous Aging Exposure

Phase I consisted of simultaneous thermal and radiation aging of the cables. The aging was performed in Sandia's Low Intensity Cobalt Array (LICA) facility. A photograph of one of the test fixtures used in the LICA facility with a test chamber placed in it is shown in Figure 1. When located at the bottom of the LICA water pool, cobalt pencils were

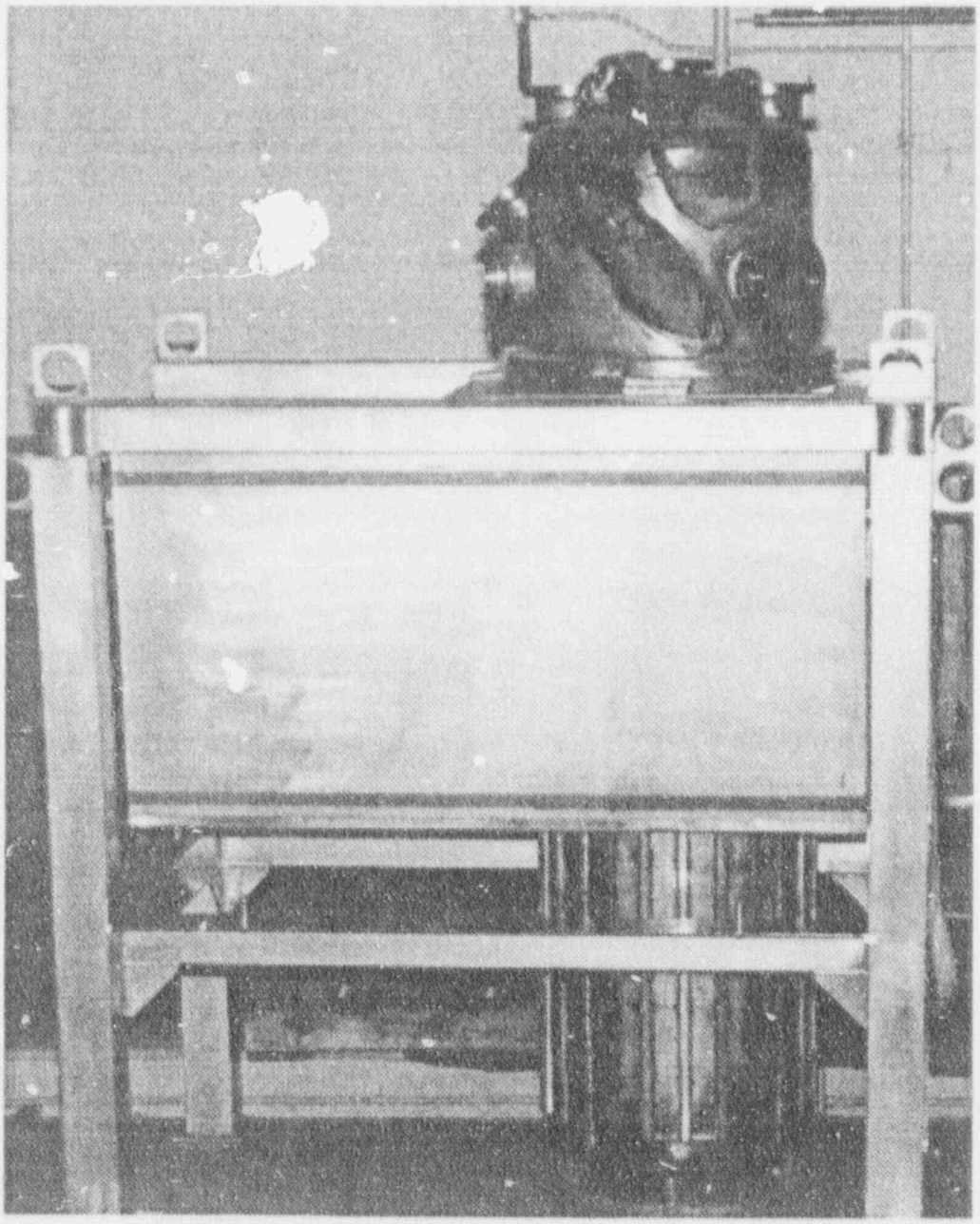

Figure 1 Test Chamber in Fixture Used for Aging

placed into the test fixture. Test chambers could then be lowered into the fixture and located as shown in Figure 1. Three different sets of specimens were included in this phase, one aged to a nominal lifetime of 20 years, a second to 40 years, and a third to 60 years. Actual simulated lifetimes vary greatly because of different activation energies of the specimens, because of the assumed service temperature, and because of test temperature gradients. A single value of activation energy had to be chosen to keep aging times and temperatures constant for different cables, which were all located in common test chambers for each exposure. A value of 1.15 eV was chosen since it is in the range of typical values for many of the polymer material that were being tested. Based on meeting a realistic schedule together with the desire to accelerate the aging of the cables as little as possible, periods of three, six, and nine months were chosen as the accelerated aging times. The aging conditions assumed a plant ambient temperature of 55°C with no conductor heat rise. Conductor heat rise during normal plant operations is rarely significant for qualified cables in containments of nuclear power plants because most qualified power circuits are not energized during normal operation and other circuits (control and instrumentation with low currents) have minimal heat rise. The well-known Arrhenius equation was used to calculate the aging temperature:

$$\frac{t_2}{t_1} = \exp\left[\frac{E_a}{k_b}\left(T_2^{-1} - T_1^{-1}\right)\right] \qquad (1)$$

where t_1 and t_2 are two aging times (one normally being the life to be simulated), E_a is the activation energy of the material, k_b is Boltzmann's constant, and T_1 and T_2 are the absolute aging temperatures corresponding to t_1 and t_2, respectively. With the desired aging times, the assumed activation energy, and the assumed ambient conditions, the desired aging temperature was calculated to be 95°C. The total aging dose used in previous Sandia tests was typically 400 kGy for 40-year samples [3,5,6]. To provide a basis for comparison to this study, the 20-year cables were aged to a nominal total dose of 200 kGy, the 40-year cables to a nominal 400 kGy, and the 60-year cables to a nominal 600 kGy. Each of these total aging doses required a dose rate of about 0.09 kGy/hr. During the aging exposure, cable lead wires and penetrations were shielded to reduce their radiation and thermal exposures and reduce artificial failures that might occur at these locations.

2.1.2 Phase II--Accident Exposure

Phase II consisted of exposing the cables to a simulated LOCA environment in Sandia's Area I facility. The cables were first exposed to an accident radiation dose of approximately 1100 kGy at a dose rate of about 6 kGy/hr. This radiation exposure was performed in Sandia's LICA facility by reconfiguring the cobalt-60 pencils for higher dose rate conditions. During the radiation exposure, the cable leads and penetrations remained shielded from the radiation environment as much as possible. The samples were then exposed to a high temperature and pressure steam environment. The test profile was similar to the one given in IEEE 323-1974 [1] for "generic" qualification. The cables were energized at 110 Vdc during the accident simulation. Insulation resistance measurements (IRs) were performed on-line throughout the test. IRs were also measured periodically with an independent measurement technique that is more accurate than the on-line measurement system for IRs above 10^8 Ω. No chemical spray was used during the steam exposure, but a post-LOCA submergence test was performed on the cables aged to a nominal equivalent of 40 years [7].

2.2 Test Specimens

2.2.1 Sample Selection

Samples were selected on the basis of cable availability, application in safety systems, abundance of cable in use, and cable materials. Information gained from the NRC Equipment Qualification Inspection Program was a major input for assessing current plant usage of cables. Also considered in specimen selection was the current EPRI/University of Connecticut aging study [8].

2.2.2 Sample Preparation

For each cable type, 23-m (76-ft) lengths of cable were wrapped around a mandrel. The effective cable length inside the test chamber was typically 4.6-6.1 m (15-20 ft), with the remainder of the cable used for external connections. A typical mandrel hanging from a test chamber head is shown in Figure 2. Where both single and multiconductor samples of the same cable were tested, the single conductors were obtained by stripping the jacket from the multiconductor and removing all filler materials.

Additional test samples included in the aging exposure consisted of insulation and jacket specimens that were 15 cm. (6 in.) long and single and multiconductor cable samples that were 36 cm. (14 in.) long. The insulation and jacket samples (hereafter referred to as tensile specimens) were used for tensile strength and elongation testing. The copper conductors were removed from these cable samples prior to the beginning of aging. The 36-cm cable samples (hereafter referred to as complete cable specimens) were used for hardness and modulus testing. They were prepared by simply cutting the cables to the desired length and stripping the insulation from the ends of the cable. Figure 3 shows a typical sample basket that these samples were placed in during aging. This basket was then located inside the mandrel shown in Figure 2.

2.3 Test Description

Table 2 gives a list of the 23-m cables tested in each chamber and the associated conductor numbers that will be used in the remainder of this report. The notation used to describe the samples removed from the baskets inside the test chambers is shown in Table 3. The sample identifications ending in 1, 2, and 3L from the 6-month chamber were generated by replacing the 5-, 4-, and 3F-month samples, respectively, when they were removed from the 6-month chamber. Similarly, the sample identifications ending in 1, 2, and 3 from the 9-month chamber were generated by replacing the 8-, 7-, and 6-month samples when they were removed from the 9-month chamber. Sample identifications that include an R designator were included in the accident radiation. Table 4 lists the number of 15-cm. insulation and jacket specimens that were removed from each chamber, along with the months of aging that the specimens received. Table 5 gives similar information for the 36-cm. single and multiconductor samples.

2.3.1 Radiation and Thermal Aging

Irradiation and thermal aging were performed in Sandia's LICA facility. Dose rates in the chambers were determined using thermoluminescent dosimeters (TLDs). The cables were installed in one of three test chambers, which were lowered into the LICA facility. The test chamber temperature was maintained using electric wall heaters and electric inlet air heaters. Temperature uniformity was controlled to the extent possible by insulating the chamber and by providing air circulation. Approximately 4.7 l/s (10 ft^3/min) of outside air (about 40 air changes per hour) was introduced into the chamber to maintain circulation and ambient oxygen concentration. Some of the piping used for air circulation can be seen in Figure 2.

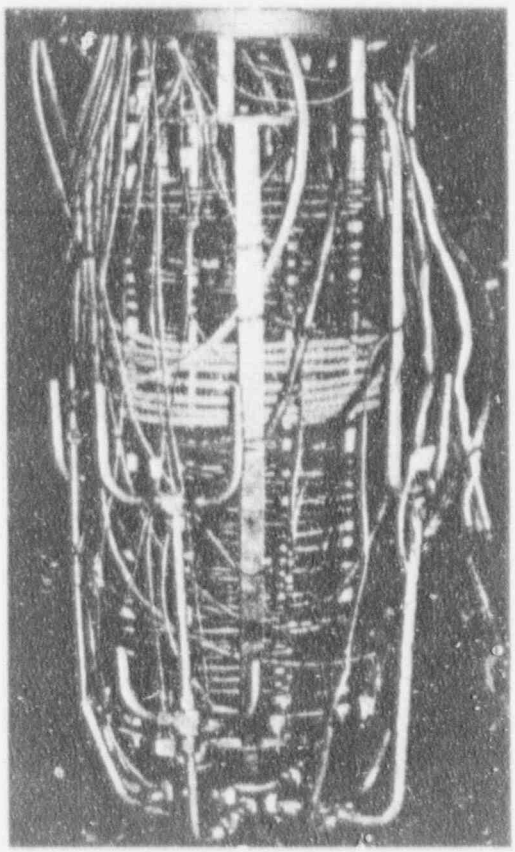

Figure 2 Typical Test Mandrel Hanging from a Test Chamber Head

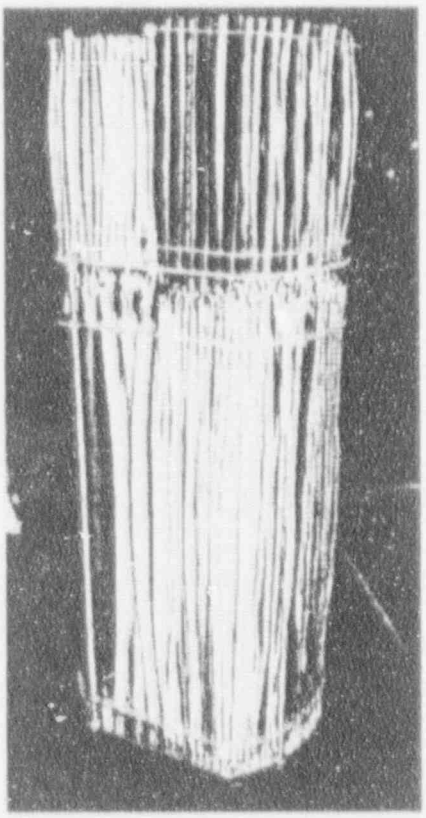

Figure 3 Typical Sample Basket

2.3.2 Loss-of-Coolant Accident Simulation

The accident simulation consisted of an exposure to a nominal radiation dose of 1100 kGy at 6 kGy/hr and ambient temperature, followed by a simulated LOCA steam exposure. The intended LOCA temperature and pressure profiles are given in Table 6 and were applied following the accident radiation exposure. Also given in Table 6 is the IEEE 323-1974 [1] suggested profile for a combined BWR/PWR generic test. The only significant difference in the profiles is that the final portion of our tests was at a higher temperature and for a shorter duration than IEEE 323 suggests. Four separate LOCA tests were performed, one for each test chamber. However, this volume only discusses the three LOCA tests that included XLPO cables.

2.3.2.1 Saturated Versus Superheated Steam

The LOCA profile used in these tests consisted of superheated steam conditions during the initial ramp and until 6 hours after the start of the second transient. It then continued as saturated steam. Whether saturated or superheated steam is more severe is not known: superheated conditions may tend to dry out the insulations and cause them to crack, while saturated conditions provide moisture to penetrate connections or insulations and cause shorts. However, it is generally believed that saturated conditions tend to be more severe. The LOCA profile used in this test program was chosen because it is representative of profiles used by the industry during actual qualification tests (i.e., IEEE 383-1974 [2] qualification tests).

Table 2 Cables Tested in Each Chamber and Conductor Identification

Cable Type (see Table 1)	Conductor Number	Tested Length	Location on Mandrel * (below chamber flange)
Cables Aged for 3 Months			
Brand Rex--1	1 (Red) 2 (White) 3 (Black)	5.2 m (17 ft)	28 cm (11 in)
Firewall III--2	12 White) 13 (Black) 14 (Red)	5.3 m (18 ft)	48 cm (19 in)
Polyset--4	19 (#1) 20 (#2) 21 (#3)	5.8 m (19 ft)	64 cm (25 in)
Raychem--3	27	4.5 m (15 ft)	38 cm (15 in)
Raychem--3	28	4.5 m (15 ft)	41 cm (16 in)
Shield for cond. 19-21	41		
Cables Aged for 6 Months			
Brand Rex--1	1 (Red) 2 (White) 3 (Black)	4.6 m (15 ft)	28 cm (11 in)
Firewall III--2	12 White) 13 (Black) 14 (Red)	5.0 m (16 ft)	46 cm (18 in)
Polyset--4	19 (#1) 20 (#2) 21 (#3)	5.9 m (19 ft)	61 cm (24 in)
Raychem--3	27	4.7 m (15 ft)	36 cm (14 in)
Raychem--3	28	4.9 m (16 ft)	38 cm (15 in)
Shield for cond. 19-21	41		
Cables Aged for 9 Months			
Brand Rex--1	1 (Red) 2 (White) 3 (Black)	5.3 m (17 ft)	18 cm (7 in)
Firewall III--2	14 White) 15 (Black) 16 (Red)	6.0 m (20 ft)	43 cm (17 in)

Table 2 Cables Tested in Each Chamber and Conductor Identification (cont.)

Cables Aged for 9 Months (cont.)

Cable Type (see Table 1)	Conductor Number	Tested Length	Location on Mandrel * (below chamber flange)
Firewall III--2	17 (White) 18 (Black) 19 (Red)	6.8 m (22 ft)	48 cm (19 in)
Polyset--4	24 (#1) 25 (#2) 26 (#3)	6.7 m (22 ft)	66 cm (26 in)
Polyset--4	27 (#1) 28 (#2) 29 (#3)	6.9 m (23 ft)	71 cm (28 in)
Raychem--3	35	4.9 m (16 ft)	28 cm (11 in)
Raychem--3	36	4.4 m (14 ft)	30 cm (12 in)
Raychem--3	37	4.4 m (14 ft)	33 cm (13 in)
Shield for cond. 24-26	55		
Shield for cond. 27-29	56		

* For the 3- and 6-month chambers, conductors 1-21 were wrapped on the outside of the mandrel and conductors 22-39 were wrapped on the inside of the mandrel. For the 9-month chamber, conductors 1-29 were wrapped on the outside of the mandrel and conductors 30-50 were wrapped on the inside of the mandrel.

2.4 Monitoring During Testing

2.4.1 Cable Condition Monitoring During Aging

This section describes the condition monitoring measurements that were performed on the cables during the aging exposure.

2.4.1.1 Electrical Techniques

a. Insulation resistance (IR) and polarization index (PI, the ratio of IR at two different times) between each conductor and all other conductors connected together. We performed the measurements at nominal voltages of 50, 100, and 250 Vdc. IR/PI measurements for single conductors are much more difficult to interpret than those for shielded and/or multiconductor cables because the single conductor cables have a much less precisely defined ground plane. Our measurements were always performed relative to the same ground plane in the same configuration. Thus, the single conductor measurements will at least indicate trends in IR that result from global degradation. Local degradation of a single conductor cable may be outside the effective ground plane and may therefore not be detected. Such undetectable

local degradation is not limited to single conductors, however, since the ground plane for unshielded multiconductors is, at least in part, based on insulated conductors. Appendix A gives a discussion of IR and PI measurements and the circuitry used to measure them.

Table 3 Identification of Samples in Baskets

Sample ID #	Chamber	Months aging
xx-3-3 *	3	Entire 3 month exposure
xx-3-3R	3	Entire 3 month exposure and accident radiation
xx-6-3F	6	First 3 months of exposure
xx-6-4	6	First 4 months of exposure
xx-6-5	6	First 5 months of exposure
xx-6-6	6	Entire 6 month exposure
xx-6-6R	6	Entire 6 month exposure and accident radiation
xx-6-R	6	Accident radiation exposure only
xx-6-3L	6	Last 3 months of exposure
xx-6-2	6	Last 2 months of exposure
xx-6-1	6	Last 1 month of exposure
xx-9-6	9	First 6 months of exposure
xx-9-7	9	First 7 months of exposure
xx-9-8	9	First 8 months of exposure
xx-9-9	9	Entire 9 month exposure
xx-9-9R	9	Entire 9 month exposure and accident radiation
xx-9-3	9	Last 3 months of exposure
xx-9-2	9	Last 2 months of exposure
xx-9-1	9	Last 1 month of exposure

* xx denotes the cable number as given by Table 1.

b. Capacitance and dissipation factor between each conductor and all other conductors connected together. Capacitance measurements give an indication of the dielectric charge/voltage characteristics and dissipation factor gives a measure of the AC resistive leakage current in the cables. These measurements, like IR/PI, are more difficult to apply and interpret when single conductor cables are tested. Note that once capacitance and dissipation factor are known, many other cable parameters can be calculated, such as complex transfer function magnitude and phase, effective cable resistance, power factor, real and imaginary (loss) components of complex capacitance, and loss angle.

2.4.1.2 Mechanical Techniques

a. Elongation at failure of the tensile specimens. This measurement determines the amount that the cable will stretch prior to failure. We performed these

measurements with an Instron Model 1000 load tester and an incremental extensometer that has a resolution of 10% elongation. The samples were stretched at a rate of 127 mm/min (5 in/min). The measurements were performed on the small test specimens discussed in Section 2.2. This is, of course, a destructive test.

The force output from the load tester was fed into a data logger that was interfaced with a Hewlett Packard Model 216 computer. The incremental extensometer triggered the data logger to make a force reading each time the specimen stretched an additional 10%. In this way, a complete force-elongation (or stress-strain) curve was obtained with data at every 10% elongation.

b. Ultimate tensile strength of the tensile specimens. This measurement was made together with elongation measurements and is defined as the force at break divided by the initial cross sectional area of the material.

Table 4 Number of 15-cm Specimens Removed at Each Test Condition

Insulation

Cham. #	3	3	6	6	6	6	6	6	9	9	9	9	9
Month #	3	3R	3F/3L*	4/2	5/1	6	6R	R	6/3	7/2	8/1	9	9R
Cable Type													
Brand Rex	12	9	7	9	11	14	4	10	7	9	11	14	4
Rockbestos	13	9	7	9	11	13	4	10	7	9	11	13	4
Raychem	10	6	5	6	7	10	4	9	5	6	7	10	4
Dekoron	13	9	7	9	11	14	4	10	7	9	11	14	4

Jacket

Cham. #	3	3	6	6	6	6	6	6	9	9	9	9	9
Month #	3	3R	3F/3L*	4/2	5/1	6	6R	R	6/3	7/2	8/1	9	9R
Cable Type													
Brand Rex	13	10	3	5	6	9	3	6	3	5	6	9	3
Rockbestos	13	10	3	5	6	9	3	6	3	5	6	9	3
Raychem	0	0	0	0	0	0	0	0	0	0	0	0	0
Dekoron	13	10	3	5	6	9	3	6	3	5	6	9	3

* When the 3-, 4-, and 5-month specimens were removed from the 6-month chamber and when the 6-, 7-, and 8-month specimens were removed from the 9-month chamber, they were replaced with an equal number of unaged specimens. Thus, the values shown for these cases represent two different sets of specimens.

Table 5 Number of 36-cm Specimens Removed at Each Test Condition

Single Conductor

Cham. #	3	3	6	6	6	6	6	6	9	9	9	9	9
Month #	3	3R	3F/3L*	4/2	5/1	6	6R	R	6/3	7/2	8/1	9	9R
Cable Type													
Brand Rex	8	6	4	5	7	10	3	7	4	5	7	10	3
Rockbestos	8	6	4	6	7	11	3	10	4	6	7	11	3
Raychem	8	6	4	6	7	10	3	7	4	6	7	10	3
Dekoron	8	6	3	5	6	8	3	10	3	5	6	8	3

Multiconductor

Cham. #	3	3	6	6	6	6	6	6	9	9	9	9	9
Month #	3	3R	3F/3L*	4/2	5/1	6	6R	R	6/3	7/2	8/1	9	9R
Cable Type													
Brand Rex	1	2	1	1	1	1	1	2	1	1	1	1	1
Rockbestos	2	2	1	1	1	1	1	2	1	1	1	1	1
Raychem	0	0	0	0	0	0	0	0	0	0	0	0	0
Dekoron	1	2	1	1	1	1	1	2	1	1	1	1	1

* See footnote to table 4.

c. Modulus profiling of selected complete cable specimens. Modulus profiles were acquired using an apparatus developed at Sandia [9,10]. The modulus is the slope of the stress versus strain curve in the initial linear portion of the curve. The modulus profile gives information on the modulus of the sample across its cross section. It also gives an indication of the uniformity of the aging process [9,10]. The primary purpose for using modulus profiling was to establish the uniformity of the aging process, and therefore, this technique was used only on a few selected samples.

To perform the modulus profiles, 1.25-cm samples were cut from the 36-cm cable specimens. For cable products that were tested in both single and multiconductor configurations, samples were only removed from the multiconductor 36-cm specimens because oxygen diffusion effects will be most severe in the multiconductors. In some cases, the 1.25-cm samples were surrounded with heat shrinkable tubing to hold them in place. The samples were then encapsulated in epoxy, allowed to cure, and polished prior to the modulus measurements. Figure 4 shows a diagram of a typical multiconductor cable prepared for testing. For cable products supplied as single conductors, modulus profile samples were prepared in a similar fashion, but four single conductor samples were typically grouped in a diamond pattern for potting in epoxy. For the multiconductors, modulus testing

would typically proceed across the centerline of two specimens from the point labelled "start measurement" to the point labelled "end measurement." The measurements would be performed on the first cable's insulation, wrap (if used), and jacket, and then measurements would be performed on the second cable's jacket, wrap (if used), and insulation. For single conductors, a similar path through two cable samples was followed.

Table 6 Intended LOCA Profile and IEEE 323-1974 [1]
PWR/BWR Combined Temperature Profile

	Intended Profile		IEEE 323 Profile
Time	Temperature (°C)	Absolute Pressure (kPa)	Temperature (°C)
0 - 10 s	Ambient-138	101-339	57-138
10 s - 5 min	138-171	339-584	138-171
5 min - 3 hr	171	584	171
3 - 5 hr	171-60	584-101	171-60
Reset time to 0 for the next portion of the tests			
0 - 10 s	60-138	101-339	60-138
10 s - 5 min	138-171	339-584	138-171
5 min - 3 hr	171	584	171
3 hr - 6 hr	160	584	160
6 hr - 10 hr	149	462	149
10 hr - 91 hr	121	206	121
91 hr - end *	121	206	93

* IEEE 323-1974 implies that the test should be continued for 100 days for a combined PWR/BWR simulation. Our intended test profile was at a higher temperature and lasted until 240 hr (10 days) after the beginning of the second transient.

d. Modulus tests using Franklin Research Center's cable indenter developed under EPRI funding [12,13]. This test measures penetration force of a blunt conical probe as a function of penetration depth. The compressive modulus is defined as $\Delta F/\Delta x$, where Δx is the change in depth of penetration for a given change in force ΔF. In all of our tests, ΔF was defined as 6.7 N (1.5 lb), beginning at 2.2 N (0.5 lb) and ending at 8.9 N (2.0 lb). A key advantage of this indenter modulus measurement is that it is a nondestructive test and therefore may be realistic for use in the field.

The outputs of the cable indenter were fed into a data logger that was interfaced to a Hewlett Packard Model 216 computer. Thus, the entire force-displacement curve was obtained. A sample curve is shown in Figure 5. As the indenter penetrates the material, the force increases as shown on the left part of the figure. The force during retraction of the indenter, as shown on the right part of the figure, is substantially lower at the same displacement because of hysteresis in the material.

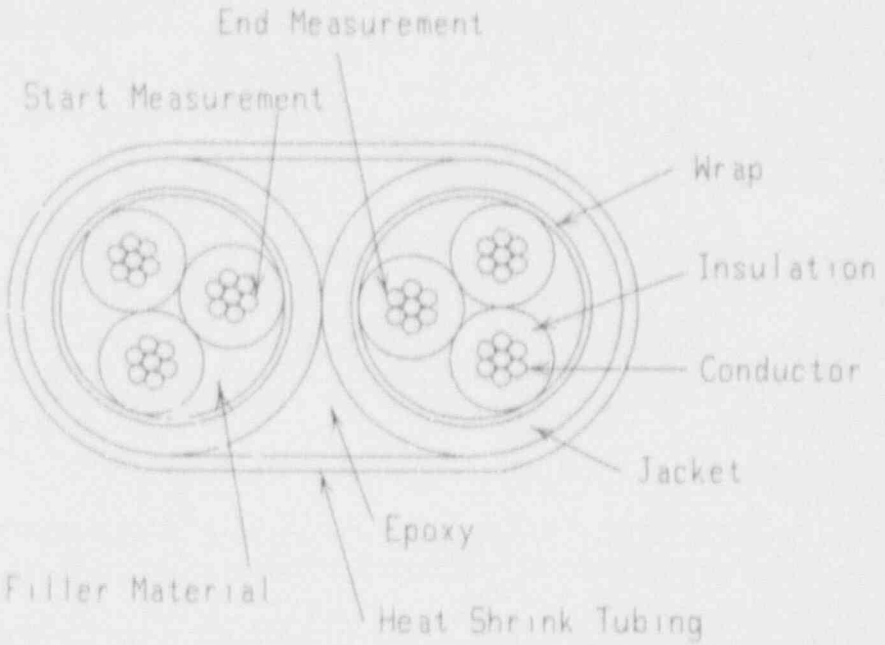

Figure 4 Diagram of Multiconductor Prepared for Modulus Profiling

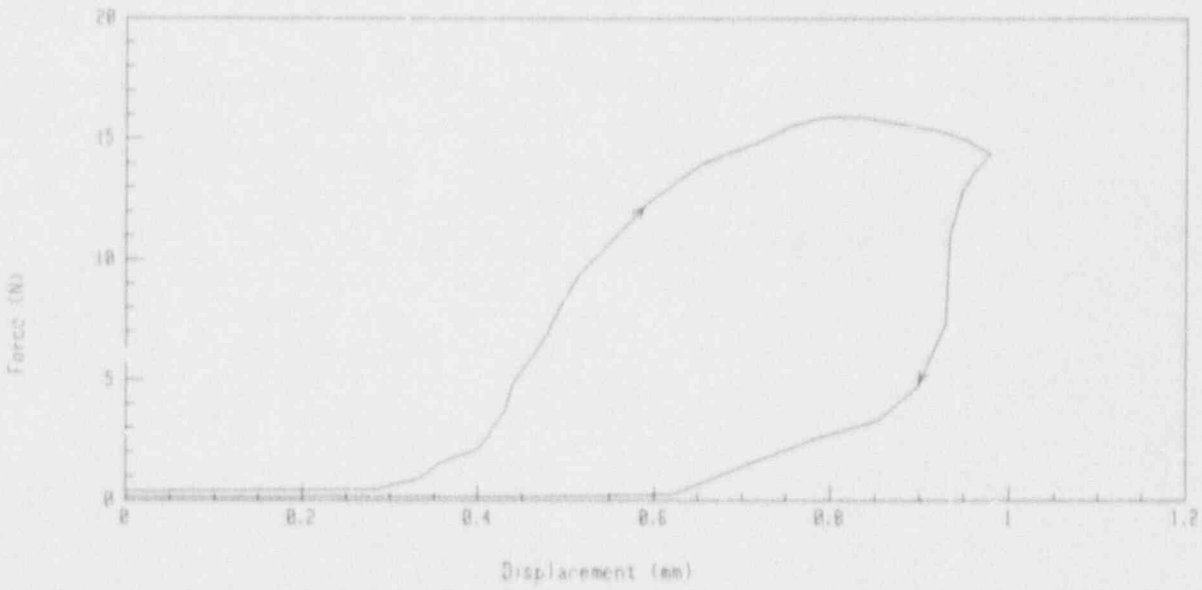

Figure 5 Sample Force Versus Displacement Curve from Cable Indenter for Unaged Dekoron Polyset Insulation

e. Hardness testing of cable insulation and jacket materials. Hardness is a measure of the material's resistance to local penetration. In this program, a Shore Durometer Type A2 was used for the measurements. The previously discussed techniques of modulus profiling and indenter modulus testing give more quantitative information, but the hardness tests were included since they represent a very simple, nondestructive field measurement technique.

f. Bulk density of small samples. Samples for density measurement were on the order of 5 mm^3 and were removed from 15-cm insulation and jacket specimens that were not used for tensile testing. Density profiling has demonstrated that density tends to increase with aging [10, 11], but similar to modulus, density may be subject to gradients resulting from oxygen diffusion effects. In this program, bulk density was measured and the modulus profiling was used to give an indication of the gradients resulting from oxygen diffusion. Density profiling was not performed because it is considerably more tedious than modulus profiling and tends to yield complementary information. The density measurements were performed in density gradient columns covering a range from 1.20 to 1.55 g/cm^3.

2.4.2 Monitoring of Test Environment

Nominally 18 type K thermocouples were positioned near the cables in each test chamber. Additional thermocouples were positioned near the baskets of tensile and complete cable specimens. Two of the thermocouples in each chamber were connected to a strip chart recorder during aging and other thermocouples were used for control of the aging temperature as needed. All of the thermocouples were connected to a data logger, which recorded the thermal aging temperature histories. The data logger was interfaced to a computer for storage of data. A pressure transducer monitored chamber pressure during aging and a flow meter monitored the air flow delivered to the chamber during aging. A similar configuration of temperature and pressure monitoring was used during the accident exposure.

Automated measurements of temperature and pressure during the accident exposure were made at intervals varying from 10 seconds during transient ramps in the profile to 5 minutes during long steady portions of the profile. Measurements during aging were typically made at 1-hour intervals.

2.4.3 Cable Monitoring During Accident Simulations

Throughout the accident simulations, the cables were normally powered at a nominal voltage of 110 Vdc with no current. Because many instrumentation circuits operate at voltages below 110 Vdc, during the second steam exposure at 171°C (340°F) of AT3, the voltage was reduced to 45 Vdc for 1 hour as shown in Figure 6. Similarly, during AT6, the voltage was reduced to 45 Vdc for 20 hours as shown in Figure 7. During all other LOCA testing, the voltage was at the nominal 110 Vdc. Insulation resistance (IR) was monitored using the circuits and apparatus shown in Figures 8-9. The conductor numbers used in the figures are based on the conductor numbers in Table 2. As shown in the figures, some individual conductors of some multiconductors were connected to ground to help provide a ground plane. The IRs were measured at intervals ranging from 10 seconds to 5 minutes. These IRs will subsequently be referred to as continuous IRs, even though they were not truly continuous. IRs were also measured at discrete intervals using the Keithley electrometer apparatus that is discussed in Appendix A. These will subsequently be referred to as the Keithley IRs. The Keithley IRs were performed at nominal voltages of 50 V, 100 V, and 250 V. The actual applied voltage during a given measurement can be approximated from Table A-1 in Appendix A. In general, the actual applied voltage was not more than 10% below the nominal except for cables with IRs below 18 kΩ at 50 V, 18 kΩ at 100 V, or 556 kΩ at 250 V.

While the continuous IRs are quite accurate down as low as about 100 Ω, a number of factors limit the upper IR that can be measured with reasonable accuracy. The data logger resolution and accuracy are important factors. Under the conditions during testing, the Hewlett Packard 3497A data loggers have an accuracy of about ±4 μV with a resolution of 1 μV. This would give an apparent upper limit of about 25 MΩ (for the tested length) to maintain 10% accuracy in the measurement (or about 1 MΩ-100 m). Because the method of measurement relies on measuring a small voltage change on top of a floating voltage of 110 V, further inaccuracy can result in the IR measurements as a result of capacitive charging effects in the data logger circuitry, which are greatest when the scan rate is fastest. In spite of these effects, the Keithley measurements show that in most cases (particularly when the scan rate was slow), the continuous system effectively measured IRs that were somewhat higher than 1 MΩ-100 m.

2.5 Environmental Data

2.5.1 Thermal Exposure Data

The temperatures and air flow rates to each chamber are given in Appendix B. The pressure in each chamber was maintained slightly above ambient to prevent water leakage into the chamber. The pressure was not continuously recorded nor controlled. With Albuquerque's altitude reducing ambient pressure by about 20% from sea level conditions, the positive gage pressure in the test chamber resulted in an actual absolute pressure close to ambient pressure at sea level.

2.5.2 Radiation Exposure Data

The radiation dose rates that the complete cable samples were exposed to are given in Table 7. Similar data for the small cable samples and the tensile samples may be found in Appendix B. As a result of test chamber rotations (the 6- and 9-month chambers were rotated half way through the exposures), the radiation aging data in Appendix B include two dose rates for some samples. The radiation exposure data includes shielding effects caused by the large number of cables in the sample baskets. It should be noted that the actual total doses were lower than the nominal desired values primarily because of shielding effects and radiation gradients in the test chambers. The estimated uncertainty in the radiation aging exposure data is ±20%.

2.5.3 Accident Radiation Exposure

The accident radiation exposure followed the aging exposure. The dose rates to the complete cable samples during the accident radiation exposures are given in Table 7, along with the total integrated dose to the complete cables. Similar data for the small cable samples and the tensile samples may be found in Appendix B. The estimated uncertainty in the accident exposure data is ±10%. The accident radiation exposure time was 209 hours for AT3, 193 hours for AT6, and 192.5 hours for AT9. Different times were used for each exposure to account for radioactive source decay.

2.5.4 Loss-of-Coolant Accident Simulation Environmental Data

The temperature and pressure profiles during AT3 are shown in Figures 10-11. The temperature and pressure profiles during AT6 are shown in Figures 12-13. The temperature and pressure profiles during AT9 are shown in Figures 14-15. As these figures demonstrate, all of the accident test profiles were very similar. The temperatures during the transients to 171°C are given in Table B-5 in Appendix B.

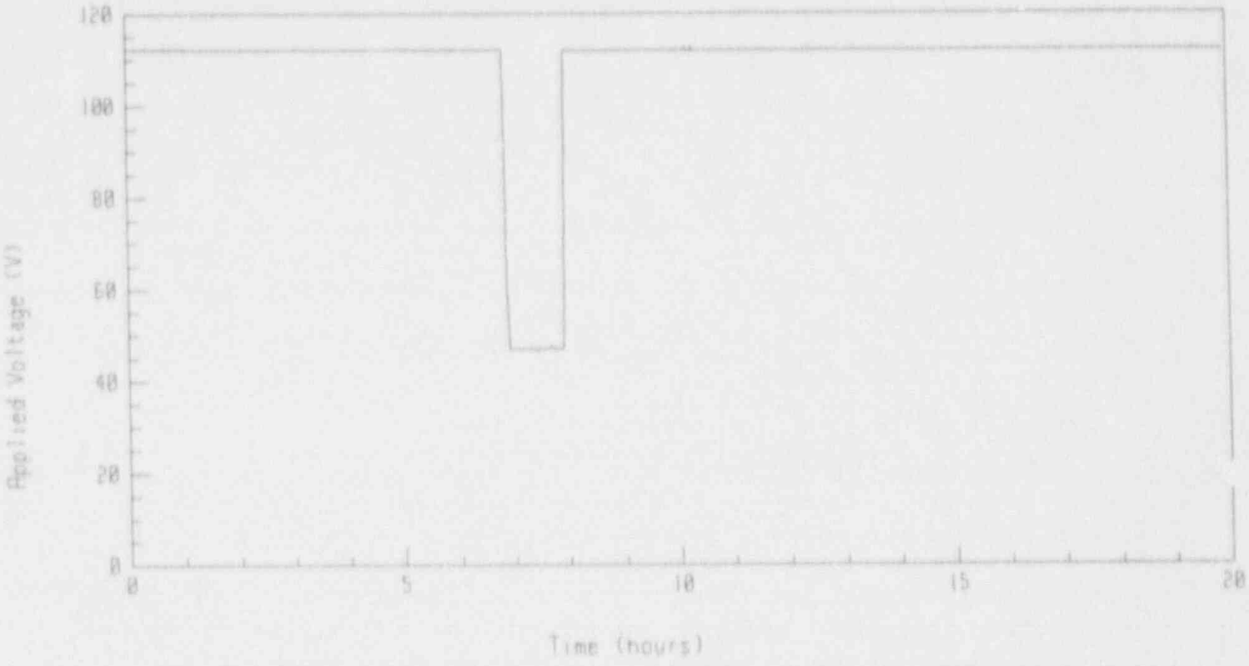

Figure 6 Applied Voltage for the First 20 Hours of AT3

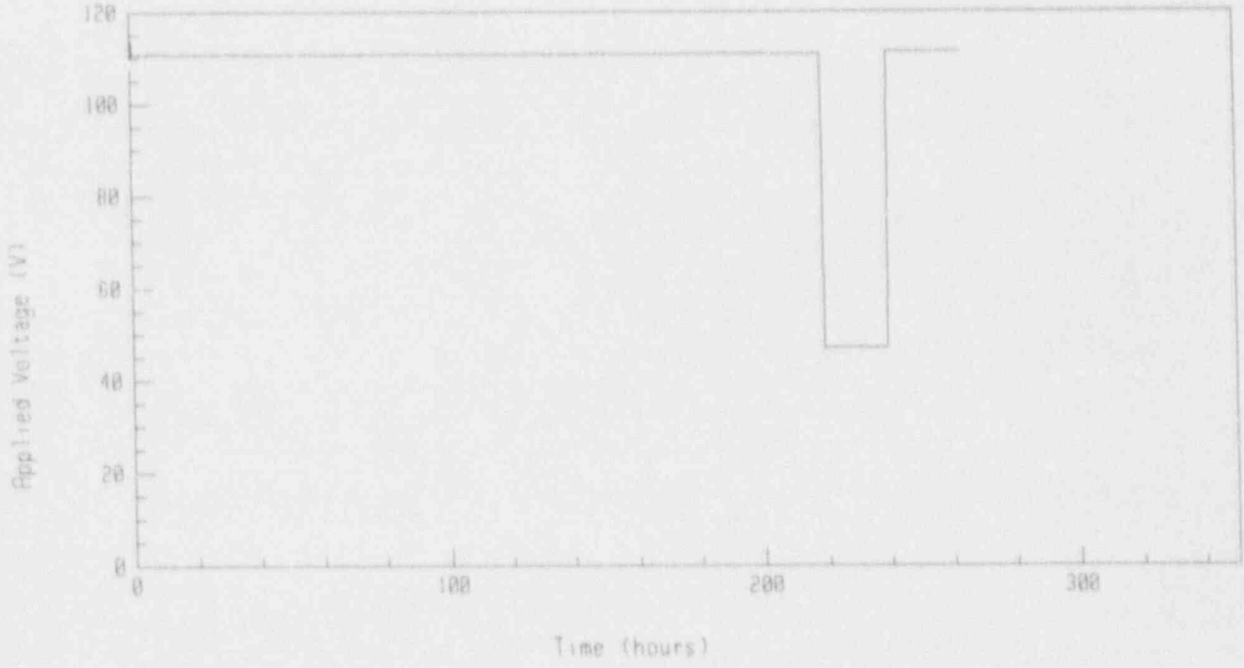

Figure 7 Applied Voltage During AT6

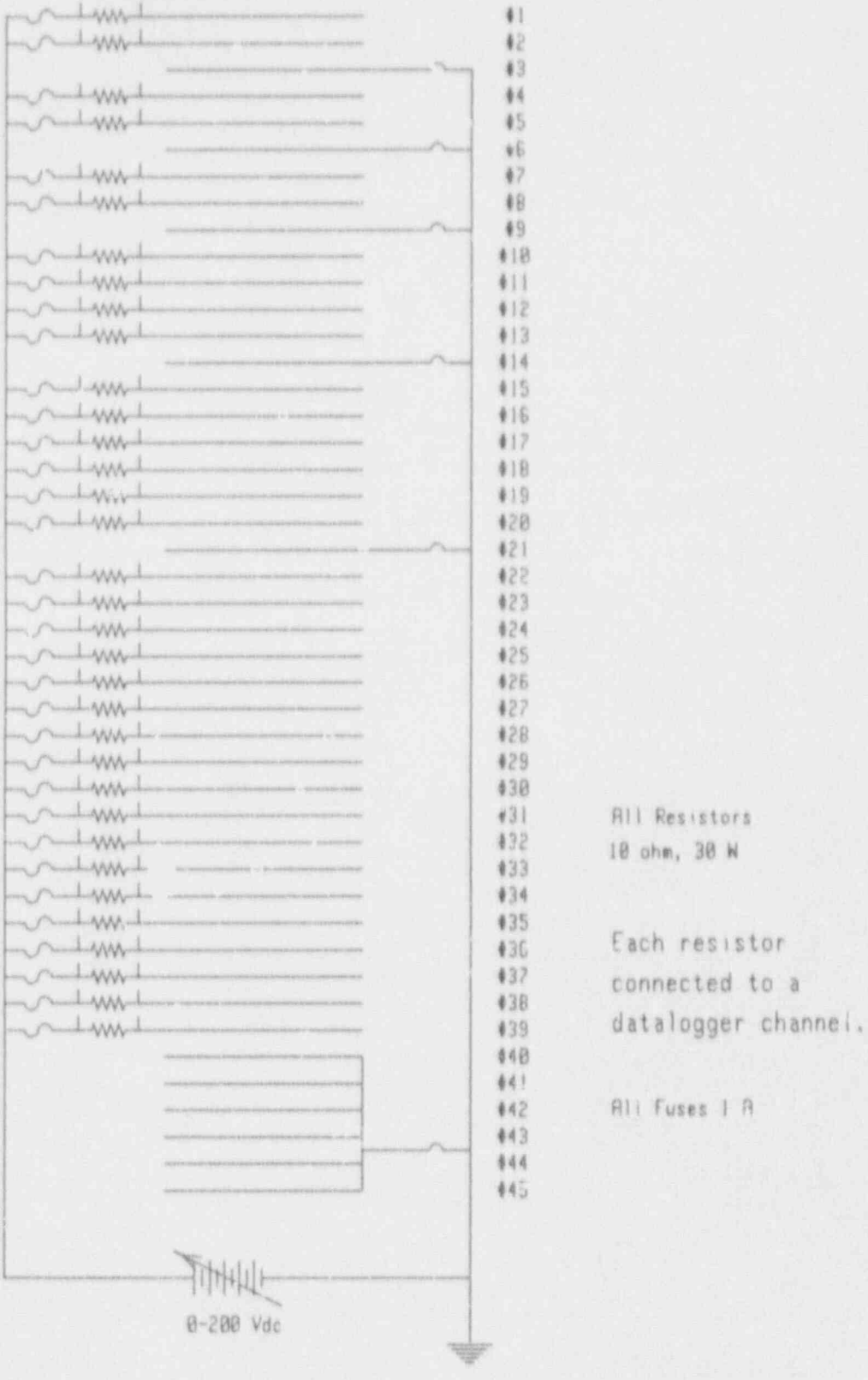

Figure 8 Circuitry Used to Monitor IRs During AT3 and AT6

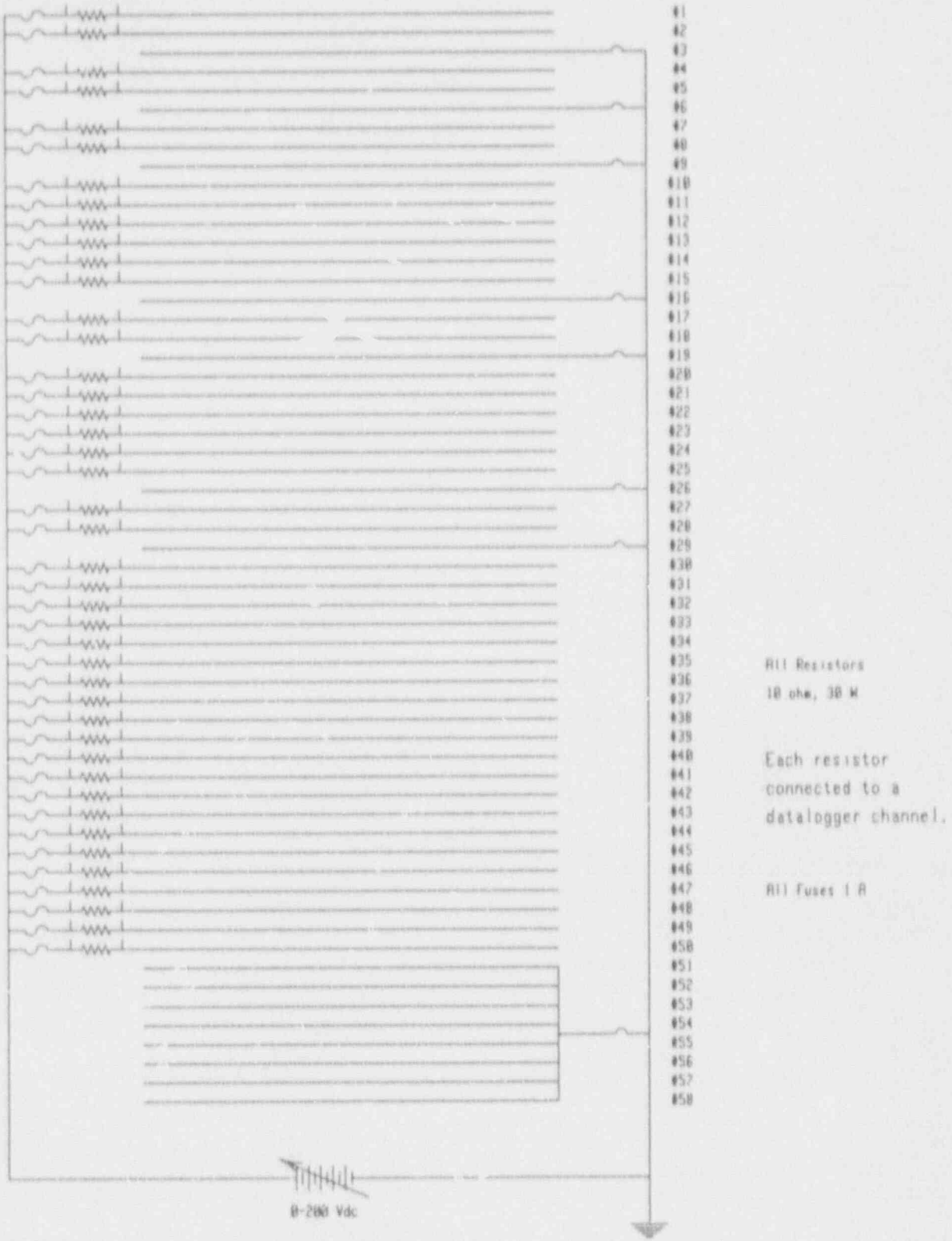

Figure 9 Circuitry Used to Monitor IRs During AT9

Table 7 Exposure Data for Complete Cables

Conductors	Aging Dose Rate (Gy/hr) Min	Avg	Max	Aging Dose (kGy) Avg	Accident Dose Rate (Gy/hr) Avg	Total Dose (kGy) Min	Avg	Max	
Cables Aged for 3 Months									
1-3	28	72	120	160	5000	1110	1190	1300	Brand Rex
12-14	34	78	130	170	5400	1210	1290	1400	Rockbestos
19-21	31	75	120	160	4600	1050	1130	1240	Polyset
27	33	77	130	170	5400	1210	1290	1400	Raychem
28	33	77	130	170	5400	1220	1300	1410	Raychem
Cables Aged for 6 Months									
1-3	25	62	110	280	5200	1220	1280	1330	Brand Rex
12-14	27	64	110	290	5700	1330	1390	1430	Rockbestos
19-21	25	62	110	280	5100	1190	1250	1300	Polyset
27	26	64	110	290	5600	1310	1360	1410	Raychem
28	27	64	110	290	5700	1320	1380	1430	Raychem
Cables Aged for 9 Months									
1-3	20	68	120	450	4200	1250	1270	1300	Brand Rex
14-16	35	84	140	560	5700	1640	1660	1690	Rockbestos
17-19	35	84	140	560	5600	1630	1650	1670	Rockbestos
24-26	31	80	140	530	4700	1410	1430	1460	Polyset
27-29	29	77	130	520	4200	1310	1330	1360	Polyset
35	30	78	130	520	5200	1500	1520	1550	Raychem
36	31	80	140	530	5400	1550	1560	1590	Raychem
37	32	81	140	540	5500	1580	1600	1630	Raychem

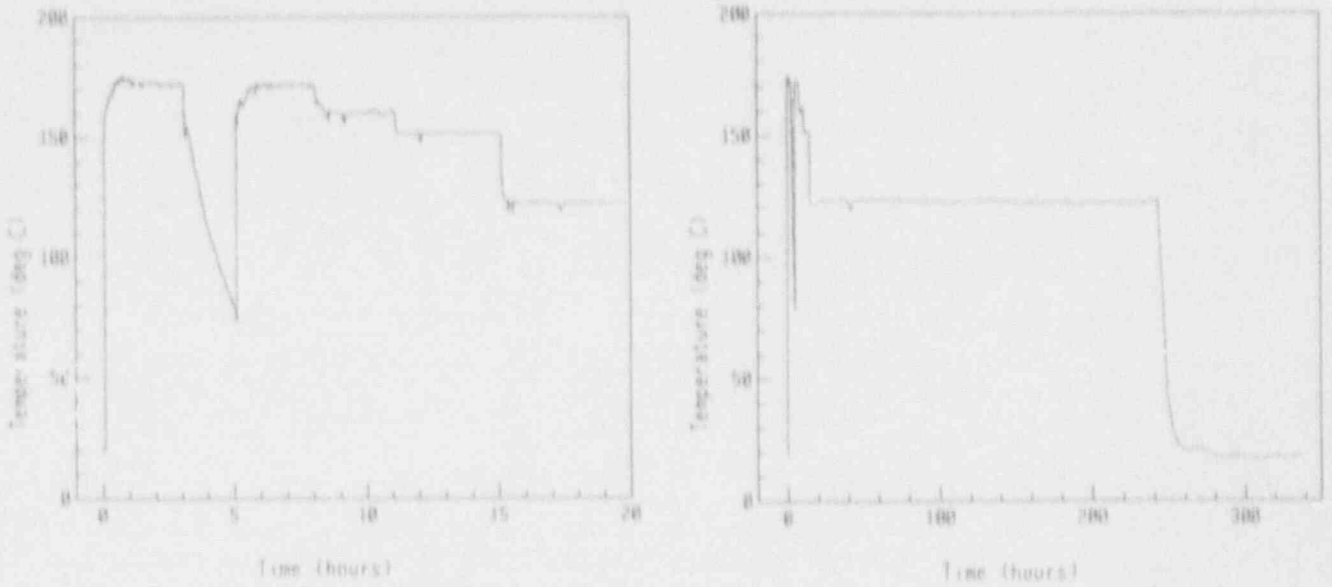

Figure 10 Temperature Profile During AT3

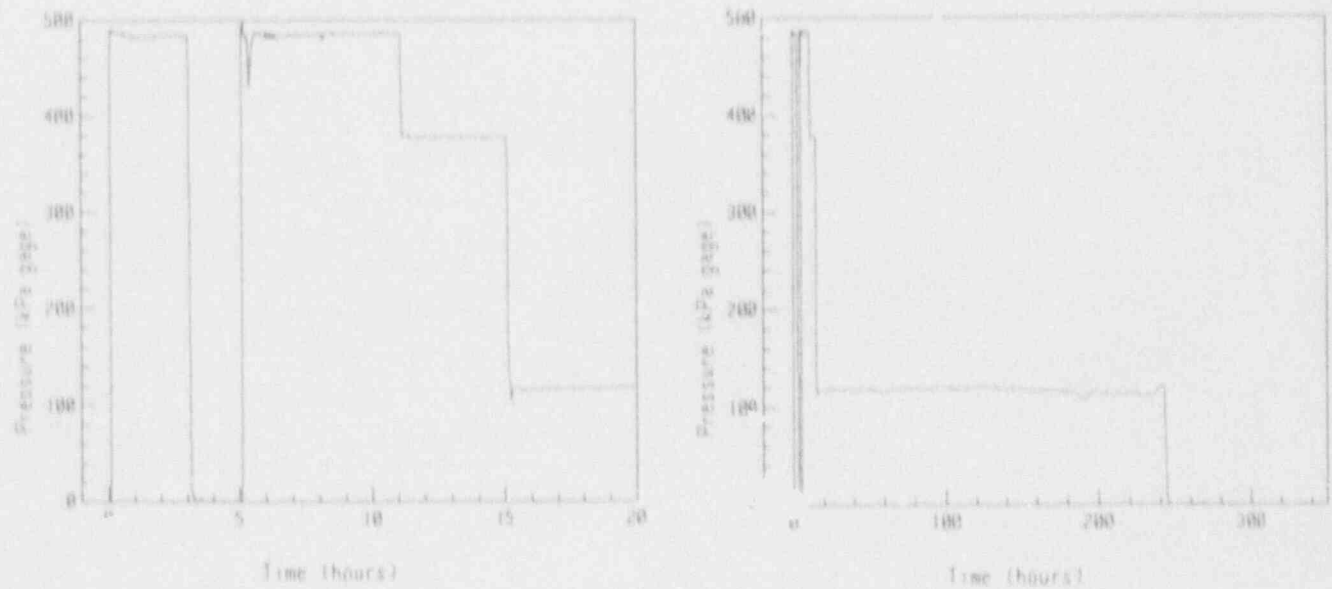

Figure 11 Pressure Profile During AT3

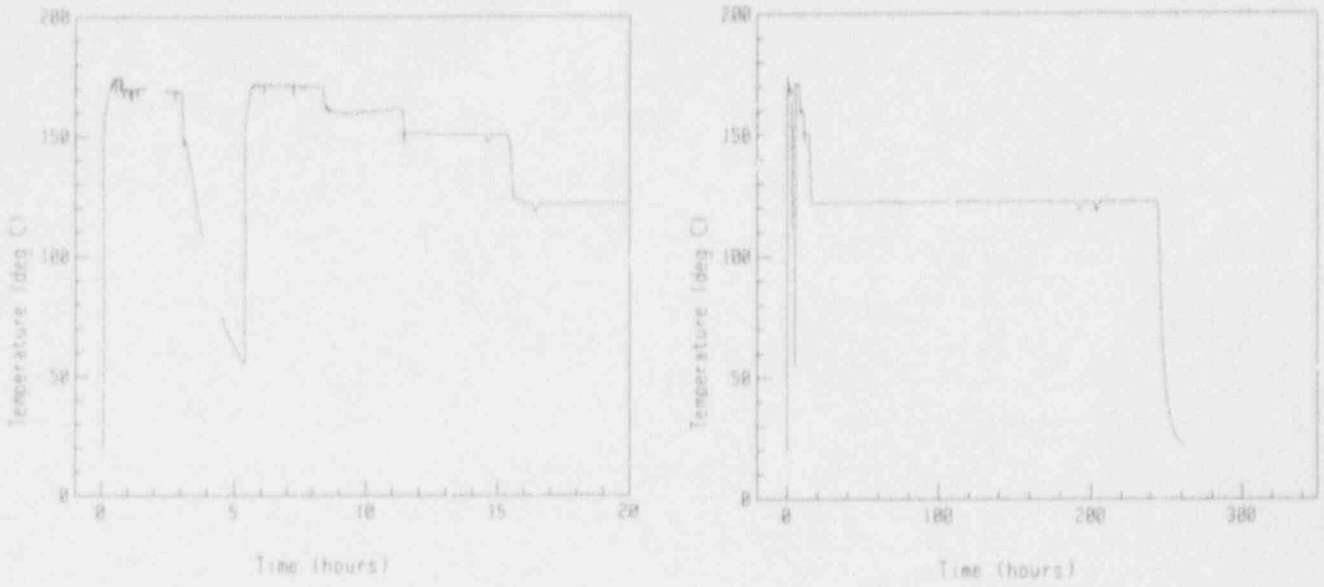

Figure 12 Temperature Profile During AT6

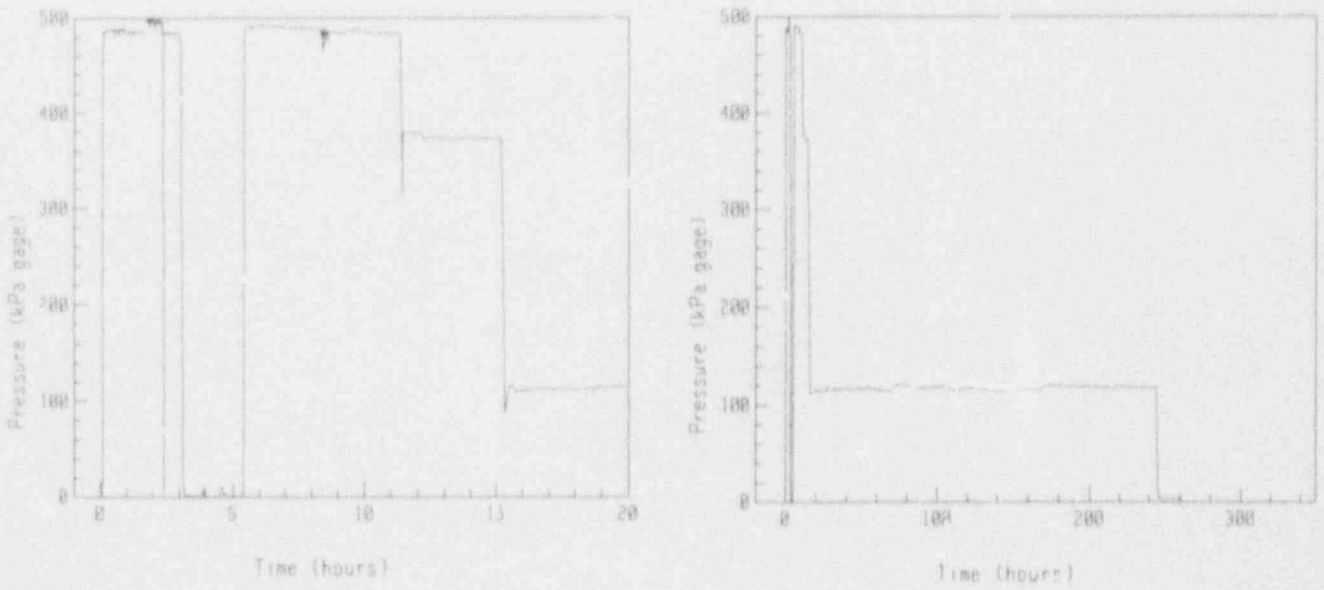

Figure 13 Pressure Profile During AT6

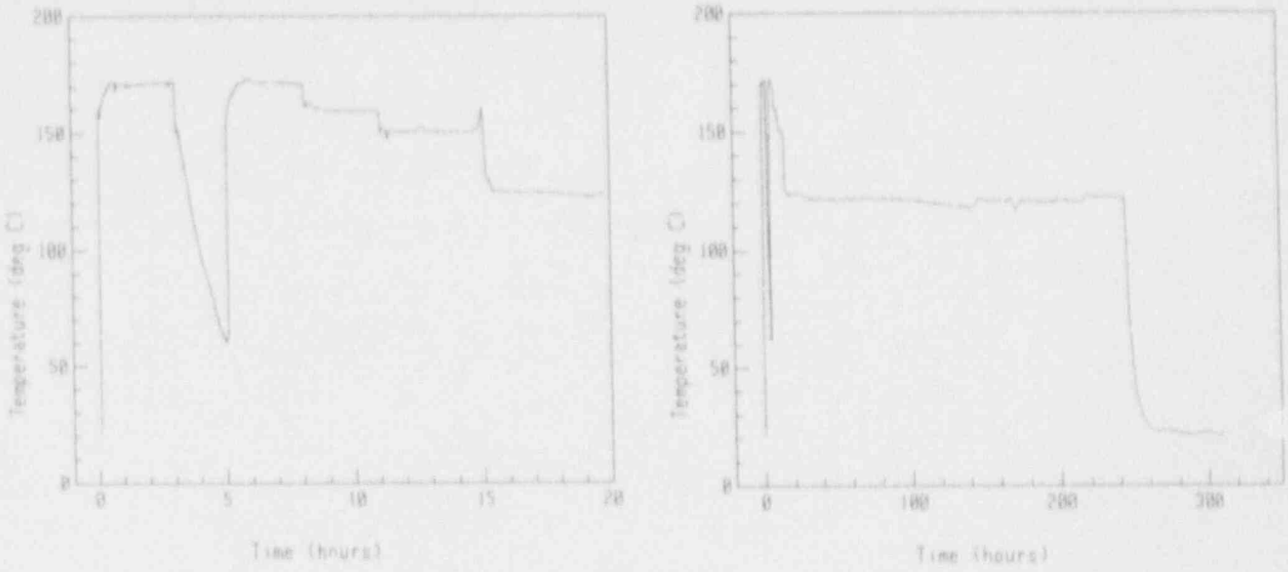

Figure 14 Temperature Profile During AT9

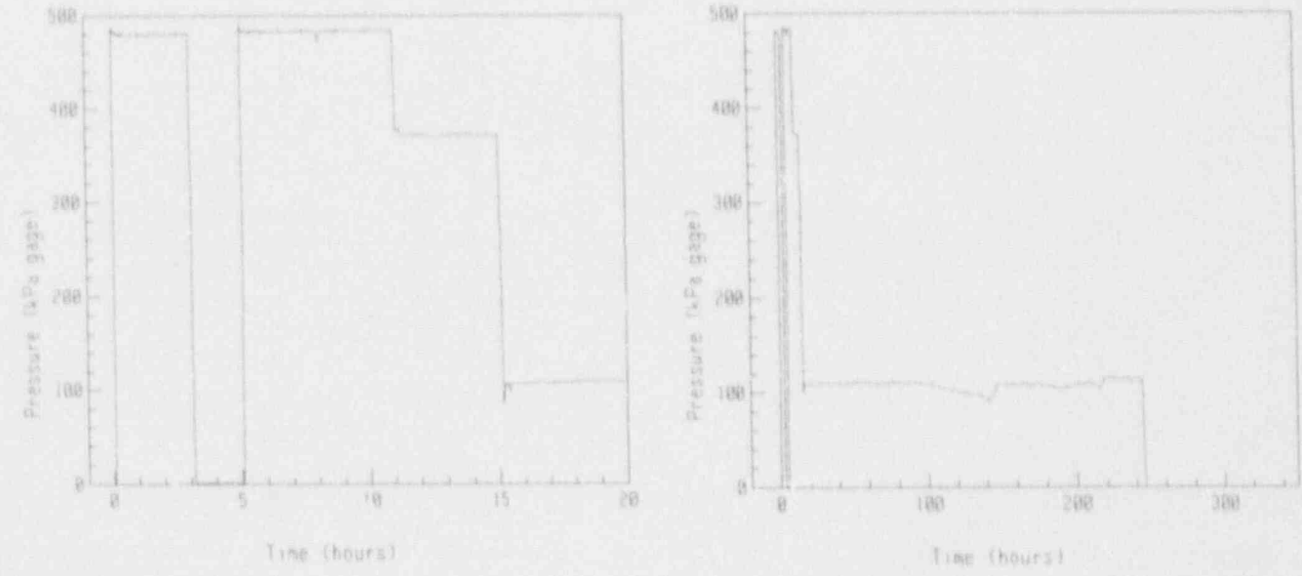

Figure 15 Pressure Profile During AT9

3.0 CONDITION MONITORING TEST DATA AND RESULTS

Plots of test data from the different condition monitoring measurements are presented in this section and the referenced appendices. Because different parts of each complete cable were exposed to different total doses (due to spatial dose rate variations in the test chambers), there was no unique total dose for the complete cables when the electrical properties were measured. Thus, electrical property data is plotted against months of exposure. Mechanical property data, on the other hand, is plotted against total radiation dose since the small aged samples had unique total doses. Because of radiation gradients in the test chambers, equal total dose does not necessarily imply an equal amount of simultaneous thermal aging, although it does to a first approximation. Plots of mechanical properties versus aging time are similar to, but not as consistent as the plots versus radiation dose, tending to indicate that radiation degradation was probably dominant over thermal aging for most of the materials tested under our simultaneous aging conditions. In the mechanical property plots, data from the aging portion of the exposure is coupled with data for the aging plus accident radiation exposures. The data below 600 kGy is from the aging exposures. The data above 600 kGy is from the aging plus accident radiation exposures, including, in many cases, data from unaged samples that were exposed to accident radiation only. Unaged samples that were exposed to accident radiation only give a data point at about 800-1000 kGy.

3.1 Insulation Resistance During Aging and Accident Radiation

Insulation resistance measurements were performed prior to the combined thermal and radiation aging; at one-month intervals during aging; after aging, but before accident radiation; and after accident radiation. Plots of the IR data during aging at 50 V, 100 V, and 250 V and of the PI data during aging at 250 V are given in Appendix C. The plots in Appendix C show the averages and one standard deviation range (shown as error bars about each point) of the cables from the three test chambers. The standard deviation is the directly calculated standard deviation of the data, not the standard deviation of the mean. It should be recognized that standard deviations are of somewhat limited value when only two or three samples exist. However, the standard deviation bands do give some idea of the range of the measurements for different samples. The IR is calculated on a 100-m basis, with only the length of the cable inside the test chamber considered in the calculation. This is a very good assumption for measurements performed at the aging temperature, since the cable inside the chamber dominates the measurement. However, for ambient temperature measurements, the length of cable outside the chamber may have a significant impact on the measurement. The discussion that follows will focus on the measurements performed at the aging temperature. The IR plots in Appendix C include the data from the ambient temperature measurements.

In the plots of Appendix C, data from the cables in the three different test chambers are plotted together. Although the same amount of aging time in the different chambers does not produce exactly the same conditions, the variation is not significant for these plots. The data generally show excellent agreement for cables that were aged in different test chambers. The PI that was used for the plots in Appendix C is the ratio of the IR at 5 min to the IR at 30 s.

The IRs of the Brand Rex cables (Figures C1-C3) at the aging temperature were largely constant throughout aging, but they did decrease slightly during the first four months of aging and increase slightly during the last five months of aging. The Rockbestos Firewall III cables (Figures C4-C6) had IR decreases of 2 orders of magnitude at all voltage levels during the first 3-4 months of aging. However, after 4 months, the IRs began increasing

again and recovered almost an order of magnitude over the last 6 months. The behaviors of the Brand Rex and Rockbestos IRs were somewhat similar, but the change in IR of the Rockbestos cable was much more significant. The IR of the Polyset cables (Figures C7-C9) increased by about a factor of two during the entire aging, while the IR of the Polyset jacket (Figures C10-C12) was constant until about 7 months of aging, where it began an order of magnitude decrease. The IR of the Raychem cables (Figures C13-C15) at the aging temperature was essentially constant throughout aging.

The PI of the Brand Rex cable (Figure C16) dropped from 1.8 to 1.2 during the first 4 months of aging, but then increased back to about 1.5. The PI of the Rockbestos cable (Figure C17) had a trend very similar to that of the Brand Rex, with the PI decreasing from 1.6 to 1.0 during the first 3 months of aging, followed by an increase back to 1.2. The PI of the Polyset cable (Figure C18) increased slightly from 1.8 to 2.0, but then decreased slightly back to about 1.9. The Polyset jacket (Figure C19) had a fairly constant PI of 1.06 during the first 4 months of aging, but then began a consistent decrease to 1.0 at the end of the 9-month exposure. Because of the high IRs of the Raychem cables, the PIs (Figure C20) were more difficult to measure and they had much more variability than the PIs of other cables. Therefore, no clear trends could be established.

The last part of Appendix C presents the results of some additional IR and PI measurements that were not included in the figures of Appendix C. These include measurements of IR and PI that were performed after accident radiation and PI measurements that were performed at ambient temperature.

3.2 Capacitance and Dissipation Factor During Aging

Capacitance and dissipation factor were measured as described in Appendix A. The measurements were performed monthly on the cables in the 6- and 9-month test chambers and covered a frequency range from about 0.3 Hz-500 kHz. In this report, only the data from the cables contained in the 9-month chamber will be presented in detail. However, limited data from the 6-month chamber will be discussed as appropriate. Figures 16 and 17 show sample capacitance and dissipation factor data plotted against frequency with months of aging as a parameter. Only five selected monthly intervals are plotted to prevent the plots from becoming unreadable. In Appendix D, plots of capacitance and dissipation factor are given for each individual conductor versus amount of aging, with frequency as a parameter. The five frequencies selected for the plots were chosen in the lower frequency range, where the greatest changes were typically observed with aging (when notable changes did occur). Plots that are shown in this section use the averages of several tested conductors of the same cable type.

The capacitance of the Brand Rex conductors (Figures D1-D3) had a slight increase during the first 2 months of aging and was essentially constant beyond that point. The changes were not highly dependent on frequency over a wide frequency range. The baseline capacitance of the Brand Rex cables varied by about 25% over the frequency range tested. Figure 18 shows the average capacitance of all of the Brand Rex conductors in the 6-month chamber. The data in Figure 18 compares very well with Figures D1-D3. The capacitance of the Rockbestos conductors (Figures D4-D9) increased by about 30% with aging over much of the frequency range tested. The capacitance was also largely independent of frequency at all aging times. As with the Brand Rex cable, capacitance data from the cables in the 6-month chamber matched that in Figures D4-D9 very well. The capacitance of the Dekoron Polyset conductors (Figures D10-D15) did not change significantly with either aging or frequency. The capacitance of the Raychem conductors (Figures D16-D18) had no change with aging. There was a slight dependence on frequency, with the capacitance decreasing at

increased frequency. Data from the cables in the 6-month chamber gave results that were very similar to that from the 9-month chamber for both the Polyset and Raychem cables.

The dissipation factor of the Brand Rex conductors (Figures D19-D21) dropped from about 0.07 to 0.03 at 1.52 Hz, with most of the change during the first 3 months of aging. Dissipation factor data from the 6-month chamber cables did not show as great a change,

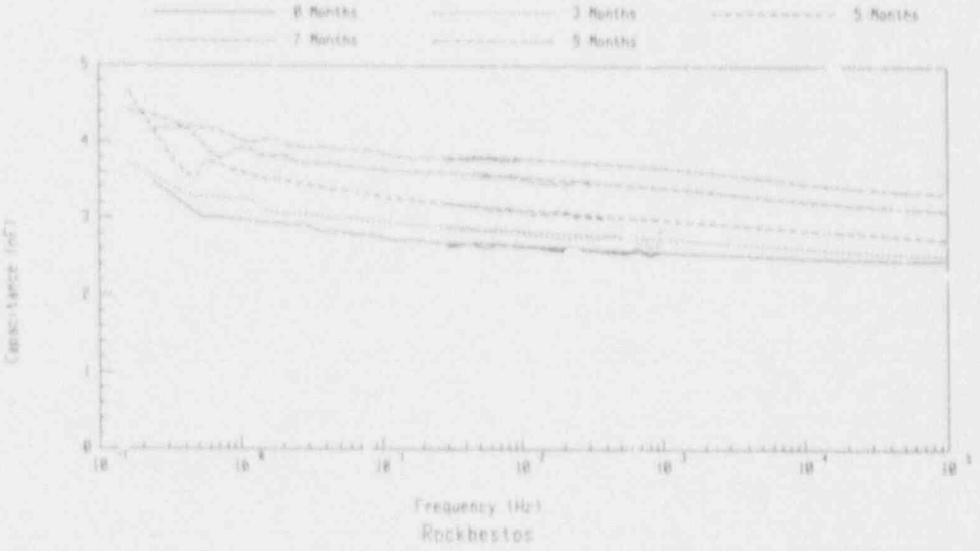

Figure 16 Capacitance Versus Frequency for Rockbestos Conductor #14

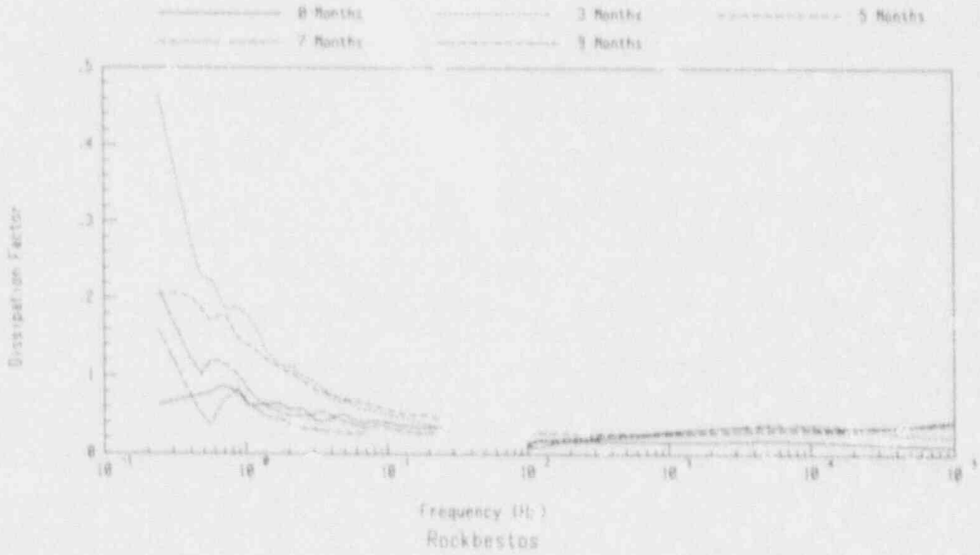

Figure 17 Dissipation Factor Versus Frequency for Rockbestos Conductor #14

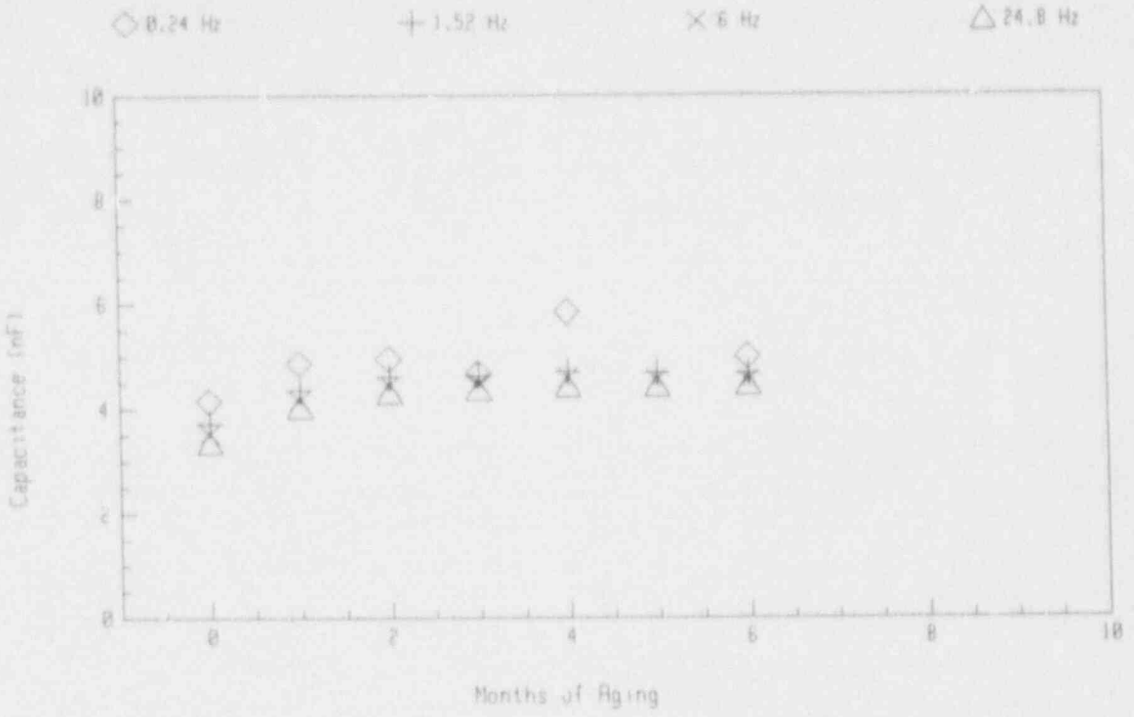

Figure 18 Average Capacitance of Brand Rex Conductors During Aging in the 6-month Chamber

decreasing from 0.06 to 0.05 at 1.52 Hz during the first 3 months of aging. The 0.24 Hz data for the Brand Rex cables was quite variable, with no consistent trend. Figure 19 shows the Brand Rex dissipation factor plotted against frequency from the conductors in the 9-month chamber. Figure 20 gives the same plot from the conductors in the 6-month chamber. A very significant dissipation factor increase is noted between the baseline and 3-month measurements at frequencies from 1-100 kHz for the conductors from both the 6- and 9-month chambers. This change is in contrast to the decreases in dissipation factor that occurred at lower frequencies. As shown in Figures 19 and 20, a significant part of the increase at frequencies between 1 and 100 kHz occurred during the first month of aging.

The dissipation factor at 0.24 Hz of the Rockbestos conductors (Figures D22-D27) from the 9-month chamber tended to show a peak at 3-5 months of aging. This peak occurred at nearly the same time that the minimum IRs of the Rockbestos conductors occurred (see Figures C4-C6). At other frequencies, peaks with aging also occurred at about 3-5 months of aging. For comparison, the average dissipation factor at 0.24 Hz for the Rockbestos conductors in the 6-month test chamber was 0.46 after 3 months of aging, 0.86 after 4 months of aging, and 0.18 after 5 months of aging. These values compare well with the values from the 9-month chamber shown in Appendix D. The dissipation factors of the Dekoron conductors (Figures D28-D33) and the Raychem conductors (Figures D34-D36) did not show any consistent trends with aging.

3.3 Elongation and Tensile Strength During Aging

Plots of T/T_0, tensile strength normalized to unaged values, and of e/e_0, absolute elongation relative to the unaged values, are shown in Appendix E. In the plots, tensile

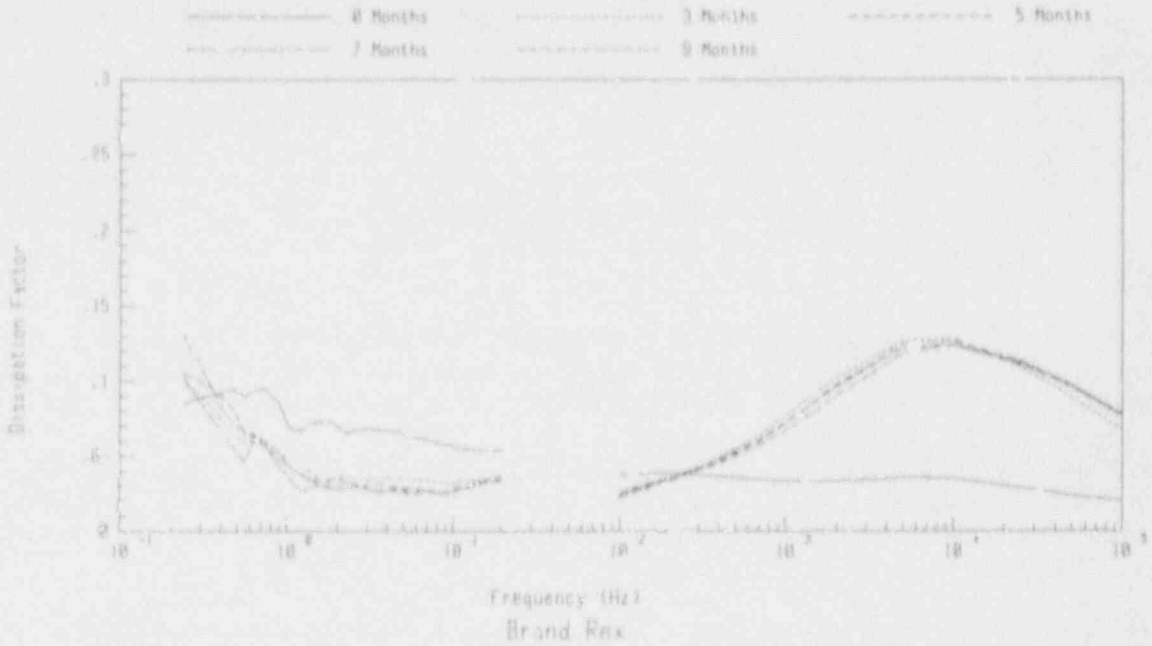

Figure 19 Average Dissipation Factor Versus Frequency for Brand Rex Conductors in 9-month Chamber

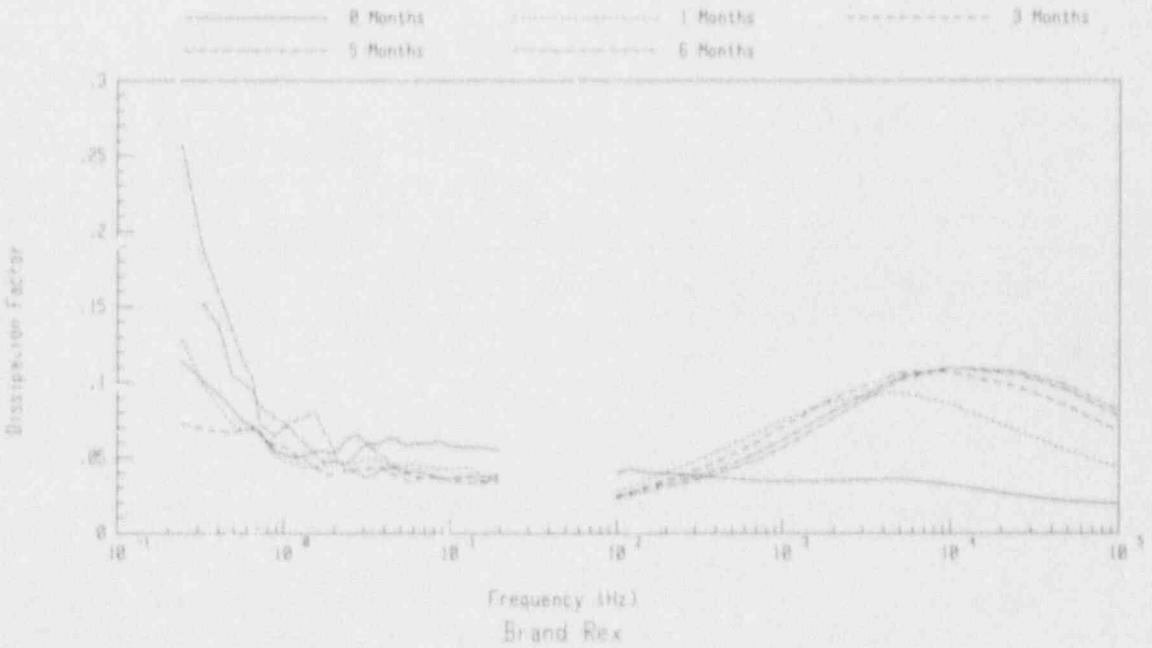

Figure 20 Average Dissipation Factor Versus Frequency for Brand Rex Conductors in 6-month Chamber

strength is defined as the force at break of the specimen divided by the original cross-sectional area of the unaged specimen. Although the force at break is also usually the maximum force applied to the specimen, such is not necessarily the case. Since the unaged area of a given cable type is nominally a constant, T/T_0 reduces to the ratio of the force required to break an aged specimen to the force required to break an unaged specimen. Thus, the precise cross-sectional area is only necessary to provide absolute scaling for the plots. For reference, the tensile strength of the unaged specimens is noted on each plot. Similarly, the elongation at break of unaged specimens, e_0, is noted on the e/e_0 plots.

In Appendix E, all plots are shown versus total radiation dose. Where a tensile strength is shown on the plots as 0%, this indicates that the sample broke before reaching 10% elongation, and therefore, no tensile strength measurement was obtained. It should also be recalled that the resolution of the elongation measurements was 10% absolute. Thus, measurements at 0-20% elongation have somewhat more uncertainty than measurements of higher elongations. Note that unmeasurable elongation, especially of the jacket material, does not imply that a cable is no longer functional. Results from accident tests of the cables are discussed in Section 4.0.

Figure E-1 shows that the elongation of the Brand Rex insulation decreased to 20% of its initial value after a total aging dose of 400 kGy. The accident radiation caused a further decrease to below 10% of initial elongation. Interestingly, three unaged samples that were exposed only to accident radiation broke at elongations below 10%. Figure E-2 shows that tensile strength of the Brand Rex insulation increased by about 30% with a total aging dose of 400 kGy. The accident radiation exposure resulted in mixed behavior with a significant decrease in tensile strength after the 6- and 9-month aging exposures, but very little decrease after the 3-month exposure. Tensile strength of the samples with accident radiation only could not be obtained because of the low elongation of those specimens.

Figure E-3 shows that the elongation of the Brand Rex jacket decreased to 0% of its initial value after a total aging dose of 200 kGy. Following accident radiation, all samples except those that had not been aged were down to 0% elongation. The samples that received only accident radiation had their elongations fall to about 30% of their initial values. Figure E-4 shows that the tensile strength of the Brand Rex jacket decreased to 10% of its initial value after 200 kGy. Beyond that point, tensile strength could not be measured because the elongation was below 10%. The only tensile strength that could be measured after the accident radiation exposure was for the unaged cables, which showed almost no change as a result of the accident radiation exposure.

Figure E-5 shows that the elongation of the Rockbestos insulation first increased by about 10% of its initial value, then fell to 25% of its initial value after 400 kGy of aging exposure. In all cases, no elongations were measurable after the accident irradiations. The initial increase in elongation is probably a result of radiation causing additional curing (i.e., crosslinking) of the XLPO insulation. Tensile strength of the Rockbestos insulation, as shown in Figure E-6, remained essentially constant throughout the aging exposures. After the accident radiations, the tensile strength could not be measured.

Figure E-7 shows that the relative elongation of the Rockbestos neoprene jacket fell to 0% within the first 100 kGy of aging exposure. Because thermal aging is expected to dominate the degradation of neoprene at our conditions [14], the data from Figure E-7 should not be used to make assessments of the generic radiation damage threshold of neoprene. The tensile strength of neoprene, as shown in Figure E-8, also decreased with aging exposure, but only a few valid data points could be obtained because the elongation fell below 10% very quickly.

Figure E-9 shows that the elongation of the Dekoron insulation fell to 40% of its original value after 400 kGy of exposure. The accident radiation caused further decreases in elongation, down to about 10% of the initial value when coupled with aging exposures. The tensile strength of the Dekoron insulation, shown in Figure E-10, had very little change with aging or accident radiation exposure.

Figure E-11 shows that the elongation of the Dekoron CSPE jacket fell to 3% of its initial value after 400 kGy of aging exposure. The accident exposure caused a further, consistent decrease in elongation in each case tested. Figure E-12 shows that the tensile strength of the Dekoron CSPE jacket decreased to 70% of its initial value by 400 kGy. The final tensile strength measurement, at about 400 kGy, was somewhat variable, but notably lower than the previous measurements. The accident radiation exposure caused mixed results. The unaged jacket and the jacket aged for 3 months had little change with accident radiation. The jacket aged for 6 months had a fairly significant decrease in tensile strength after the accident radiation exposure, but the results displayed some scatter. The data points at 400 kGy and at 1100 kGy indicate the possibility of a threshold effect, above which the tensile strength decreases significantly.

Figure E-13 shows that elongation of the Raychem insulation decreased to about 3% of its initial value after 400 kGy of aging exposure. After all accident irradiations, no elongations were measurable. Tensile strength of the Raychem insulation, as shown in Figure E-14, first decreased to 85% of its initial value by 100 kGy of aging exposure, then increased to 120% of its initial value by 400 kGy of aging exposure. After the accident radiations, the tensile strength could not be measured because the elongation was below 10%.

In summary, elongation consistently decreases with aging (except for the early exposure of the Rockbestos insulation). Based on the data in Appendix E, Table 8 gives estimates of the total dose (under our simultaneous aging conditions) to retention of 75%, 50%, 25%, and 10% of initial elongation of each insulation and jacket material, except for the Rockbestos neoprene jacket. The neoprene is not included because, under the conditions of our test, thermal aging dominates the degradation. The data in Table 8 and in Appendix E indicate that elongation is generally a fairly sensitive measure of the amount of aging up to the total dose where very little residual elongation remains. When using the data in Appendix D or Table 8 to compare different cable materials, it is important to note baseline elongation differences. For example, Rockbestos XLPE insulation at $e/e_0 = 0.25$ corresponds to an elongation of 60%, while Raychem XLPE insulation at $e/e_0 = 0.25$ corresponds to an elongation of 130%.

Tensile strength showed some change with aging for the Brand Rex and Raychem XLPOs, but almost no change for the Rockbestos and Dekoron materials. Tensile strength of the Rockbestos jacket showed a rapid decrease, but only a few points could be measured because the elongation quickly fell below 10%. The Brand Rex jacket had a fairly consistent and significant decrease in tensile strength, while the Dekoron jacket had only a slight decrease in tensile strength.

3.4 Modulus During Aging Using the EPRI Cable Indenter

Plots of indenter modulus relative to the initial value (M/M_0) are presented in Appendix F as a function of total radiation dose. For reference, the baseline modulus, M_0, is shown on the plots.

The indenter modulus of the Brand Rex insulation (Figure F-1), the Rockbestos insulation (Figure F-3), the Dekoron insulation (Figure F-5), and the Raychem insulation (Figure F-7) all had somewhat inconsistent behavior, although an increase of

perhaps 50% in modulus is possibly indicated. The Dekoron and Raychem insulations had the more consistent behavior, especially the Raychem insulation after accident radiations.

Table 8 Estimated Total Doses to Retention of Various Elongations

Material	ε_0	Total Dose (kGy) to $\varepsilon/\varepsilon_0$ of *			
		75%	50%	25%	10%
Brand Rex XLPE	320%	80	140	300	**
Rockbestos XLPE	240%	200	300	400	**
Dekoron XLPO	350%	100	230	**	**
Raychem XLPE	520%	50	80	100	230
Brand Rex CSPE Jacket	330%	20	80	100	140
Dekoron CSPE Jacket	360%	20	70	200	280

* Total dose with simultaneous thermal aging at 95-100°C.
** These material never reached the indicated $\varepsilon/\varepsilon_0$ during aging.

Figure F-2 shows the indenter modulus of the Brand Rex CSPE jacket. This material shows a strong upward trend with aging, especially when the total dose exceeds 200 kGy. It is interesting to note that 200 kGy is just about the point where the elongation fell to near 0%. The accident radiation exposures caused the indenter modulus to increase in all cases.

Figure F-4 shows the indenter modulus for the Rockbestos neoprene jacket. A strong upward trend is evident, with the indenter modulus reaching 2000% of its original value at about 400 kGy. Note that elongation measurements (see Figure E-7) showed no change on this material beyond a total radiation dose of about 50 kGy (the material was below 10% elongation). It should be recalled that at our simultaneous aging conditions, neoprene degradation is dominated by thermal aging rather than radiation aging. Thus, the trends during the aging portion of the exposure should be interpreted as applying more to thermal aging, rather than radiation aging. The accident radiation exposure caused mixed results, with the modulus increasing for the materials that were unaged or aged for 6 months and the modulus decreasing for the materials that were aged for 3 or 9 months.

Figure F-6 shows the indenter modulus of the Dekoron CSPE jacket. The initial trend is upward but inconsistent. At about 400 kGy, a sharp upward trend occurs. Note that the elongation was essentially at 0% by 400 kGy (see Figure E-11), just where the indenter modulus began its most significant changes. The accident radiation exposure caused increases in indenter modulus under all test conditions.

3.5 Hardness During Aging

Plots of hardness relative to the initial value (H/H_0) are presented in the second part of Appendix F as a function of total radiation dose. For reference, the baseline hardness, H_0, is shown on the plots.

The hardness of the XLPO insulations are not presented because they were all too hard (Shore "A2" readings of 88-96) prior to aging to detect any significant changes with the tester we were using (effective upper limit of our tester was about 92). Hardness of the Brand Rex jacket (Figure F-8) increased by 75% during aging, hardness of the Rockbestos jacket (Figure F-9) increased by 25% during aging, and hardness of the Dekoron jacket (Figure F-10) increased by 15% during aging. In each case, the upward trends were quite consistent. It is important to note that some of the measurements were close to, or beyond, the effective upper limit of the tester range. Readings above 92 are not included on the plots. Hence, although the plots in Appendix F do not reflect it, the hardness may continue to increase beyond what is shown on the plots. An attempt at using a Shore "D2" durometer that could measure harder materials caused permanent damage to a sample that was tested, and hence no additional testing was conducted.

3.6 Bulk Density During Aging

Plots of density relative to the initial value (D/D_0) are presented in Appendix G as a function of total radiation dose. For reference, the baseline density, D_0, is shown on the plots. Note that small changes in density are readily detectable, so that a change of only 1-2% can be significant.

The density of Brand Rex insulation (Figure G-1) had a consistent increase to 1.5% above the initial value. The accident radiation generally increased the density slightly, but after the 9-month aging exposure, the density decreased slightly as a result of the accident radiation exposure. The density of Brand Rex CSPE jacket (Figure G-2) first increased until the total dose reached 100 kGy, then decreased during the remainder of the aging exposure. The accident radiation exposure did not produce any notable effects on the density.

The density of Rockbestos insulation (Figure G-3) changed significantly during aging, increasing to 3.5% above the baseline value. For the conditions tested, accident radiation also caused increases in density. The density of the Rockbestos neoprene jacket was too high to be measured with our density gradient columns.

The density of Dekoron insulation (Figure G-4) did not change consistently with either aging or accident radiation exposures. However, the Dekoron CSPE jacket (Figure G-5) had a very consistent trend with aging, increasing by 3% over the 400 kGy exposure. The accident radiation exposure did not affect the density of the Dekoron jacket.

The density of Raychem insulation (Figure G-5) appeared to increase with aging, but the trend was somewhat inconsistent. The effects of the accident radiation exposure on density was mixed.

3.7 Modulus Profiles During Aging

Plots of modulus profiles are presented in Appendix H. In most cases, only baseline samples and samples that were aged for 9 months are included. The figures indicate which data is for the insulations and which data is for the jackets (see Figure 4). Each of the figures includes data for one pair of cable samples removed from the same 36-cm cable specimen. The center line of the plot represents the intersection of the two surfaces that were exposed to air during aging. A flat profile through a material is generally expected for unaged samples. A flat profile after aging (assuming a reasonable change in modulus from baseline conditions) generally indicates the absence of significant oxygen diffusion effects.

Oxygen diffusion effects occur when aging reactions use oxygen in the material more rapidly than it can be replenished through diffusion. In such cases, material further from

the oxygen supply (i.e., the ambient air) participates less fully in reactions involving oxygen, leading to non-uniform aging. Because aging generally increases the modulus of the materials used in this study, diffusion effects normally result in larger modulus increases at edges that have been exposed to oxygen. Oxygen diffusion effects generally increase with higher temperatures and with higher radiation dose rates. Also, when the modulus increases as the material ages, oxygen permeation through the material decreases, which can lead to diffusion effects only in the later stages of aging [15].

The more that oxygen diffusion effects can be eliminated in a test, the closer the test simulates natural aging conditions. Thus, in this section, we are concerned primarily with a simple evaluation of the shape of the profiles, although we will also consider changes in the magnitude of the modulus. It should be noted that oxygen diffusion effects may not be the only dose rate effect that a material exhibits. Thus, absence of diffusion effects does not necessarily imply the absence of all dose rate effects.

Figures H-1 through H-4 show modulus profiles for the Brand Rex cable. The baseline modulus is flat and consistent for both the insulation and jacket materials. After 3 months of aging, the jacket profile is still flat and the jacket modulus has doubled. After 6 months of aging, an oxygen diffusion profile has begun to appear in the jacket and after 9 months of aging, the profile has become more significant. Thus, oxygen diffusion effects have not been completely eliminated for this cable. By the end of aging, the average modulus in the jacket increased by a factor of about 100, with a factor of 2-5 gradient in the modulus. The jacket surface exposed to the ambient conditions had higher modulus increases than the jacket material that was next to the insulation, as is generally expected when oxygen diffusion effects are present.

The lack of diffusion effects after 3 months of aging suggests that a significant factor contributing to the diffusion effects later in aging is the decrease in oxygen permeation rate as the jacket hardens. The indenter modulus data suggests that significant hardening of the jacket begins in the range of 200 kGy total dose. Thus, 200 kGy is where diffusion effects might be expected to begin to appear. Because the total aging doses used in this study are significantly higher than those currently postulated for most nuclear power plant locations, diffusion effects that only occur later in aging may be less significant.

The small changes in modulus of the insulation make conclusions about possible diffusion effects in the insulation difficult. Once diffusion effects become significant in the jacket, however, they become much more probable in the insulation. Thus, some oxygen depletion effects may have occurred in the Brand Rex insulation, particularly at the higher aging doses.

Figures H-5 and H-6 show modulus profiles for the Rockbestos cable. The baseline modulus is reasonably flat and consistent for both the insulation and jacket materials. After 9 months of aging, the insulation modulus has only changed slightly. The jacket modulus has increased dramatically, but the profile is still essentially flat. Thus, oxygen diffusion effects appear to have been successfully eliminated for this cable. However, recent experience with modulus profiles for heat aged neoprene has indicated that diffusion profiles can appear during the earlier stages of aging, only to disappear when the jacket becomes extremely hard. The indenter modulus data suggests that significant hardening of the jacket began in the range of 100 kGy total dose. Thus, 100 kGy is where diffusion effects could have begun to appear, followed by the diffusion effects disappearing after the jacket became extremely hard. The scatter in the modulus data for the jacket can be attributed primarily to the high values that had to be measured. The average increase in jacket modulus was a factor of 770.

Because the absolute value of the insulation modulus did not change greatly, the sensitivity of the modulus to diffusion effects in the insulation is limited. With the high hardness of the neoprene jacket later in aging, however, the greatly reduced oxygen permeation rate may have largely prevented oxygen from reaching the insulation. Thus, at the higher aging doses, some oxygen depletion effects may have occurred in the Rockbestos insulation. Such effects would not be expected during typical natural aging conditions.

Figures H-7 and H-8 show modulus profiles for the Raychem cable. The baseline modulus is flat and consistent for the insulation. After 9 months of aging, the insulation modulus has only changed slightly, with the profile still being essentially flat. Thus, within the limits of the sensitivity of this method, no oxygen diffusion effects are evident. Note that because this cable has no jacket, diffusion effects in the insulation are much less likely than for jacketed cables.

Figures H-9 through H-12 show modulus profiles for the Dekoron Polyset cable. Figures H-10 and H-11 show profiles for only jacket materials. The baseline modulus is quite flat for both the insulation and jacket materials. After 9 months of aging, the insulation modulus has only changed slightly and is still essentially flat. The jacket modulus increased by a factor of 15, with greater changes at the inside edge (near the insulation). This is opposite from the effect that was observed for the Brand Rex cable. Figures H-10 and H-11 show the modulus of the jacket material after 246 kGy and 406 kGy, respectively. Both of these profiles are relatively flat, indicating that any nonuniform aging does not become significant until somewhere after 400 kGy. Note that the indenter modulus data suggests that the jacket begins hardening significantly at about 400 kGy. The lack of a flat profile through the material may be a result of oxygen diffusion effects that appear later in aging when the jacket has hardened, reducing the oxygen permeation rate. Alternatively, it may be a result of other effects, such as an initially nonuniform antioxidant profile in the jacket, which could cause the antioxidant to be depleted earlier at the inside edge of the jacket. In any case, the lack of a flat profile should not be significant for most applications because it occurs at such high total doses. The small changes in insulation modulus make conclusions about possible diffusion effects in the insulation difficult.

Defining the upper limits of test parameters (dose rate and temperature) that reasonably eliminate oxygen diffusion effects was beyond the scope of this test program. However, the reader is referred to Reference 16 for more detailed studies of this subject.

3.8 Comparison of Indenter Modulus, Modulus Profiles, and Elongation Data

This section briefly considers correlation of data from the indenter testing, the modulus profiles, and the elongation testing. Table 9 presents a summary of the changes in indenter modulus and average modulus from the modulus profiles. Except for the modulus of the Dekoron insulation as measured by the modulus profiles, the modulus always increased. In general, XLPO insulation modulus increased by about 40% during aging using either method, although some data variability is evident. The jackets all had significant modulus increases, with the modulus profiling technique showing greater increases than the indenter modulus.

Because a complete stress-strain curve was obtained during the elongation measurements, the results of the modulus profiling measurements can be compared in an approximate sense with the elongation measurements. If the material behaves in an elastic fashion for more than about 20% strain, a reasonable estimate of the modulus may be calculated from the linear part of the stress-strain curve. However, if plastic behavior begins early, then the modulus is very difficult to calculate from the elongation data. In general, the insulations experienced early plastic behavior, while the jackets

tended to be somewhat more elastic. Elastic modulus is given by the expression $E = \Delta\sigma/\Delta\epsilon = (\Delta F/A)/\Delta e$, where E is the elastic modulus, $\Delta\sigma$ is the difference in stress at two different points on the linear portion of force-elongation curve, $\Delta\epsilon$ is the corresponding change in strain, ΔF is the corresponding change in force, Δe is the corresponding change in elongation, and A is the cross-sectional area of the material. Normally, one of the two points used to calculate the differences in the above expression is a point prior to the application of force (no stress and no strain).

Table 9 Summary of Indenter Modulus and Modulus Profile Data

Cable	Average Modulus from Profile			Indenter Modulus Change
	Baseline (MPa)	9 Month Aging (MPa)	Change	
Brand Rex Insulation	330±22	554±51	1.68	1.4
Brand Rex Jacket	5.39±0.36	665±351	123	15
Rockbestos Insulation	425±38	522±41	1.23	1.5
Rockbestos Jacket	9.23±0.35	7120±1470	771	25
Raychem Insulation	398±52	643±121	1.62	1.4
Dekoron Insulation	88.9±12.1	80.3±9.8	0.90	1.2
Dekoron Jacket	14.5±0.7	224±42	15.4	6

Figure 21 shows a case where the material behavior was quite linear during the elongation test. Many materials exhibited plastic deformation by the time the first force point was taken. Figure 22 shows an example of such behavior. From Figure 21, using the cross sectional area of 0.097 cm^2 (0.015 in^2), the modulus calculated using the 0% and 100% elongation points is 3.32 MPa. Using the 300% and 350% points, the modulus is 5.85 MPa. These values compare favorably with 5.39 MPa, the average value from the modulus profile for this material.

3.9 Visual Examinations During Aging

Visual examinations of the complete cable specimens were performed during aging when the chamber was opened to remove small test samples. The XLPO cables generally appeared to be in good condition in all cases, except for the neoprene jacket on the Rockbestos cable product after six months or more of aging. After six months of aging, circumfrential cracks about 0.5 cm (0.2 in) wide were noted in the neoprene jackets. Some discoloration was also noted on most of the samples.

3.10 Summary of Condition Monitoring Measurements

The following summarizes the condition monitoring data presented in this section and apply under the conditions of our tests:

a. Of the parameters tested, elongation at break tends to show the most consistent correlation with aging. This is particularly true at lower radiation doses. Unfortunately, the test is destructive.

b. Tensile strength generally has only minimal correlation with aging. The major exceptions were the Brand Rex and Rockbestos jacket materials, which both had strong decreases in tensile strength.

c. Hardness increased by 15-75% with aging for the jacket materials. In a number of cases, the hardness was above the effective measuring range of our instrument. This was the case for all of the XLPO insulation materials.

d. Modulus, which was measured with the EPRI/Franklin cable indenter, showed good correlation with aging for the jacket materials discussed in this paper, but not for the XLPOs. The trend in indenter modulus was most evident at higher aging doses.

e. The modulus profiles did not indicate any significant oxygen diffusion effects for the aging conditions used in these tests. The Brand Rex and possibly the Dekoron product did experience some diffusion effects, but evidence indicated that the effects would not likely be significant for many applications. For the jacket materials, the absolute value of the modulus had large changes from the baseline samples to the samples that were aged for 9 months.

f. For the jacket materials, which had good aging correlations using both elongation and indenter modulus, elongation was the more sensitive aging indicator up to the total dose where the elongation approached 0%, with indenter modulus the more sensitive aging indicator beyond that point.

g. Density is a good indicator of aging for several materials, increasing by up to 3.5%. The density of the Brand Rex CSPE jacket first increased, then decreased at higher total doses. Density of the Dekoron Polyset insulation did not change in any significant way during aging.

h. Insulation resistance, polarization index, capacitance, and dissipation factor changes with aging were observed for some materials, but they were not nearly as sensitive to aging as the mechanical measurements.

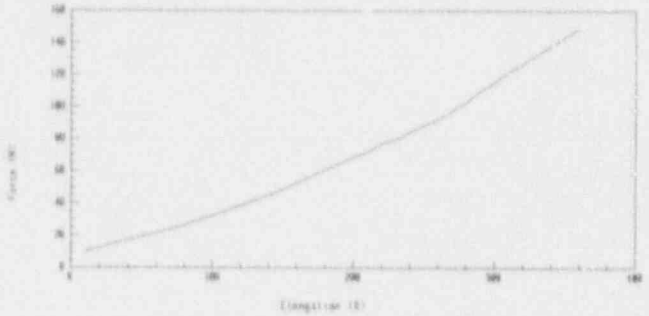

Figure 21 Force Versus Elongation for Unaged Brand Rex Jacket

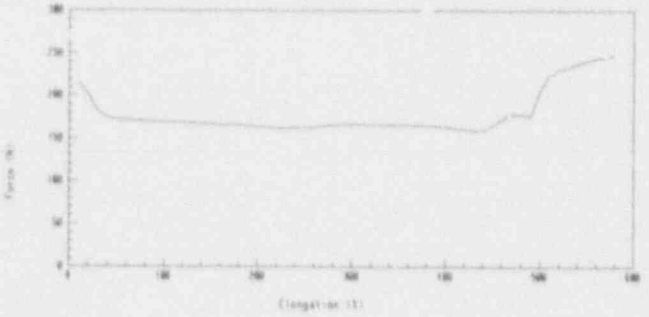

Figure 22 Force Versus Elongation for Unaged Raychem Insulation

4.0 ACCIDENT EXPOSURE INSULATION RESISTANCE DATA

This section discusses the performance of the cables during exposure to the accident simulations. In addition to environmental monitoring during the tests, on-line insulation resistance measurements were made as discussed in Section 2.4.3. The IR data as a function of time for each conductor of each cable is shown in Appendix I. For clarity in presentation of the data, figures in this section will generally show the averages of multiple samples and will usually be limited to the first 20 hours of the tests.

4.1 Cable Failures During the Accident Exposure

While no conductors failed during the aging or accident radiation exposures, one XLPO conductor, Rockbestos Firewall III conductor #15 in the 9-month chamber, did experience failure sufficient to cause the opening of a 1 A fuse during the accident steam exposures. Conductor #15 was one conductor of a three conductor cable. Figure 23 shows the details of the failure. A sudden IR decrease of almost two orders of magnitude occurred just before 83 hours into the test. Further IR degradation occurred over the next hour of the test. At that point, the fuse on the monitoring circuit opened. One other conductor of the same three conductor cable was continuously monitored during the accident exposure. This conductor did not experience a failure, but Figure I-16 tends to indicate the beginning of a gradual IR degradation at the end of the test.

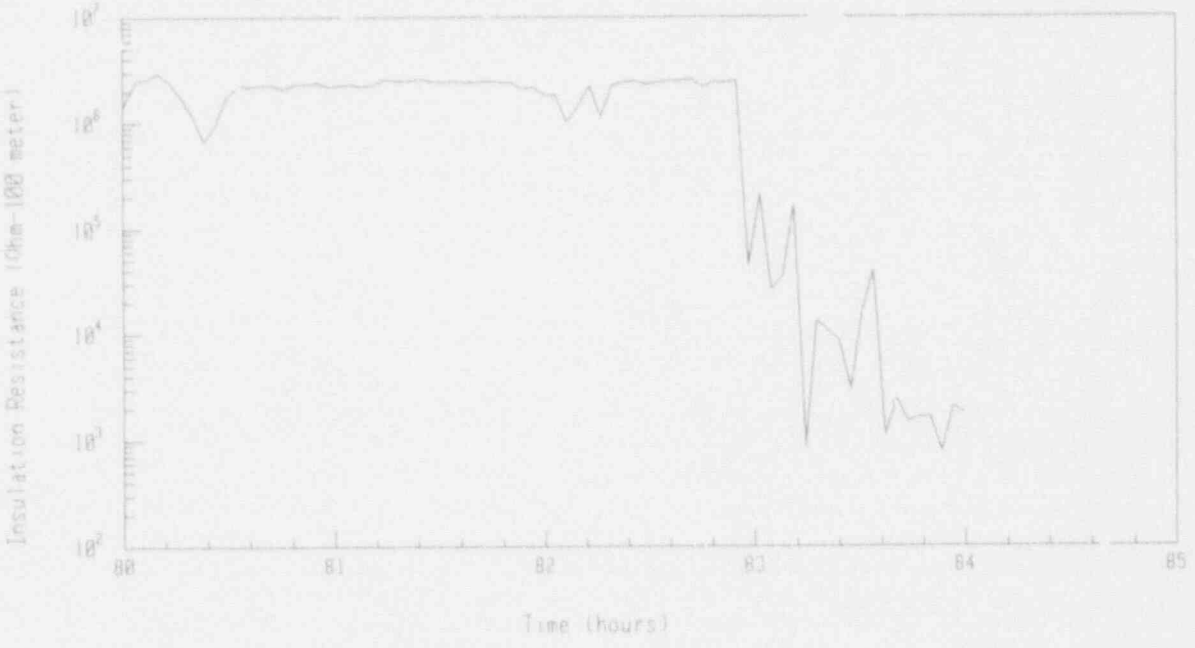

Figure 23 IR of Rockbestos Conductor #15 Prior to Failure

After completion of the post-LOCA dielectric withstand testing (see Section 5.0), the cables were removed from the mandrel for inspection. The failure point of the Rockbestos conductor was identified using a bucket of water and an ohmmeter. One lead of the ohmmeter was connected to the metal bucket and the other end was connected to the defective conductor. By carefully placing different parts of the cable into the water, the failure point was readily identified. The failure was a hole about 1.2 cm (0.5 in) along the cable length and about 0.6 cm (0.25 in) around the cable. With the cable coiled up in the same configuration as when on the aging mandrel, the failure

point was on the side of the coil of wire. There was no indication that the failure was caused by inadvertent damage or any test anomalies. The failure was a local failure, rather than global degradation leading to failure along significant portions of the cable (this latter type of degradation will be described in Volume 2 of this report for some EPR cable products). Because this conductor had been subjected to post-LOCA dielectric withstand testing, the failure point was somewhat enlarged and additional failure analysis was not pursued.

4.2 Insulation Resistance Versus Amount of Aging

Figure 24 shows the average IRs during the LOCA tests for Brand Rex multiconductor cables aged to the three different lifetimes. Each point on the plots is based on the conductors that were energized. Similar data for the Rockbestos Firewall III and the Dekorad Polyset are shown in Figures 25 and 26, respectively. Data for the Raychem single conductors are not shown because the IR was very high in all cases. The IR of the Brand Rex cables improved by up to almost an order of magnitude with aging, while the IR of the Rockbestos cables decreased by up to an order of magnitude with aging. The major difference in the IR of the Rockbestos cables occurred between the cables that were aged for 3 months and the cables that were aged for 6 months; the cables aged for 9 months behaved very much like the cables aged for 6 months. The Dekoron Polyset cables behaved very much like the Rockbestos cables.

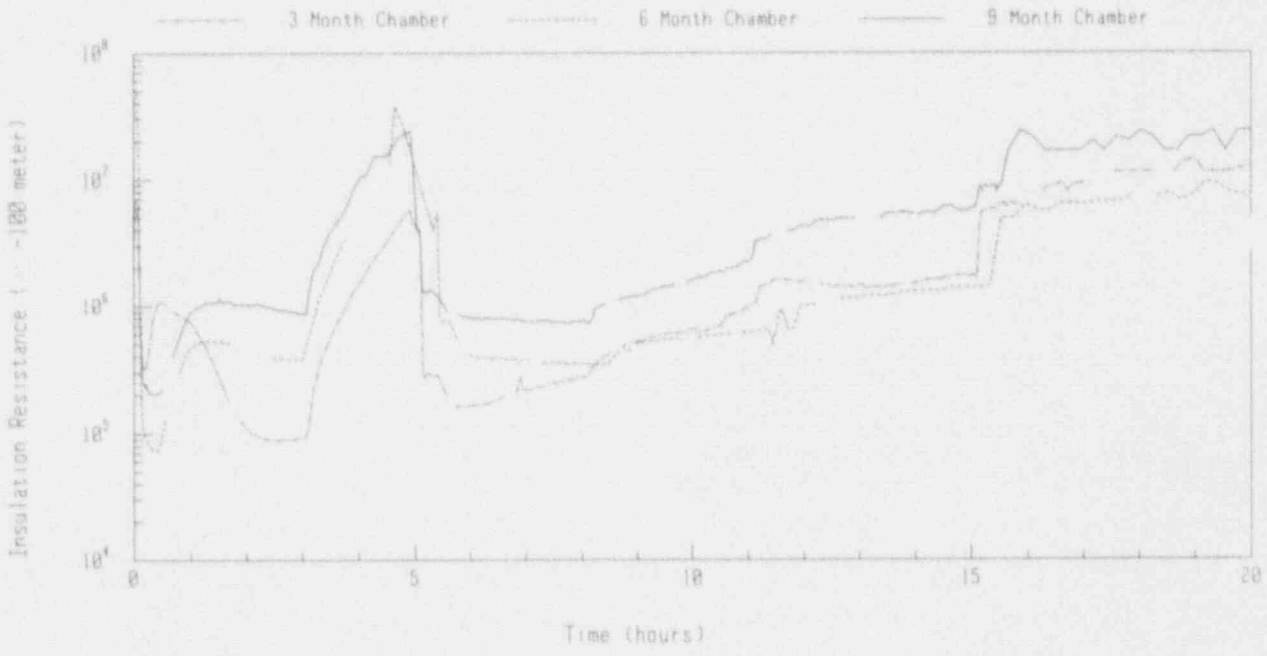

Figure 24 IR of Brand Rex Cables During Accident Exposures for Different Aging Treatments

4.3 Insulation Resistance Versus Applied Voltage

During several of the long steady-state portions of the test, IR measurements using the Keithley electrometer (see Appendix A) were performed at 50, 100, and 250 V. These measurements show how insulation resistance depends on applied voltage. Table 10

shows some data that may be used to perform this comparison. The values in the table are averages of the number of samples shown. When a given conductor had a

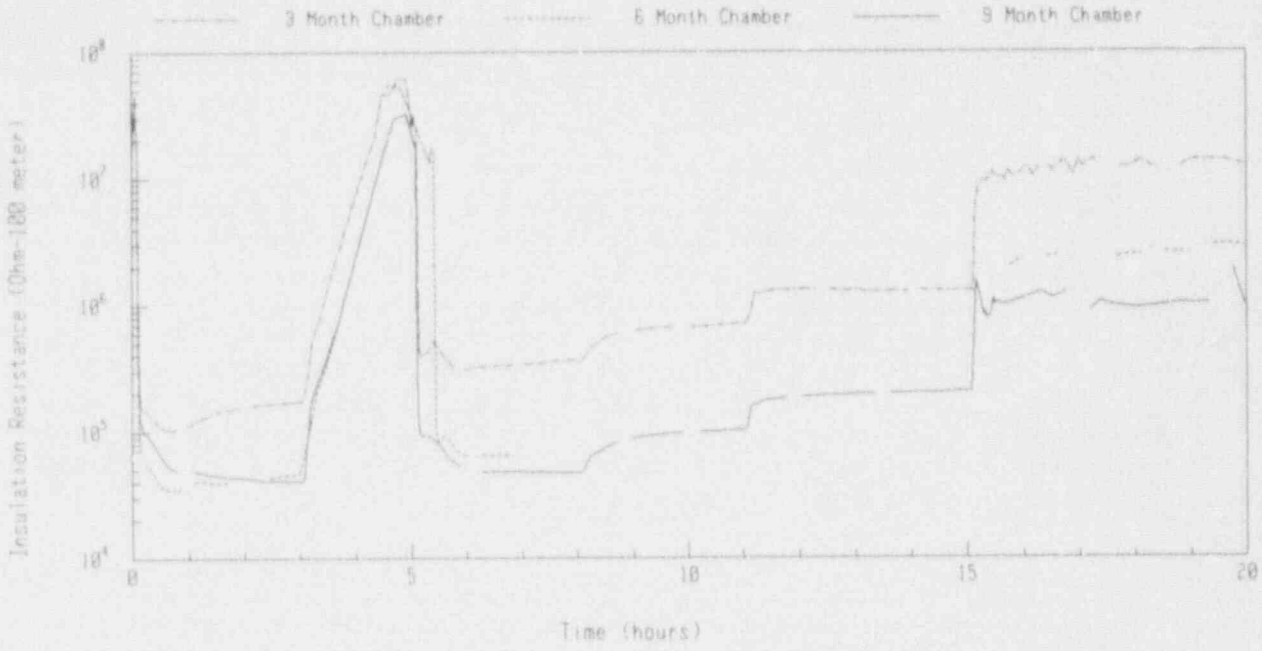

Figure 25 IR of Rockbestos Cables During Accident Exposures for Different Aging Treatments

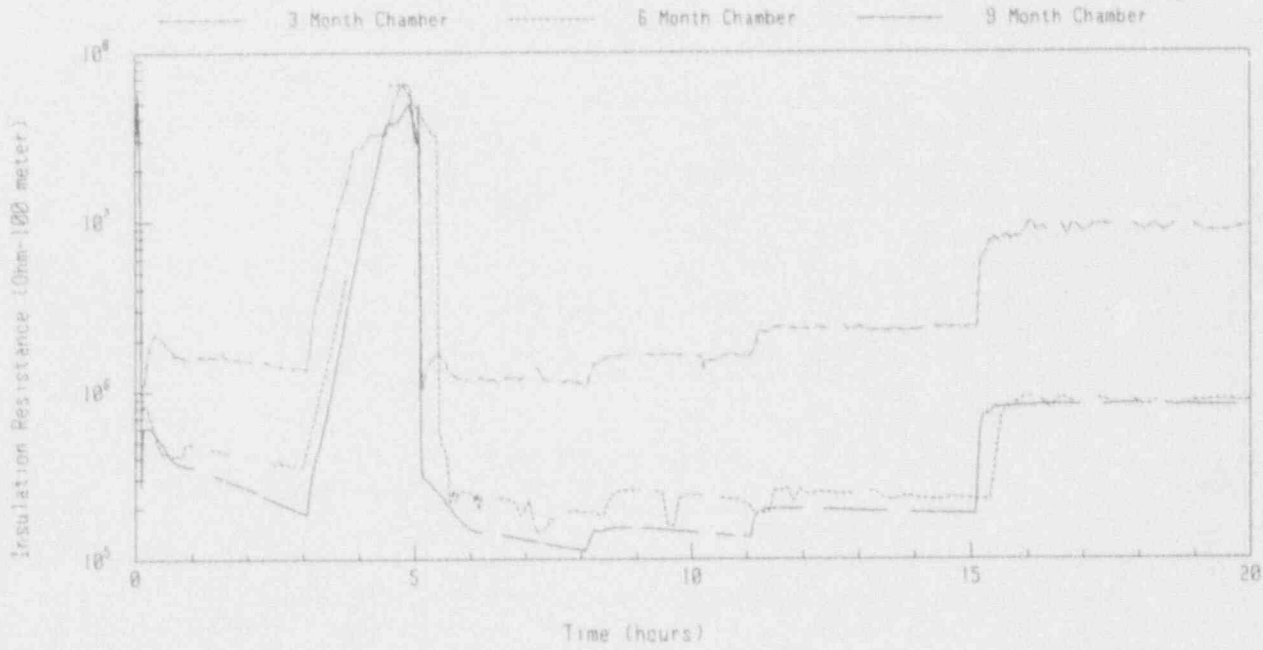

Figure 26 IR of Dekoron Polyset Cables During Accident Exposures for Different Aging Treatments

Table 10 Insulation Resistance Versus Applied Voltage During LOCA

Cable Type	Nominal Temperature (°C)	Number of Samples*	IR (50 V) (MΩ-100 m)	IR (100 V) (MΩ-100 m)	IR (250 V) (MΩ-1.. m)
Rock. FW III	171 (AT3)	3	---	0.10	0.16
	121 (AT9)	5	1.4	1.3	1.3
Brand Rex	171 (AT3)	3	---	1.2	0.15
	121 (AT9)	3	57	58	59
Polyset	171 (AT3)	3	---	1.5	1.4
	121 (AT9)	5	0.58	0.56	0.56
Raychem	171 (AT3)	2	---	1.6	1.9
	121 (AT9)	3	96	99	101

* Number of samples averaged, not necessarily total number of samples tested.

significantly different IR than the other conductors, that conductor was not included in the averages shown in Table 10. Thus, the number of samples averaged does not necessarily include all samples tested.

As Table 10 clearly shows, the IR is not strongly dependent on applied voltage over the range of voltages tested. This result implies that the cables behave as linear resistors over the range of voltages tested. This observation does not necessarily apply if the cables are close to failure. The only case in Table 10 that shows a significant decrease in IR with applied voltage was the Brand Rex multiconductor at 171°C in AT3, where the IR dropped by an order of magnitude between 100 V and 250 V. This decrease was consistent across all three conductors tested. Only one of the other cases shown had IRs that deviated by more than 20%. Additional data that can be used to assess IR dependence on applied voltage is shown in the figures of Appendix I.

4.4 Insulation Resistance Versus Temperature

Most of the XLPO cables tested behaved in a very consistent inverse temperature fashion. As examples, Figures 27 and 28 plot cable IRs versus temperature using the Keithley IR data from AT6. The IR of the Dekoron Polyset cables was much less consistent in this regard than the other cable products. Appendix I contains additional cable IR plots that can be compared to the temperature plots in Figures 10, 12, and 14.

4.5 Cable Behavior During Transients

Most of the XLPO cables behaved in a fairly consistent fashion during the transient portions of the test. In several instances, however, the IR fell below the eventual steady state value at the peak temperature before recovering to the steady state value. This section will focus on those conductors that showed such behavior. Although not as detailed as the plots in this section, the plots in Appendix I show the IR of each cable throughout each test.

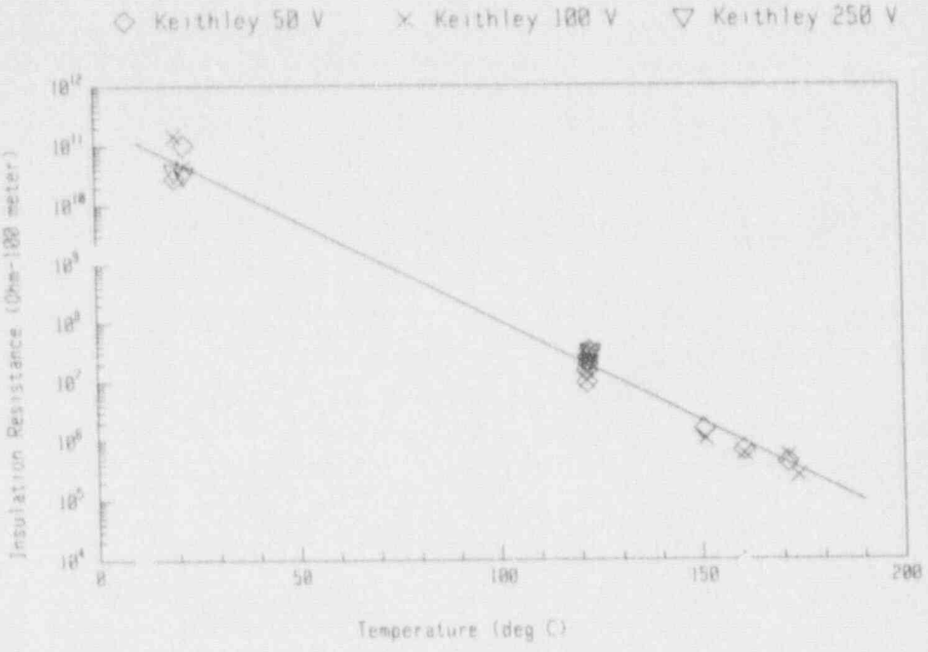

Figure 27 Average IR Behavior with Temperature for Brand Rex Cables (AT6)

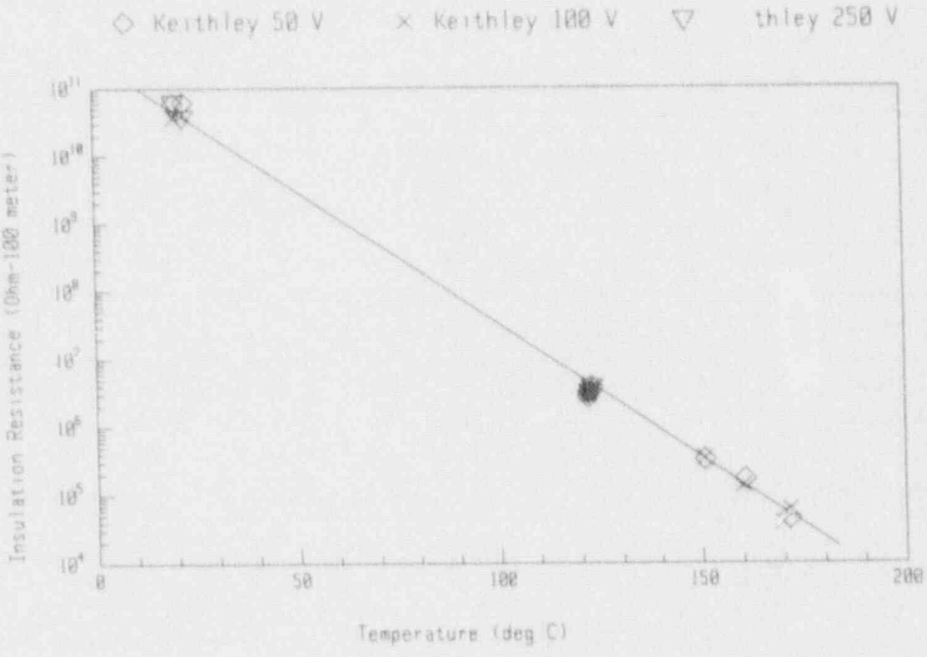

Figure 28 Average IR Behavior with Temperature for Rockbestos Cables (AT6)

As shown in Figure 29, the Brand Rex cables in AT3 had a slight thermal lag during the first transient of AT3, followed by an IR dip, somewhat of a recovery, and then a decrease over a longer term. Similar behavior was noted in AT6 and AT9. During the second transients, the amount that the IR fell below the eventual steady state value was generally less, probably because of the higher initial temperature for the second

transients. A sample IR plot during the first transient of AT3 for one of the Rockbestos conductors is shown in Figure 30, and a sample IR plot during the first transient of AT9 for one of the Polyset conductors is shown in Figure 31. The Raychem single conductor cable IRs remained above the range that could be effectively measured by our continuous measurement system.

During the second transient of AT9, the IR of the two monitored conductors of one of the Rockbestos cables fell below the eventual steady state value, recovered to a value above the steady state, and then settled to the steady state value. The behavior of one of these two conductors is shown in Figure 32. One of the conductors of this cable was the only Rockbestos conductor to fail during any of the accident tests.

The effects of transient IR reductions on nuclear power plant circuitry would be circuit specific and could range from no adverse effects to a temporary reduction in the accuracy of some instrument circuits.

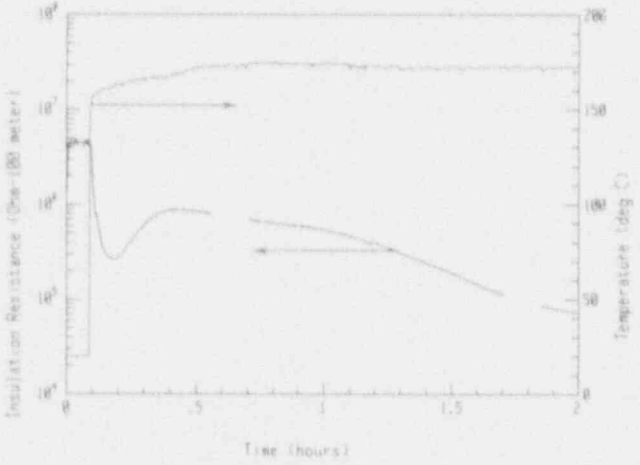

Figure 29 IR Behavior of Brand Rex Conductor #1 During First Transient of AT3

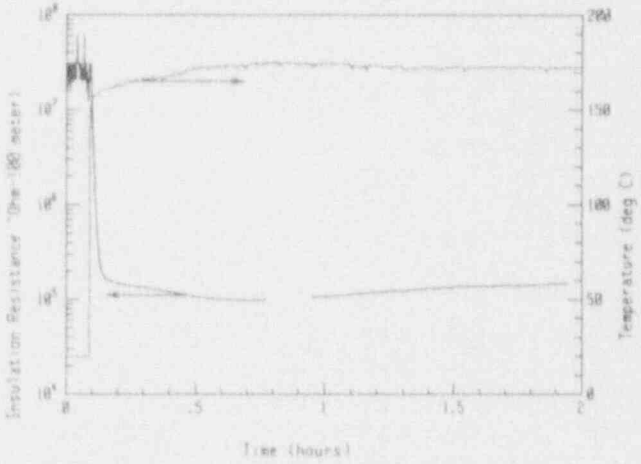

Figure 30 IR Behavior of Rockbestos Conductor #13 During First Transient of AT3

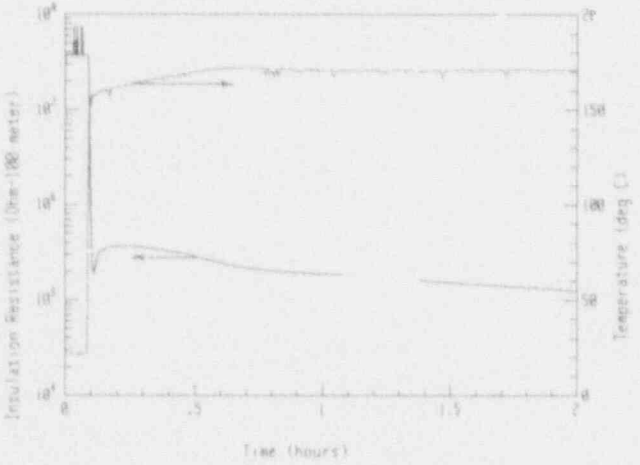

Figure 31 IR Behavior of Dekoron Polyset Conductor #24 During First Transient of AT9

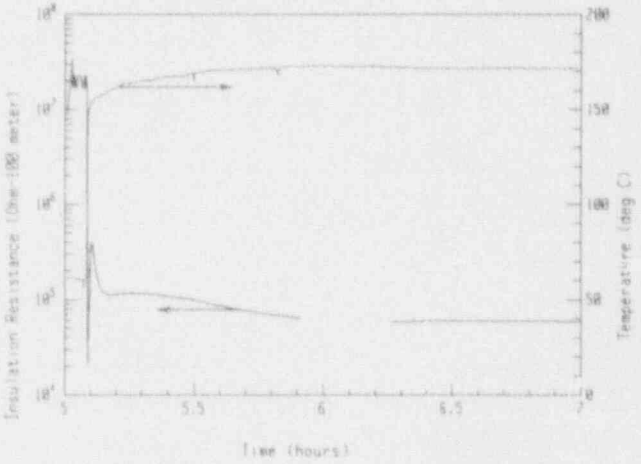

Figure 32 IR Behavior of Rockbestos Conductor #15 During Second Transient of AT9

4.6 Discrete Versus Continuous Insulation Resistance Measurements

Current cable qualification is typically based on IR data that is taken at discrete time periods. The data may include only one measurement on each conductor at each of the high temperature dwells. In this test program, many measurements were performed throughout the accident test. In general, periodic measurements would have been sufficient to indicate cable performance. The major exception was during the initial transient portions of the steam exposures where some cables experienced transient IRs that were lower than the subsequent steady state IRs. This phenomenon was discussed in Section 4.5.

4.7 Comparison of IR Data for Cables from Different Manufacturers

Table 11 compares the IRs of different XLPO cable products. The values in the table are approximate minimum values during the 171°C (340°F) exposures, based on Figures 24-26. The data indicates a large difference between the IRs of the various cable products during the same LOCA conditions, particularly when the single conductor Raychem is compared to the multiconductor cables. The data for the different multiconductors generally fall within an order of magnitude of each other. EPR testing reported in Volume 2 of this report compares IR data of multiconductors with the IR of single conductors removed from the multiconductors. Although the single conductors had up to a factor of six higher IRs for two cable types, a third cable type exhibited virtually no difference between the single and multiconductor samples. Some differences between single and multiconductor IRs may be expected because of differences in the effectiveness of the ground return path. Cables with continuous shields would have the best ground return path. Much of the return path for single conductors is in the form of surface conductivity. Unshielded multiconductors might be expected to have a good ground return through the other conductors, but these other conductors are also insulated and there may also be an insulated path through the jacket to the grounded test mandrel. Thus, it is not clear what the net effect of ground return paths should be on the differences in IRs of single and multiconductors. However, the IRs of the EPR cables indicate that any effects may be quite small since one type of EPR cable had no difference between single and multiconductor IRs.

Table 11 Approximate Minimum IRs (MΩ-100 m) of XLPO Cables Tested

Condition	Brand Rex Multi	Rockbestos Multi	Polyset Multi	Raychem * Single
AT3--1st 171°C	0.089	0.10	1.3	150
AT3--2nd 171°C	0.16	0.31	1.1	240
AT6--1st 171°C	0.073	0.034	0.35	66
AT6--2nd 171°C	0.34	0.064	0.14	37
AT9--1st 171°C	0.20	0.041	0.19	30
AT9--2nd 171°C	0.73	0.048	0.11	15

* Data for this cable from the 100 V Keithley measurements

5.0 POST-ACCIDENT MEASUREMENTS

After completion of the accidents tests, visual examinations of the specimens were performed, followed by dielectric withstand tests as follows:

a. Cables aged for 3 months were tested after the LOCA exposure. The cables were not disturbed prior to the dielectric test. These cables were then exposed to a high temperature steam test. Reference [7] contains details of the high temperature steam test.
b. Cables aged for 6 months were tested after the LOCA exposure. The cables were not disturbed prior to the dielectric test. These cables were then submergence tested in a chemical solution, with IEEE 383-1974 [2] mandrel bends and additional dielectric tests following the submergence test. Reference [7] contains details of the submergence test and the additional dielectric tests.
c. Cables aged for 9 months were tested after the LOCA test. The cables were not disturbed prior to the dielectric test. Following these tests, mandrel bends and additional dielectric tests were performed. These tests included ultimate breakdown strength of some of the cables.

In this section where the term "leakage" current is used, it should be taken to mean the resistive leakage current plus the capacitive charging currents. Note that a very large portion of the "leakage" current can be a result of the charging current.

5.1 Visual Examinations

All of the cable jackets were discolored to some extent by the accident exposures. The jackets on the Rockbestos Firewall III cables were moderately to severely damaged after all three accident tests (AT3, AT6, and AT9). The cracking was both longitudinal and circumfrential in both tests.

All of the XLPO cable jackets, except for one of the two Polyset cables, had evidence of cracking and damage after AT9. After AT3 and AT6, all of the jackets except the Rockbestos Firewall III jacket were in relatively good shape with no open cracks.

5.2 Dielectric Withstand Tests With Cables on Test Mandrels

The dielectric tests discussed in this section were performed with the cables still on the test mandrels, without disturbing them in any way. The dielectric tester was set for an automatic voltage rise of 500 Vac/s to the desired peak voltage, a hold at the peak voltage for 5 minutes, and finally a return to 0 voltage at -500 Vac/s. In cases where the leakage current was increasing significantly, the applied voltage usually decreased in response. In the automatic mode of our dielectric tester, there is no provision for readjusting the voltage back to the desired peak. The discussions below indicate where the voltage varied significantly during the 5-minute hold period. The dielectric testing described in this section was performed with the cables submerged in tap water after a soak period of at least 1 hour.

The test voltage for the individual conductors was nominally 80 Vac/mil of insulation thickness. The jackets (for cables with shields) were tested at 600 Vac. Table 12 is a summary of the dielectric test results. For purposes of Table 12, a conductor was defined as failing if the maximum leakage/charging current exceeded 20 mA during any part of the test. This failure criterion is well above the normal charging currents for all cable types tested and therefore represents a level where significant leakage currents are occurring. The actual applied voltage at steady state is given in parenthesis for those cables that passed the test. For cables that failed, the number in parenthesis is the

Table 12 Maximum Leakage/Charging Current (mA) in Dielectric Tests ("--" denotes No Sample)

Cable Type	Desired Voltage (kV)	3-month Post-LOCA	6-month Post-LOCA	9-month Post-LOCA
Multiconductors				
Brand Rex	2.4	3.9 (2.4)*	3.4 (2.4)	3.4 (2.6)
Brand Rex	2.4	3.9 (2.4)	3.4 (2.4)	2.3 (2.6)
Brand Rex	2.4	4.0 (2.4)	3.4 (2.4)	2.4 (2.6)
Rockbestos	2.4	3.6 (2.5)	3.5 (2.5)	3.3 (2.7)
Rockbestos	2.4	3.7 (2.5)	3.4 (2.5)	Fail (1.5)
Rockbestos	2.4	4.0 (2.6)	3.4 (2.5)	4.1 (2.6)
Rockbestos	2.4	--	--	4.2 (2.7)
Rockbestos	2.4	--	--	4.3 (2.7)
Rockbestos	2.4	--	--	4.0 (2.7)
Polyset	2.4	6.4 (2.6)	5.2 (2.4)	5.5 (2.7)
Polyset	2.4	6.3 (2.6)	5.2 (2.4)	5.3 (2.6)
Polyset	2.4	6.4 (2.6)	5.3 (2.4)	5.2 (2.6)
Polyset	2.4	--	--	4.8 (2.5)
Polyset	2.4	--	--	4.8 (2.5)
Polyset	2.4	--	--	4.8 (2.5)
Single Conductors				
Raychem	2.4	1.6 (2.5)	1.6 (2.4)	1.5 (2.7)
Raychem	2.4	1.6 (2.5)	1.6 (2.4)	1.7 (2.7)
Raychem	2.4	--	--	1.6 (2.7)
Jackets				
Polyset	0.6	8.0 (0.7)	6.0 (0.7)	Fail (0)
Polyset	0.6	--	--	Fail (0)

* Numbers in parenthesis denote average sustained voltage (kV) for cables that passed or peak voltage for cables that failed (see additional information in text).

maximum voltage that was applied to the cables during the transient voltage rise. The peak voltages normally lasted 2 seconds or less. The discussion below gives details of those failures that did not occur immediately. For cables with a peak value of 0, no readable voltage could be applied to the specimen, using the 0-10 kV scale on the dielectric tester. In Table 12, the individual conductor numbers are in the same order as in Table 2. For example, the third Rockbestos conductor listed under multiconductors in Table 12 corresponds to conductor #14 of the cables aged for 3 or 6 months, and conductor #16 of the cables aged for 9 months.

Table 12 indicates that all of the Brand Rex conductors and all of the Raychem Flamtrol conductors passed the post-LOCA dielectric withstand tests. The active conductors of the Polyset cables also passed the post-LOCA dielectric withstand tests. The shields of the Polyset cables passed the dielectric withstand tests after AT3 and AT6, but failed after AT9 (two samples). The Rockbestos Firewall III conductors passed all of the dielectric tests following the LOCA tests, with the exception of one conductor failing (out of six tested) after AT9. This conductor took a peak voltage of about 1500 Vac, but the test lasted only about 5 seconds.

5.3 Mandrel Bends and Dielectric Tests of Cables Aged for 9 Months

Following the tests described above, the cables from AT9 were subjected to a series of mandrel bends and high potential tests. Because conductor #15 had failed during AT9, conductors #14-16 (all part of the same cable) were not included in these tests. The results of the mandrel bend and high potential tests are summarized in Table 13. To verify that no damage had been done during removal of the cables from the aging mandrel, all of the conductors were subjected to an 80 Vac/mil high potential for 1 minute after a minimum of 1 hour in the water bath. All of the cables were then straightened, reverse bent around a nominal 40xD mandrel (i.e., the mandrel diameter was 40 times the cable outer diameter), returned to the water, and then subjected to a 5 minute high potential test at 80 Vac/mil in accordance with IEEE 383-1974 [2]. All the conductors passed the high potential test after the mandrel bend except the three conductors (#24-26) of one of the Dekoron Polyset cables. Upon examination, one crack was found in each of the conductors. All three cracks were within about 5 cm (2 in) of each other near the location where the cable had begun wrapping on the aging mandrel, but in an area where the cable had not been wrapped on the aging mandrel. It is very possible that this local area of the cable was closer to the wall heater than the rest of the cable, and thus, it may have been exposed to (unknown) higher temperatures (and more thermal aging). The section with the cracks was removed and the cable passed a retest with the shorter length.

During the 40xD and subsequent mandrel bends, extensive damage was done to the cable jackets. By the completion of the mandrel bends described below, most of the cable jackets had fallen completely off. It should be noted that all of the cable diameters, for purposes of calculating mandrel diameter to cable diameter ratio, were taken as the outer diameter of the cable with the jacket intact.

The next mandrel bend was nominally 30xD on all of the multiconductors, followed by 1 minute high potential tests at 80 Vac/mil. This bend was performed by tightening the 40xD bend, rather than straightening and recoiling the cables. All cables withstood this test, including the Polyset cable with the damaged section removed. Next all of the cables were wrapped around a nominal 20xD mandrel and another 80 Vac/mil high potential test was performed. Again all conductors passed the test.

The next mandrel was a 10xD nominal diameter mandrel, followed by an 80 Vac/mil withstand test. Dekoron Polyset conductor #24 was the only cable to fail during this test. The failure was located roughly in the middle of the cable, an area that was located on

Table 13 Mandrel Bends and Dielectric Tests After AT9

Cable Type	Bend mandrel diameter/ Cable diameter	Test Voltage (kV)	Maximum Current (mA)	Test Time (min)	Test Length (m)
Brand Rex-1	Off aging mandrel-no bend	2.6	0.9	1	4.4
	39	2.6	1.0	5	4.4
	31	2.5	0.9	1	4.4
	17	2.5	1.0	1	4.4
	9.9	2.5	1.0	1	4.4
	5.2	2.5	1.1	1	4.4
	Step breakdown test	13.0	6.2	See text	4.4
Brand Rex-2	Off aging mandrel-no bend	2.6	0.9	1	4.4
	39	2.6	0.9	5	4.4
	31	2.5	0.9	1	4.4
	17	2.5	1.0	1	4.4
	9.9	2.6	1.0	1	4.4
	5.2	2.5	1.1	1	4.4
	Step breakdown test	14.0	6.6	See text	4.4
Brand Rex-3	Off aging mandrel-no bend	2.6	0.9	1	4.4
	39	2.5	1.0	5	4.4
	31	2.5	0.9	1	4.4
	17	2.5	1.0	1	4.4
	9.9	2.5	1.0	1	4.4
	5.2	2.5	1.1	1	4.4
	Step breakdown test	14.0	6.8	See text	4.4
Rockbestos-17	Off aging mandrel-no bend	2.5	2.0	1	5.9
	40	2.6	2.2	5	5.9
	32	2.4	1.9	1	5.9
	18	2.6	2.0	1	5.9
	11	2.5	2.1	1	5.9
	5.4	2.5	2.3	1	5.9
	2.6--Cracked	--	--		5.9
Rockbestos-18	Off aging mandrel-no bend	2.4	2.0	1	5.9
	40	2.6	2.3	5	5.9
	32	2.4	1.9	1	5.9
	18	2.6	2.2	1	5.9
	11	2.5	2.2	1	5.9
	5.4	2.5	2.4	1	5.9
	2.6--Cracked	--	--		5.9

Table 13 Mandrel Bends and Dielectric Tests After AT9 (cont)

Cable Type	Bend mandrel diameter/ Cable diameter	Test Voltage (kV)	Maximum Current (mA)	Test Time (min)	Test Length (m)
Rockbestos-19	Off aging mandrel-no bend	2.4	1.8	1	5.9
	40	2.5	2.1	5	5.9
	32	2.5	1.9	1	5.9
	18	2.5	2.0	1	5.9
	11	2.5	2.1	1	5.9
	5.4	2.2	2.3	1	5.9
	2.6--Cracked	--	--		5.9
Polyset-24	Off aging mandrel-no bend	2.5	1.7	1	6.0
	41--Cracked	--	Fail		6.0
	Damaged section removed				
	32	2.5	1.5	1	4.9
	18	2.6	1.5	1	4.9
	10--Cracked	--	--		4.9
Polyset-25	Off aging mandrel-no bend	2.5	1.7	1	6.0
	41--Cracked	--	--		6.0
	Damaged section removed				
	32	2.5	1.5	1	4.9
	18	2.6	[illegible]	1	4.9
	10	2.5	1.5	1	4.9
	5.5	2.5	1.6	1	4.9
	5.5	2.5	1.5	2	4.9
	2.7--Cracked	--	--		4.9
Polyset-26	Off aging mandrel-no bend	2.6	1.8	1	6.0
	41--Cracked	--	Fail		6.0
	Damaged section removed				
	32	2.5	1.5	1	4.9
	18	2.6	1.5	1	4.9
	10	2.5	1.5	1	4.9
	5.5	2.5	1.6	1	4.9
	2.7	2.4	1.5	2	4.9
	Step breakdown test	21.0	12.5	See text	
Polyset-27	Off aging mandrel-no bend	2.6	1.8	1	6.2
	41	2.6	1.8	5	6.2
	32	2.5	1.8	1	6.2
	18	2.5	1.8	1	6.2
	10	2.5	1.5	1	6.2
	5.5--Cracked	--	Fail		6.2

Table 13 Mandrel Bends and Dielectric Tests After AT9 (cont)

Cable Type	Bend mandrel diameter/ Cable diameter	Test Voltage (kV)	Maximum Current (mA)	Test Time (min)	Test Length (m)
Polyset-27 (cont)	Damaged section removed Step breakdown test	20.0	12.8	See text	5.2
Polyset-28	Off aging mandrel-no bend	2.6	1.8	1	6.2
	41	2.6	1.8	5	6.2
	32	2.6	1.8	1	6.2
	18	2.5	1.8	1	6.2
	10	2.5	1.8	1	6.2
	5.5--Cracked	--	Fail		6.2
Polyset-29	Off aging mandrel-no bend	2.6	1.8	1	6.2
	41	2.6	1.8	5	6.2
	32	2.5	1.8	1	6.2
	18	2.6	1.8	1	6.2
	10	2.5	1.8	1	6.2
	5.5	2.6	2.0	1	6.2
	Step breakdown test	19.0	14.5	See text	6.2
Raychem-35	Off aging mandrel-no bend	2.5	0.9	1	4.1
	41	2.5	0.9	5	4.1
	24	2.5	0.8	1	4.1
	11	2.5	0.8	1	4.1
	5.3	2.5	0.8	1	4.1
	2.6	2.5	0.7	1	4.1
	1.3--Cracked	--	--		4.1
Raychem-36	Off aging mandrel-no bend	2.5	0.8	1	4.0
	41	2.6	0.9	5	4.0
	24	2.5	0.8	1	4.0
	11	2.5	0.9	1	4.0
	5.3	2.5	0.7	1	4.0
	2.6	2.5	0.8	1	4.0
	Step breakdown test	21.1	7.2	See text	4.0
Raychem-37	Off aging mandrel-no bend	2.5	0.8	1	4.0
	41	2.5	0.8	5	4.0
	24	2.5	0.8	1	4.0
	11	2.5	0.8	1	4.0
	5.3	2.4	0.8	1	4.0
	2.6	2.4	0.7	1	4.0
	1.3--Cracked	--	--		4.0

the test mandrel during aging and accident exposures. The failure (crack) was in an area where a small amount of jacket still remained on the cable. The brittleness of the jacket may have caused some damage during the 10xD bend.

The next mandrel was a 5xD nominal diameter mandrel, followed by an 80 Vac/mil withstand test. Dekoron Polyset conductors #27 and 28 were the only two conductors to fail during this test. The insulations on both of these conductors were observed to be cracked prior to the dielectric test, and both failures were located near where the cable had begun wrapping around the aging mandrel. These two conductors failed in locations similar to those of the three conductors (#24-26) of the Dekoron Polyset cable that failed after the 40xD mandrel bend. Again, the area of failures may have been closer to the wall heaters and hence exposed to a higher temperature than the cable on the mandrel, causing additional thermal aging.

At this point, to provide additional insights on the behavior of both electrical and mechanical properties of the cables in the post-LOCA state, different tests were performed on different cables. Thus, each of the remaining cables will be described individually.

Each conductor of the Brand Rex cable was exposed to a step breakdown test. Voltage was held for 30 seconds at each voltage, then raised to the next voltage. The test voltage began at 2400 Vac with 1200 Vac increments until the voltage reached 9600 Vac. The test was continued at 11000 Vac and incremented 1000 Vac at a time until breakdown of each conductor occurred. One conductor broke down at 13000 Vac after 3 seconds, the second conductor broke down at 14000 Vac after 3 seconds, and the third conductor broke down at 14000 Vac after 15 seconds.

The Rockbestos cable (conductors #17-19) was subjected to a 2.6xD mandrel bend. After this bend, cracking through to all conductors was evident. Thus, this cable was not tested further.

The first Dekoron Polyset cable (conductors #24-26) was subjected to a 2.7xD mandrel bend and a 1 minute dielectric test at 80 Vac/mil. Conductor #25 cracked during the bend, but conductor #26 passed the dielectric test after the bend (conductor #24 had previously failed during the 10xD test). Conductor #26 was then subjected to a step breakdown test, with the voltages as defined above for the Brand Rex conductors. The cable began arcing and the test set tripped at a voltage of 21000 Vac after 17 seconds. The leakage current before tripping was 12.5 mA. A retest of the cable allowed a voltage of 20000 Vac to be applied for 5 seconds with a leakage current of 20 mA. After this last test, the breakdown point was located toward the middle of the cable.

Conductor #29 of the second Dekoron Polyset cable (conductors #27 and 28 had previously failed during the 5xD test) was subjected to a step breakdown test, with the voltages as defined above for the Brand Rex conductors. The cable broke down at a voltage of 19000 Vac after 19 seconds. The leakage current just before breakdown was 14.5 mA. Following this breakdown test, a section of the entire cable was removed where conductors #27-28 had been mechanically damaged. As a result of the handling, another through-wall crack was noted in the insulation of conductor #28 and this conductor was not tested further. Conductor #27 (now shorter) was exposed to the step voltage breakdown test and broke down at 20000 Vac after 8 seconds. The leakage current just before breakdown was 12.8 mA.

Raychem single conductors #35 and 37 were both exposed to successively tighter bends, with 80 Vac/mil dielectric tests after each bend. Both conductors survived the testing with a 2.6xD mandrel, but both cracked when subjected to a bend around a 1.3xD mandrel. Raychem conductor #36 survived a similar 2.6xD mandrel bend and high

potential test. This conductor was then exposed to a step voltage breakdown test as described above. The cable broke down at a voltage of 21100 Vac after 20 seconds. The leakage current just before breakdown was 7.2 mA.

5.4 Post-Accident Elongation Tests of Cables Aged for 9 Months

Following completion of the mandrel bends and dielectric tests described in Section 5.2, the insulation of each cable product was subjected to elongation testing. Test samples were cut from near the middle of the cables and the copper conductors were removed. The samples were then tested using an Instron Model 1000 tester. Table 14 gives the results of the elongation testing, along with the baseline tensile strength and elongation values. The following compares the approximate absolute elongation at the end of the accident radiation exposure (before AT9) with the approximate absolute elongation of each insulation material after AT9:

Cable Type	Before AT9	After AT9
Brand Rex	10%	40%
Rockbestos	<10%	20%
Dekoron Polyset	40%	30%
Raychem	<10%	50%

The above data indicates that elongations of three of the XLPO materials improved with the exposure to the accident environment. (It should be noted that the "After AT9" elongation measurements were performed a long time after completion of the accident exposure.) To provide some additional verification of the aging elongation data, three of the 36-cm complete cable samples that had been aged for 9 months and exposed to accident radiation were cut into thirds and the copper conductors were removed for elongation testing. Two Raychem specimens both broke at less than 10% elongation. One Brand Rex specimen broke at 20% elongation and one broke at less than 10% elongation. The three Polyset specimens broke at 10, 20, and 30% elongation. The above data compare very favorably with the data from the 15-cm tensile specimens. The 36-cm Polyset specimens had average elongation of 20% as compared to the 15-cm specimen elongation of 40%. Tables B-1 and B-3 in Appendix B indicate that the 36-cm specimens received a total radiation dose about 10% higher than the 15-cm specimens, which probably accounts for the small differences in elongations.

With the likelihood that the accident environment had actually improved the properties of some of the XLPO materials, we decided to boil several samples in water for 30 minutes to see if that affected the elongations of the materials. We boiled three samples, one Brand Rex and one Raychem (from the third third of the 36-cm specimen of each) and one spare Rockbestos 15-cm tensile specimen. After boiling, the Raychem conductor broke at 10%, the Brand Rex conductor broke at 40%, and the Rockbestos conductor broke at 50%. Note that these values are each higher than comparable samples that were not boiled, indicating that the boiling had a positive effect on the elongation properties of these XLPO materials, consistent with the observed effects of the accident simulation. The increase in flexibility may result from plasticizer effects of the moisture and/or the possibility of melting and reforming the crystalline structure of the material. This data provides several potential insights into the behavior of XLPO materials:

a. The effects of humidity during aging may be more important than previously believed, possibly providing a positive benefit for XLPO materials.
b. The effects of humidity during aging may account for some differences between natural and artificial aging experiences. Historically, it has been argued that artificial aging is more severe than natural aging, with differences

attributable to "non-Arrhenius" behavior. Since artificial aging is conducted at high temperatures, the humidity is always lower than during natural aging conditions. The lack of "matched" moisture conditions may account for some "non-Arrhenius" behavior. The effects of crystalline melting during aging have also been identified as a mechanism for "non-Arrhenius" behavior [16].

c. If very degraded XLPO materials consistently "improve" their elongation as a result of LOCA exposures, the risks of operating nuclear plants with XLPO cables having severely degraded mechanical properties may be somewhat lower than what would have previously been expected.

Table 14 Tensile Strength and Elongation After AT9

Cable Type	Conductor Number	Elongation at Break (%)	Peak Force (N)	Tensile Strength (MPa)
Brand Rex	1	30	89.0	9.4
e_0 = 320	2	50	94.3	9.9
T_0 = 11.8	3	40	95.6	10.1
Rockbestos	14	20	94.7	9.5
e_0 = 240	14	20	92.1	9.2
T_0 = 12.4	15	30	101.4	10.1
	15	10	93.4	9.3
	16	10	104.1	10.4
	16	10	98.7	9.9
	16	20	96.1	9.6
	16	10	96.1	9.6
Polyset	27	20	92.5	8.8
e_0 = 350	27	30	110.8	10.5
T_0 = 12.9	28	20	106.3	10.1
	29	30	120.1	11.4
	29	40	125.4	11.9
Raychem	35	60	232.6	14.7
e_0 = 520	35	60	230.0	14.6
T_0 = 14.6	35	70	236.2	14.9
	35	60	222.0	14.0
	36	20	212.2	13.4
	36	20	211.3	13.4
	36	40	225.5	14.3
	36	50	226.4	14.3
	36	40	223.3	14.1
	36	50	229.5	14.5
	36	50	227.7	14.4

6.0 CONCLUSIONS

This conclusions section is divided into three parts. First, general conclusions regarding aging and condition monitoring are presented. Next, general conclusions regarding the accident behavior of aged cables are presented. Finally, a summary of conclusions that address each of the objectives of this study is presented.

6.1 Aging and Condition Monitoring

a. Of the condition monitoring parameters tested, elongation at break tends to show the most correlation with amount of aging for the most cable types.

b. Hardness and indenter modulus both increased with aging of jacket materials, but they did not change consistently for the XLPO insulation materials. Indenter modulus measurements were clearly more sensitive than hardness measurements.

c. Density increased with aging for most of the insulation and jacket materials. However, no consistent change was noted for one material and the density of another material initially increased, but later began decreasing.

d. Although there were isolated exceptions, neither tensile strength nor any of the electrical measurements had any significant, consistent trend with aging.

e. The modulus profiles did not indicate any significant oxygen diffusion effects for the aging conditions used in these tests. The Brand Rex and possibly the Dekoron product did experience some diffusion effects, but evidence indicated that the effects would not likely be significant for many applications. Defining the upper limits of test parameters (dose rate and temperature) that reasonably eliminate oxygen diffusion effects was beyond the scope of this test program.

6.2 Accident Performance of Aged Cables

a. Only one XLPO conductor (out of 40 tested) failed during the accident tests. This was one of three conductors of a Rockbestos multiconductor cable in the accident test of cables aged for 9 months (AT9).

b. A statistically significant conclusion regarding the number of failures versus the amount of aging is not possible. However, the only conductor that failed during an accident test was one that had been aged for the maximum amount of time.

c. The maximum difference in the accident IR performance of a given cable type aged to the three different lifetimes was about an order of magnitude. In one case, the accident IR was higher for more highly aged cables, and in three cases, the IR was lower. The significance of this order of magnitude change would be application dependent, but it is expected to be negligible for many applications.

d. The accident IR performance of our XLPO cables aged to three different lifetimes under simultaneous, slow rate aging was comparable to the accident performance of aged XLPO cables in industry tests that used high rate sequential aging to nominally more severe conditions (total dose and thermal equivalent lifetime).

c. The three multiconductor cable products tested had accident IRs that were within an order of magnitude of each other. The single conductor cable product tested had IRs that were 2-3 orders of magnitude higher than the multiconductors. Part of the difference between single and multiconductors may reflect differences in ground plane effectiveness, but a significant portion of the difference is expected to be a result of actual differences in the cable materials.

f. Over the range from 50-250 V, IR was largely independent of test voltage during both aging and accident testing (as long as the cable was not close to failure).

g. During accident testing, the IR of the XLPO cables consistently varied inversely with temperature, i.e., the IR increased as the temperature decreased.

h. During the initial steam transients, some cables had lower IRs than their eventual steady state values. Except for this transient phenomenon, periodic measurements of IR would have been sufficient to indicate cable performance. The effects of these transient IR variations would be circuit specific and could range from no adverse effects to a temporary reduction in the accuracy of some instrument circuits.

i. With the exception of the one conductor that failed during the LOCA test, all conductors successfully passed high voltage tests at an applied voltage of 80 Vac/mil following the accident tests. Three conductors failed a similar high voltage test after an IEEE 383-1974 [2] post-accident mandrel bend test. However, the location of the failures may have received more thermal aging than the rest of the cable.

j. Following the accident exposure, dielectric withstand voltages of XLPO cables were on the order of 13-21 kVac. Mechanical damage (cracking) was generally necessary to cause breakdown voltages to occur at voltages below 80 Vac/mil of insulation. Such cracking during mandrel bend tests frequently required mandrel bends much more severe than that specified in IEEE 383-1974 [2].

k. When cracking was observed after mandrel bends, it was usually through to the conductor and very obvious.

l. For three of the four XLPO materials, the elongation was greater after AT9 than before AT9. This may be a result of moisture being absorbed into the cable and acting as a plasticizer or of the crystalline structure of the XLPO materials being melted and reformed.

m. Although the IEEE 383-1974 [2] mandrel bend requirement is quite severe, most of the XLPO materials tested to our conditions survived mandrel bends significantly more severe than the IEEE 383 requirement (using successively tighter mandrel bends until failure occurred).

6.3 Summary of Conclusions

The conclusions of this experimental effort with regard to both the broad and specific objectives of the program are addressed below:

Objective: To determine the long term aging degradation behavior of popular cable products used in nuclear power plants.

Conclusion: The test results indicate that most properly installed XLPO cables should be able to survive an accident after 60 years for total aging doses up to 400 kGy and for moderate ambient temperatures on the order of 50-55°C (potentially higher or lower, depending on material specific activation energies).

Objective: To determine the potential of condition monitoring (CM) for residual life assessment.

Conclusion: Of the measurements tested, elongation is the best condition monitoring method. Although a quantitative generic acceptance criterion is difficult to establish based on these tests, a reasonable range (that is likely to be fairly conservative) would be about 50-100% absolute elongation remaining. Compressive modulus and density could also be somewhat effective for monitoring residual life, although acceptance criteria would be much more difficult to establish for these measurements because extensive testing has not been performed to demonstrate that modulus and density respond consistently for varied test conditions. The electrical measurements were not effective for monitoring residual life.

Objective: To assess the accident performance of cables aged more slowly (e.g. low temperature and low radiation dose rate) than in typical industry tests and under simultaneous conditions.

Conclusion: The accident performance (in terms of electrical properties) of the XLPO cables did not differ substantially from the accident performance of cables aged at more highly accelerated (both sequential and simultaneous) conditions in past Sandia tests, as well as in industry tests. However, it must be noted that this conclusion only applies up to the limits of the aging conditions simulated in this test program since the testing does not prove or disprove whether highly accelerated tests to much higher total exposure conditions would produce the same results if the acceleration were greatly reduced.

Objective: To assess the conservatism associated with the IEEE 383-1974 [2] post-accident mandrel bend and high potential testing.

Conclusion: The IEEE 383-1974 [2] post-LOCA mandrel bend test on the cables that had been aged for 9 months induced cracking of three conductors of one cable type. The high potential test did not induce any cable failures (assuming the cable did not crack during the mandrel bend), even after bends significantly more severe than the IEEE requirement. Thus, for XLPO cables, the most severe part of the post-accident exposure appears to be the bend test.

Objective: To assess what additional qualification requirements might be needed as cables age beyond their current nominal 40-year qualified life.

Conclusion: The accident performance of cables aged to the three different lifetimes was not significantly different. Thus, for XLPO cables exposed to

environments less severe than those simulated in this test program, these tests do not indicate the need for additional qualification requirements as cables age beyond their current qualified life. This conclusion is based on the technical finding that the cables tested did not fail (with only one exception) when exposed to the environments defined in this test program. It does not prove or disprove the adequacy of current qualification practices and requirements.

7.0 REFERENCES

1. IEEE Standard for Qualifying Class 1E Equipment for Nuclear Power Generating Stations, IEEE Standard 323-1974, New York, NY.

2. IEEE Standard for Type Test of Class 1E Electric Cables, Field Splices, and Connections for Nuclear Power Generating Stations, ANSI/IEEE Standard 383-1974 (ANSI N41.1C-1975), New York, NY.

3. Bustard, L. D., *The Effect of LOCA Simulation Procedures on Ethylene Propylene Rubber's Mechanical and Electrical Properties,* NUREG/CR-3538, SAND83-1258, Sandia National Laboratories, Albuquerque, New Mexico, October 1983.

4. Bustard, L. D., et al., *The Effect of Thermal and Irradiation Aging Simulation Procedures on Polymer Properties,* NUREG/CR-3629, SAND83-2651, Sandia National Laboratories, Albuquerque, New Mexico, April 1984.

5. Bustard, L. D., *The Effect of LOCA Simulation Procedures on Cross-Linked Polyolefin Cable's Performance,* NUREG/CR-3588, SAND83-2406, Sandia National Laboratories, Albuquerque, New Mexico, April 1984.

6. Bennett, P. R., S. D. St. Clair, and T. W. Gilmore, *Superheated-Steam Test of Ethylene Propylene Rubber Cables Using a Simultaneous Aging and Accident Environment,* NUREG/CR-4536, SAND86-0450, Sandia National Laboratories, Albuquerque, New Mexico, June 1986.

7. Jacobus, M. J. and G. F. Fuehrer, *Submergence and High Temperature Steam Testing of Class 1E Electrical Cables,* NUREG/CR-5655, SAND90-2629, Sandia National Laboratories, Albuquerque, New Mexico, April 1991.

8. Shaw, M. T., *Natural Versus Artificial Aging of Materials in Nuclear Plant Equipment,* EPRI NP-4997, Electric Power Research Institute, Palo Alto, CA, December 1986.

9. Gillen, K. T., R. L. Clough, and C. A. Quintana, "Modulus Profiling of Polymers," *Polymer Degradation and Stability,* Vol. 17, p. 31, 1987.

10. Clough, R. L., K. T. Gillen, and C. A. Quintana, *Heterogeneous Oxidative Degradation in Irradiated Polymers,* NUREG/CR-3643, SAND83-2493, Sandia National Laboratories, Albuquerque, New Mexico, April 1984.

11. Clough, R. L., K. T. Gillen, and C. A. Quintana, "Heterogeneous Oxidative Degradation in Irradiated Polymers," *Journal of Polymer Science, Polymer Chemistry Edition,* Vol. 23, p. 359, 1985.

12. Toman, G. J. and G. Sliter, "Development of a Nondestructive Mechanical Condition Evaluation Test for Cable Insulation," *Proceedings: Operability of Nuclear Power Systems in Normal and Adverse Environments,* Albuquerque, New Mexico, September 29-October 3, 1986.

13. Gardner, J. B. and T. A. Shook, "Status and Prospective Application of Methodologies from an EPRI Sponsored Indenter Test Project," Appears in *Proceedings: Workshop on Power Plant Cable Condition Monitoring,* EPRI EL/NP/CS-5914-SR, July 1988.

14. Gillen, K. T. and R. L. Clough, *Predictive Aging Results for Cable Materials in Nuclear Power Plants,* SAND90-2009, Sandia National Laboratories, Albuquerque, New Mexico, November 1990.

15. Clough, R. T. and K. T. Gillen, "Detailed Studies of Thermal Oxidation," *Polymer Materials Science and Engineering,* , Vol. 58, p. 209, 1988.

16. Gillen, K. T. and R. L. Clough, *Aging Predictions in Nuclear Power Plants--Crosslinked Polyolefin and EPR Cable Insulation Materials,* SAND91-0822, Sandia National Laboratories, Albuquerque, New Mexico, June 1991.

Appendix A Description of Electrical Measurement Equipment

A.1 BACKGROUND

For our tests, insulation resistance (IR) measurements were performed between each conductor and ground with all other conductors connected to ground. Measurements were taken at 3 voltages: 50, 100, and 250 V. Leakage current (or IR) data were taken at discrete times from 2 seconds to 1 minute for 50 and 100 V measurements and from 2 seconds to 5 minutes for 250 V measurements. IR gives a measure of the resistive component of the dielectric impedance. It is typically used in industry as a go/no-go test of insulation. However, no technical basis is available to set an acceptance criteria related to age-related degradation [A-1]. Rather, the test is usually used to assist detection of locally damaged cable (e.g. insulation windings that are wet or a gouged cable that is "sufficiently close" to the ground plane in the test).

Some common criticisms of IR measurements are that they are subject to uncontrollable temperature and humidity effects along the cable. Because they are dimensionless quantities, polarization indices are sometimes used to determine the condition of an insulation structure. Reference [A-2] indicates that polarization index is independent of temperature. However, the data presented in Appendix C and discussed in Section 3.0 indicates that the PI was dependent on temperature in our tests.

A polarization index lower than normal suggests excessive surface leakage or deteriorated insulation [A-3, A-4]. IEEE 62-1978 [A-4] defines polarization index as the ratio of the IR at 10 minutes to the IR at 1 minute, which should normally be greater than 1. It should be noted, however, that other definitions of polarization index may be used. In this study two definitions were used. At all voltage levels, a polarization index ratio of 1 minute to 30 seconds was used; at 250 V, a polarization index ratio of 5 minutes to 1 minute was also used.

Transfer function measurement techniques are described in References A-5, A-6, A-7, A-8, and A-9. The transfer function gives an indication of the variation of dielectric impedance (principally due to the bulk cable capacitance and conductance) as a function of frequency. The imaginary component of the transfer function gives an indication of the dielectric charge/voltage characteristics at the given frequency, and the phase angle δ between the real and imaginary components gives an indication of the dielectric losses as a function of frequency. The tangent of the phase angle δ is commonly referred to as the dissipation factor (DF) and is often measured only at a single frequency. Dissipation factor also gives an indication of the power factor (PF) since the two are related as $PF = DF/(1+DF^2)$. If δ is a small angle, then PF≈DF.

References A-5, A-6, and A-7 describe a number of bridge techniques, including the famous Schering Bridge. Typically in bridge techniques, a sinusoidal voltage is applied to a bridge containing the unknown sample as one leg. Other reference legs are adjusted until bridge balance is obtained. The unknown capacitance and resistance at the discrete frequency can then be calculated based on the reference values.

We made capacitance and dissipation factor measurements using two different instruments, covering the range of frequencies from about 0.3 Hz to 500 kHz. We used a Hewlett Packard Model 4192A Low Frequency (LF) Analyzer to make these measurements at the "higher" frequencies, ranging from about 100 Hz to 500 kHz and a Hewlett Packard Model 3192A Spectrum Analyzer combined with a low noise preamplifier to make the measurements at the lower frequencies, from about 0.3-1000 Hz. The overlapping portion of the ranges provided a check between

measurements made by two independent techniques. As with IR, the transfer function in our tests was evaluated between each conductor and ground with all other conductors connected to ground.

A.2 INSULATION RESISTANCE

The test apparatus for measuring IR is shown in Figure A-1. An HP Model 216 computer was used to control the data acquisition. A Keithley electrometer was used to measure the voltage across a dropping resistor. The output of the Keithley was then fed, either directly or via the HP 3497A data logger, to the computer for storage on disc. In addition to data acquisition and storage, the computer also directed the data logger to automatically select the proper voltage level using the 0-250 Vdc power supply and to select the proper dropping resistor using a set of computer-controlled relays.

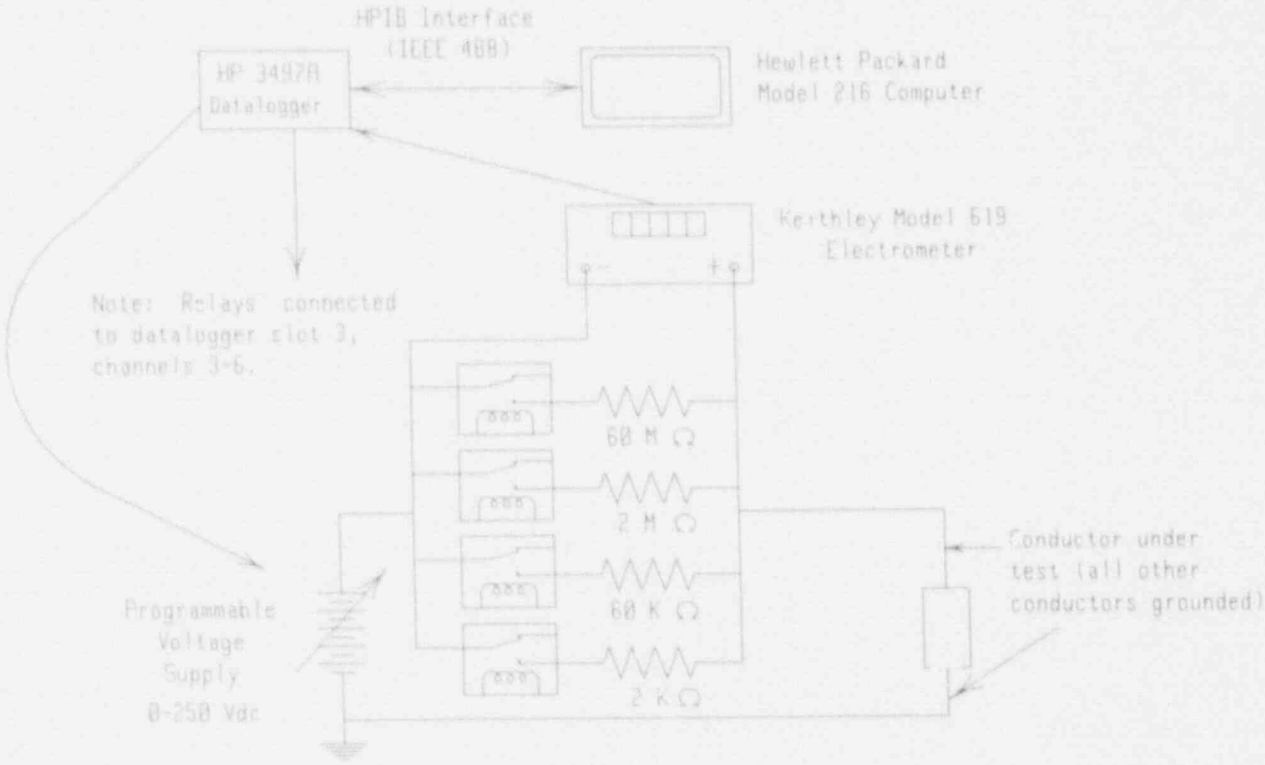

Figure A-1 Circuitry to Measure Insulation Resistance

A.2.1 Operational Description

A given measurement involved the following steps, all performed automatically by the acquisition system:

a. Close the relay connected to the 2 MΩ resistor.
b. Raise the power supply voltage to desired level (50, 100, or 250 V).
c. Perform 3 measurements of the voltage across the 2 MΩ resistor during the first 7 seconds (to assure stability).
d. Change the range of the instrument if necessary by closing the relay connected to the desired measuring resistor and then opening the relay connected to the previous measuring resistor.

e. Perform 2 measurements of the voltage across the dropping resistor during the next 7 seconds (to assure stability).
f. Repeat step d).
g. Measure the voltage across the dropping resistor 10 more times during the next 46 seconds.
h. Measure the actual power supply output voltage.

For a 250 V, 5-minute measurement, the above procedure is used except that 28 measurements are performed during 4 minutes and 46 seconds in step g.

The rules used to perform a dropping resistor change were as follows:

a. If the measured voltage across the dropping resistor is greater than 5 V, then select the next smaller dropping resistor.
b. If the measured voltage across the dropping resistor is less than 0.15 V, then select the next larger dropping resistor.

For 250 V measurements, the above procedure is used except that the 2 kΩ resistor is never used (to prevent excessive currents).

Based on the circuit of Figure A-1, it is evident that if the IR of the cable is not significantly higher than the dropping resistor, the actual voltage applied to the cable will be lower than the nominal. Because of the method of choosing the dropping resistors on-line, the actual voltage is almost always within 10% of nominal except when the cable IR falls below 18 kΩ at 50 V, 18 kΩ at 100 V, or 556 kΩ at 250 V. Based on simple voltage divider calculations, Table A-1 shows the approximate applied voltage on the sample, given the sample IR in kΩ and the nominal applied voltage. Because the IRs in this paper are given on a 100-m basis, the IRs must be converted back to raw data before using Table A-1. This conversion is done by multiplying the IR in Ω-100 m by 100 and dividing by the actual cable length (in meters), which is given in Table 2.

A.2.2 Implementation Problems and Solutions

Probably the major difficulty with implementing the above system is the high IRs that had to be measured. Several techniques, which are not obvious from Figure A-1, are used to overcome the difficulties associated with measuring high impedances. For illustrative purposes, assume that the IR to be measured is 10^{11} Ω at 100 V using the 60 MΩ dropping resistor. This value was exceeded by some cables in our test, even at elevated temperatures. A typical relay has an isolation resistance of 10^9 Ω between open contacts and between open contacts and the coil.

Based on the above, Figure A-2 is a circuit model that includes the input impedance of the Keithley ($5x10^{13}$ Ω), the relay IR across open contacts, and the relay isolation from the coil (which is essentially a ground connection). It should be noted that the relay coils are somewhat isolated from "plant" ground since they use rectified voltages that may float relative to "plant" ground. However, our experience has shown that this additional isolation is not significantly higher than 10^8 Ω. The effect of lack of isolation on the measurement is severe. We now have a parallel path to ground going in a reverse direction through the unused dropping resistors. This parallel path amounts to about $3.3x10^7$ Ω, and the measured IR is then the parallel combination of the specimen and $3.3x10^7$ Ω, or essentially $3.3x10^7$ Ω. This is clearly unacceptable.

These problems were solved using specialized relays that are rated at a minimum isolation of 10^{14} Ω and are capable of switching 200 V at 0.5 A and carrying 1.5 A. The minimum breakdown voltage of the relay is 300 Vac across the contacts and 1000 Vac

from the contacts to the coil. The manufacturer indicated that 250 Vdc and low currents should present no problem for the relatively few switching operations required of the relay in our application. Thus we decided to limit our test voltage to 250 V (initial plans were to go as high as 1000 V using manual instruments) and use these relays.

Table A-1 Actual Applied Voltage as a Function of Sample IR and Nominal Applied Voltage

Sample IR (kΩ)	Nominal Applied Voltage (V) 50	100	250
1000	≥45	≥90	≥225
500	≥45	≥90	223
250	≥45	≥90	200
100	≥45	≥90	155
50	≥45	≥90	112
25	≥45	≥90	72
15	44	88	**
10	42	83	**
5	36	71	**
4	33	67	**
3	30	60	**
2	25	50	**
1	17	33	**
0.8	14	29	**
0.6	12	23	**
0.4	8	17	**
0.2	5	9	**
0.1	2	5	**

** At 250 V, no measurement was possible at these conditions.

In addition to the 250 V limitation imposed by the relays, we were also limited to 250 V by the Keithley electrometer because its inputs must float to the high voltage (see Figure A-2). To work around this limitation, the Keithley could be connected on the low (return) side of the circuit. Unfortunately, there is no real access to the return line as is implied in Figure A-2. The grounded cables and the grounded test chamber form the ground reference for the measurement. As shown in Figure A-3, the return path via the cables is accessible and the return current through the cables could be measured. However, the test chamber is grounded and cannot be isolated. Thus any leakage current to the chamber (i.e., anything except conductor to conductor leakage) would not be detected if the Keithley were on the low side of the circuit.

Many measurement techniques (for both IR and transfer function) discussed in the literature [A-5, A-8, A-10 and A-11], particularly those developed for use on small insulation samples, depend on being able to have neither the cable under test nor the "ground plane" actually grounded, i.e., neither side of the insulation under test is connected to ground. Thus, field implementation of these techniques may be limited by the effect demonstrated in Figure A-3. It may be possible to use highly isolated sources (e.g., batteries) to circumvent the grounding problem, but this is not discussed in the references, nor was it used in this work.

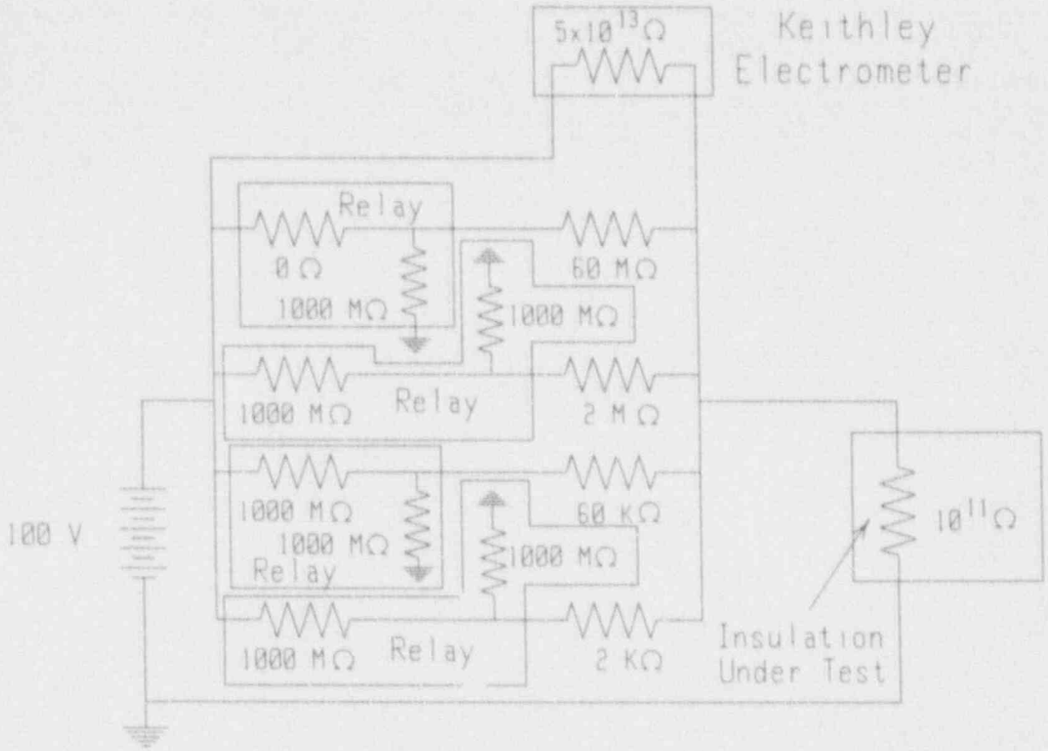

Figure A-2 Circuit Model Showing Device Isolation Resistances

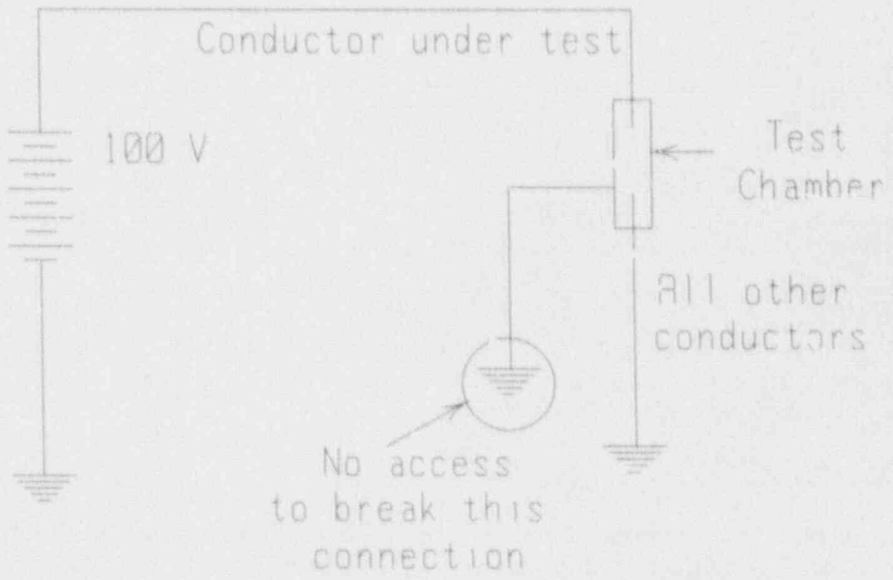

Figure A-3 Effect of Grounds

An additional problem (already solved in Figure A-1) is imposed by the Keithley itself. Anytime a high impedance measurement is being made, the characteristic impedances of the measuring device must be considered. The differential input impedance of the Keithley ($5x10^{13}$ Ω) is sufficient for accurate measurements even when the 60 MΩ dropping resistor is used. However, the impedance from the negative terminal of the Keithley to ground is only specified at 10^8 Ω. A model for the "normal" connection of the Keithley in this circuit is shown in Figure A-4. As can be seen from this figure, the impedance of 10^8 Ω acts in parallel with the cable under test and again would essentially destroy the measurement. In Figure A-1, the Keithley is connected in reverse of what would normally be expected, i.e., it measures negative voltages. In the case of reversed leads, the differential input impedance of $5x10^{13}$ Ω becomes the minimum IR to ground in parallel with the cable. The 10^8 Ω resistance simply becomes a shunt across the power supply and has essentially no effect on the measurement. When connected in this configuration, the effect of the Keithley input impedance is on the order of 2% or less at cable IRs of 10^{12} Ω. This is one of several effects that limit the upper range of our measurements.

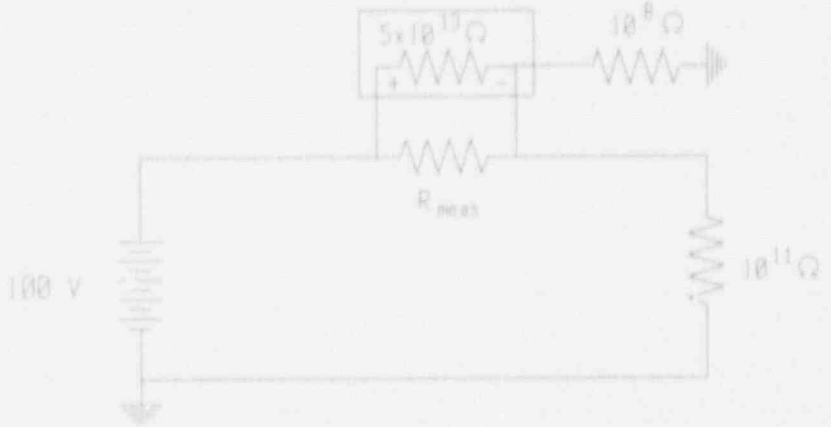

Figure A-4 Model for Normal Keithley Connection

A reasonable estimate of the maximum capability of our instrumentation as configured may be found from baseline open circuit measurements. The typical minimum IR of the open circuit is $5x10^{12}$ Ω. This IR includes limitations from aspects discussed above, interconnecting wire contributions, and inherent instrument limitations. Without using any type of baseline correction, the open circuit IR is expected to cause errors of about 20% when measuring IRs of $1x10^{12}$ Ω, or less than 2% when making typical measurements at $1x10^{11}$ Ω or below.

A.3 TRANSFER FUNCTION

The transfer function is measured using the circuit shown schematically in Figure A-5. Two different instruments are used to make the transfer function measurements, both being controlled by a Hewlett Packard Model 216 computer. At "higher" frequencies, over an effective range from about 100 to 500 kHz, the LF Analyzer is used (obviously we have different perspectives of "low" frequency than Hewlett Packard). This instrument uses an oscillator to excite the device under test in combination with a vector voltmeter to detect the complex voltage applied to the specimen and a vector ammeter to detect the complex current through the specimen. A four terminal network is used to

make the measurement, which may be displayed in a variety of formats (i.e., capacitance, dissipation factor, conductance, magnitude and angle, etc.). This instrument is capable of making measurements on a cable even when one side of the insulation under test is at ground potential. However, it should be noted that different results are obtained when one side is grounded as compared to having both sides floating. The reason for this behavior is illustrated in Figure A-6. In Figure A-6(a), neither side of the cable is grounded and the measurement is just the series combination of the two insulations between the conductors. In Figure A-6(b), with conductor #2 grounded, an additional path is introduced in parallel with the conductor #2 insulation to ground. This parallel path, which includes the jacket of multiconductor cables, consists of any paths to ground from conductor #1 except the path through the insulation of conductor #2. The significance of this path is particularly pronounced for single conductor cables which rely heavily on the parallel path to form a ground plane for the measurements. It should be noted that the effects illustrated in Figure A-6 apply to any type of electrical measurement.

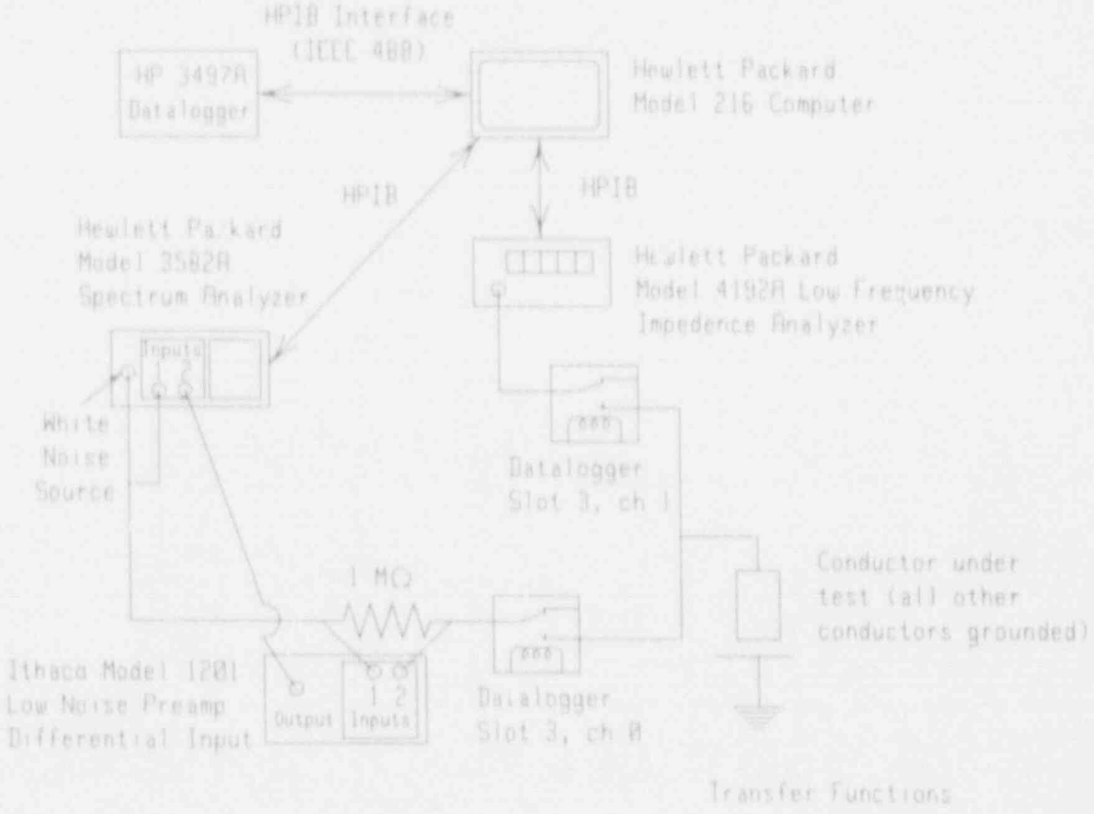

Figure A-5 Schematic of Transfer Function Measurement Circuitry

At lower frequencies, over an effective range from about 0.3 to 200 Hz, a Hewlett Packard Model 3582A spectrum analyzer (SA), driven by a white noise source is used. The white noise is provided by the spectrum analyzer and is fed to channel A of the analyzer. The input to channel B of the analyzer is from the signal across the nominal 1 MΩ resistor in series with the cable. The spectrum analyzer obtains the Fast Fourier Transform (FFT) of the transfer function between V_{in} and V_{out} and transmits the amplitude ratio and phase difference between V_{in} and V_{out} to the computer. These data are then processed by the computer to provide measures of capacitance and dissipation factor (as a function of frequency) of the cable under test.

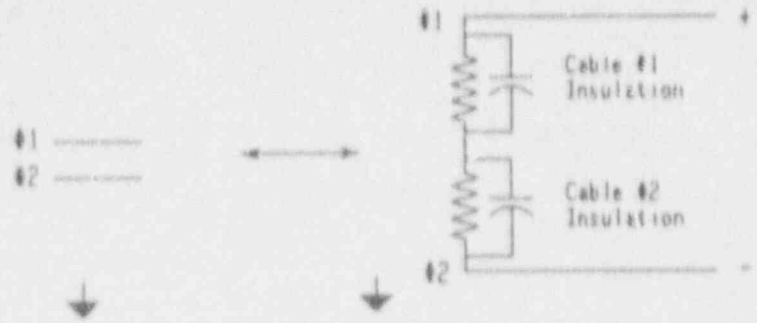

(a) Ungrounded

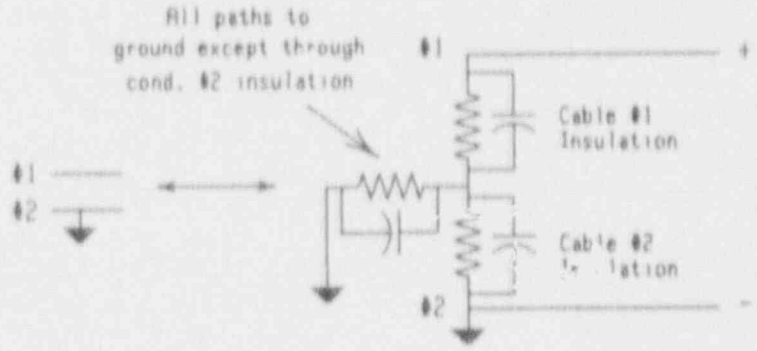

(b) Grounded

Figure A-6 Comparison of Ungrounded and Grounded Configurations

The preamplifier shown in Figure A-5 is used in the voltage follower mode (output=input). The preamplifier has an input impedance of greater than 10^9 Ω in the differential mode and a input capacitance of about 8 pF. The input capacitance of the preamplifier limits the upper frequency for effective measurements using the spectrum analyzer. For example, at 1000 Hz, impedance due to the capacitance is $1/(2 * \pi * f * C) = 1 / (2 * \pi * 1000 * 8x10^{-12}) = 20x10^6$ Ω. As this impedance is a factor of 20 above the nominal 1 MΩ resistor, it would only be expected to create errors on the order of 5%. However, in practice the phase shift associated with the capacitance can cause additional difficulty.

We were able to obtain dissipation factor data from the LF analyzer down as low as 30 Hz (by changing the instrument settings to display conductance rather than dissipation factor), but the data is somewhat variable and unreliable and the LF analyzer generally did not make effective dissipation factor measurements below about 100 Hz. To provide a reasonable overlap region for comparison with the LF measurements, we wanted the SA system to make measurements up in the range of 1000 Hz. After correcting the data reduction routines for the amplifier input capacitance, we discovered that a more significant problem is that the calculation of dissipation factor from the spectrum analyzer data becomes extremely sensitive at higher frequencies. Thus, the two independent dissipation factor measurements are each least accurate in the overlap region. When calculating capacitance, the sensitivity and amplifier input impedance problems are not very important and good agreement in the overlap region can be expected.

A.4 REFERENCES

A-1. Stone, G. C. and M. Kurtz, "Interpretations of Megohmmeter Tests on Electrical Apparatus and Circuits," *IEEE Electrical Insulation Magazine,* Vol. 2, p. 14, January 1986.

A-2. Reynolds, P. H., "Conventional Cable Testing Methods: Strengths, Weaknesses and Possibilities," Appears in *Proceedings: Workshop on Power Plant Cable Condition Monitoring*, EPRI EL/NP/CS-5914-SR, Electric Power Research Institute, July 1988.

A-3. Sugarman, A., B. Kumar, and R. Sorensen, "Condition Monitoring of Nuclear Plant Electrical Equipment," EPRI NP-3357, Research Project 1707-9, NUTECH Engineers, San Jose, California, February 1984.

A-4. IEEE Std. 62-1978, "IEEE Guide for Field Testing Power Apparatus Insulation," The Institute of Electrical and Electronic Engineers, Inc., 1978.

A-5. ASTM D150-81, "A-C Loss Characteristics and Permittivity (Dielectric Constant) of Solid Electrical Insulating Materials," American Society for Testing and Materials, 1981.

A-6. Bartnikas, R., editor, *Engineering Dielectrics, Volume IIB, Electrical Properties of Solid Insulating Materials: Measurement Techniques,* American Society for Testing and Materials Special Technical Publication 926, 1987.

A-7. Rene Seeberger, "Capacitance and Dissipation Factor Measurements," *IEEE Electrical Insulation Magazine,* Vol. 2, p. 14, January 1986.

A-8. Mopsik, F. I., "Precision Time-Domain Dielectric Spectrometer," *Rev. Sci. Instrum.,* Vol. 55, p. 79, 1984.

A-9. Mopsik, F. I., "The Transformation of Time-Domain Relaxation Data Into the Frequency Domain," *IEEE Transactions on Electrical Insulation,* Vol. EI-20, p. 957, 1985.

A-10. ANSI/ASTM D257-78, "D-C Resistance of Conductance of Insulating Materials," American Society for Testing and Materials, 1978.

A-11. IEEE Std. 402-1974, "IEEE Guide for Measuring Resistivity of Cable-Insulation Materials at High Direct Voltages," The Institute of Electrical and Electronic Engineers, Inc., 1974.

Appendix B Thermal and Radiation Data

This appendix gives radiation and thermal aging exposure data for the cables in each test chamber. The temperature data was normally recorded hourly. On several occasions over the long-term exposures, data was lost from the mass storage medium of the computer (see summary of test anomalies in Appendix J). However, review of daily logs indicated that temperatures did not deviate significantly from the trends shown in the figures. The sample ID numbers used in Table B-1 correspond to those given in Table 3. Also included in this appendix is transient temperature data from each accident simulation.

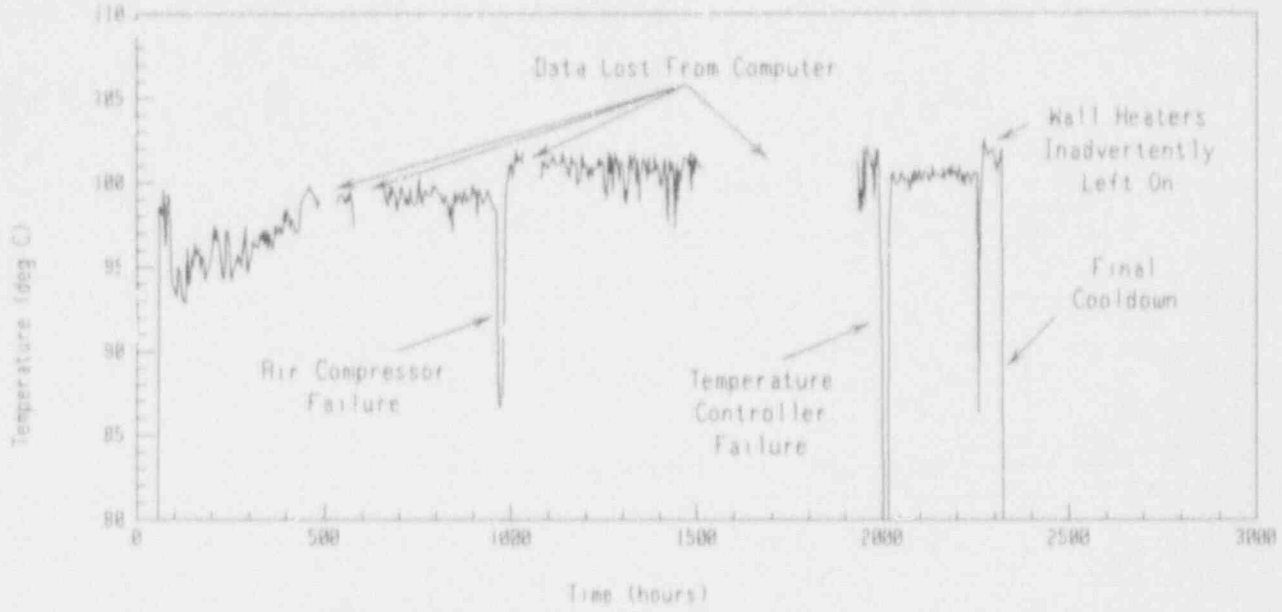

Figure B-1 Average Temperature During Aging--3-Month Chamber

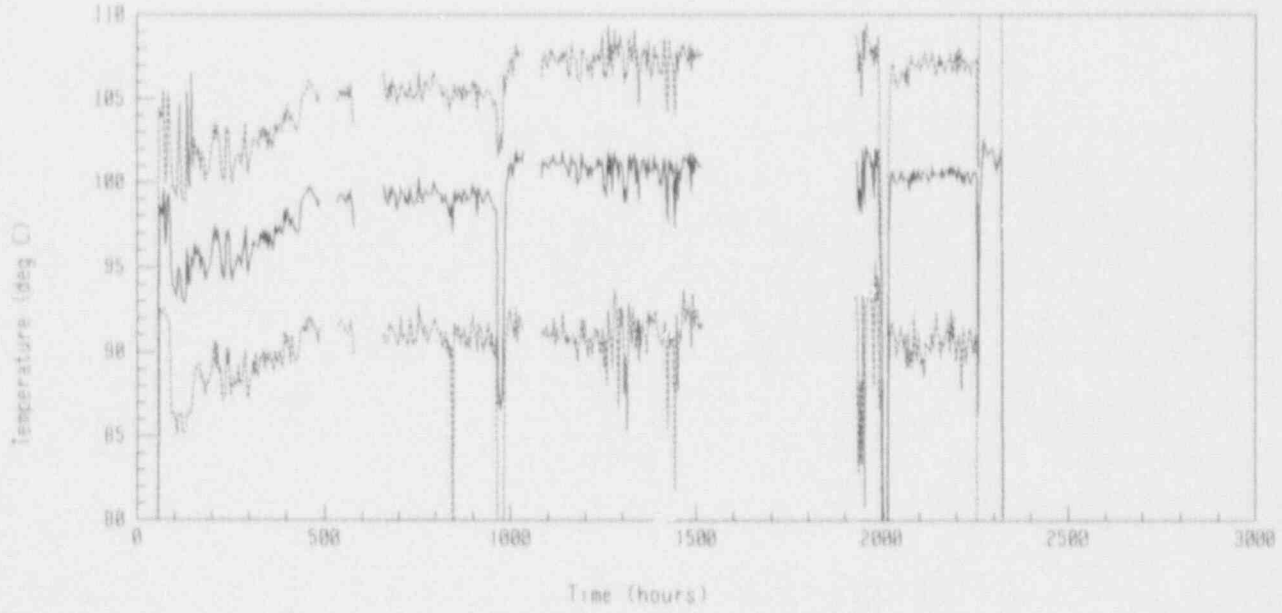

Figure B-2 Average, Minimum, and Maximum Temperature During Aging--3-Month Chamber

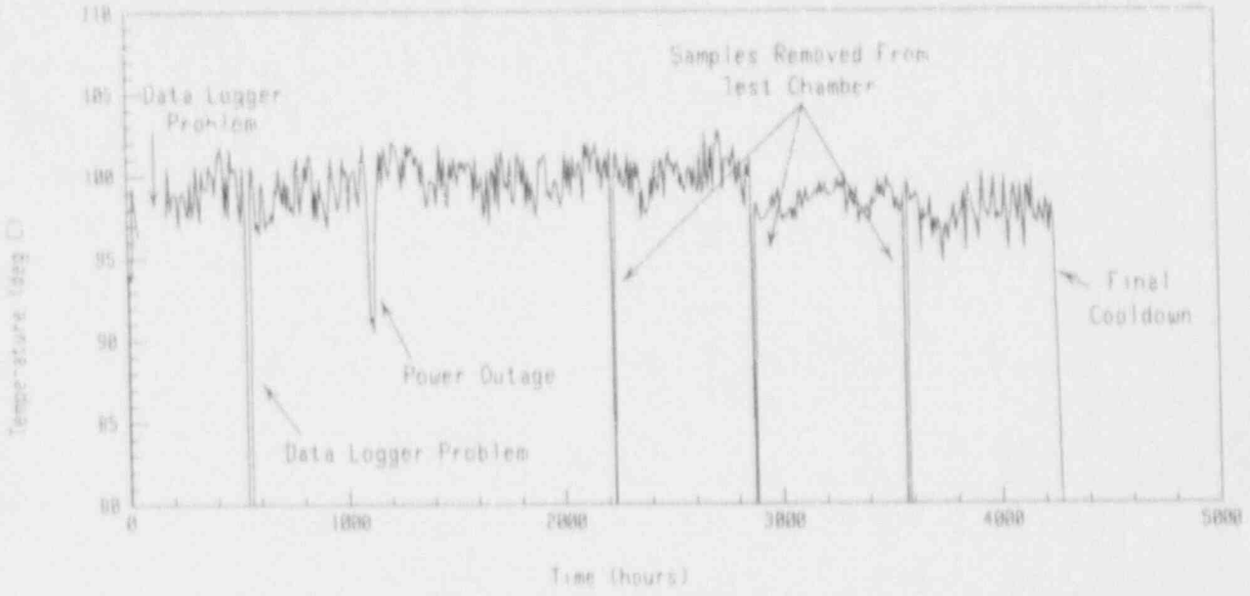

Figure B-3 Average Temperature During Aging--6-Month Chamber

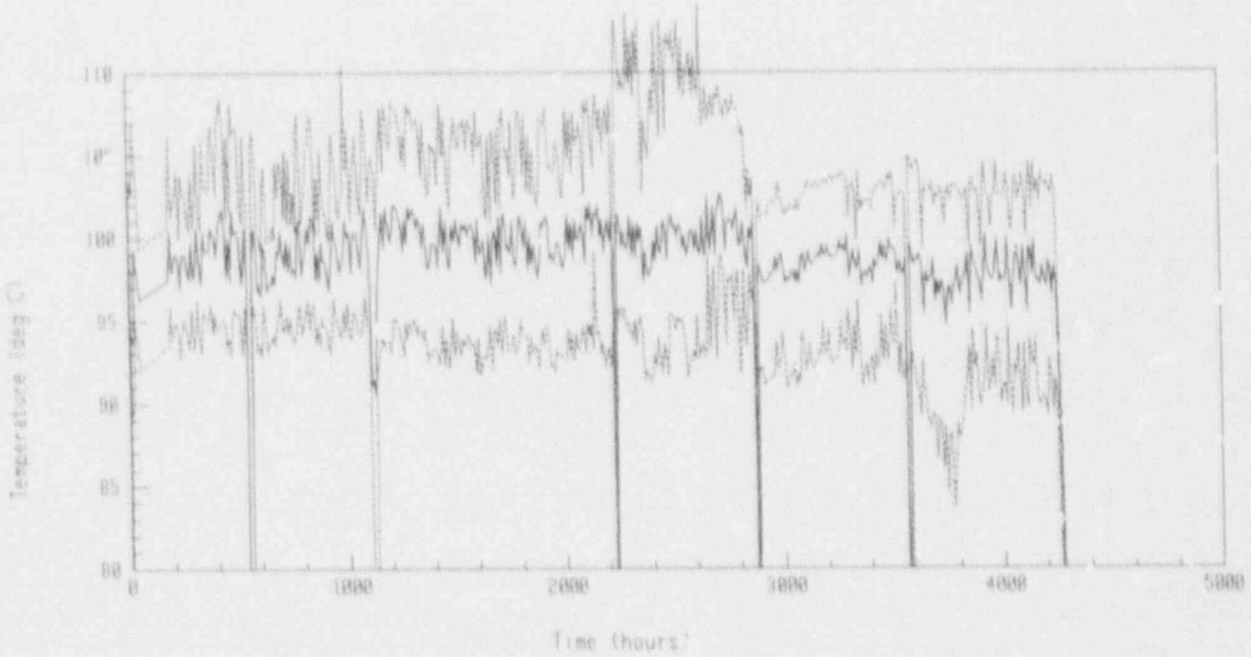

Figure B-4 Average, Minimum, and Maximum Temperature During Aging--6-Month Chamber

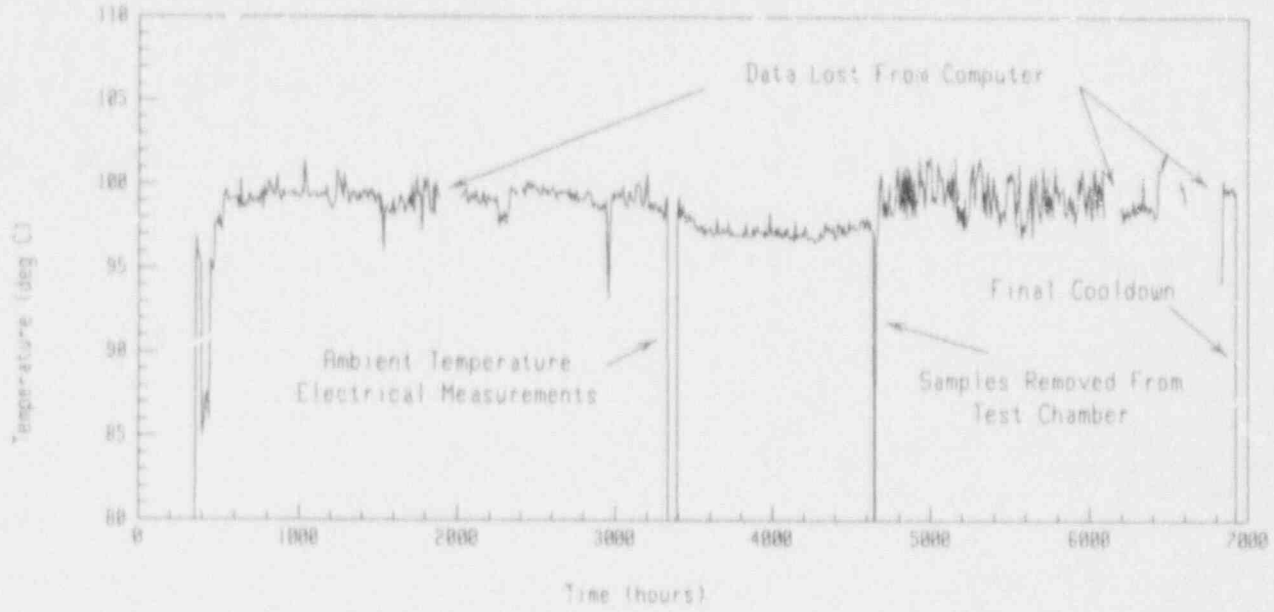

Figure B-5 Average Temperature During Aging--9-Month Chamber

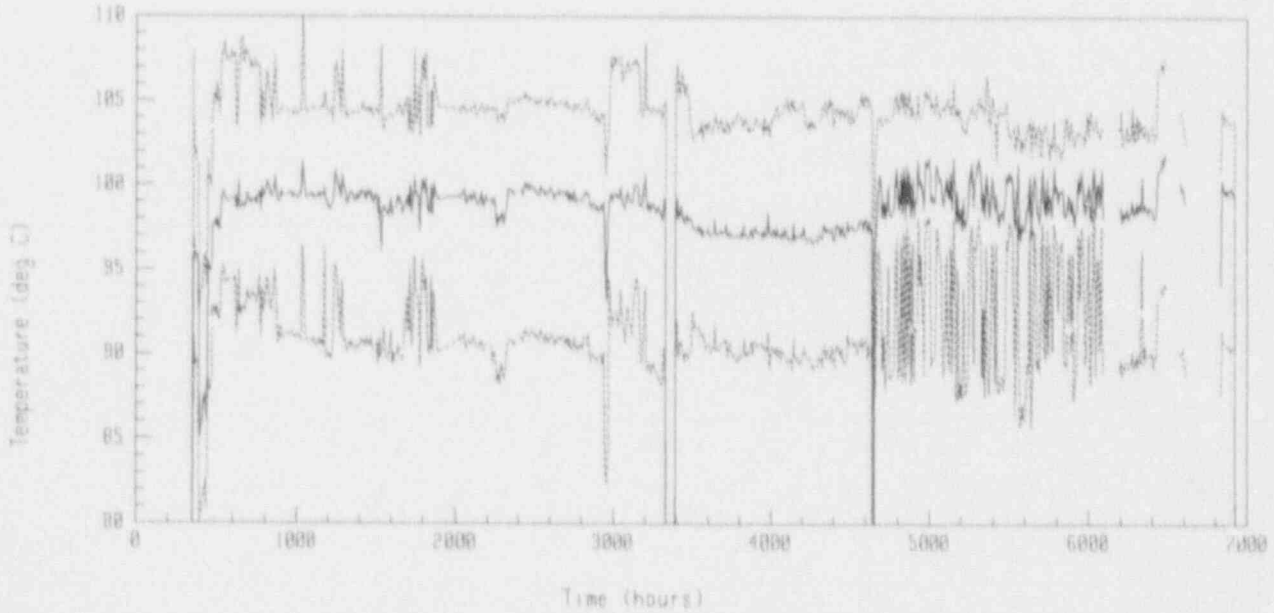

Figure B-6 Average, Minimum, and Maximum Temperature During Aging--9-Month Chamber

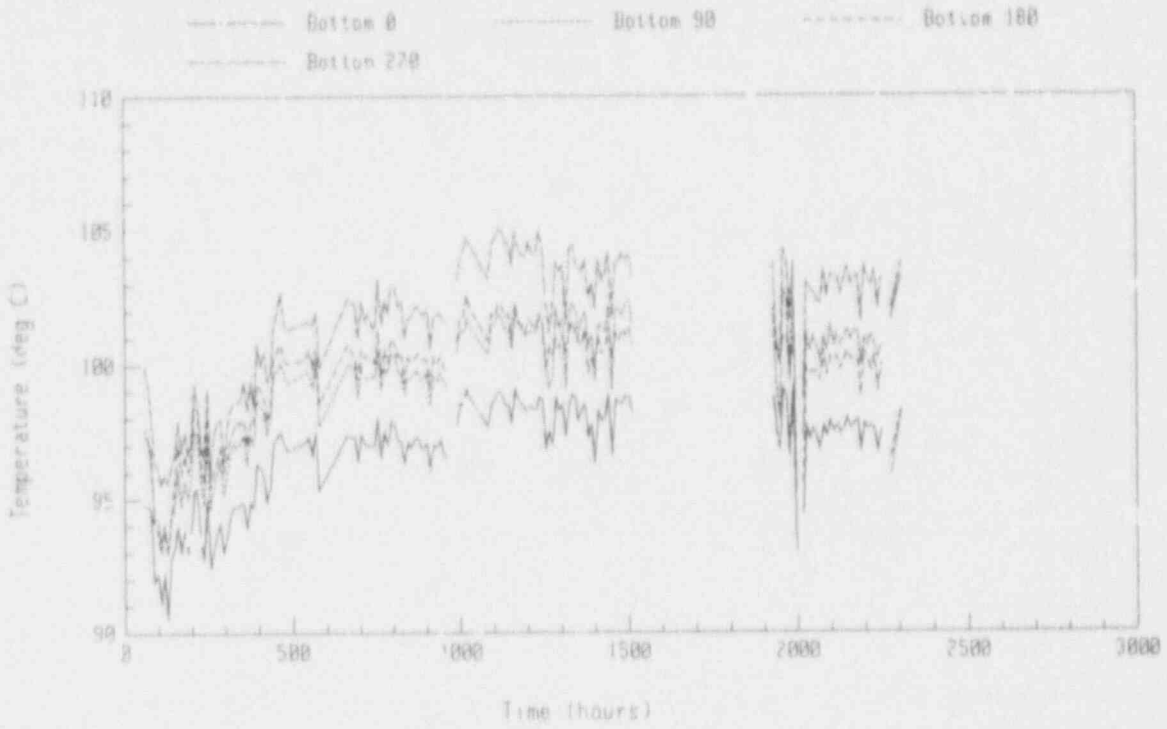

Figure B-7 Temperatures at Bottom of 3-Month Chamber During Aging

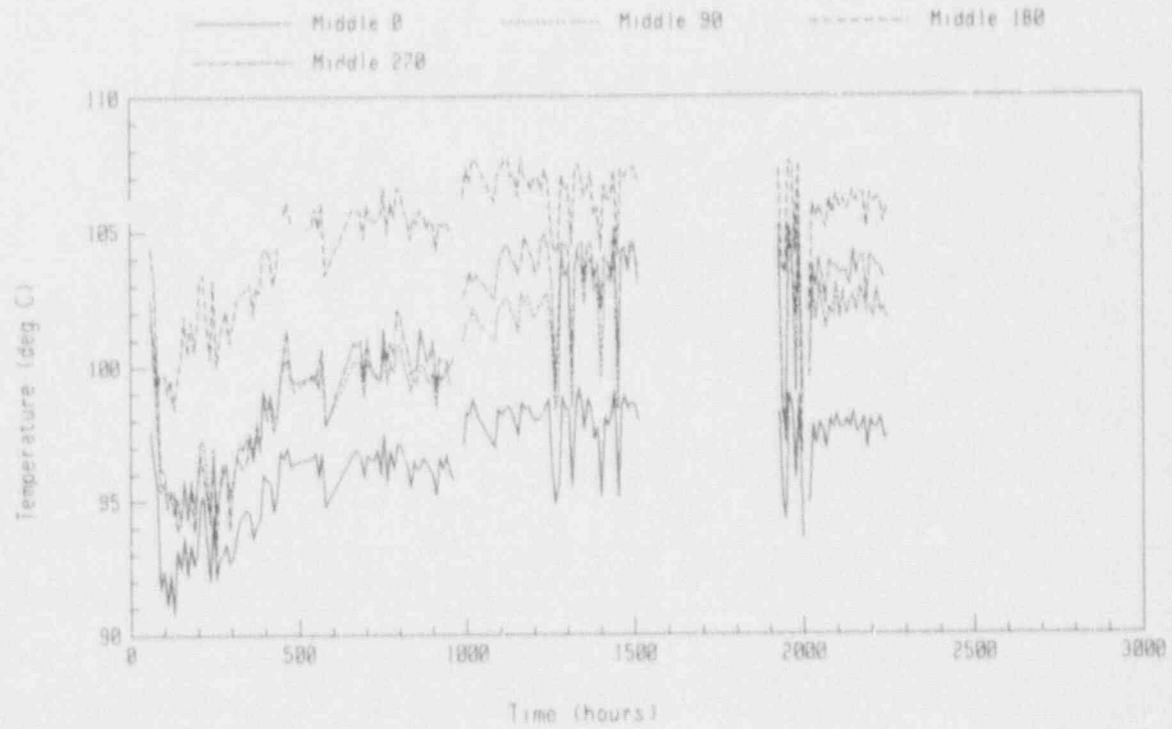

Figure B-8 Temperatures at Middle of 3-Month Chamber During Aging

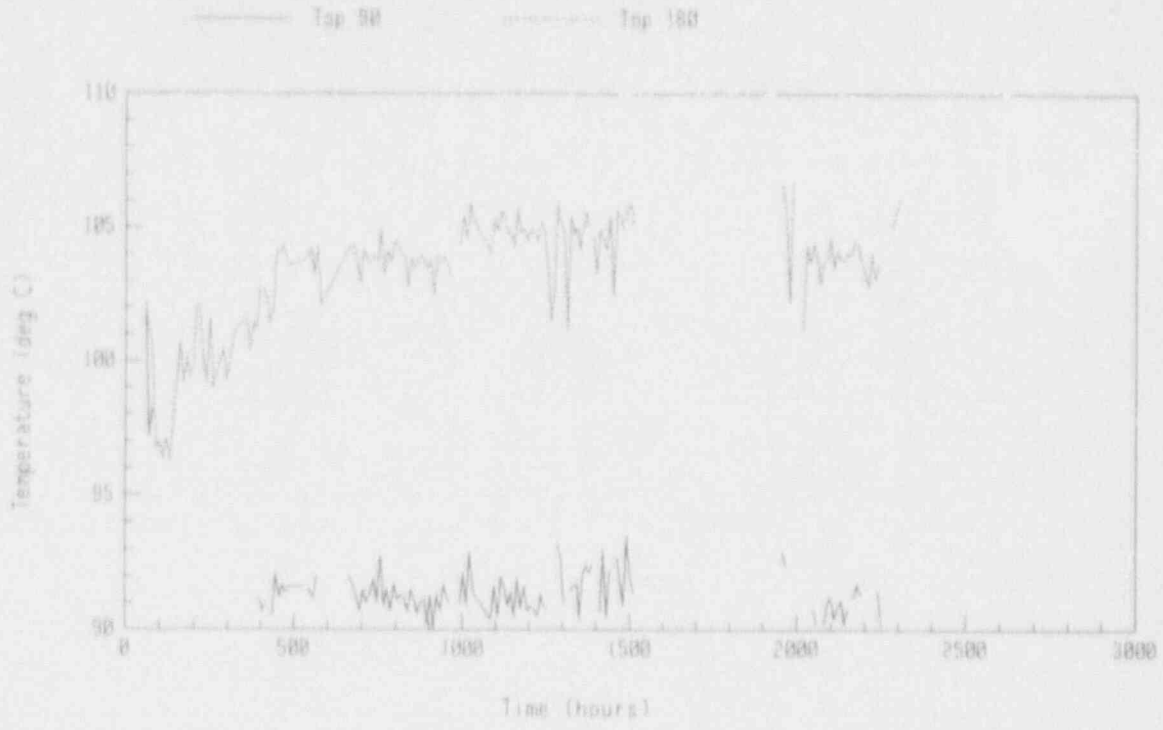

Figure B-9 Temperatures at Top of 3-Month Chamber During Aging

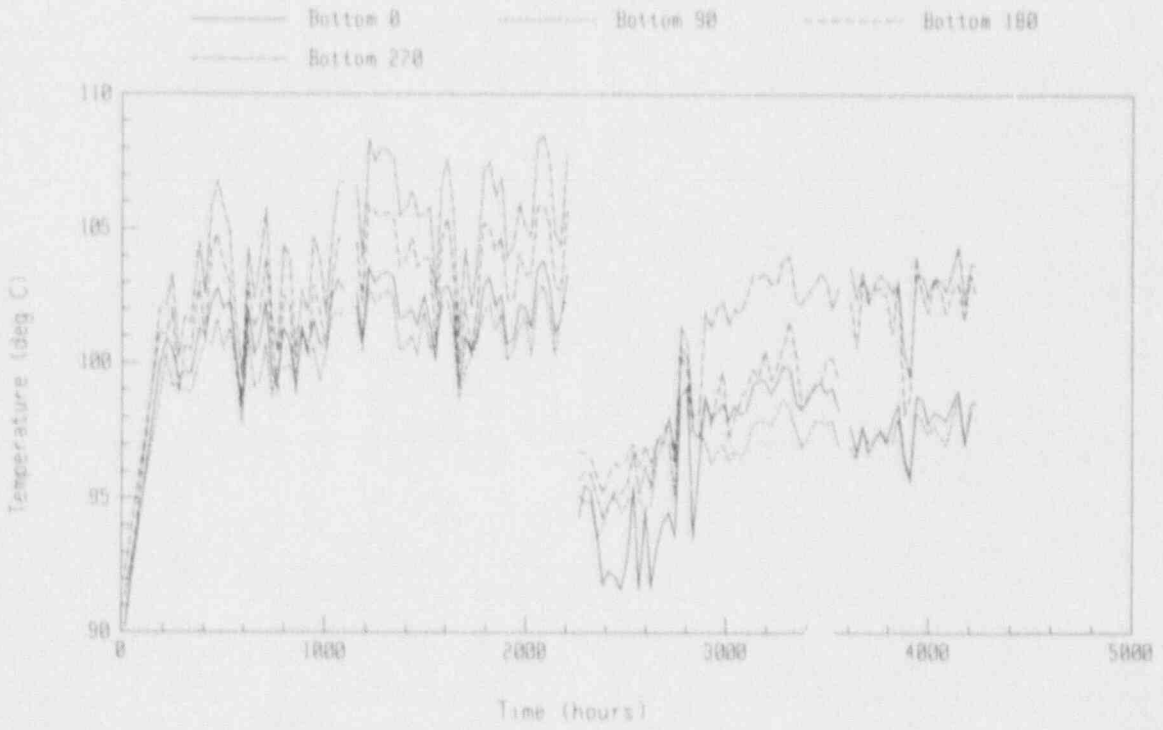

Figure B-10 Temperatures at Bottom of 6-Month Chamber During Aging

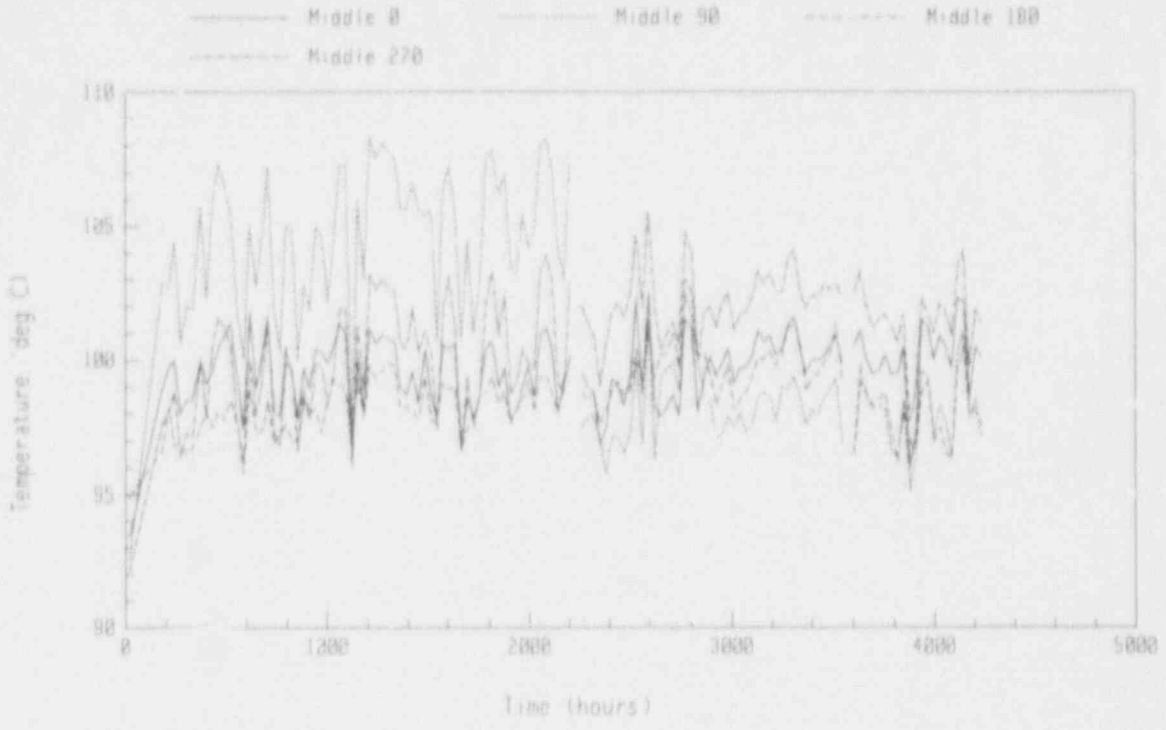

Figure B-11 Temperatures at Middle of 6-Month Chamber During Aging

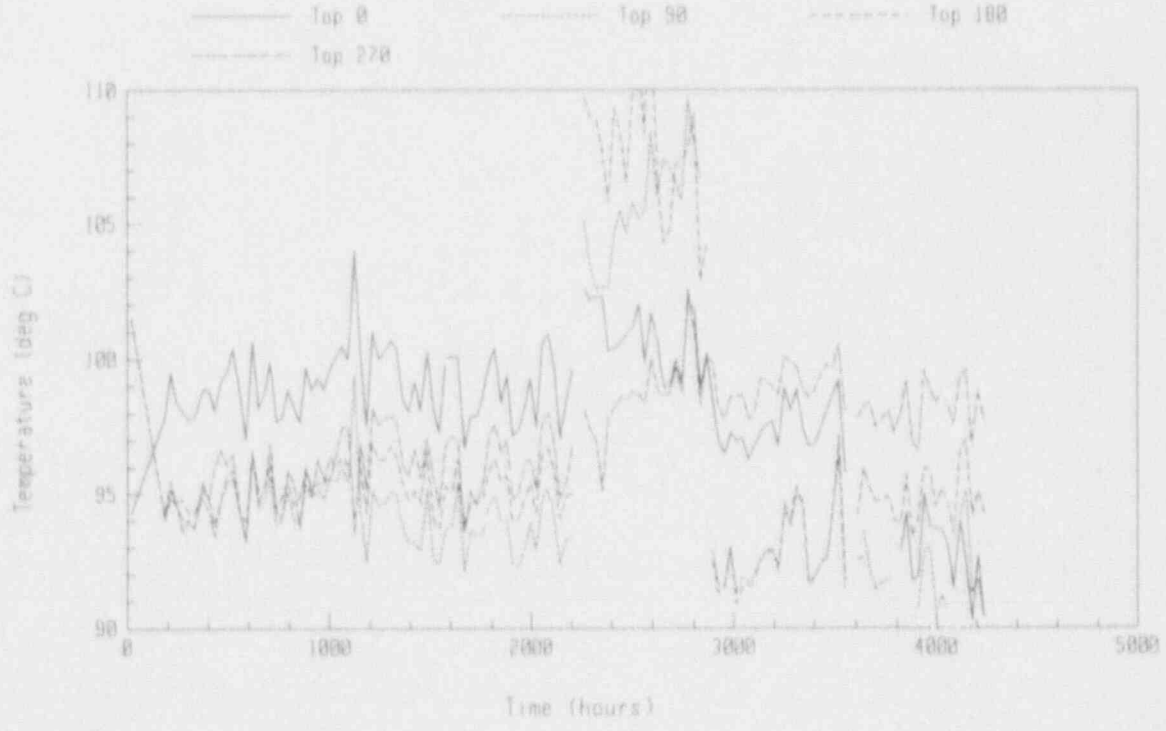

Figure B-12 Temperatures at Top of 6-Month Chamber During Aging

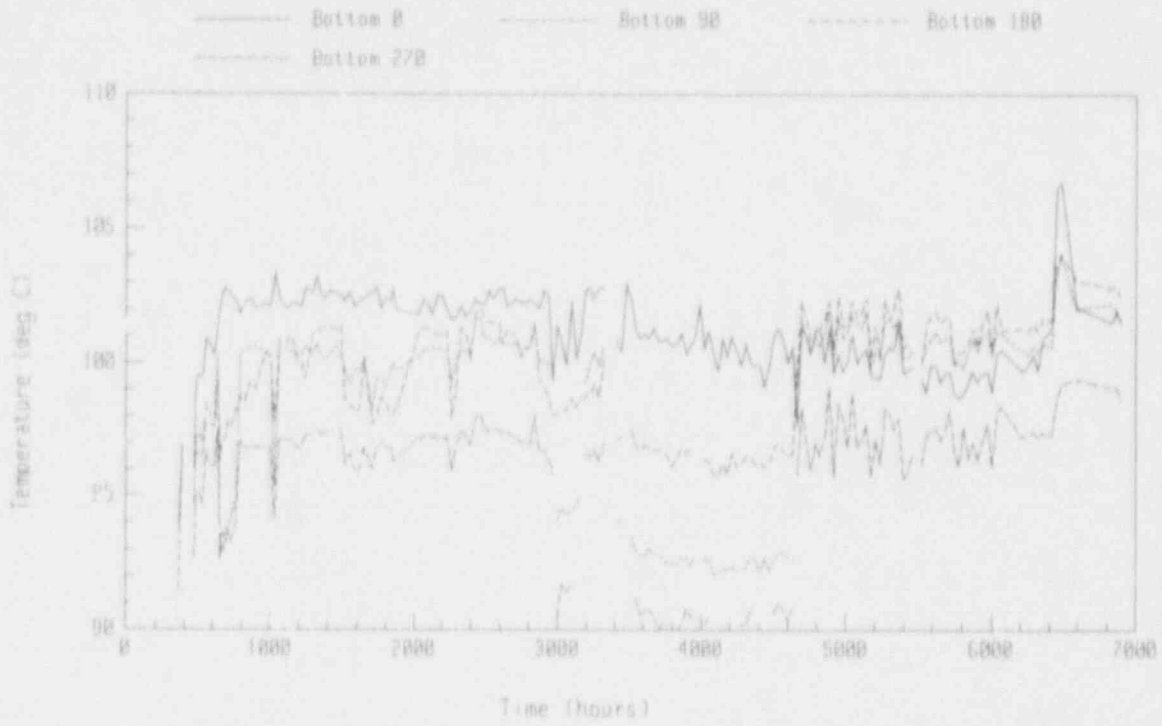

Figure B-13 Temperatures at Bottom of 9-Month Chamber During Aging

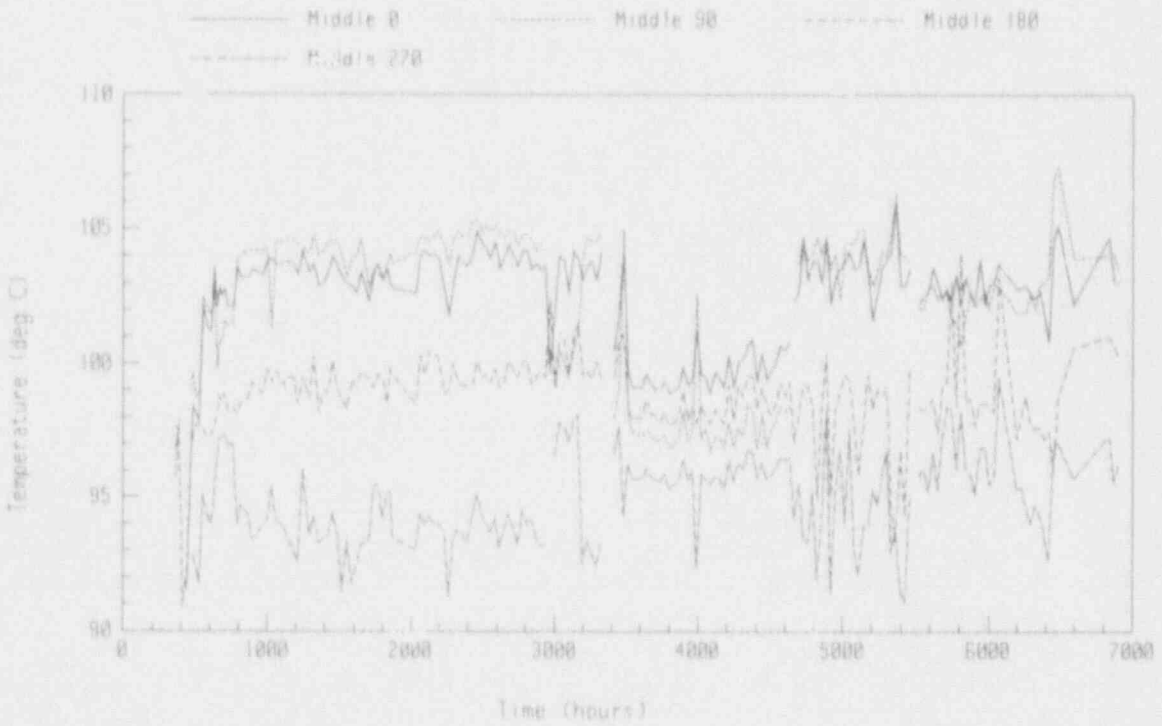

Figure B-14 Temperatures at Middle of 9-Month Chamber During Aging

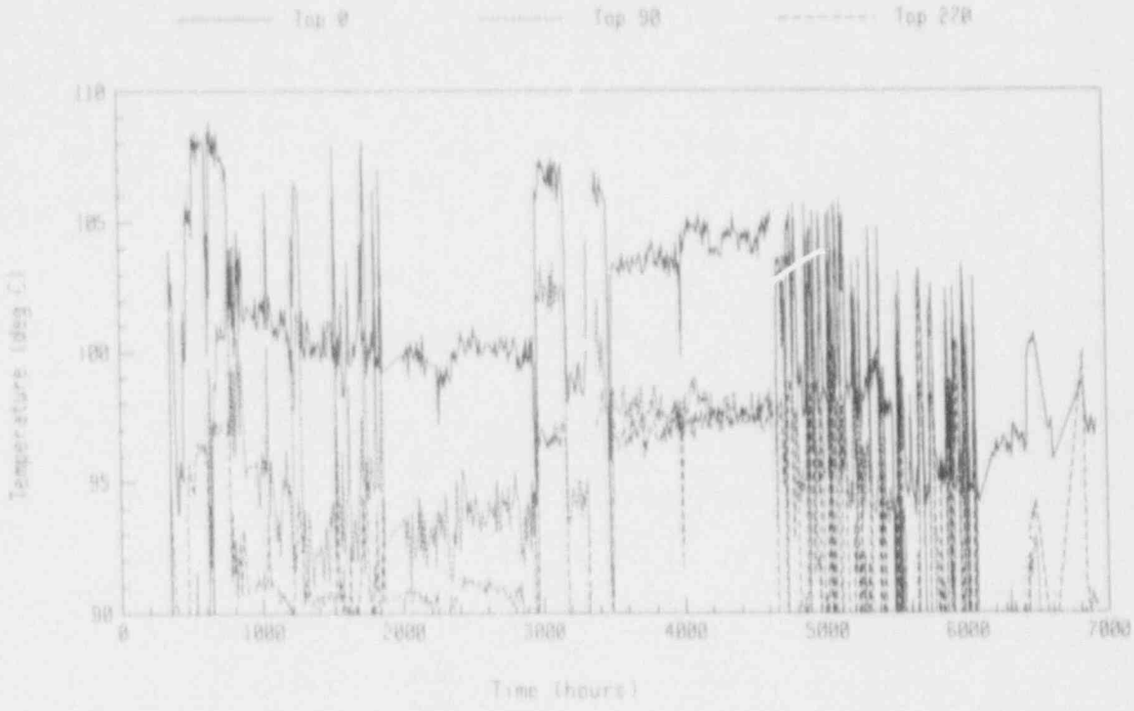

Figure B-15 Temperatures at Top of 9-Month Chamber During Aging

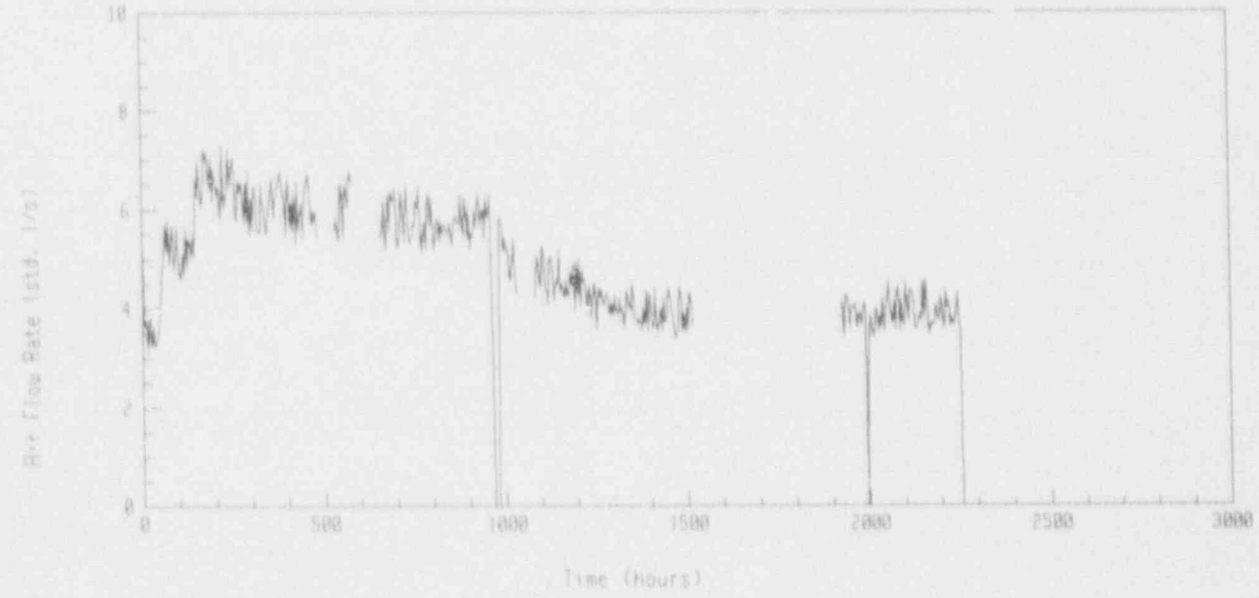

Figure B-16 Air Flow Rate During Aging--3-Month Chamber

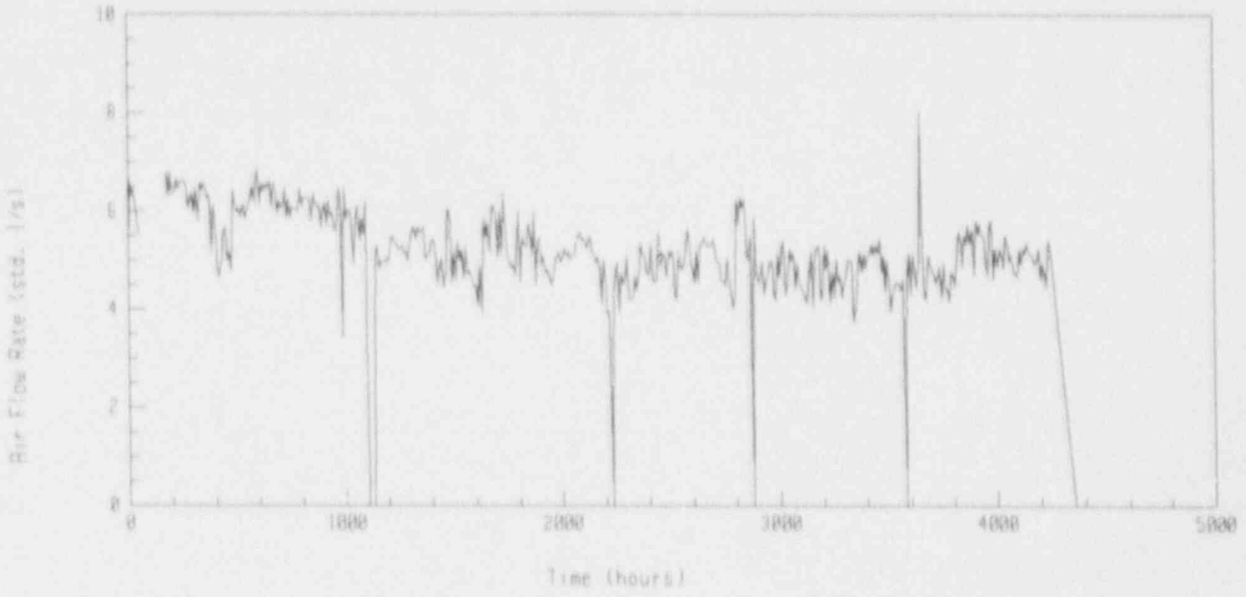

Figure B-17 Air Flow Rate During Aging--6-Month Chamber

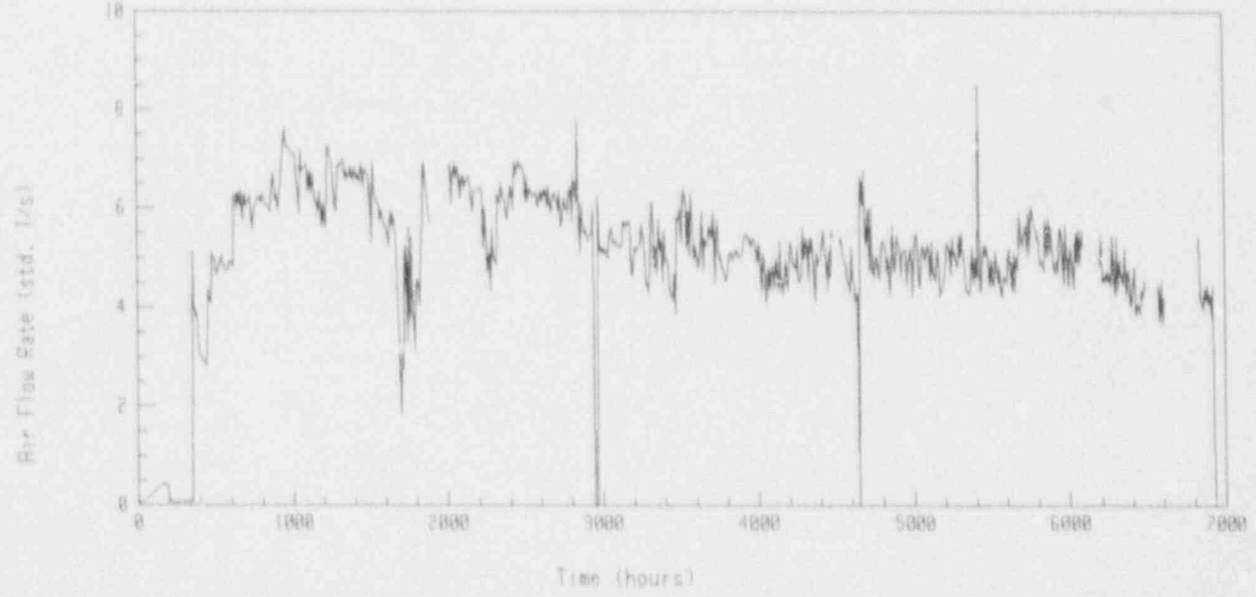

Figure B-18 Air Flow Rate During Aging--9-Month Chamber

Table B-1 Exposure Data for 15-cm. Insulation Specimens

Sample ID	Aging Dose Rate 1 (Gy/hr)	Aging Dose Rate 2 (Gy/hr)	Accident Dose Rate (kGy/hr)	Total Dose (kGy)
Brand Rex				
1-3-3	0	71.8	0	157
1-3-3R	0	74.8	4.33	1070
1-6-1	0	64.6	0	47.9
1-6-2	0	58.3	0	83.6
1-6-3L	0	61.8	0	128
1-6-3F	45.9	0	0	110
1-6-4	49.6	59.3	0	157
1-6-5	41.4	65.6	0	186
1-6-6	48.8	58.9	0	239
1-6-6R	44.3	62.5	4.58	1120
1-6-R	0	0	4.36	876
1-9-1	0	34.9	0	26.7
1-9-2	0	38.7	0	55.5
1-9-3	0	36	0	81.6
1-9-6	85.5	36.9	0	319
1-9-7	82.5	39.8	0	346
1-9-8	87.1	35.8	0	377
1-9-9	77.7	44.5	0	405
1-9-9R	82	40.2	4.56	1280
Rockbestos				
2-3-3	0	74.5	0	163
2-3-3R	0	79.5	4.35	1080
2-6-1	0	67.4	0	50
2-6-2	0	71	0	102
2-6-3L	0	69.9	0	145
2-6-3F	35.6	0	0	85.2
2-6-4	34.2	72.2	0	128
2-6-5	37.7	68.5	0	182
2-6-6	43.7	63.2	0	236
2-6-6R	40.4	65.6	4.59	1110
2-6-R	0	0	4.57	878
2-9-1	0	35.6	0	27.2
2-9-2	0	37.6	0	53.9
2-9-3	0	36.7	0	83.2
2-9-6	88.8	37.7	0	331
2-9-7	89.3	38.6	0	366
2-9-8	88.1	36.5	0	382
2-9-9	78.3	45.4	0	410
2-9-9R	82.4	41.7	4.56	1290

Table B-1 Exposure Data for 15-cm. Insulation Specimens (cont)

Sample ID	Aging Dose Rate 1 (Gy/hr)	Aging Dose Rate 2 (Gy/hr)	Accident Dose Rate (kGy/hr)	Total Dose (kGy)
Raychem				
3-3-3	0	65	0	142
3-3-3R	0	68.1	4.38	1060
3-6-1	0	77.2	0	57.2
3-6-2	0	75.2	0	108
3-6-3L	0	78	0	162
3-6-3F	57.2	0	0	137
3-6-4	60.6	76.4	0	194
3-6-5	53.7	78.4	0	233
3-6-6	56	69	0	277
3-6-6R	56.9	72.7	4.71	1190
3-6-R	0	0	4.66	896
3-9-1	0	73.3	0	56
3-9-2	0	77.8	0	112
3-9-3	0	77	0	175
3-9-6	52.7	79.1	0	267
3-9-7	48.8	79.9	0	322
3-9-8	57	75.2	0	389
3-9-9	55.6	70.4	0	425
3-9-9R	53.7	73.7	4.57	1310
Polyset				
4-3-3	0	77.8	0	170
4-3-3R	0	82.2	4.37	1090
4-6-1	0	74.1	0	54.9
4-6-2	0	72.4	0	104
4-6-3L	0	74.3	0	154
4-6-3F	31.8	0	0	76.1
4-6-4	32.7	73.6	0	126
4-6-5	32.2	75.2	0	177
4-6-6	40.9	66.2	0	235
4-6-6R	36.1	69.8	4.62	1120
4-6-R	0	0	4.59	881
4-9-1	0	45.6	0	34.9
4-9-2	0	39.6	0	56.7
4-9-3	0	42.5	0	96.3
4-9-6	88.6	43.6	0	338
4-9-7	89.1	40.6	0	369
4-9-8	86.4	46.8	0	405
4-9-9	78.2	48.1	0	419
4-9-9R	83.5	44.7	4.57	1300

Table B-2 Exposure Data for 15-cm. Jacket Specimens

Sample ID	Aging Dose Rate 1 (Gy/hr)	Aging Dose Rate 2 (Gy/hr)	Accident Dose Rate (kGy/hr)	Total Dose (kGy)
Brand Rex				
1-3-3	0	66.1	0	144
1-3-3R	0	71.6	4.35	1070
1-6-1	0	48.6	0	36.1
1-6-2	0	54.1	0	77.5
1-6-3L	0	52.5	0	109
1-6-3F	57.5	0	0	138
1-6-4	55	55	0	167
1-6-5	61.3	49.4	0	213
1-6-6	59.9	49.7	0	247
1-6-6R	59.3	50.4	4.57	1120
1-6-R	0	0	4.55	875
1-9-1	0	43.8	0	33.5
1-9-2	0	40.9	0	58.7
1-9-3	0	41.2	0	93.5
1-9-6	82.5	42.3	0	317
1-9-7	81.4	42	0	348
1-9-8	81.1	45	0	383
1-9-9	74.1	50.4	0	414
1-9-9R	77.1	47.2	4.6	1300
Rockbestos				
2-3-3	0	61.8	0	135
2-3-3R	0	68.3	4.38	1070
2-6-1	0	45	0	33.4
2-6-2	0	41.6	0	59.6
2-6-3L	0	38.2	0	79.3
2-6-3F	73.5	0	0	176
2-6-4	69.5	42.3	0	194
2-6-5	65.6	45.7	0	218
2-6-6	66.7	43.8	0	250
2-6-6R	68.3	42.7	4.6	1140
2-6-R	0	0	4.56	877
2-9-1	0	45.9	0	35.1
2-9-2	0	48.8	0	69.9
2-9-3	0	52.9	0	120
2-9-6	80.7	54.3	0	326
2-9-7	82	50.1	0	366
2-9-8	81.8	47.2	0	391
2-9-9	72.1	55.9	0	427
2-9-9R	77.1	52.5	4.67	1330

Table B-2 Exposure Data for 15-cm. Jacket Specimens (cont)

Sample ID	Aging Dose Rate 1 (Gy/hr)	Aging Dose Rate 2 (Gy/hr)	Accident Dose Rate (kGy/hr)	Total Dose (kGy)
Polyset				
4-3-3	0	55.9	0	122
4-3-3R	0	59.3	4.42	1050
4-6-1	0	36.2	0	26.9
4-6-2	0	34.6	0	49.6
4-6-3L	0	32.3	0	66.9
4-6-3F	80.2	0	0	192
4-6-4	77.1	35.2	0	207
4-6-5	75.2	36.8	0	229
4-6-6	70.1	40.6	0	252
4-6-6R	73.4	37.8	4.59	1140
4-6-R	0	0	4.56	876
4-9-1	0	55.8	0	42.7
4-9-2	0	59.6	0	85.5
4-9-3	0	63.4	0	144
4-9-6	73.5	65.1	0	316
4-9-7	75.1	61.2	0	367
4-9-8	77.8	57.3	0	406
4-9-9	68.2	61.5	0	434
4-9-9R	72.1	60.5	4.68	1340

Table B-3 Exposure Data for 36-cm. Single Conductor Specimens

Sample ID	Aging Dose Rate 1 (Gy/hr)	Aging Dose Rate 2 (Gy/hr)	Accident Dose Rate (kGy/hr)	Total Dose (kGy)
Brand Rex				
1-3-3	0	74.4	0	162
1-3-3R	0	77.1	4.75	1160
1-6-1	0	57.8	0	42.9
1-6-2	0	54.9	0	78.6
1-6-3L	0	52.6	0	109
1-6-3F	71.8	0	0	172
1-6-4	60.7	55.7	0	181
1-6-5	56.5	58.7	0	214
1-6-6	59.5	55.3	0	257
1-6-6R	60	55.2	5.01	1220
1-6-R	0	0	4.99	959
1-9-1	0	46.6	0	35.7
1-9-2	0	48.2	0	69.1
1-9-3	0	80.5	0	183
1-9-6	54.5	82.7	0	277
1-9-7	89.4	49.5	0	388
1-9-8	89.2	47.9	0	417
1-9-9	83	54.4	0	456
1-9-9R	86.1	51.5	5.04	1430
Rockbestos				
2-3-3	0	72.6	0	159
2-3-3R	0	74.8	4.77	1160
2-6-1	0	47.9	0	35.5
2-6-2	0	47.8	0	68.4
2-6-3L	0	52.2	0	108
2-6-3F	64.1	0	0	153
2-6-4	81.2	48.5	0	225
2-6-5	68.4	48.7	0	229
2-6-6	65.5	50.3	0	261
2-6-6R	65.3	50.9	5.02	1230
2-6-R	0	0	5	962
2-9-1	0	52.2	0	40
2-9-2	0	91.5	0	131
2-9-3	0	50.5	0	115
2-9-6	88.9	51.9	0	349
2-9-7	44.1	93.9	0	336
2-9-8	89.2	53.6	0	432
2-9-9	82.6	57.2	0	465
2-9-9R	86.2	53.8	5.07	1440

Table B-3 Exposure Data for 36-cm. Single Conductor Specimens (cont)

Sample ID	Aging Dose Rate 1 (Gy/hr)	Aging Dose Rate 2 (Gy/hr)	Accident Dose Rate (kGy/hr)	Total Dose (kGy)
Raychem				
3-3-3	0	51.7	0	113
3-3-3R	0	46	4.87	1120
3-6-1	0	33.1	0	24.6
3-6-2	0	35.7	0	51.1
3-6-3L	0	52.7	0	109
3-6-3F	74.7	0	0	179
3-6-4	85.6	36.2	0	228
3-6-5	86.7	33.6	0	252
3-6-6	76	42.7	0	270
3-6-6R	81.2	38.1	5.03	1240
3-6-R	0	0	5.01	963
3-9-1	0	86	0	65.8
3-9-2	0	88.7	0	127
3-9-3	0	84.9	0	192
3-9-6	49.4	87.2	0	266
3-9-7	55.4	91.1	0	366
3-9-8	60.3	88.3	0	435
3-9-9	61.1	80.3	0	477
3-9-9R	58.5	85.5	5.12	1470
Polyset				
4-3-3	0	68.6	0	150
4-3-3R	0	71.1	4.78	1150
4-6-1	0	44.7	0	33.2
4-6-2	0	41.9	0	60.1
4-6-3L	0	43.5	0	90.3
4-6-3F	73.7	0	0	177
4-6-4	75.1	42.6	0	207
4-6-5	71.8	45.4	0	233
4-6-6	68.2	47.7	0	262
4-6-6R	70.2	46.3	5.02	1230
4-6-R	0	0	4.99	959
4-9-1	0	55.9	0	42.7
4-9-2	0	58	0	83.1
4-9-3	0	56.3	0	128
4-9-6	89.3	57.8	0	357
4-9-7	87.9	59.5	0	405
4-9-8	87.2	57.4	0	437
4-9-9	79	61.8	0	470
4-9-9R	83.2	59.3	5.09	1450

Table B-4 Exposure Data for 36-cm. Multiconductor Specimens

Sample ID	Aging Dose Rate 1 (Gy/hr)	Aging Dose Rate 2 (Gy/hr)	Accident Dose Rate (kGy/hr)	Total Dose (kGy)
Brand Rex				
1-3-3	0	80.1	0	175
1-3-3R	0	86.8	4.77	1190
1-6-1	0	77	0	57.1
1-6-2	0	81.9	0	117
1-6-3L	0	85.9	0	178
1-6-3F	37.3	0	0	89.3
1-6-4	36.1	83.2	0	140
1-6-5	39.2	78.3	0	198
1-6-6	42.7	73.8	0	255
1-6-6R	46.6	69.9	5.03	1220
1-6-R	0	0	5.07	975
1-9-1	0	62.4	0	47.7
1-9-2	0	63.1	0	90.5
1-9-3	0	67.8	0	154
1-9-6	85.3	69.6	0	359
1-9-7	87.8	64.8	0	416
1-9-8	85.1	64.1	0	448
1-9-9	82	63.3	0	484
1-9-9R	78.9	63.2	4.96	1430
Rockbestos				
2-3-3	0	94.5	0	206
2-3-3R	0	85.9	4.76	1180
2-6-1	0	74.5	0	55.3
2-6-2	0	81.4	0	117
2-6-3L	0	79.5	0	165
2-6-3F	35.2	0	0	84.3
2-6-4	31.9	82.6	0	129
2-6-5	38.5	75.7	0	193
2-6-6	34.8	77.3	0	244
2-6-6R	42.3	71.4	5.04	1220
2-6-R	0	0	5.1	980
2-9-1	0	58	0	44.4
2-9-2	0	54.6	0	78.3
2-9-3	0	59.1	0	134
2-9-6	90	60.7	0	363
2-9-7	94.7	56.1	0	419
2-9-8	87	59.6	0	442
2-9-9	91.8	55.1	0	487
2-9-9R	83.8	59	4.98	1430

Table B-4 Exposure Data for 36-cm. Multiconductor Specimens (cont)

Sample ID	Aging Dose Rate 1 (Gy/hr)	Aging Dose Rate 2 (Gy/hr)	Accident Dose Rate (kGy/hr)	Total Dose (kGy)
Polyset				
4-3-3	0	91.6	0	200
4-3-3R	0	87.3	4.77	1190
4-6-1	0	72.6	0	53.8
4-6-2	0	75.4	0	108
4-6-3L	0	79.9	0	166
4-6-3F	31.7	0	0	76
4-6-4	34.9	76.6	0	133
4-6-5	38.4	73.7	0	190
4-6-6	42.5	69.6	0	246
4-6-6R	38.8	72	5.04	1210
4-6-R	0	0	5.02	966
4-9-1	0	53.7	0	41.1
4-9-2	0	49.7	0	71.3
4-9-3	0	50.4	0	114
4-9-6	96.8	51.8	0	374
4-9-7	93.7	51.1	0	406
4-9-8	88.7	55.1	0	435
4-9-9	85.7	54.8	0	466
4-9-9R	90.6	50.4	5	1430

Table B-5 Temperature During Accident Test Transients

AT3		AT6		AT9	
Time (hr)	Temp (°C)	Time (hr)	Temp (°C)	Time (hr)	Temp (°C)
0.003	19.6	0.000	19.9	0.000	21.8
0.088	20.4	0.085	20.1	0.084	22.1
0.09	132.8	0.087	120.0	0.087	55.0
0.093	151.2	0.09	149.3	0.09	138.2
0.096	152.2	0.093	154.4	0.095	156.6
0.098	155.4	0.117	158.3	0.098	154.9
0.101	156.6	0.133	160.1	0.100	152.0
0.149	161.1	0.217	164.5	0.106	157.6
0.192	163.3	0.257	166.2	0.127	159.1
0.227	164.2	0.302	168.4	0.132	159.3
0.312	166.2	0.356	171.1	0.170	160.3
0.424	169.2	0.671	174.6	0.229	162.5
0.483	171.1	0.730	170.6	0.266	164.0
0.571	172.3	0.794	174.3	0.272	164.0
0.688	173.1	0.825	170.1	0.347	166.2
0.774	175.0	0.878	166.2	0.464	167.7
0.832	174.1	0.937	170.1	0.538	170.6
0.998	174.3	0.998	169.4	1.000	170.9
5.013	79.8	5.324	56.0	5.009	61.4
5.101	78.1	5.356	55.5	5.064	60.4
5.103	111.7	5.409	54.7	5.085	61.6
5.106	152.7	5.414	139.2	5.088	133.3
5.109	159.1	5.418	155.4	5.090	147.3
5.164	160.1	5.422	157.6	5.093	148.8
5.170	160.3	5.459	159.1	5.096	151.0
5.178	161.1	5.468	159.6	5.098	152.7
5.226	163.3	5.476	160.1	5.104	153.9
5.239	163.8	5.480	160.3	5.112	155.2
5.242	164.0	5.484	161.1	5.130	156.9
5.292	165.5	5.526	163.8	5.154	158.1
5.375	163.5	5.580	167.2	5.157	158.3
5.380	163.3	5.651	169.9	5.197	161.3
5.391	162.8	5.655	170.4	5.219	163.0
5.494	166.5	5.692	171.1	5.245	163.5
5.558	167.7	5.751	170.4	5.301	165.0
5.644	169.2	5.821	171.6	5.386	167.2
5.755	170.9	5.825	171.6	5.481	168.4
5.761	171.1	5.863	171.6	5.566	170.4
5.909	171.9	5.921	171.9	5.571	170.4
6.000	171.1	6.000	171.9	5.996	173.1

Appendix C Insulation Resistance During Aging and After Accident Radiation

In this appendix, conductor identification numbers are as given in Table 2. Where measurements on more than one conductor form the basis for a data point, the error bar shown around the symbol for that data point represents one sample standard deviation of the data.

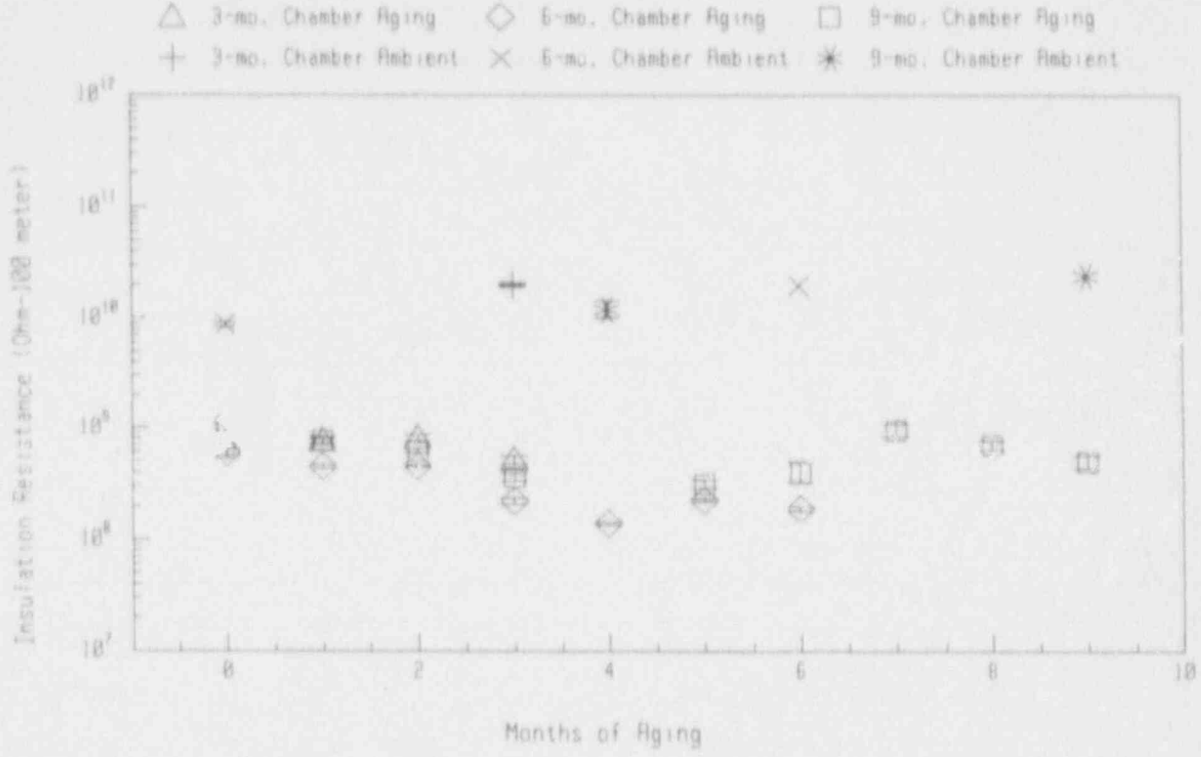

Figure C-1 50 V IR of Brand Rex Cable During Aging

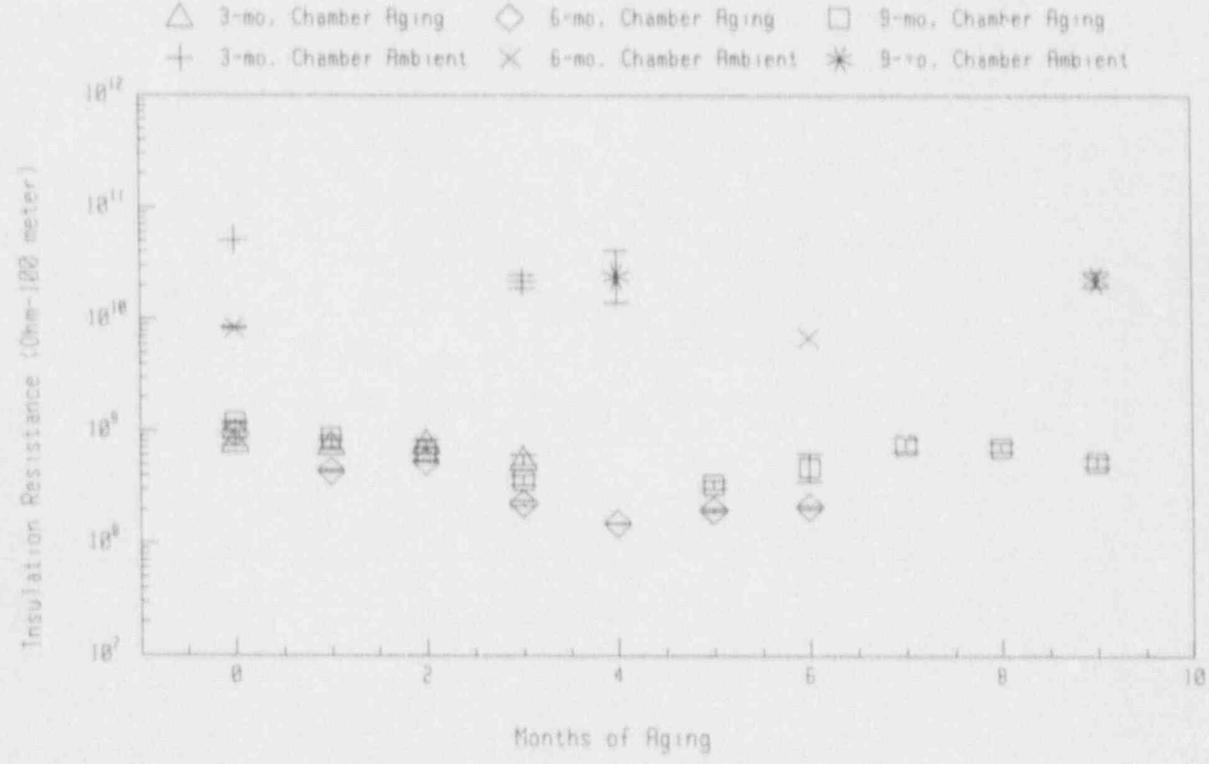

Figure C-2 100 V IR of Brand Rex Cable During Aging

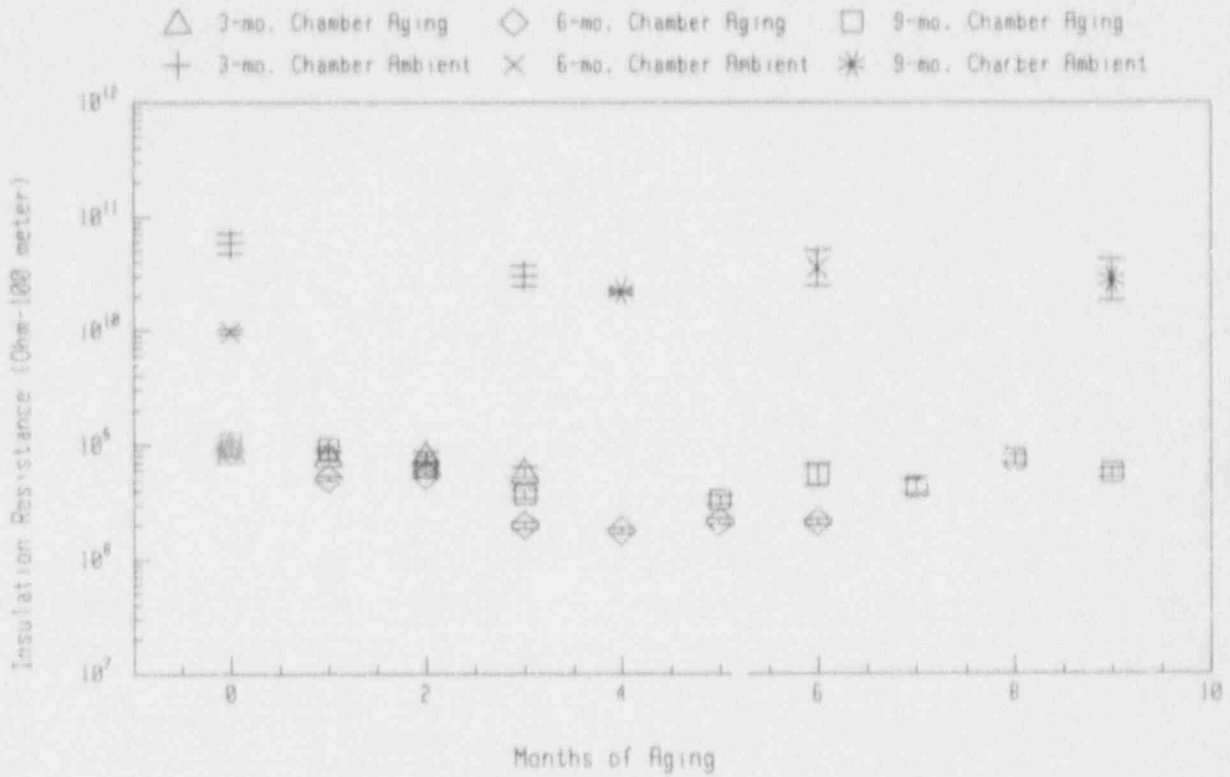

Figure C-3 250 V IR of Brand Rex Ca[illegible] aring Aging

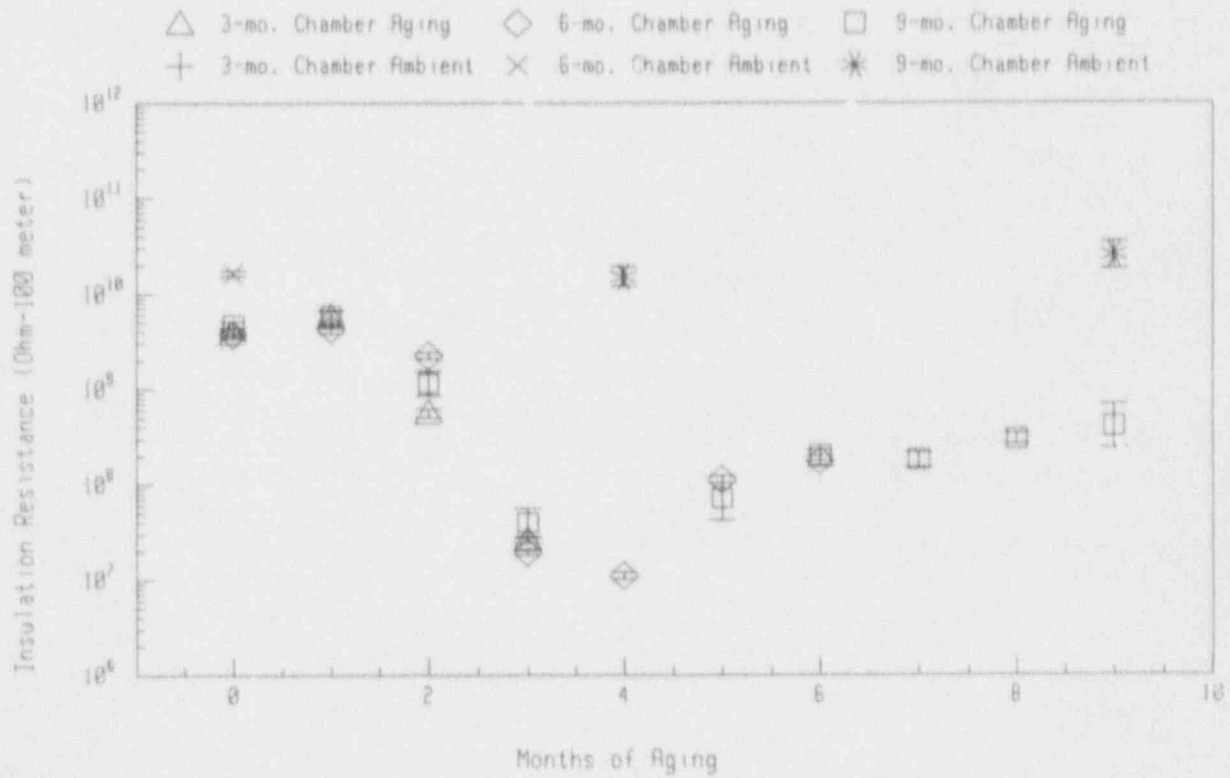

Figure C-4 50 V IR of Rockbestos Cable During Aging

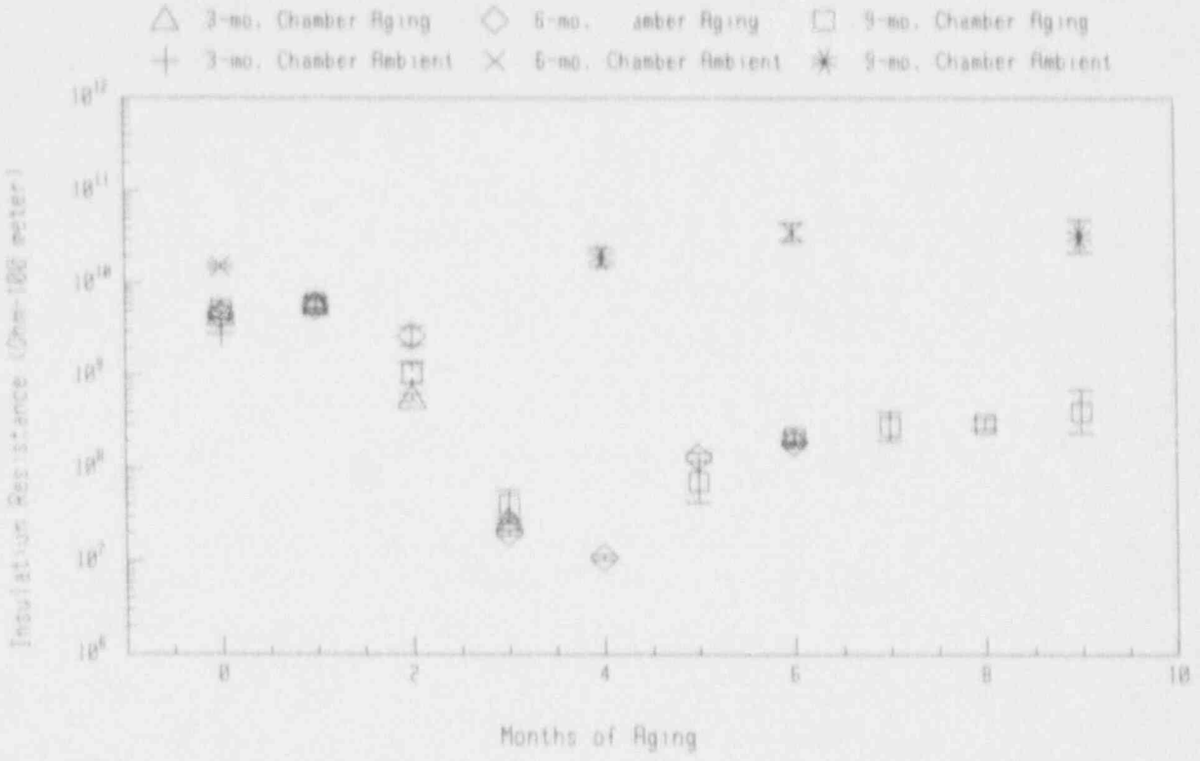

Figure C-5 100 V IR of Rockbestos Cable During Aging

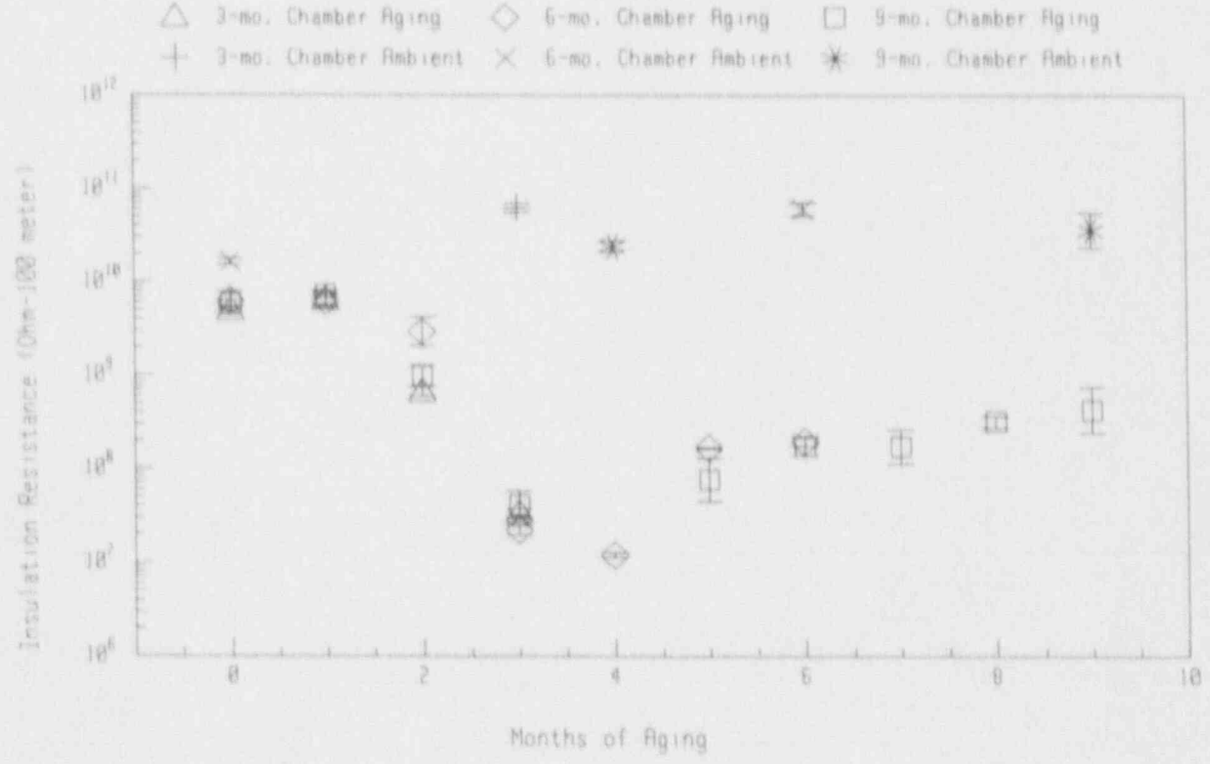

Figure C-6 250 V IR of Rockbestos Cable During Aging

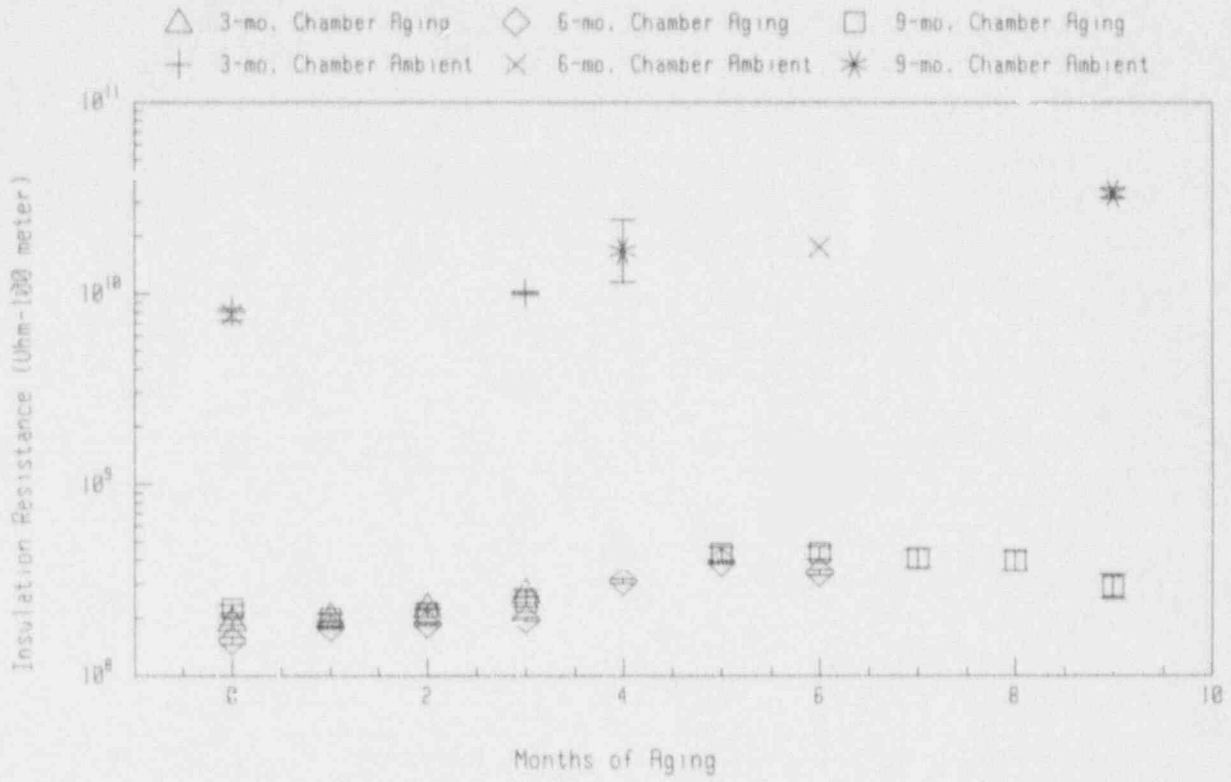

Figure C-7 50 V IR of Polyset Cable During Aging

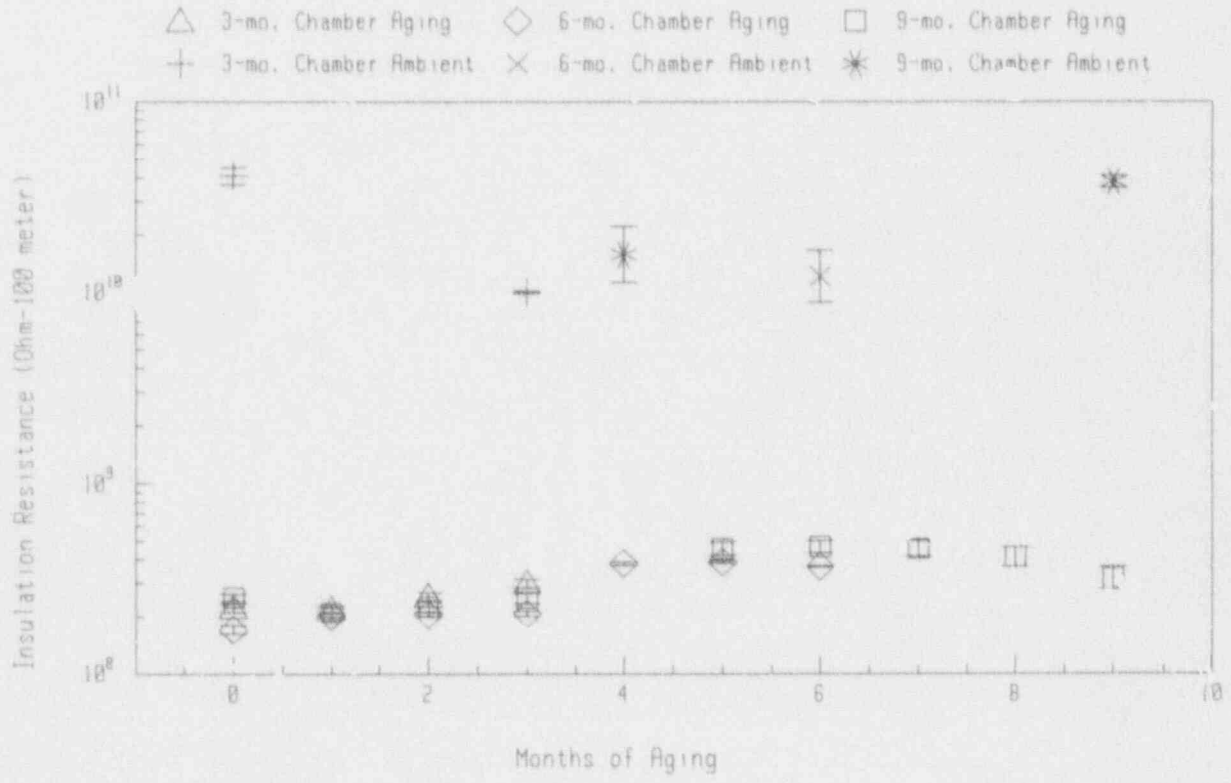

Figure C 8 100 V IR of Polyset Cable During Aging

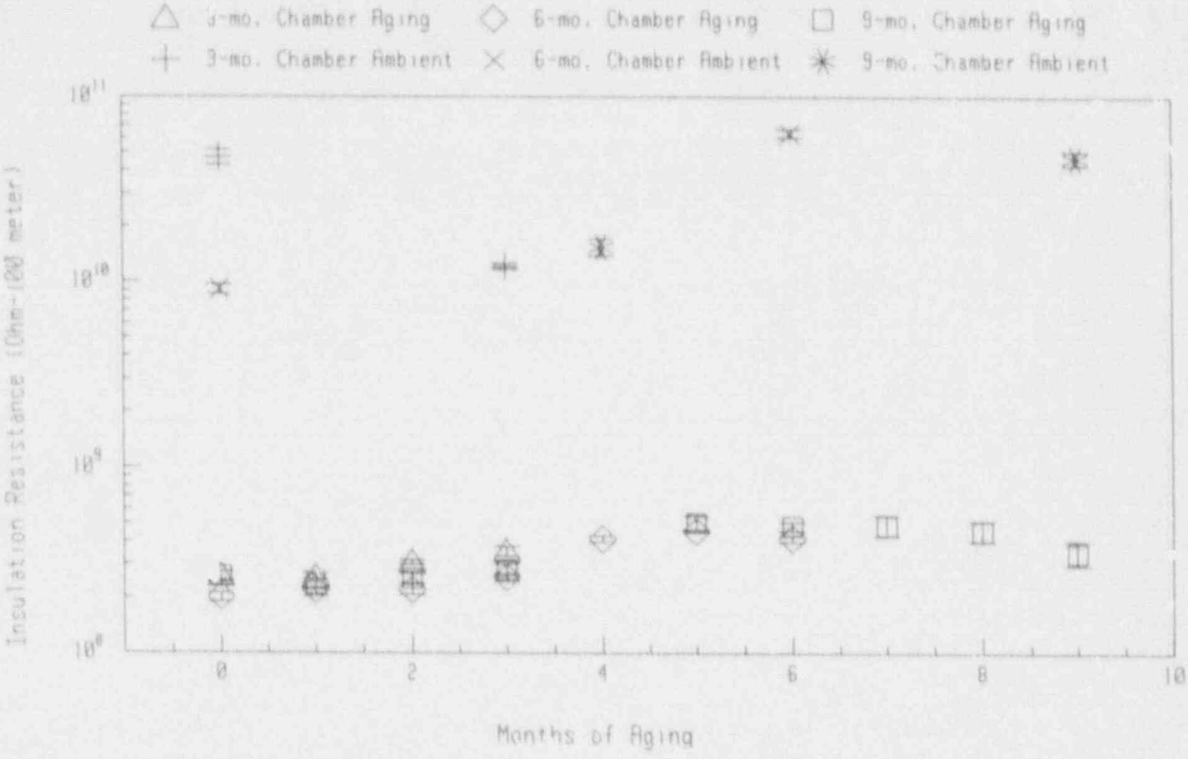

Figure C-9 250 V IR of Polyset Cable During Aging

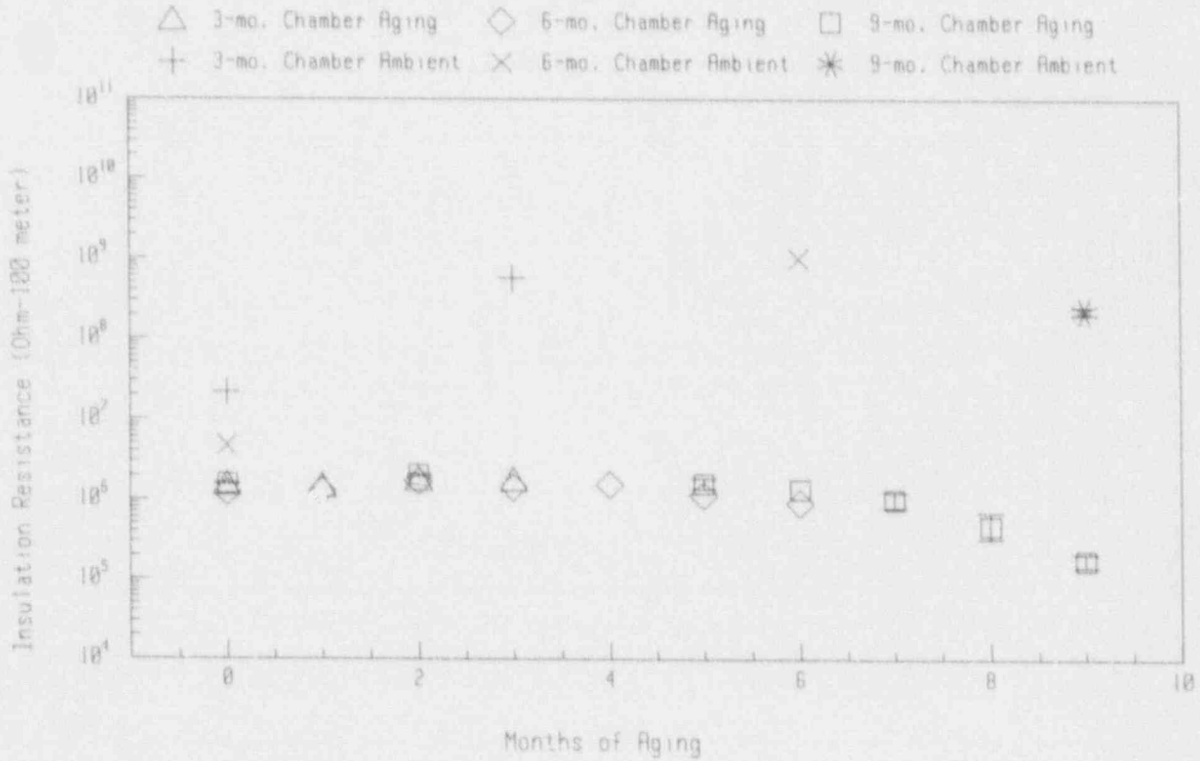

Figure C-10 50 V IR of Polyset Jacket During Aging

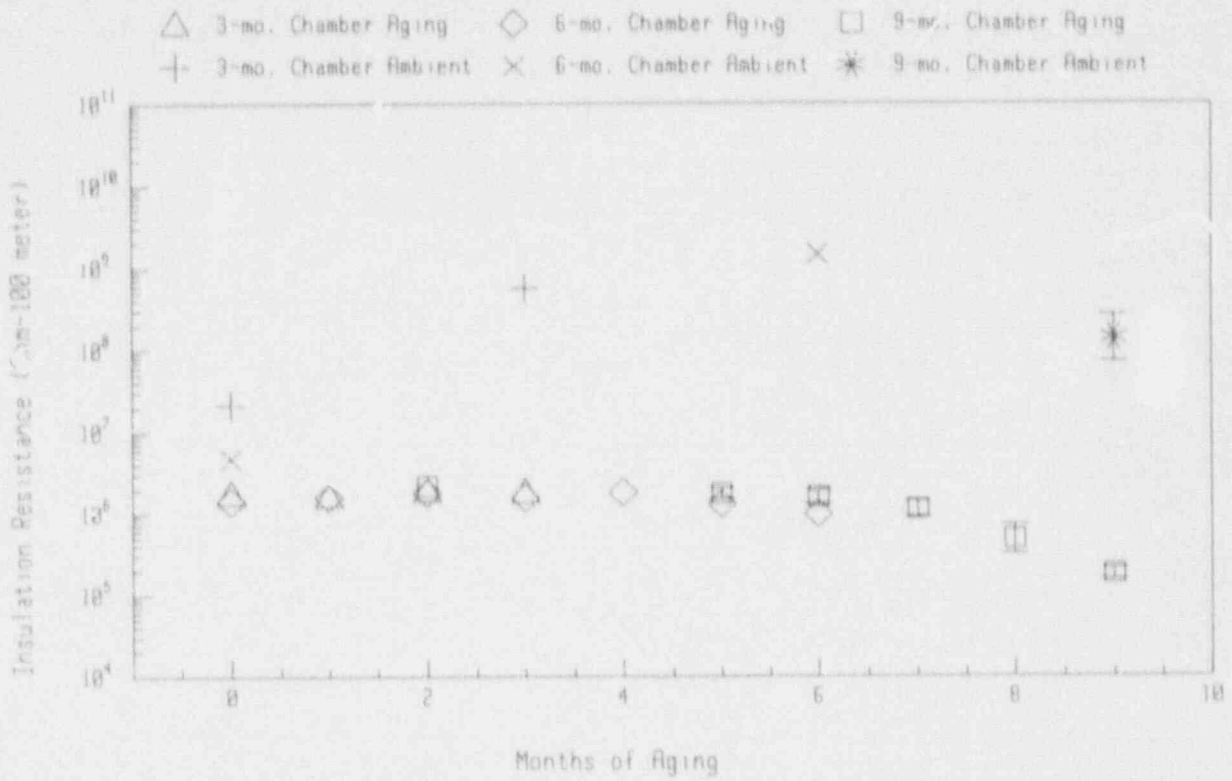

Figure C-11 100 V IR of Polyset Jacket During Aging

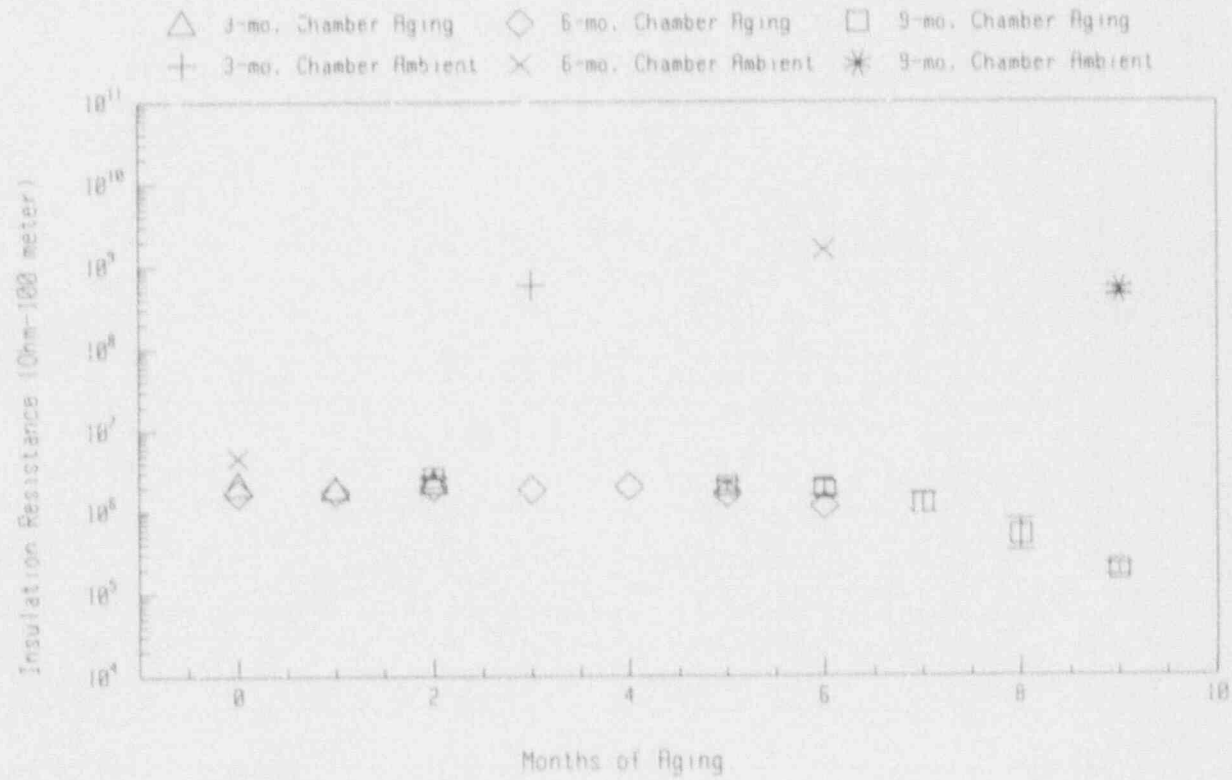

Figure C-12 250 V IR of Polyset Jacket During Aging

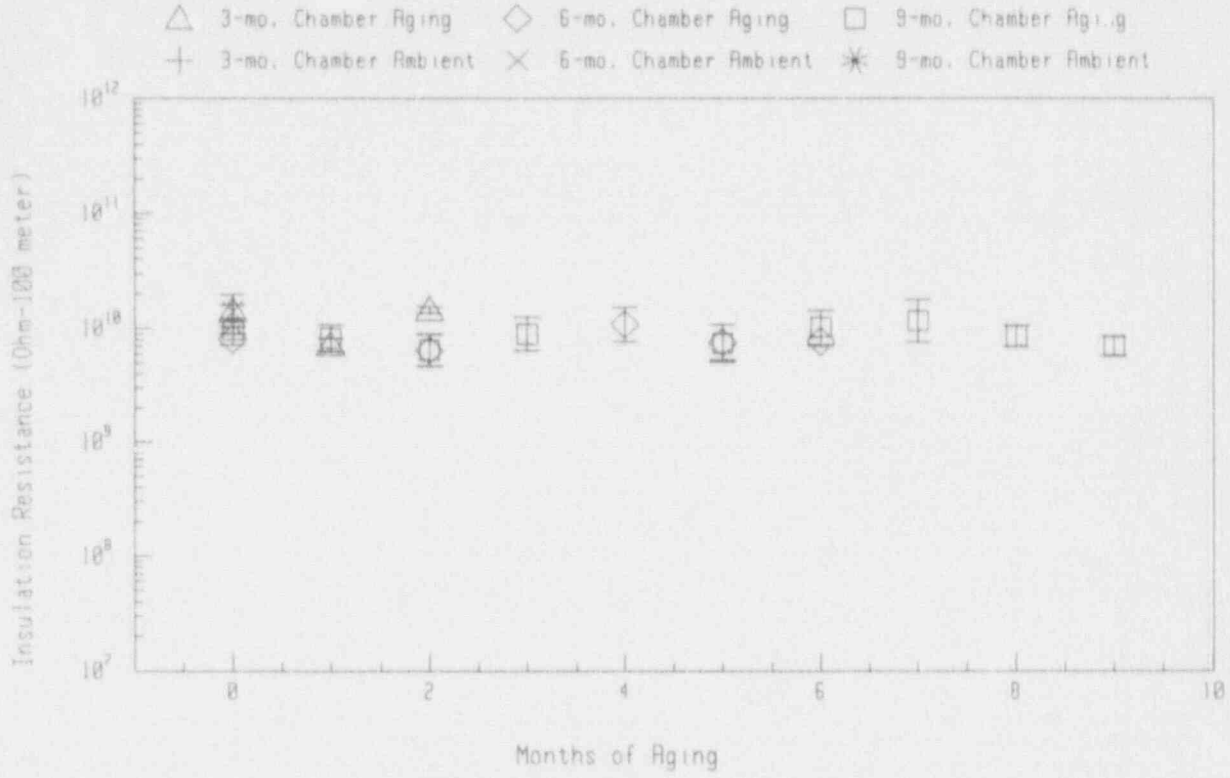

Figure C-13 50 V IR of Raychem Cable During Aging

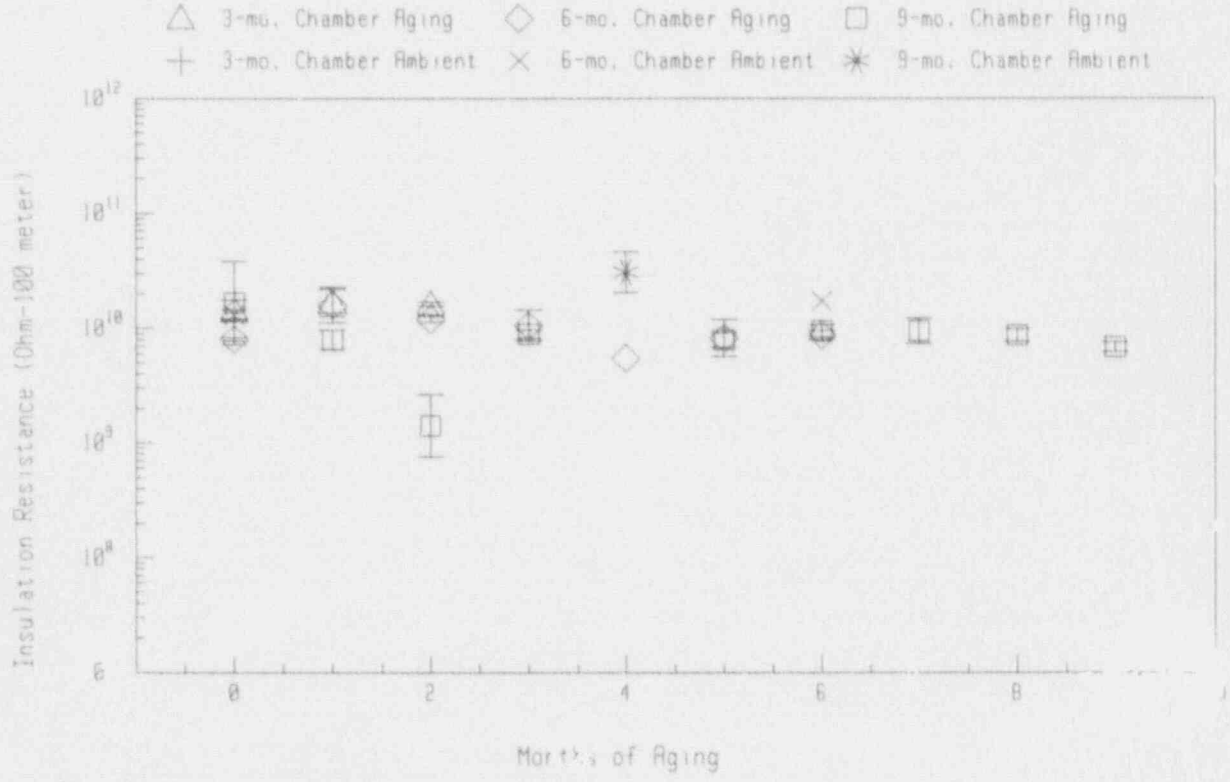

Figure C-14 100 V IR of Raychem Cable During Aging

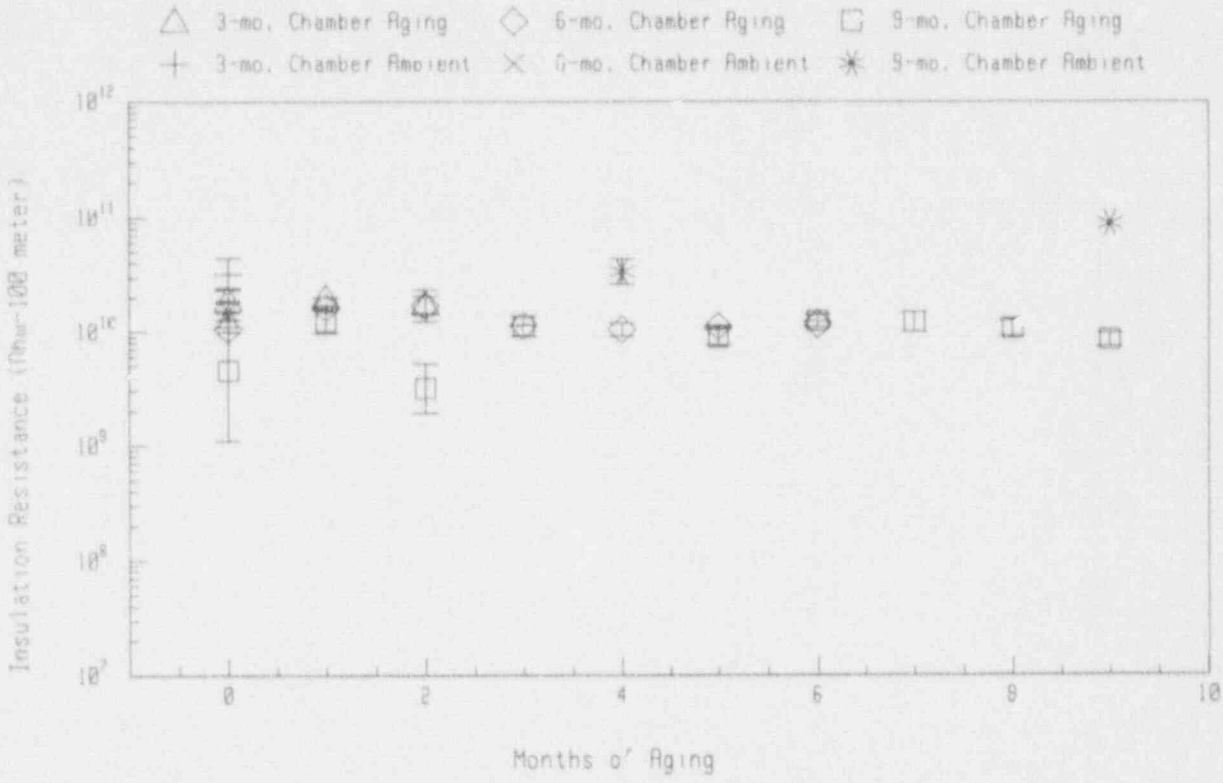

Figure C-15 250 V IR of Raychem Cable During Aging

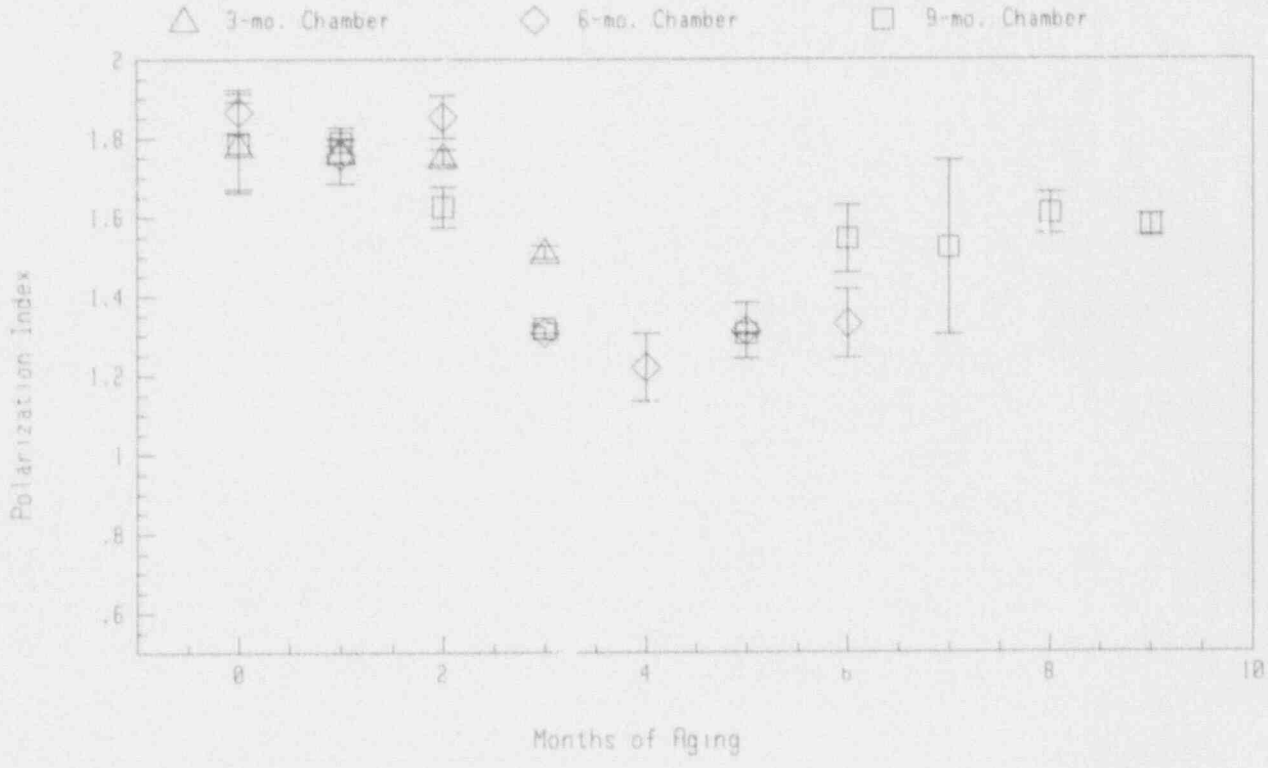

Figure C-16 250 V PI (5 min/30 s) of Brand Rex Cable During Aging

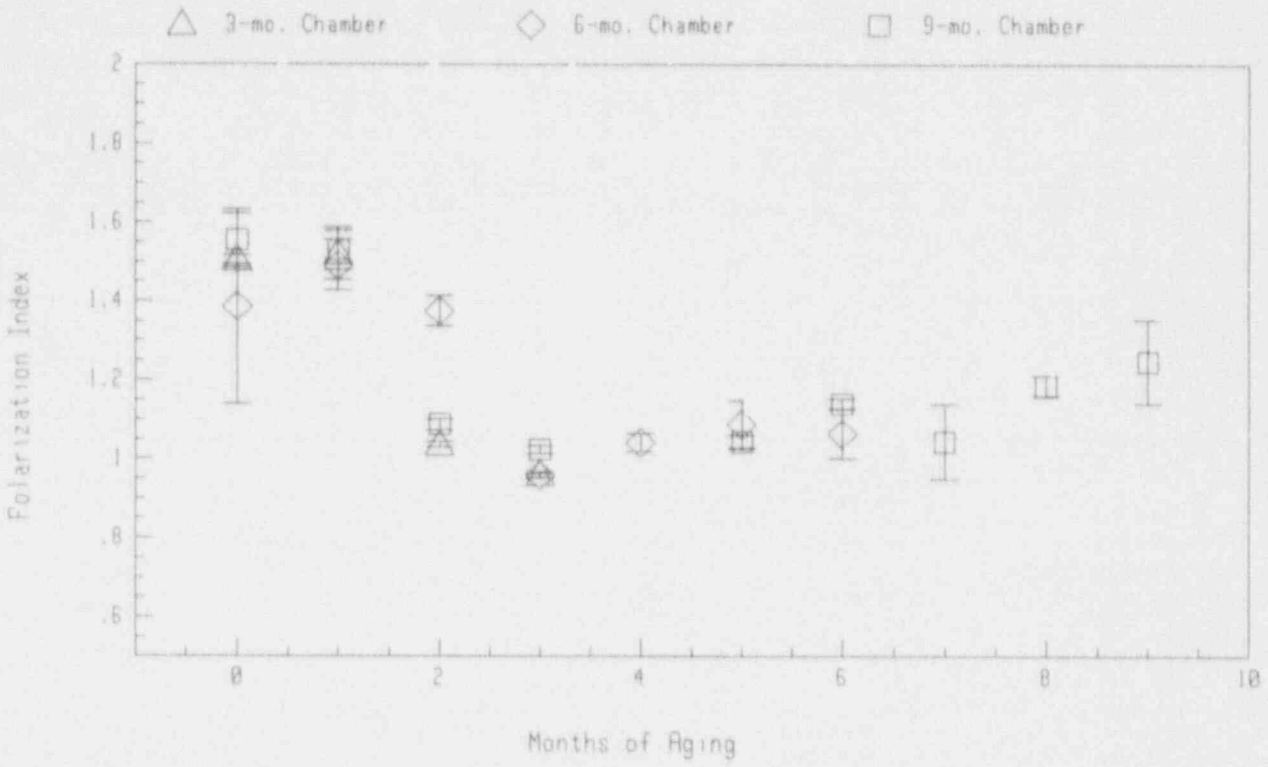

Figure C-17 250 V PI (5 min/30 s) of Rockbestos Cable During Aging

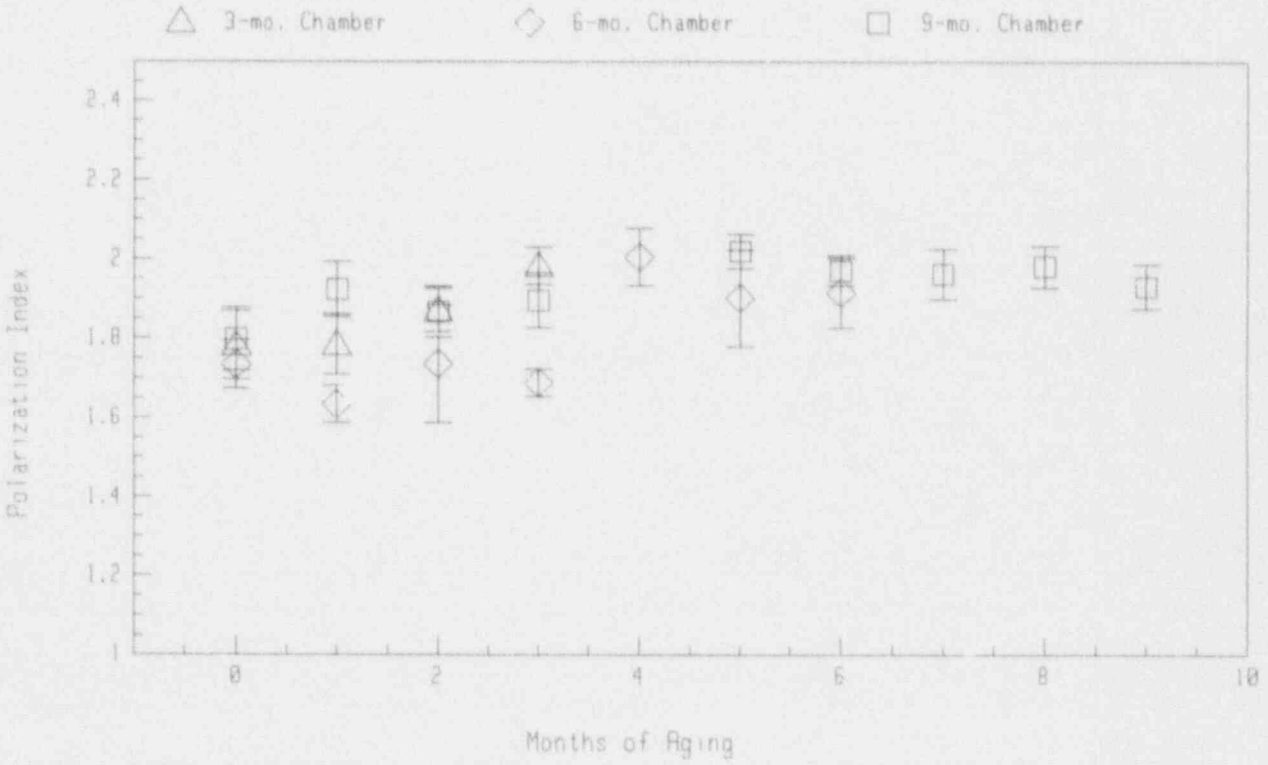

Figure C-18 250 V PI (5 min/30 s) of Polyset Cable During Aging

Figure C-19 250 V PI (5 min/30 s) of Polyset Jacket During Aging

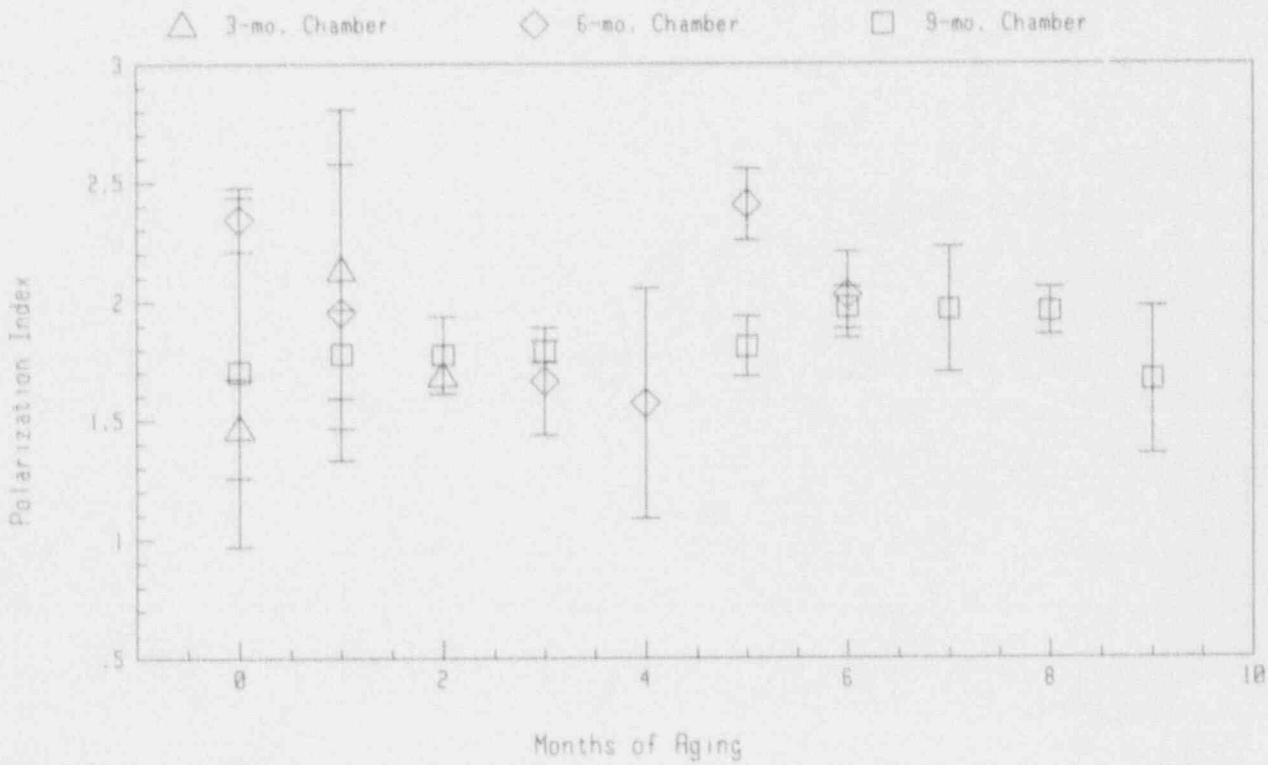

Figure C-20 250 V PI (5 min/30 s) of Raychem Cable During Aging

Table C-1 Insulation Resistance Data After Accident Radiation Exposures

3-month Chamber After Accident Radiation			9-month Chamber After Accident Radiation			
Cond #	50 V	100 V	Cond #	50 V	100 V	250 V
Brand Rex XLPO						
1	1.98E+10	1.70E+10	1	2.07E+10	1.36E+10	1.10E+10
2	2.23E+10	1.75E+10	2	1.59E+10	1.31E+10	1.73E+10
3	3.01E+10	1.41E+10	3	1.60E+10	1.69E+10	1.50E+10
Rockbestos Firewall III						
12	6.25E+10	4.89E+10	14	2.43E+10	1.84E+10	2.17E+10
13	4.77E+10	5.55E+10	15	1.51E+10	2.35E+10	2.70E+10
14	9.11E+10	5.63E+10	16	2.44E+10	1.90E+10	2.95E+10
			17	1.68E+10	1.84E+10	1.83E+10
			18	2.10E+10	1.95E+10	2.31E+10
			19	2.42E+10	2.16E+10	2.26E+10
Dekoron Polyset						
19	1.29E+10	1.28E+10	24	3.83E+09	3.13E+09	2.59E+09
20	1.21E+10	2.89E+10	25	3.29E+09	3.34E+09	2.51E+09
21	1.62E+10	1.46E+10	26	4.02E+09	3.47E+09	2.83E+09
			27	4.63E+09	3.98E+09	3.34E+09
			28	4.39E+09	4.11E+09	3.37E+09
			29	4.98E+09	4.47E+09	3.61E+09
41	4.22E+08	3.35E+08	55	7.32E+7	6.27E+7	6.51E+7
			56	8.00E+7	6.93E+7	7.13E+7
Raychem Flamtrol						
27	6.95E+10	****	35	6.59E+10	6.04E+10	6.53E+10
28	4.35E+10	5.27E+10	36	2.96E+10	4.84E+10	5.76E+10
			37	7.51E+10	****	7.33E+10

**** IR too high to measure

Table C-2 Polarization Index Data at Ambient Temperature

Note: All PIs in this table are the 250 V IR at 5 minutes divided by the 250 V IR at 30 s.

Cond #	Cham 3 Month 0	Cham 3 Month 3	Cham 6 Month 0	Cham 6 Month 6	Cond #	Cham 9 Month 4	Cham 9 Month 9	Cham 9 After Radiation
Brand Rex XLPO								
1	3.21	6.49	2.49	3.31	1	2.56	4.93	2.76
2	2.52	4.38	2.33	2.50	2	2.28	2.96	2.20
3	3.42	4.63	2.45	3.85	3	----	3.63	2.70
Rockbestos Firewall III								
12	****	4.98	2.95	****	14	5.48	----	5.70
13	****	****	2.75	****	15	4.18	----	6.15
14	****	4.31	2.92	****	16	3.97	****	6.49
					17	3.67	6.30	5.57
					18	4.54	6.32	5.08
					19	3.15	5.42	4.24
Dekoron Polyset								
19	2.57	2.23	2.08	2.92	24	2.91	2.34	1.95
20	2.11	2.17	1.98	2.26	25	2.46	2.47	1.75
21	2.27	2.07	2.01	3.14	26	2.63	2.08	2.03
					27	3.50	2.65	1.98
					28	3.35	3.24	1.83
					29	4.63	2.72	1.99
41	0	1.43	1.09	2.22	55	----	1.20	1.05
					56	----	1.17	1.04
Raychem Flamtrol								
27	****	****	3.68	****	35	1.64	****	****
28	****	****	3.49	1.81	36	2.77	****	****
					37	****	****	****

---- No measurement
**** No PI because IR too high to measure

Appendix D Capacitance and Dissipation Factor During Aging

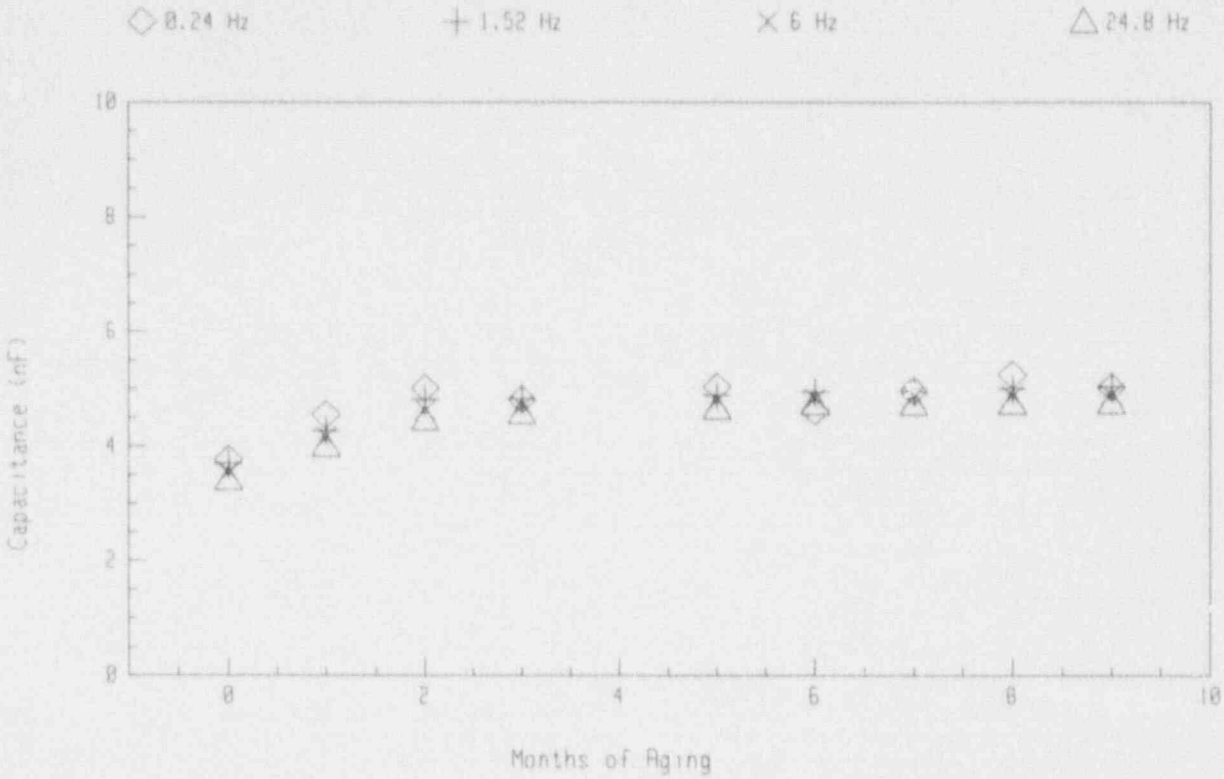

Figure D-1 Capacitance of Brand Rex Conductor #1 During Aging

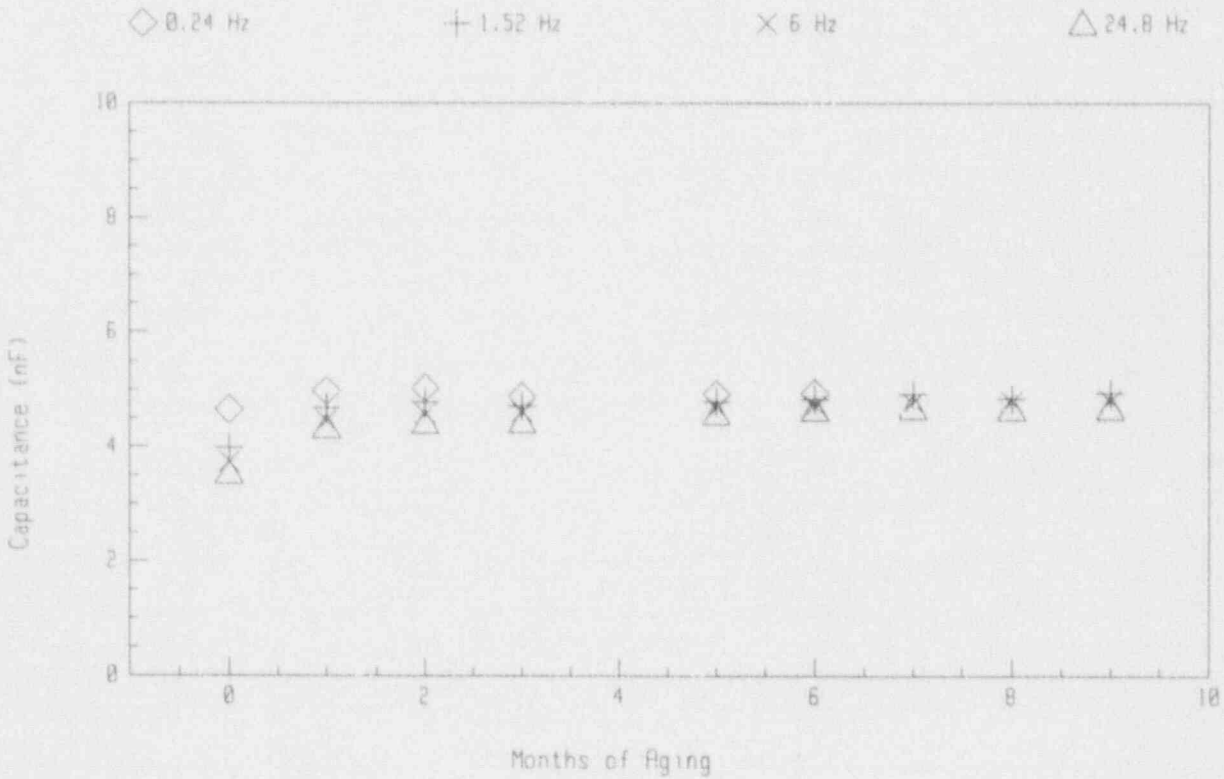

Figure D-2 Capacitance of Brand Rex Conductor #2 During Aging

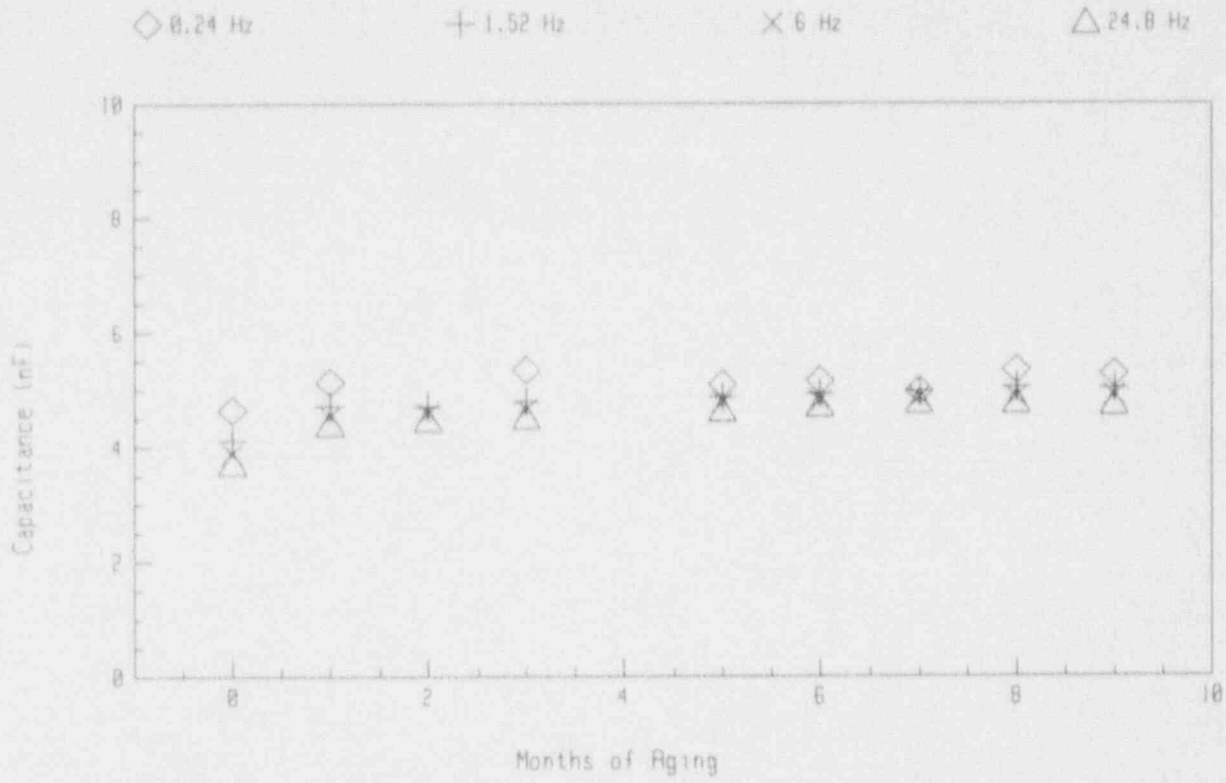

Figure D-3 Capacitance of Brand Rex Conductor #3 During Aging

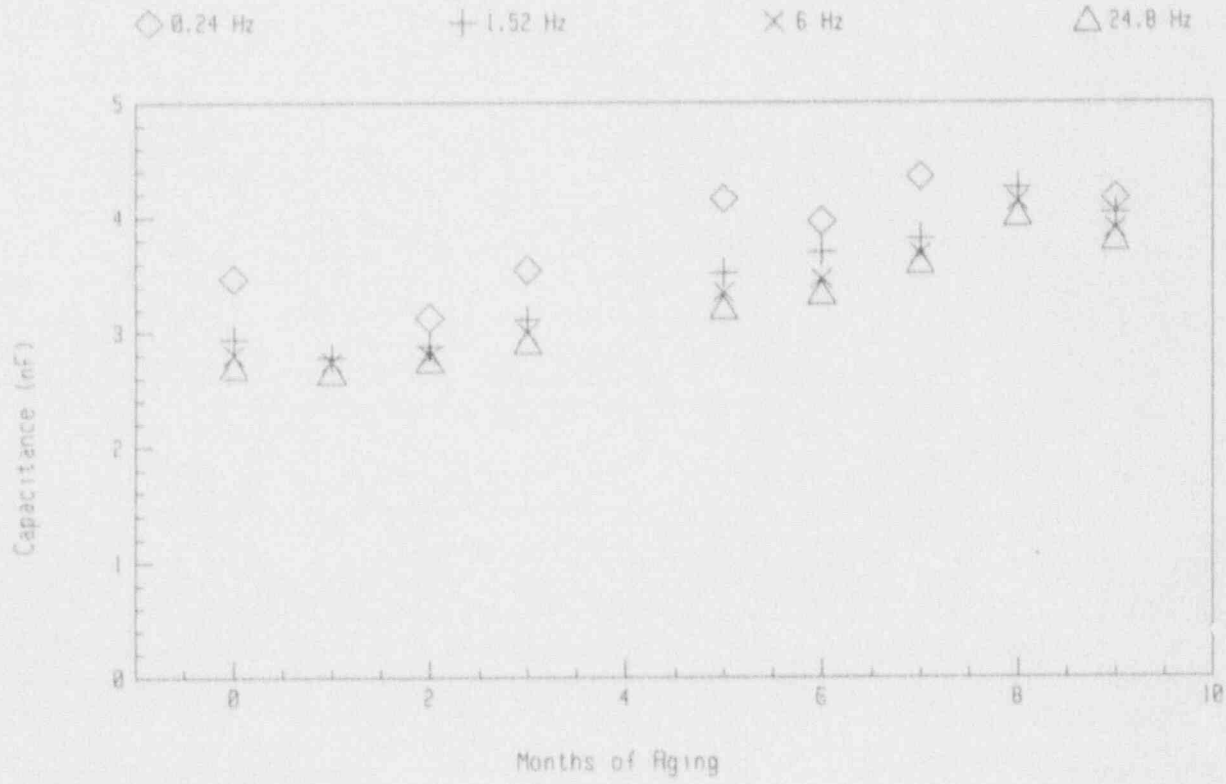

Figure D-4 Capacitance of Rockbestos Conductor #14 During Aging

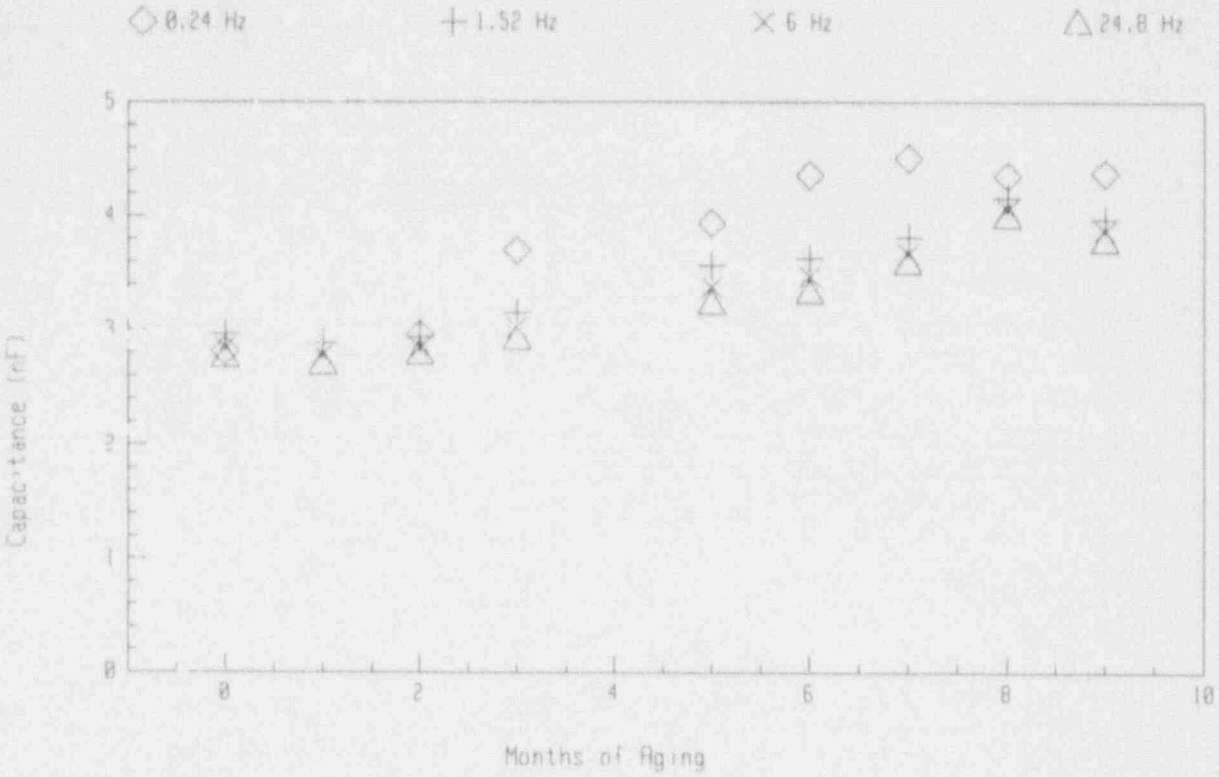

Figure D-5 Capacitance of Rockbestos Conductor #15 During Aging

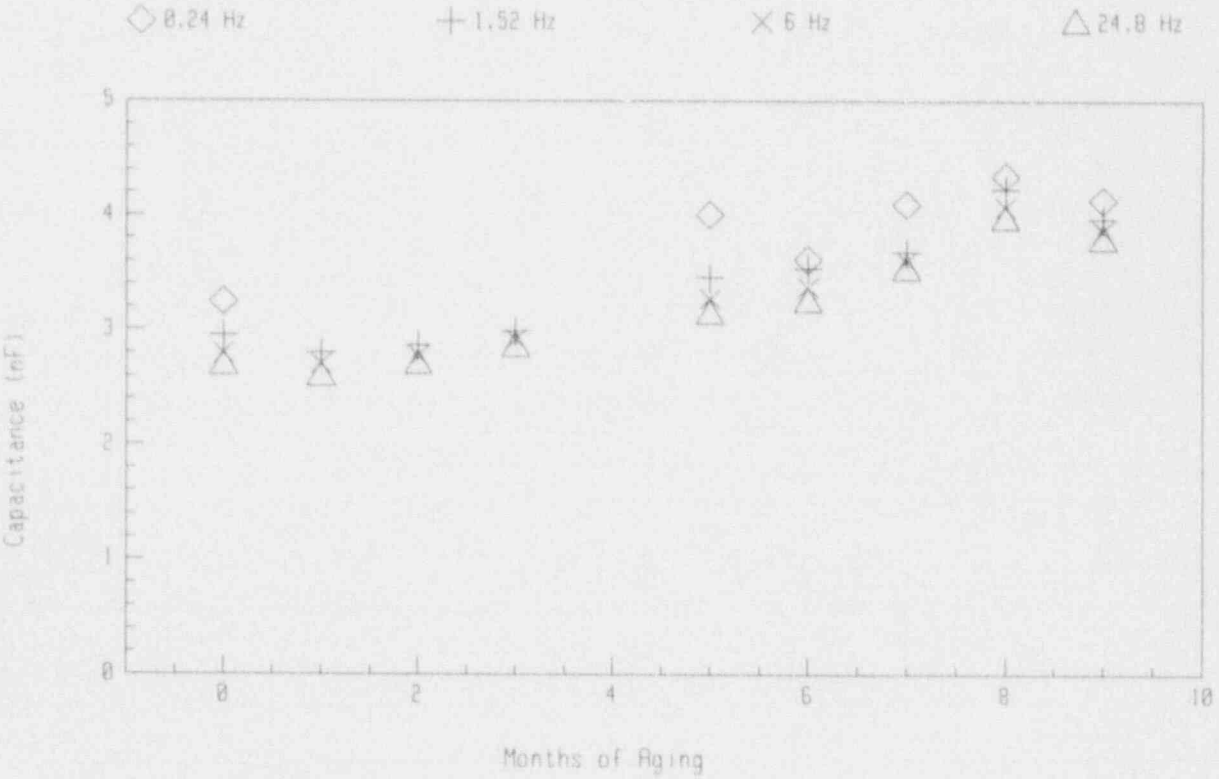

Figure D-6 Capacitance of Rockbestos Conductor #16 During Aging

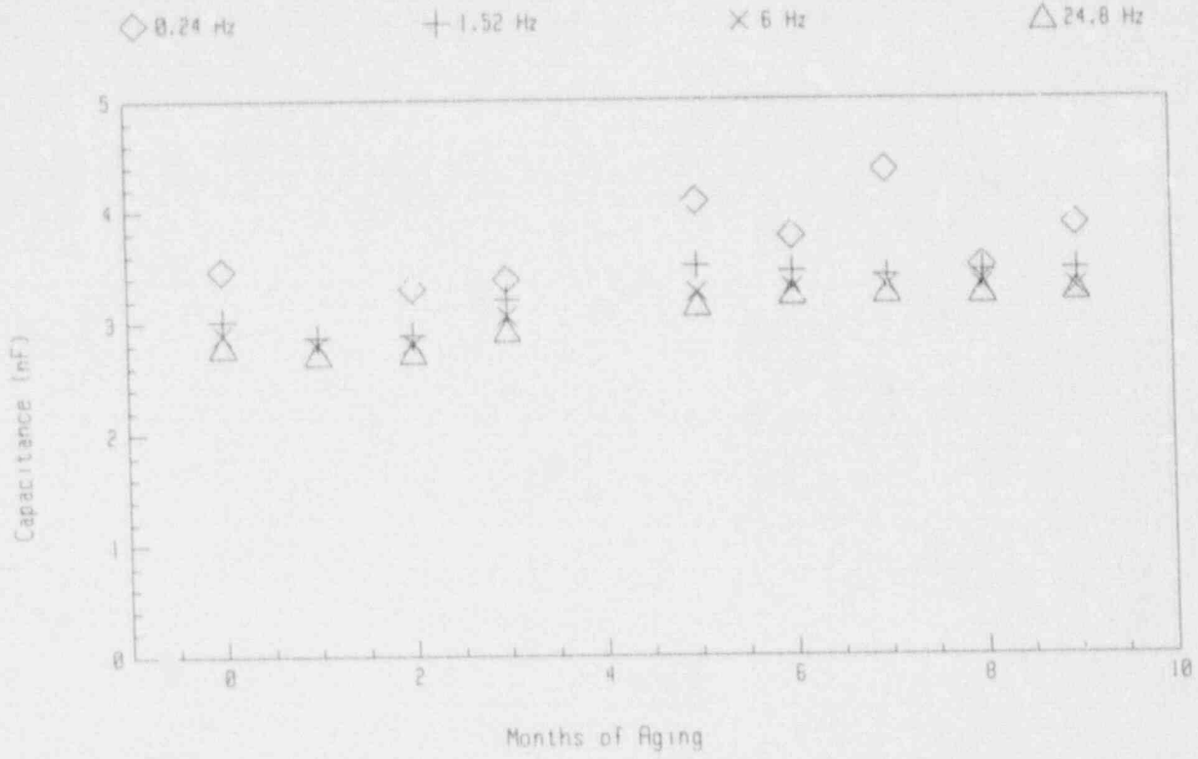

Figure D-7 Capacitance of Rockbestos Conductor #17 During Aging

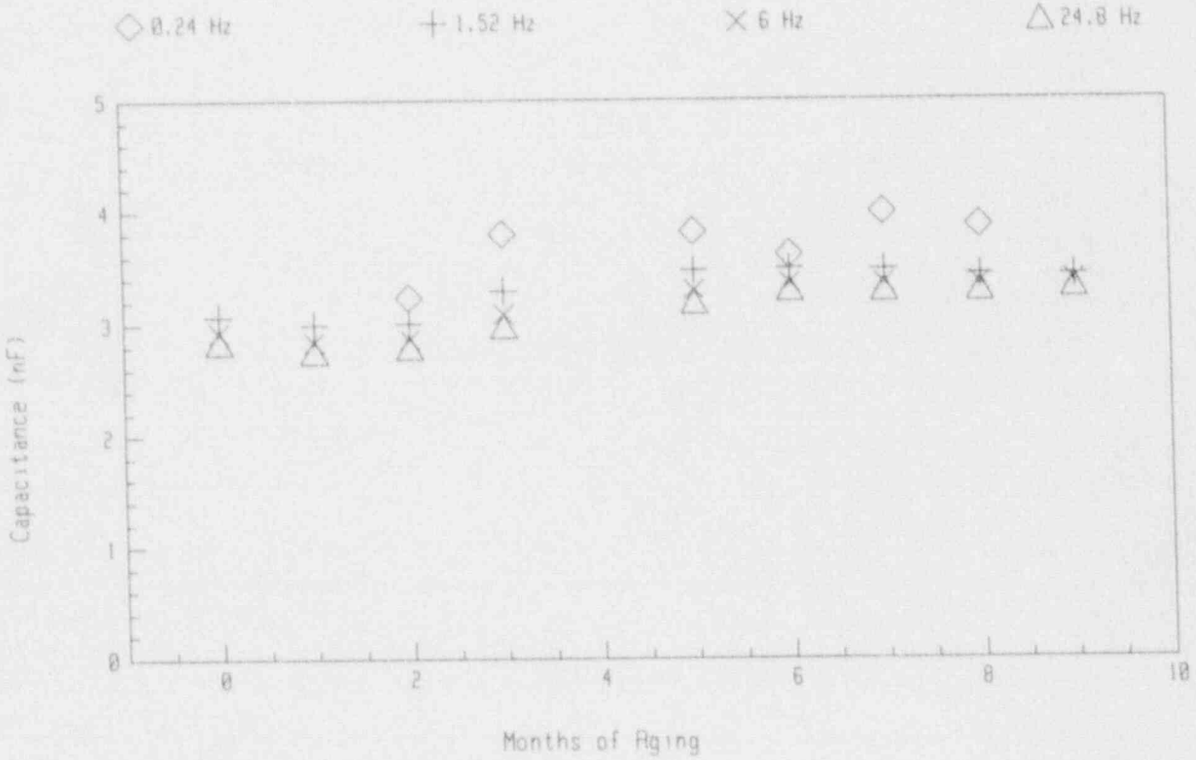

Figure D-8 Capacitance of Rockbestos Conductor #18 During Aging

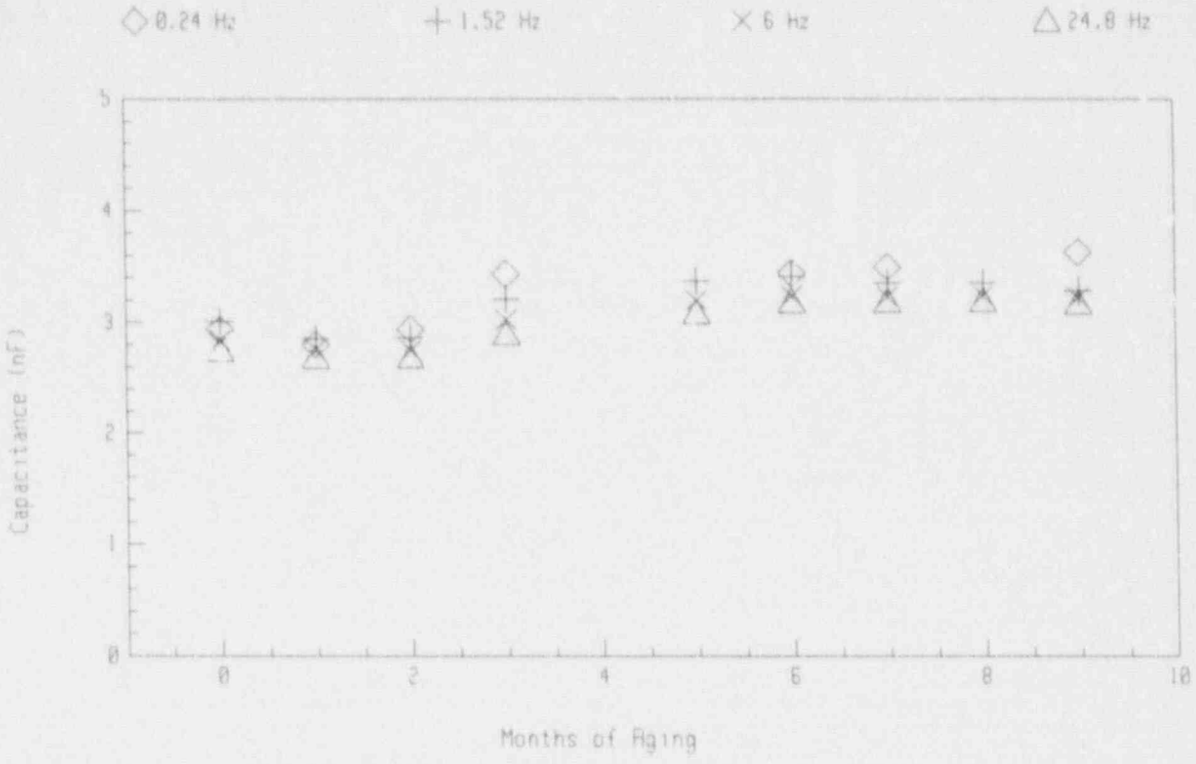

Figure D-9 Capacitance of Rockbestos Conductor #19 During Aging

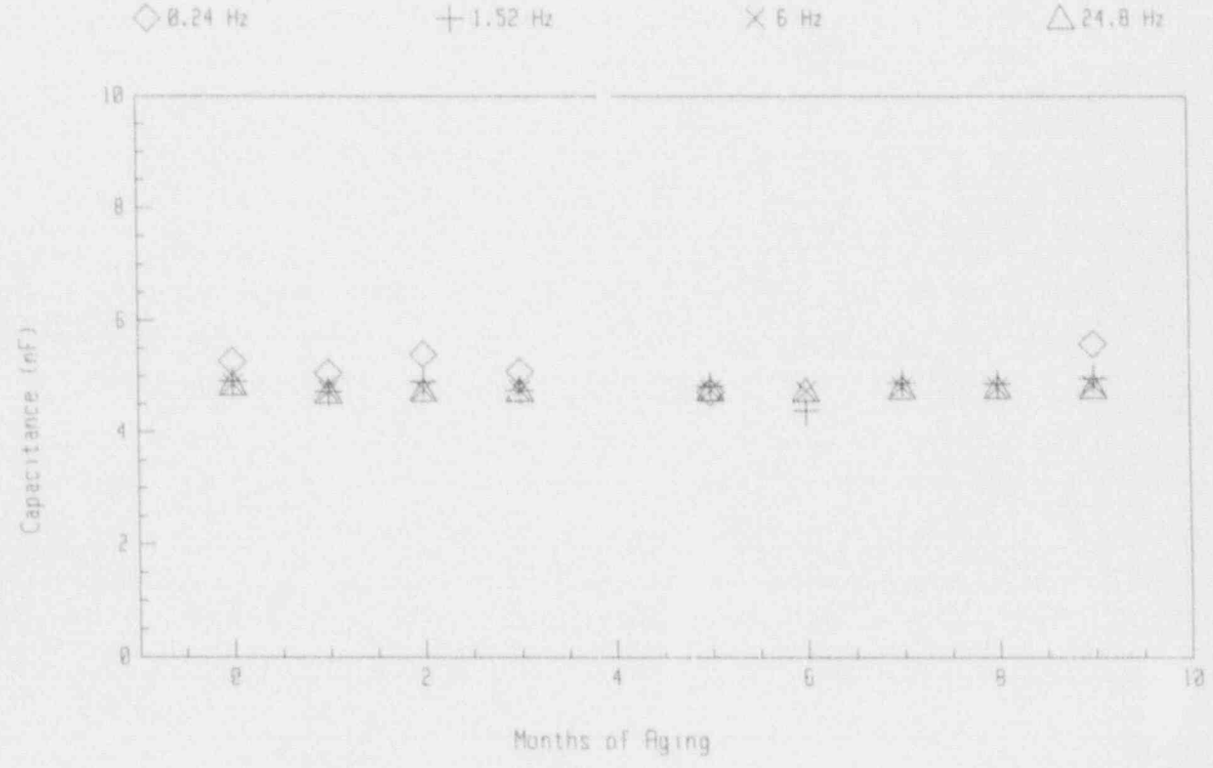

Figure D-10 Capacitance of Dekoron Polyset Conductor #24 During Aging

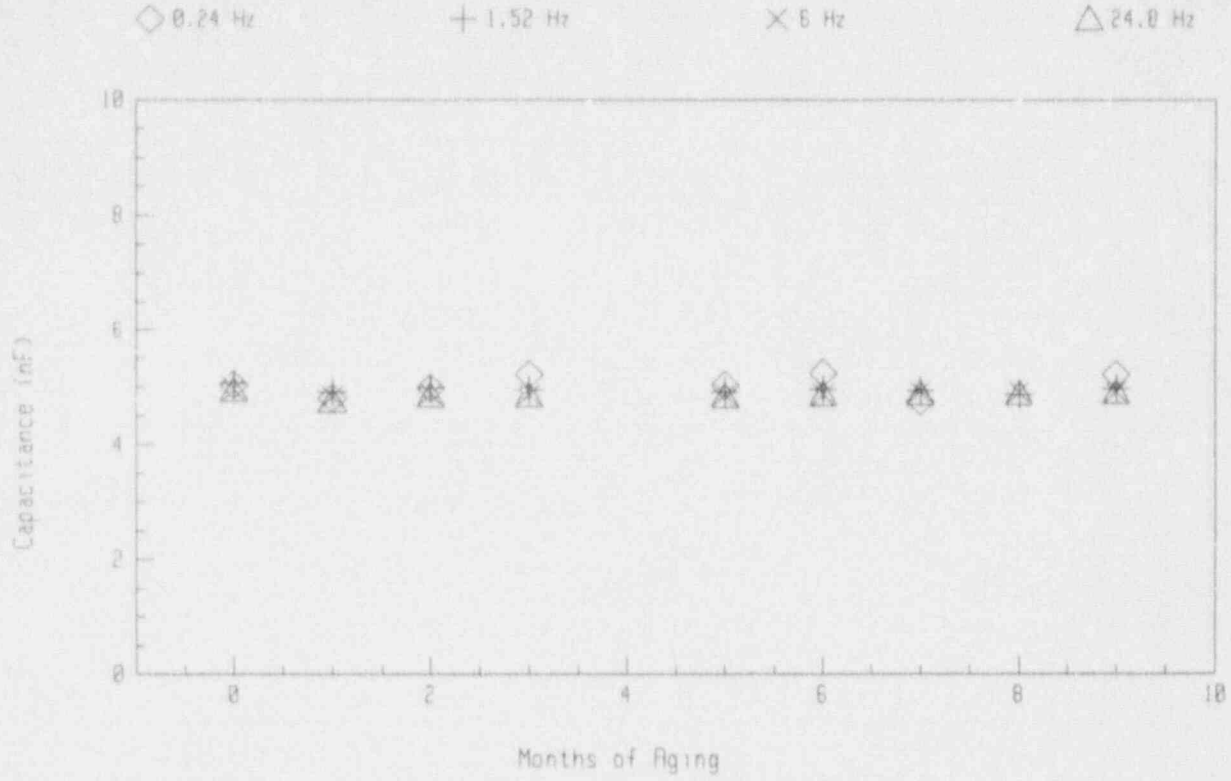

Figure D-11 Capacitance of Dekoron Polyset Conductor #25 During Aging

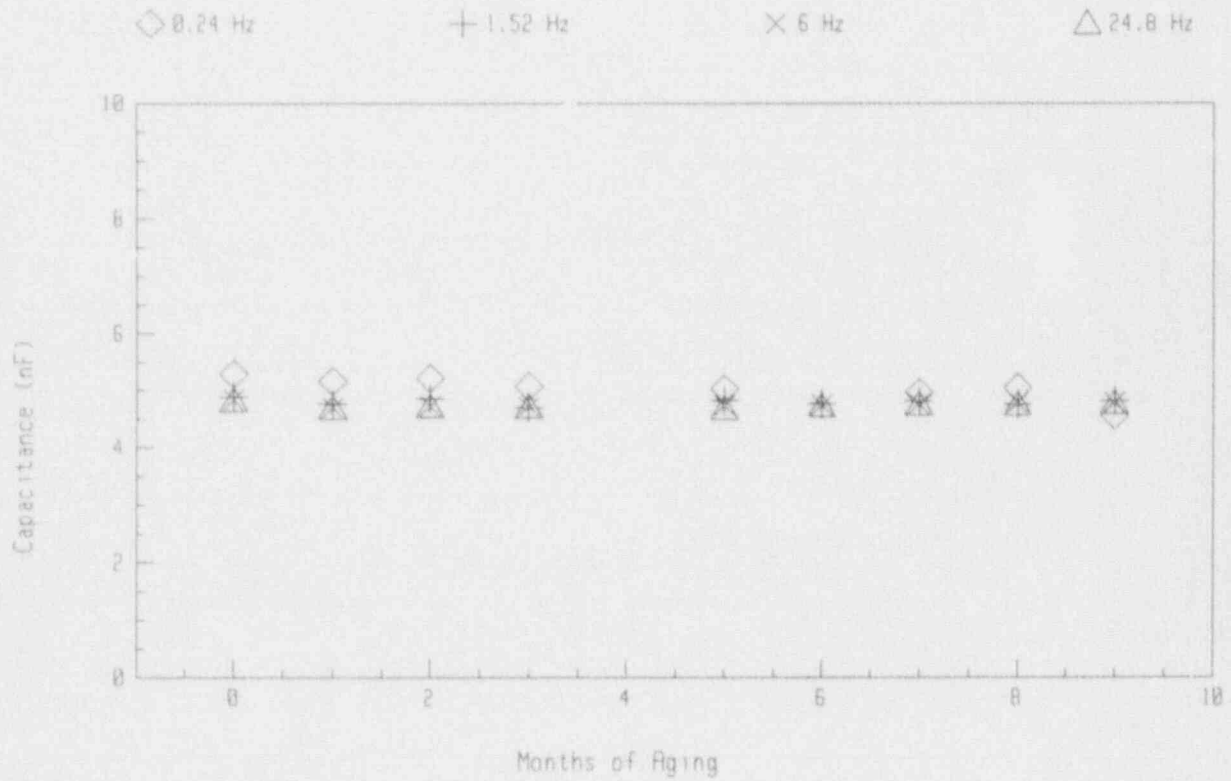

Figure D-12 Capacitance of Dekoron Polyset Conductor #26 During Aging

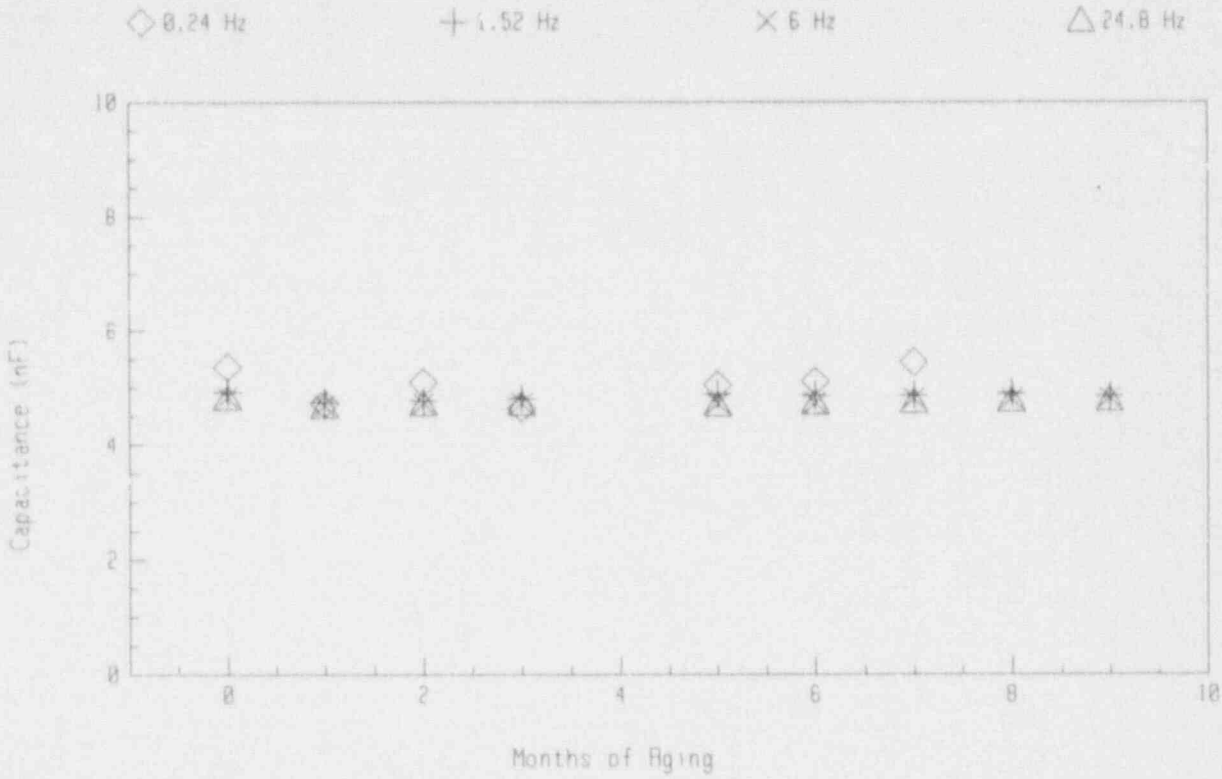

Figure D-13 Capacitance of Dekoron Polyset Conductor #27 During Aging

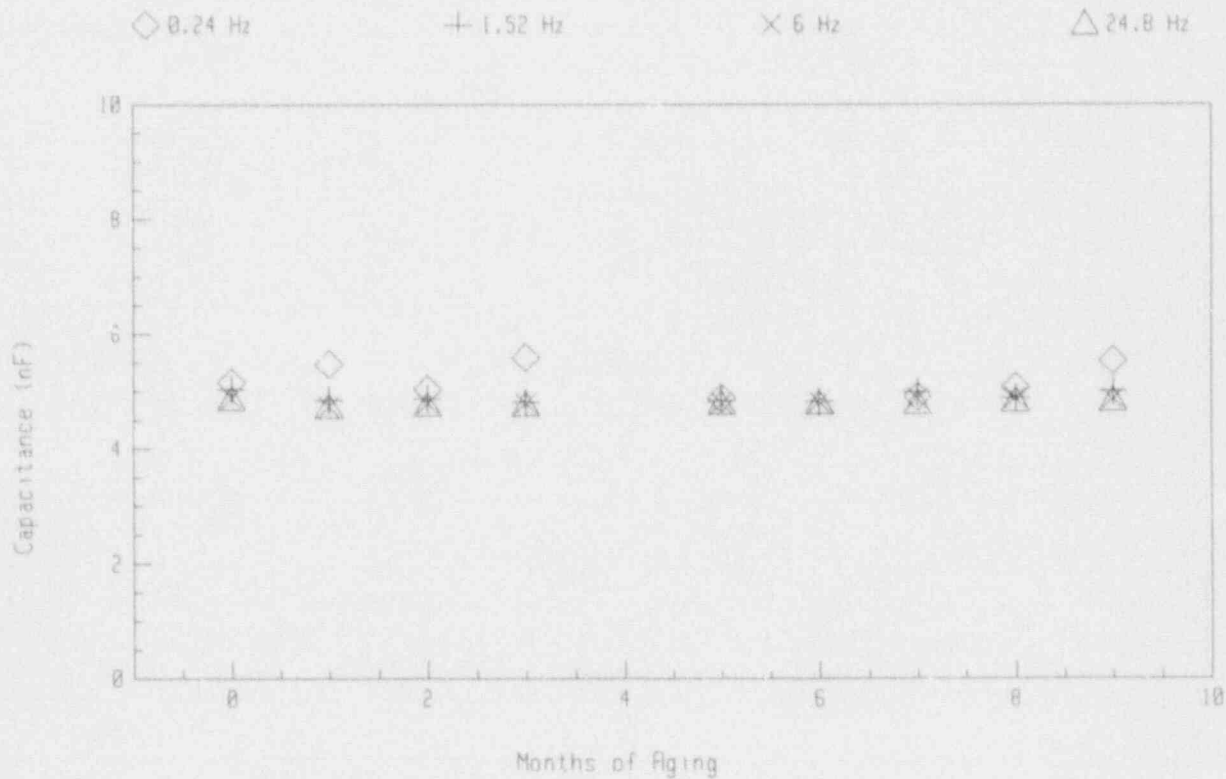

Figure D-14 Capacitance of Dekoron Polyset Conductor #28 During Aging

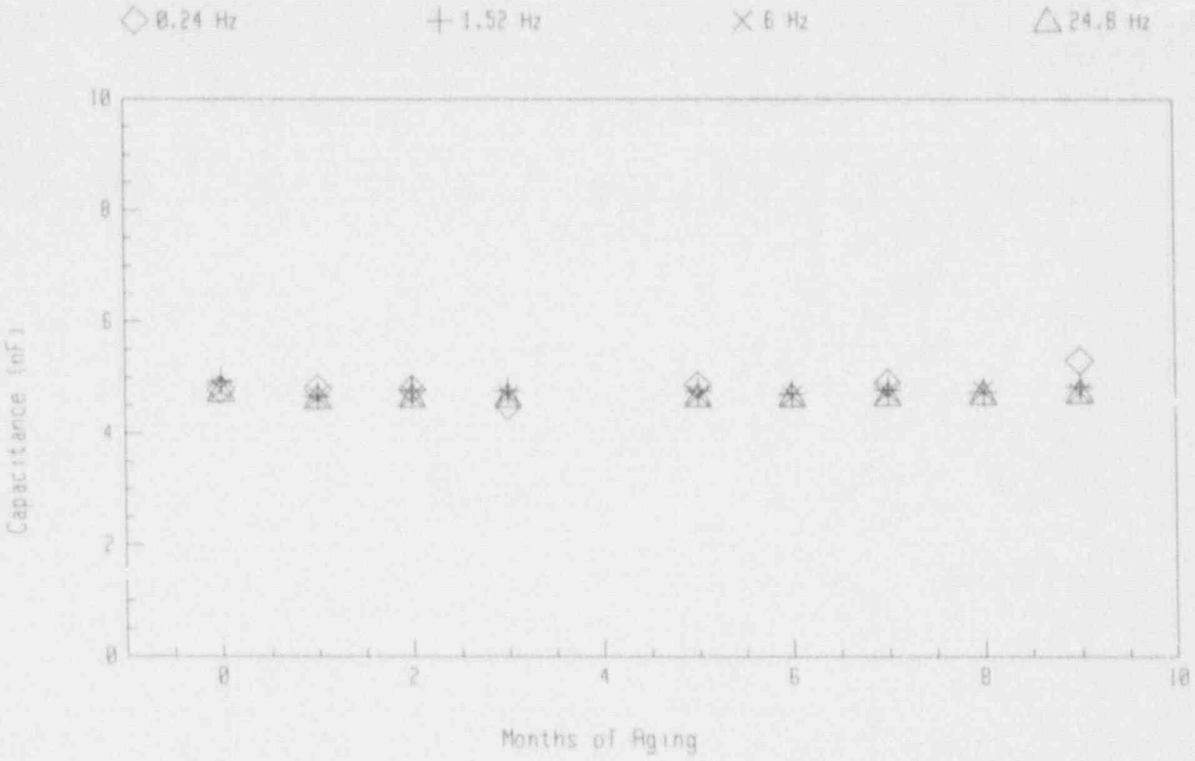

Figure D-15 Capacitance of Dekoron Polyset Conductor #29 During Aging

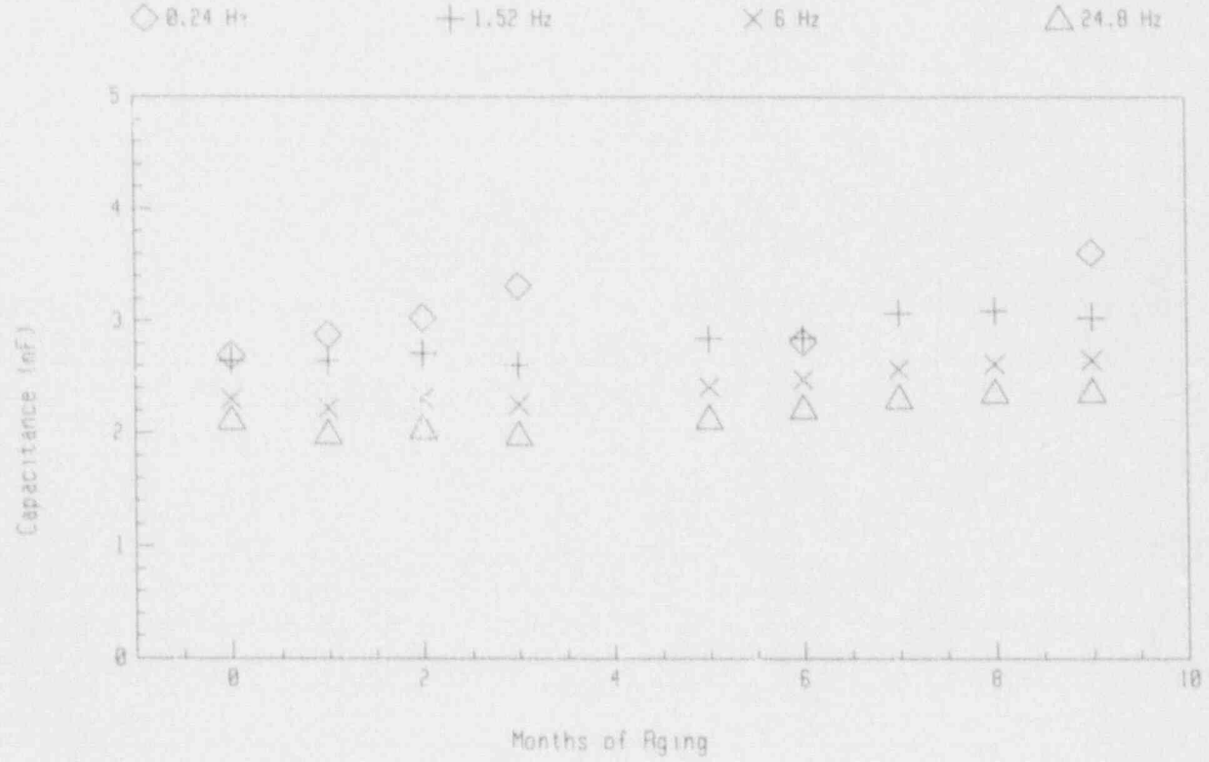

Figure D-16 Capacitance of Raychem Conductor #35 During Aging

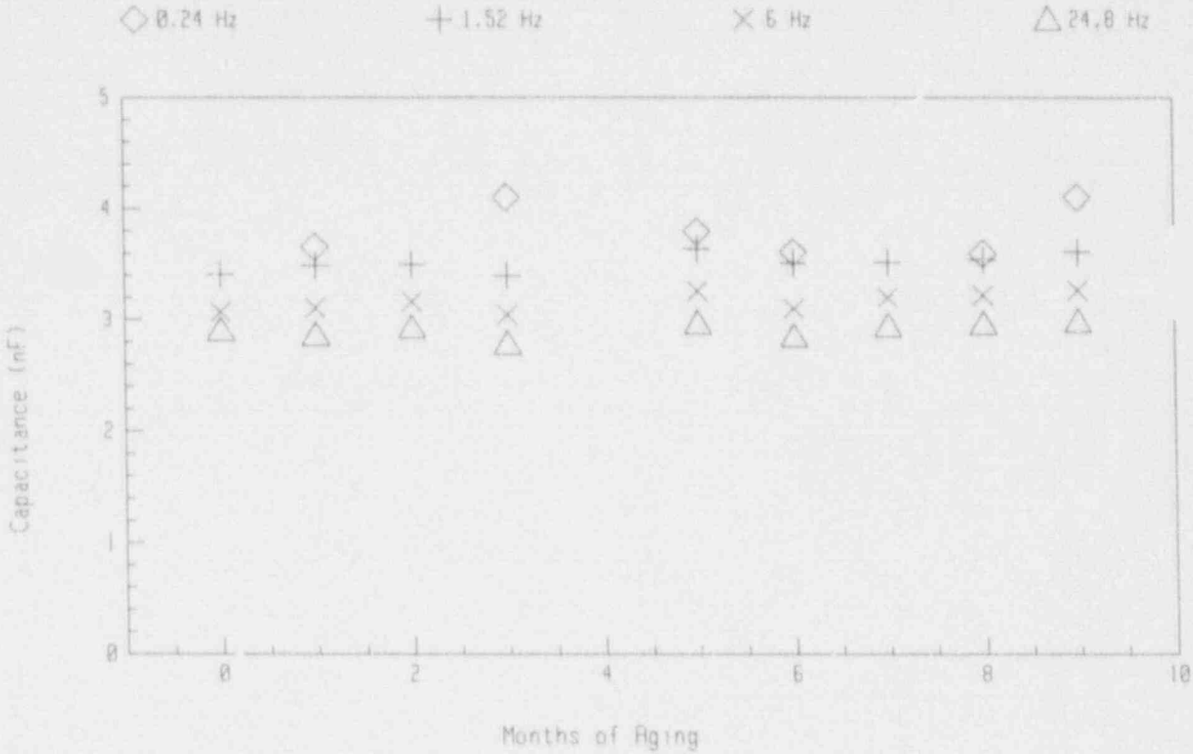

Figure D-17 Capacitance of Raychem Conductor #36 During Aging

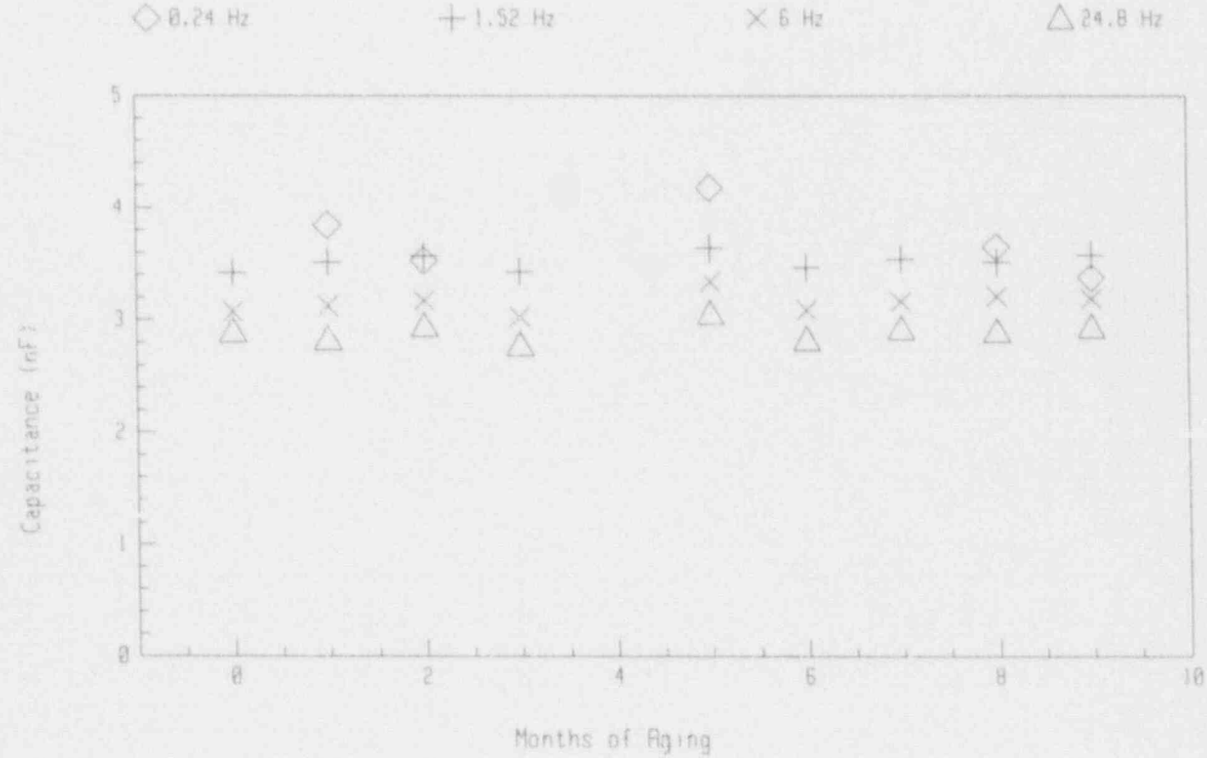

Figure D-18 Capacitance of Raychem Conductor #37 During Aging

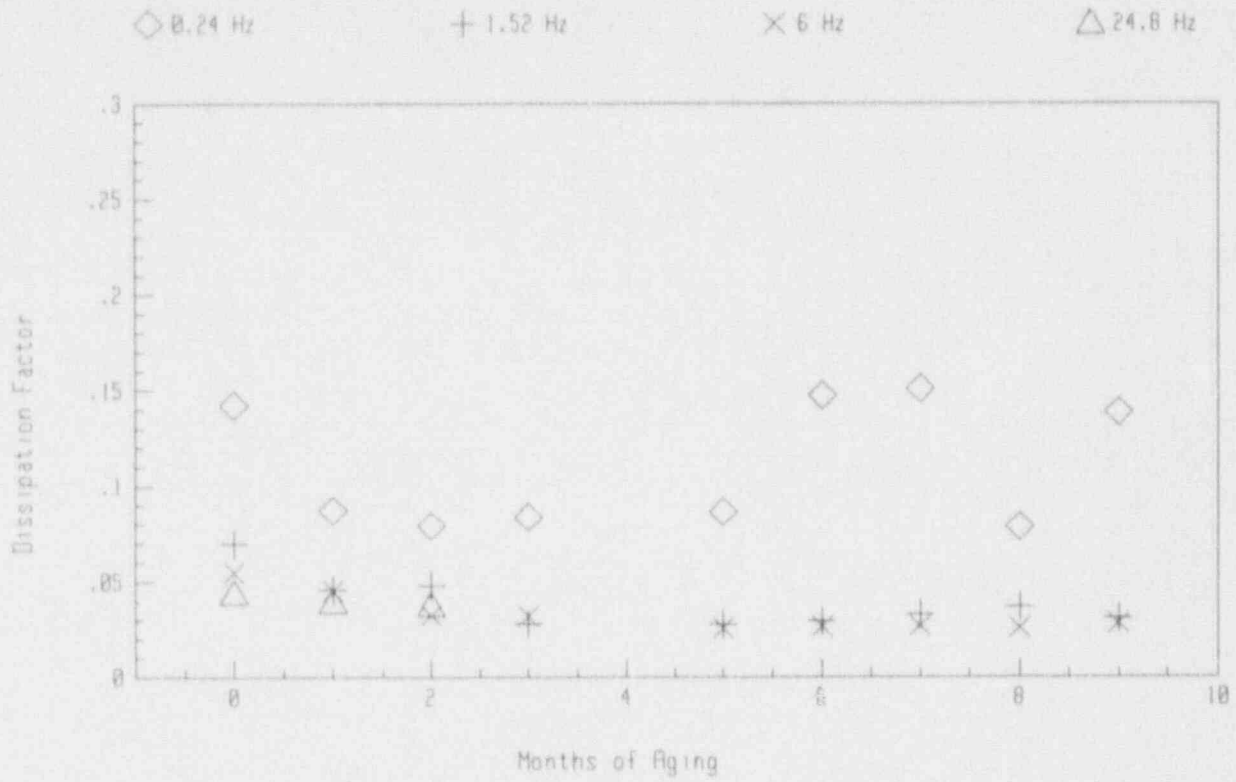

Figure D-19 DF of Brand Rex Conductor #1 During Aging

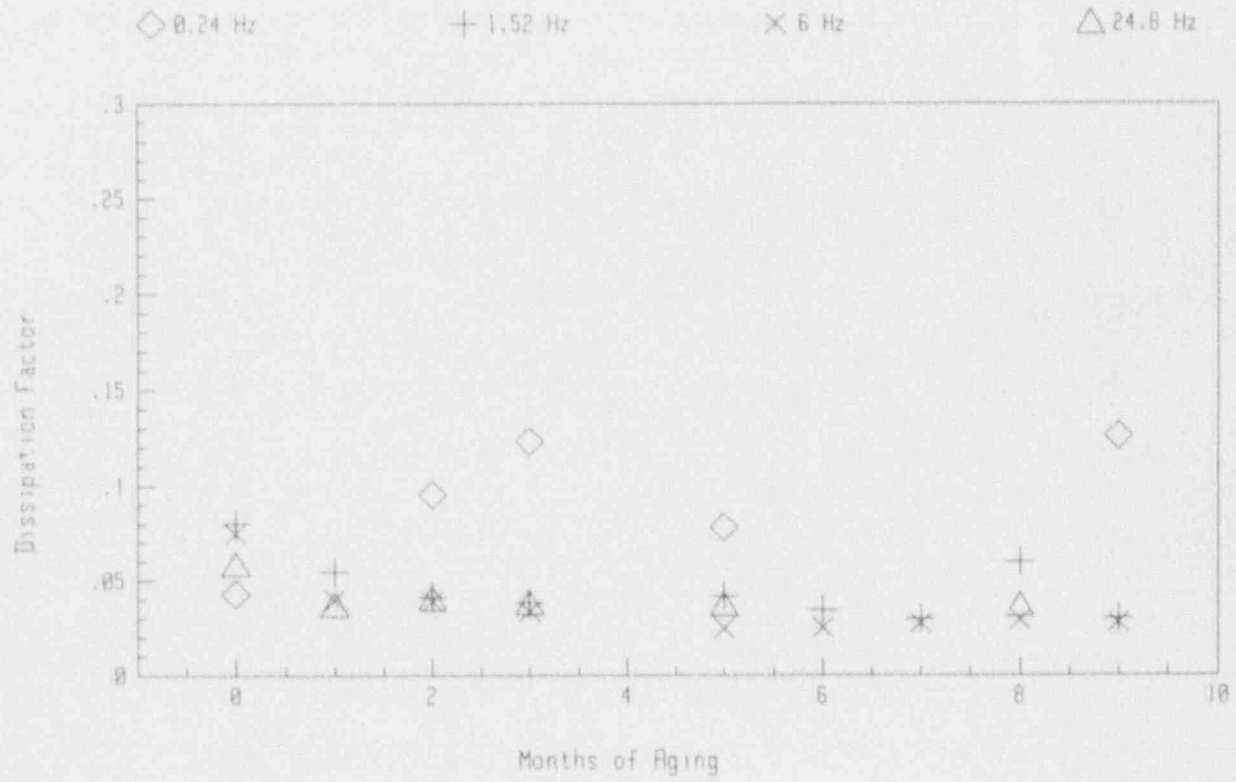

Figure D-20 DF of Brand Rex Conductor #2 During Aging

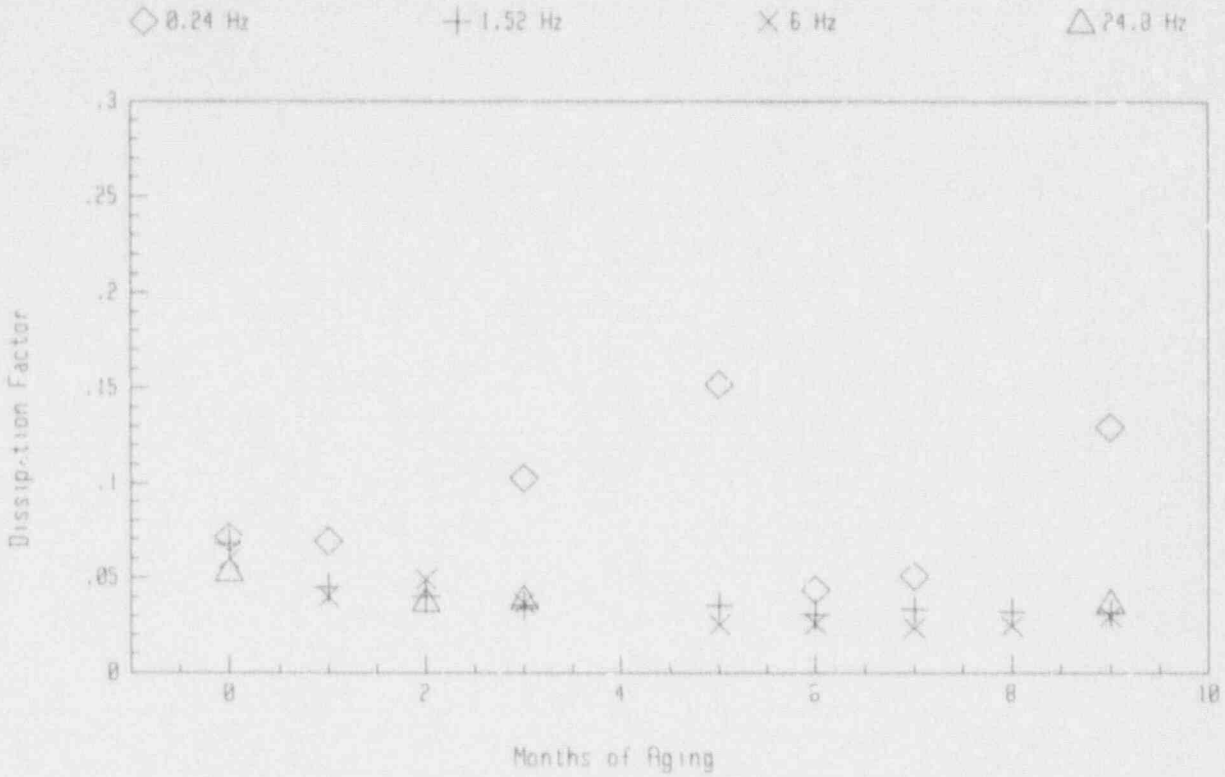

Figure D-21 DF of Brand Rex Conductor #3 During Aging

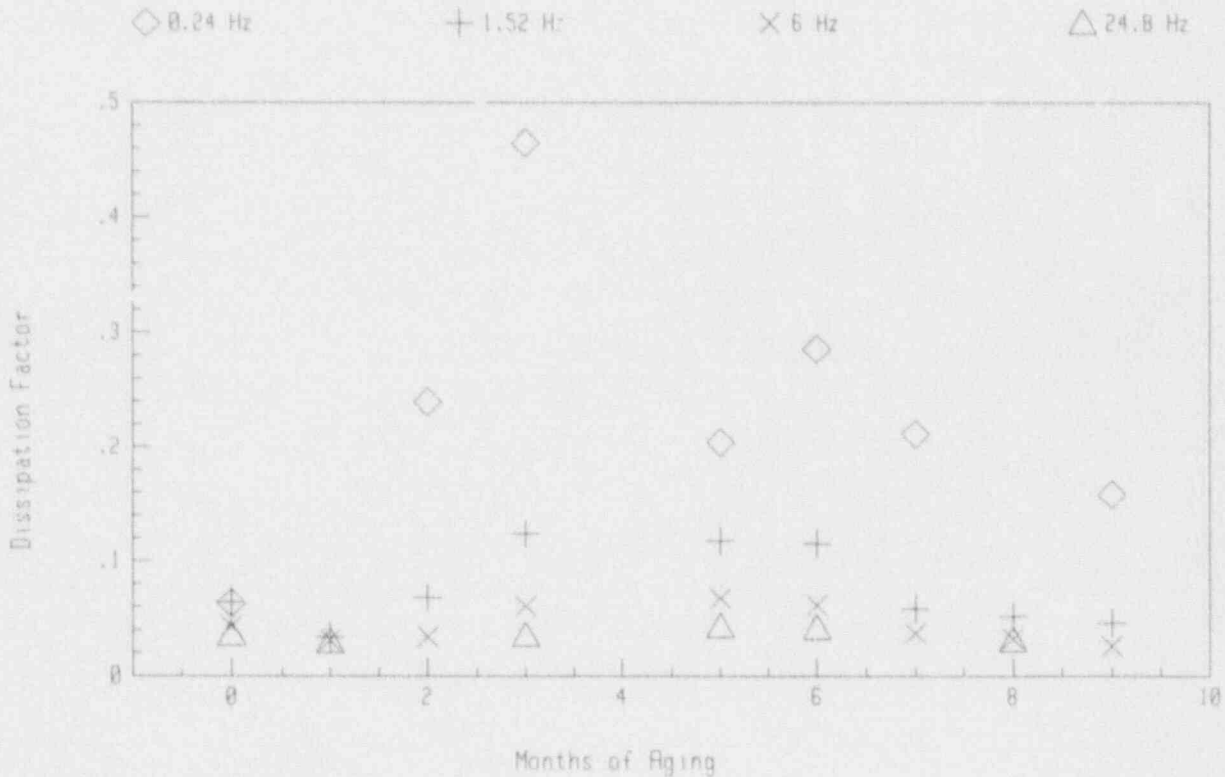

Figure D-22 DF of Rockbestos Conductor #14 During Aging

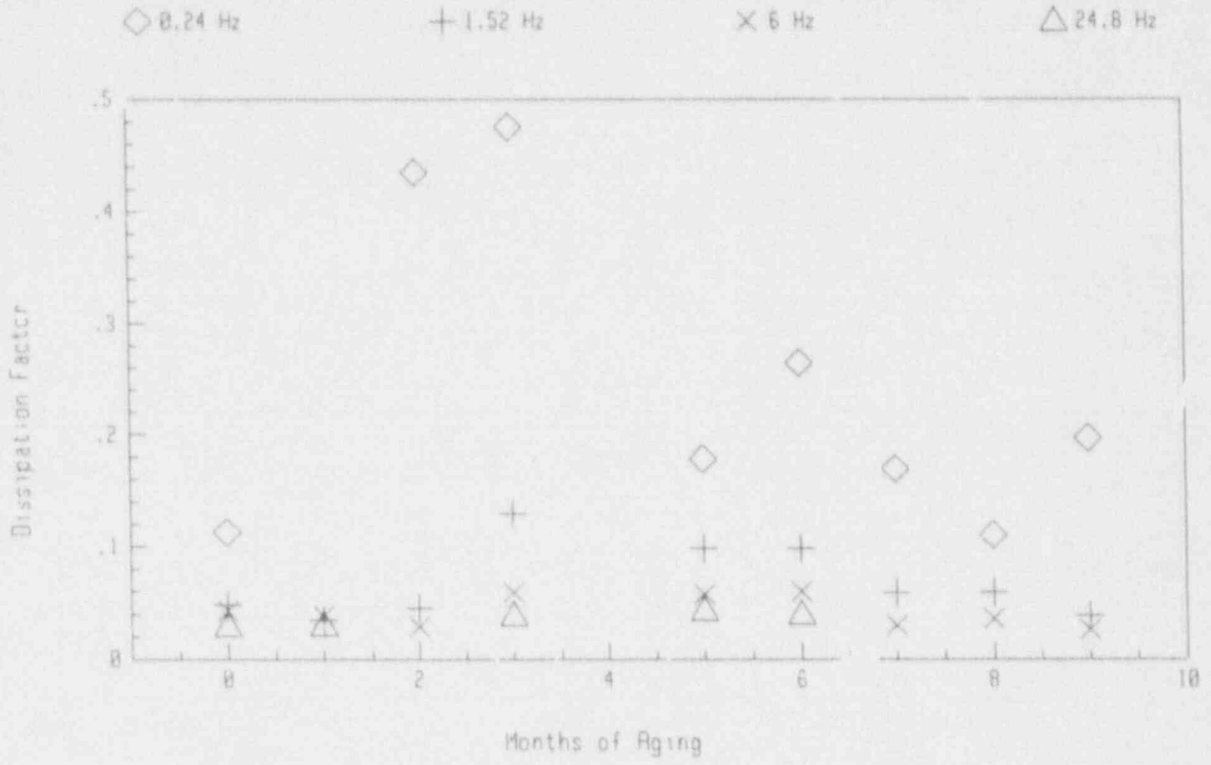

Figure D-23 DF of Rockbestos Conductor #15 During Aging

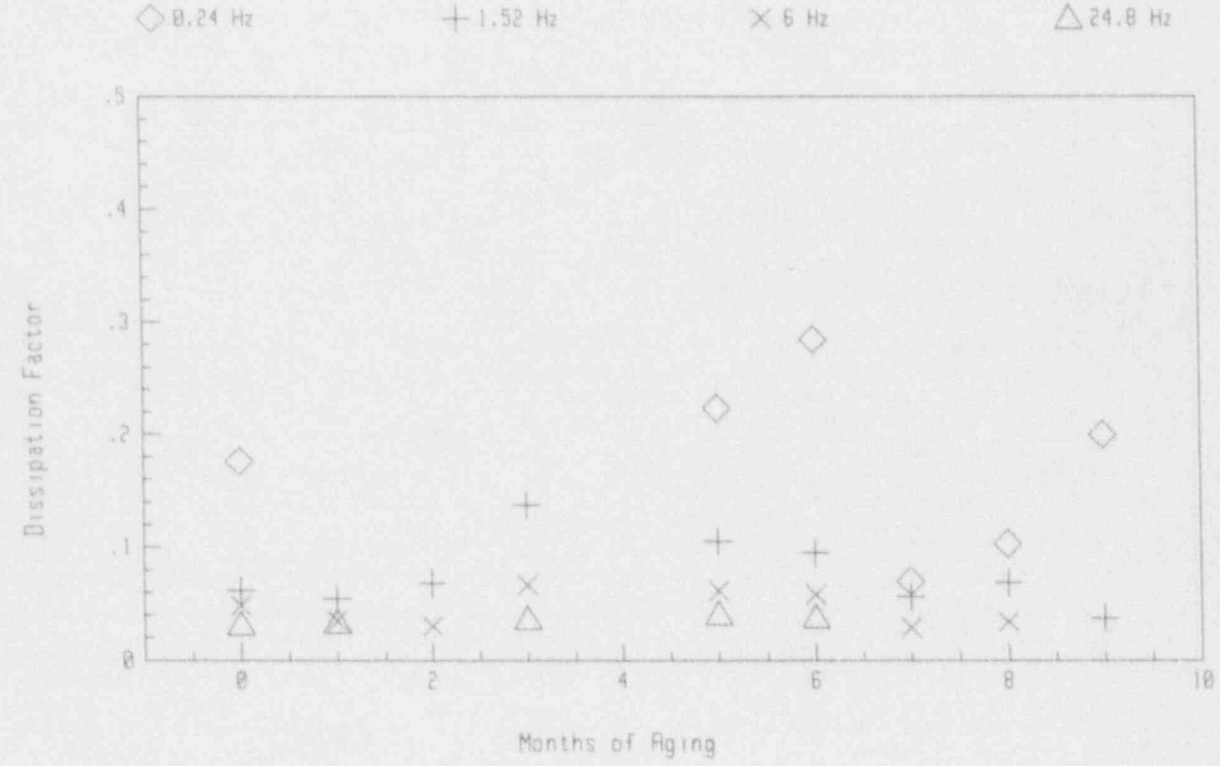

Figure D-24 DF of Rockbestos Conductor #16 During Aging

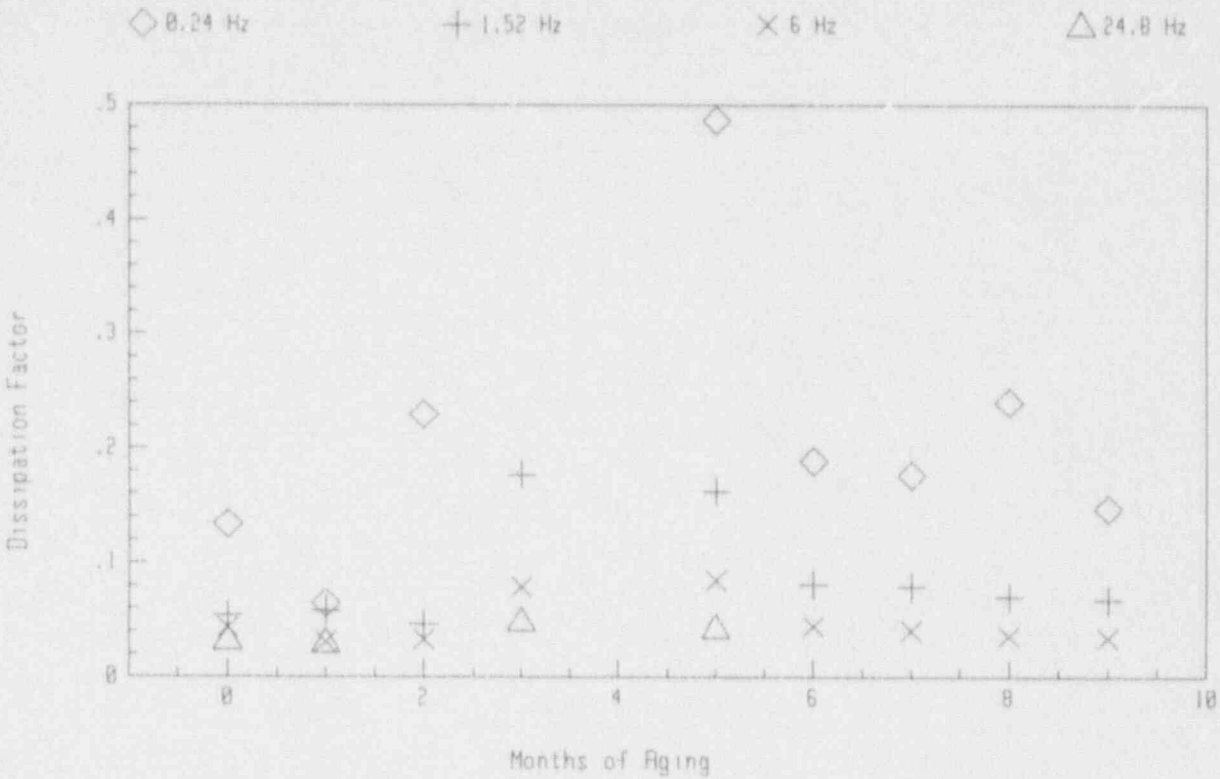

Figure D-25 DF of Rockbestos Conductor #17 During Aging

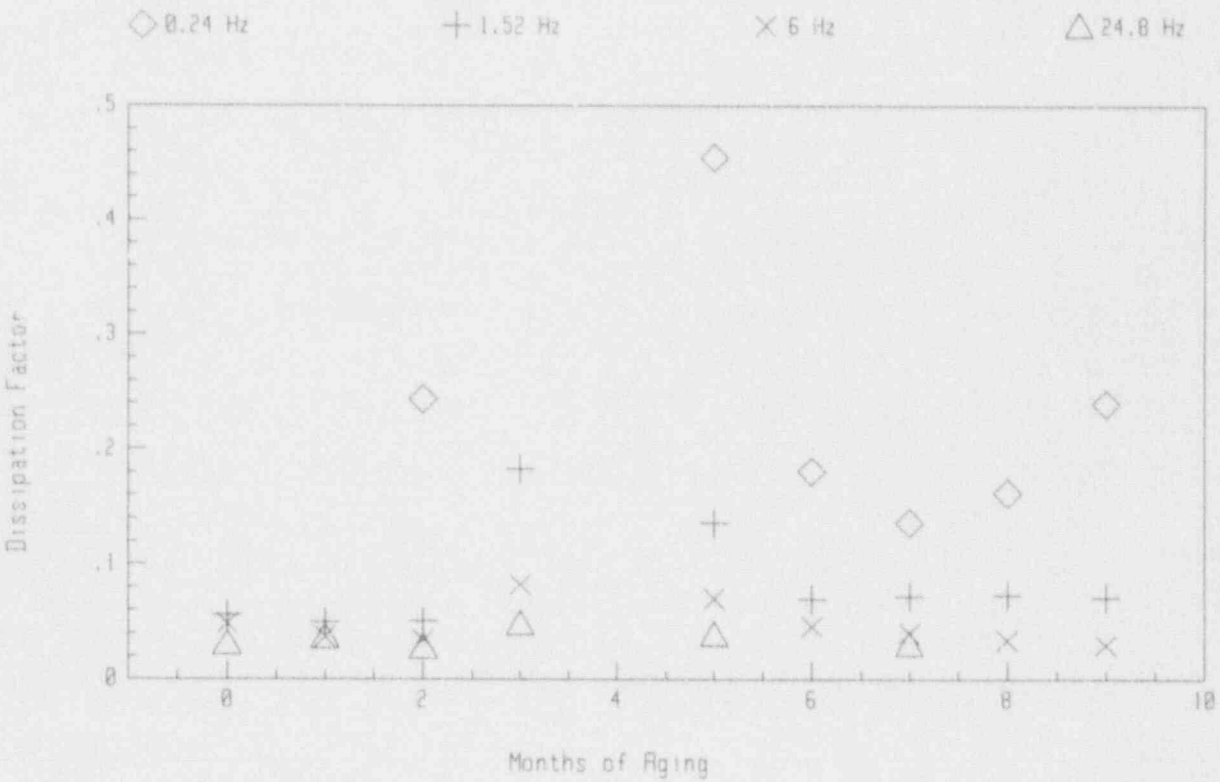

Figure D-26 DF of Rockbestos Conductor #18 During Aging

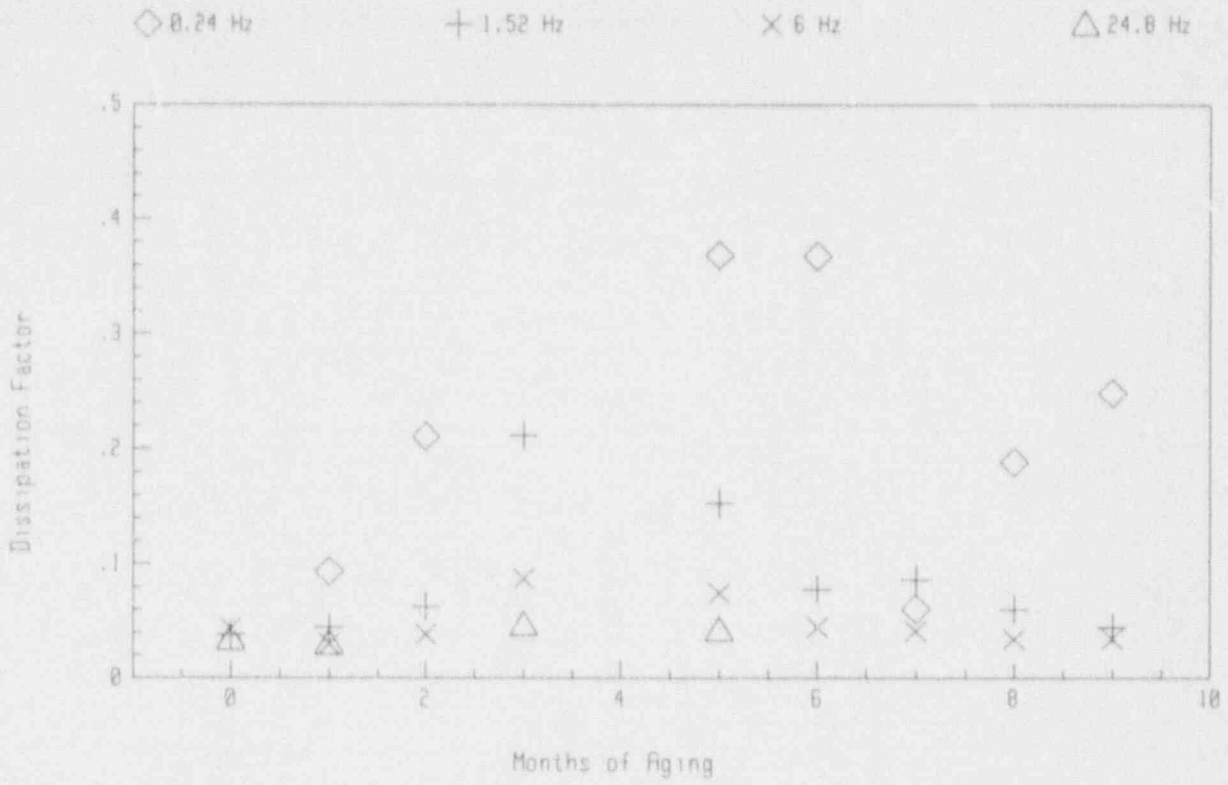

Figure D-27 DF of Rockbestos Conductor #19 During Aging

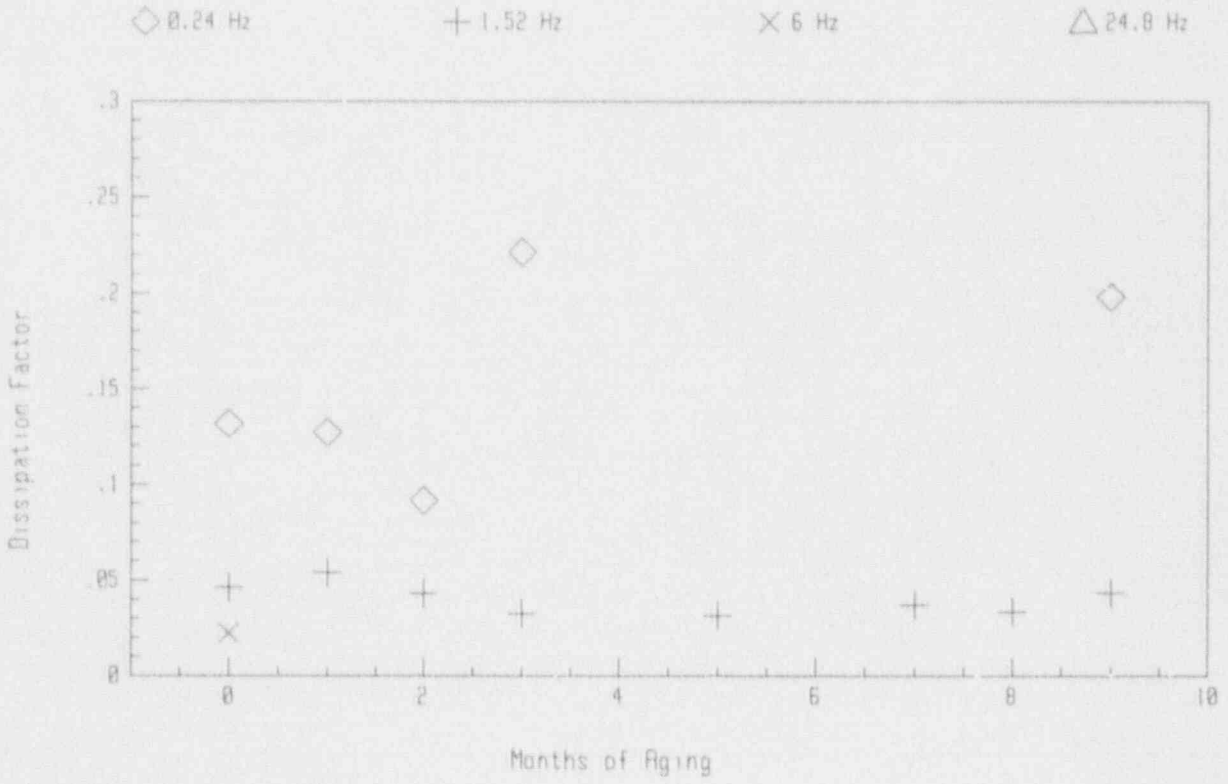

Figure D-28 DF of Dekoron Polyset Conductor #24 During Aging

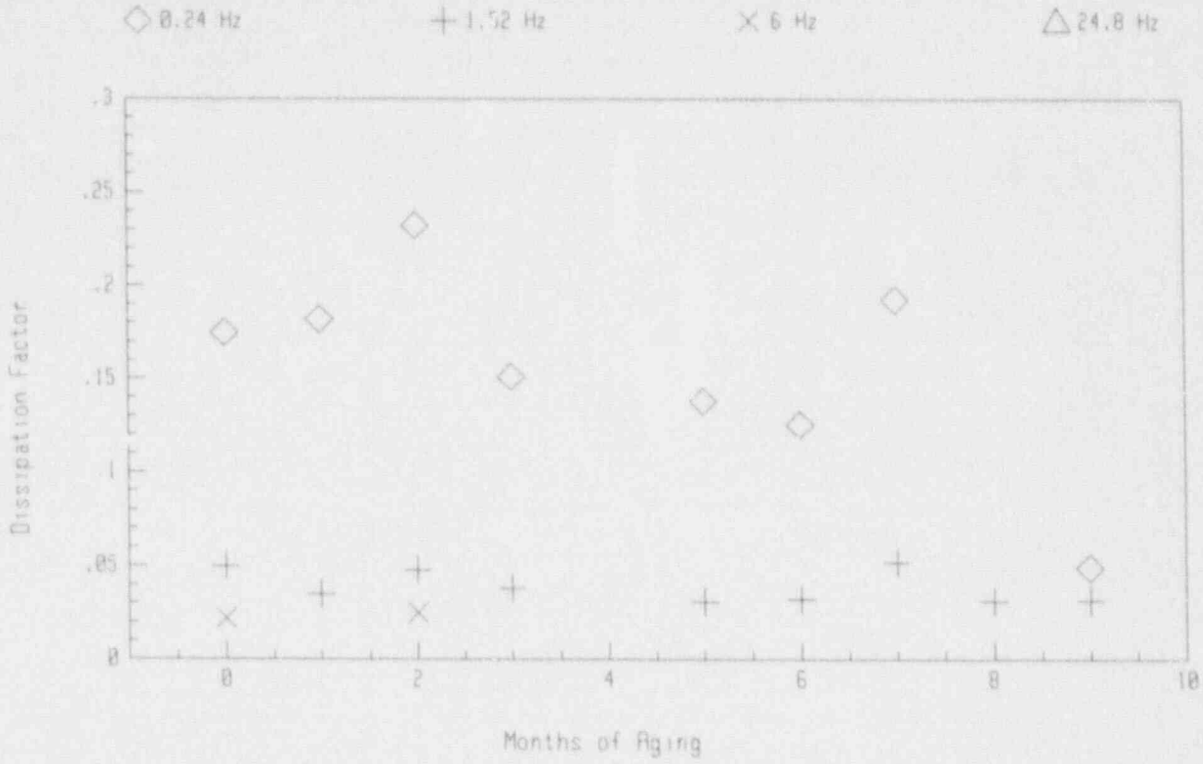

Figure D-29 DF of Dekoron Polyset Conductor #25 During Aging

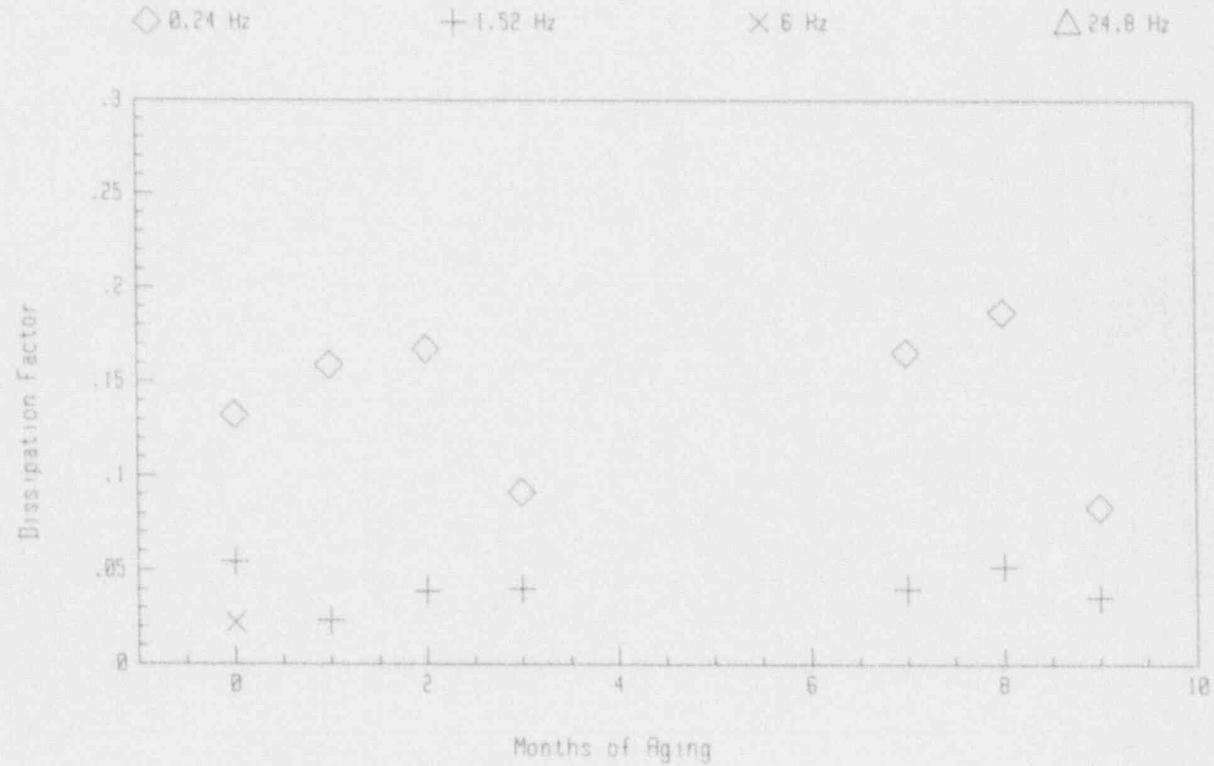

Figure D-30 DF of Dekoron Polyset Conductor #26 During Aging

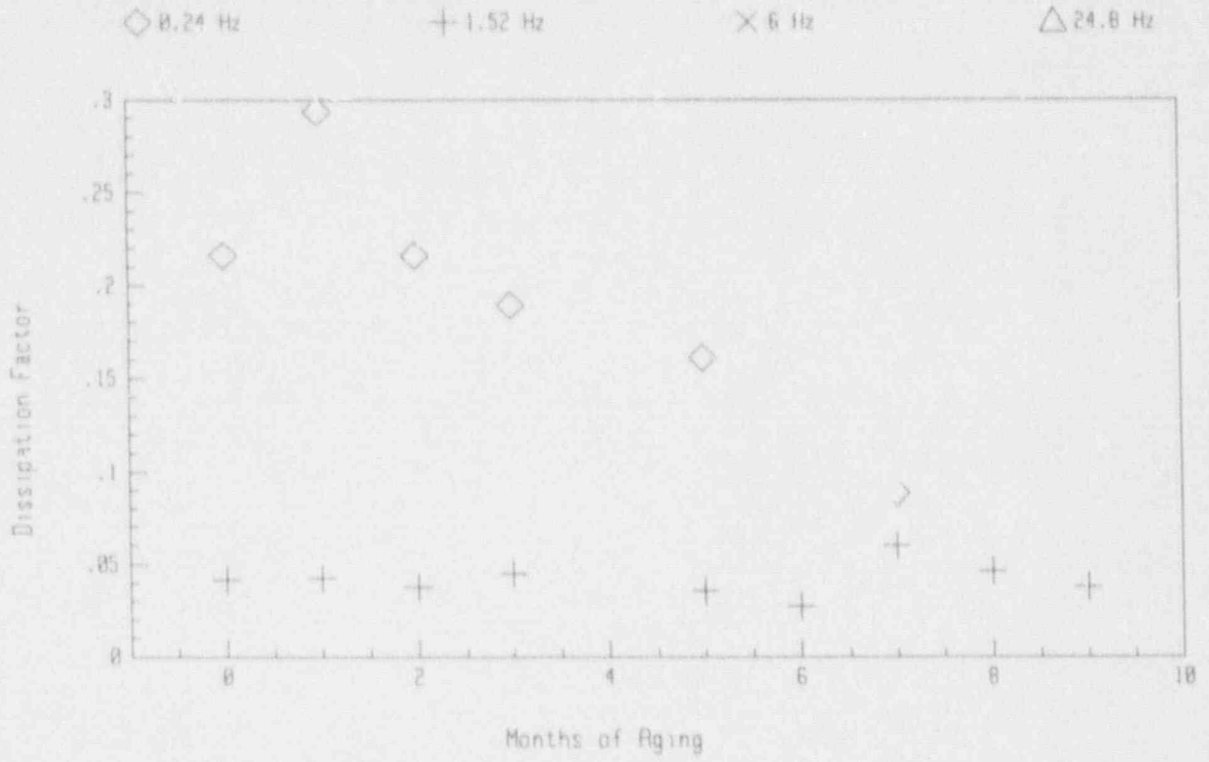

Figure D-31 DF of Dekoron Polyset Conductor #27 During Aging

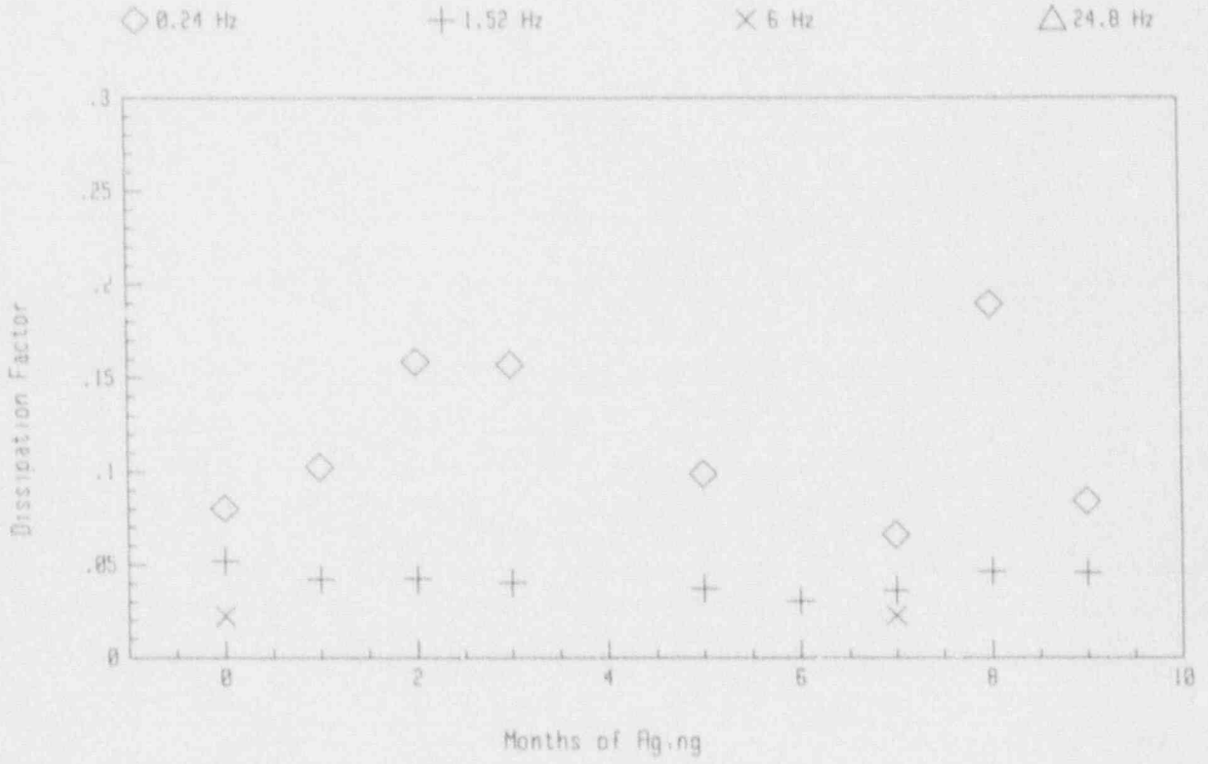

Figure D-32 DF of Dekoron Polyset Conductor #28 During Aging

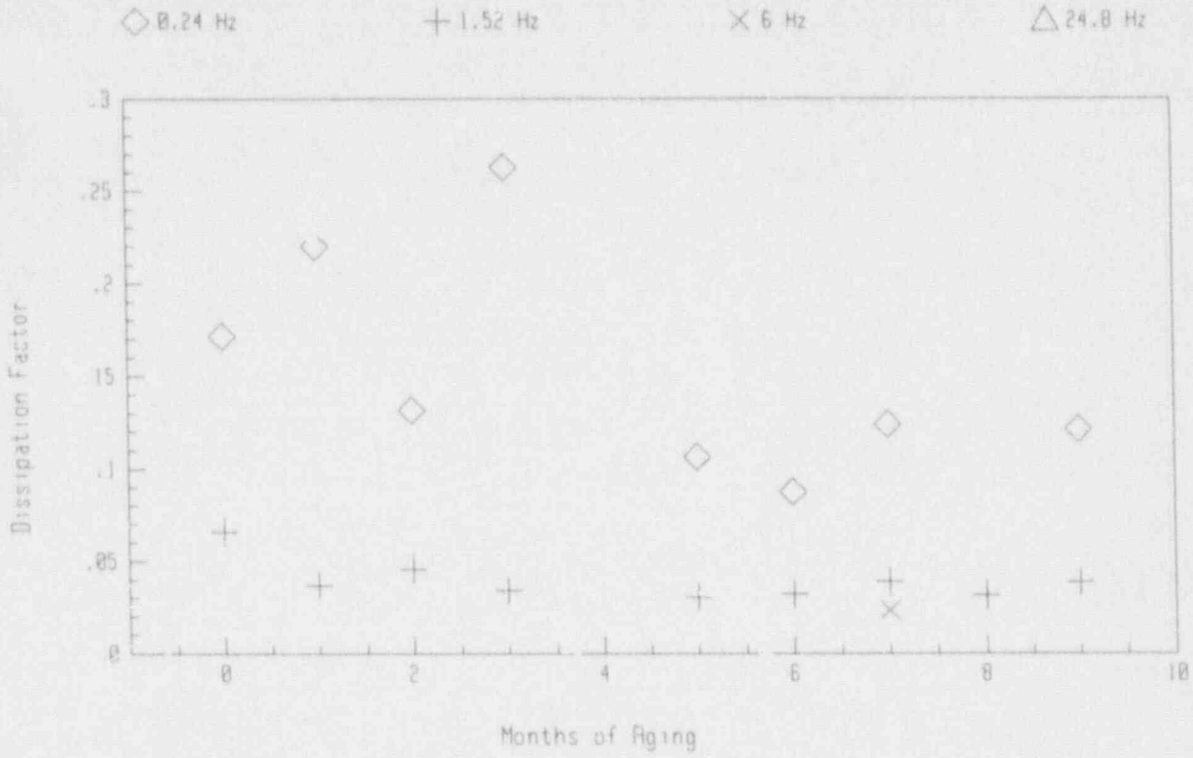

Figure D-33 DF of Dekoron Polyset Conductor #29 During Aging

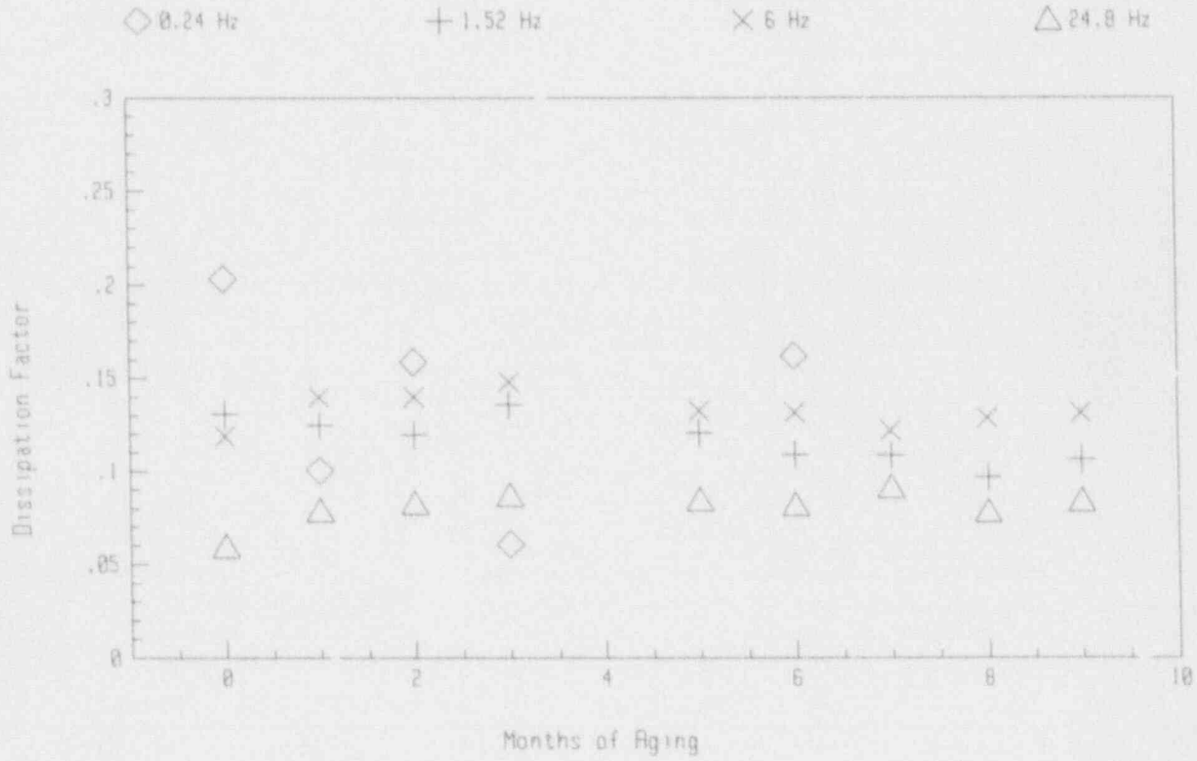

Figure D-34 DF of Raychem Conductor #35 During Aging

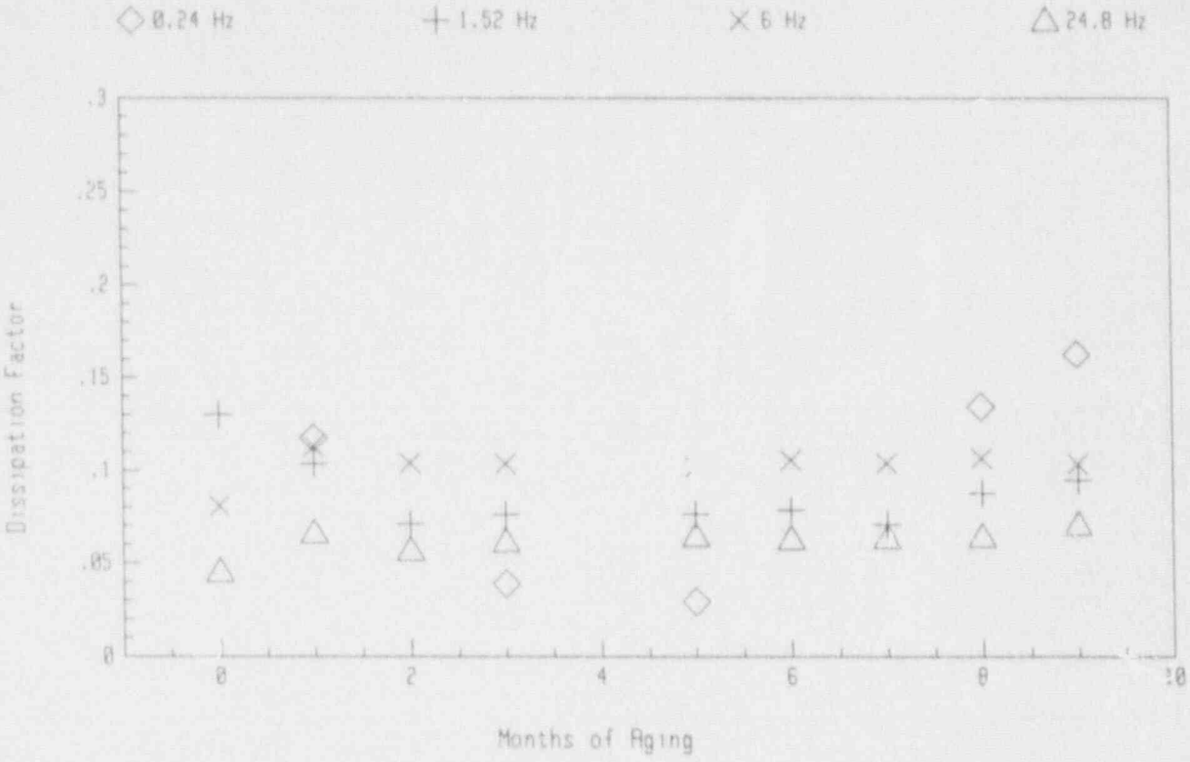

Figure D-35 DF of Raychem Conductor #36 During Aging

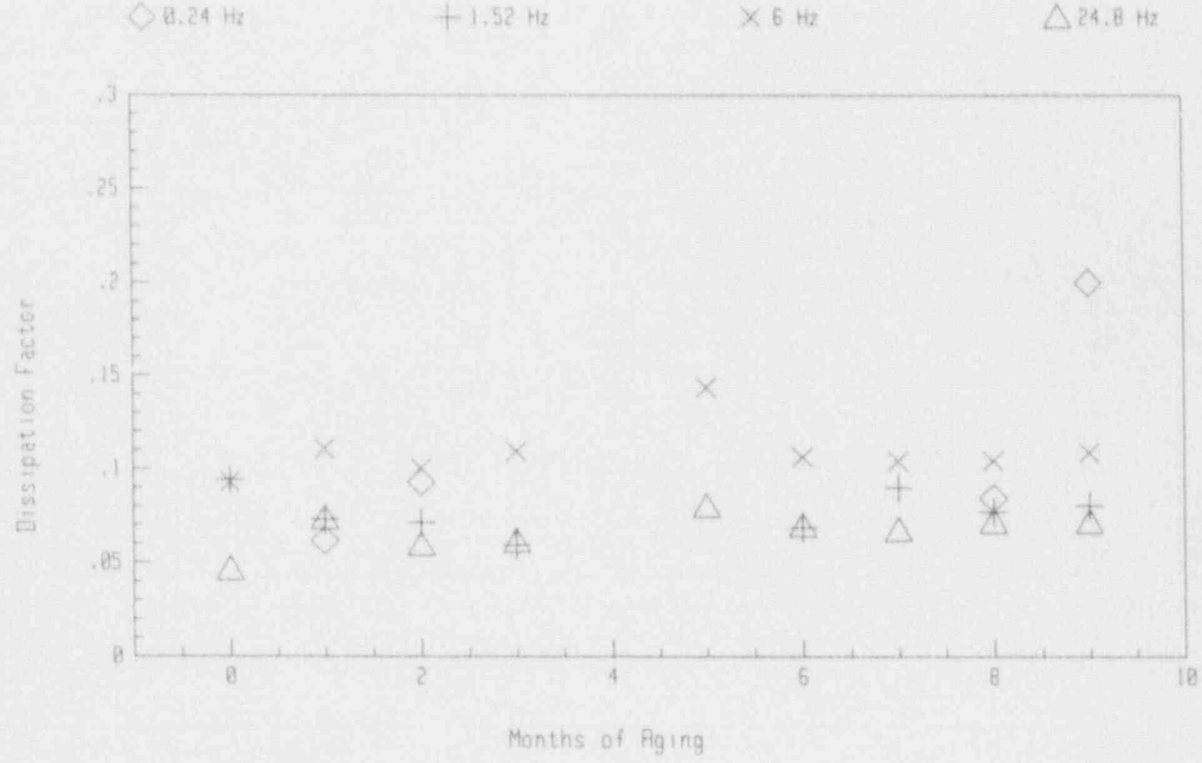

Figure D-36 DF of Raychem Conductor #37 During Aging

Appendix E Elongation and Tensile Strength Data

In this appendix, relative tensile strength and relative elongation are presented for each cable type. Error bars around each data point symbol represent one sample standard deviation of the data. The data point at 0 kGy total dose on each plot is from virgin cable specimens. The data points between 0 and 600 kGy are from samples exposed to aging only. The data points at 800-1000 kGy are from samples that were exposed only to accident radiation. (These samples were placed in the 6-month chamber after aging, but prior to the accident radiation exposure.) Finally, the data points beyond 1000 kGy are from samples exposed to both aging (either 3, 6, or 9 months) and accident radiation.

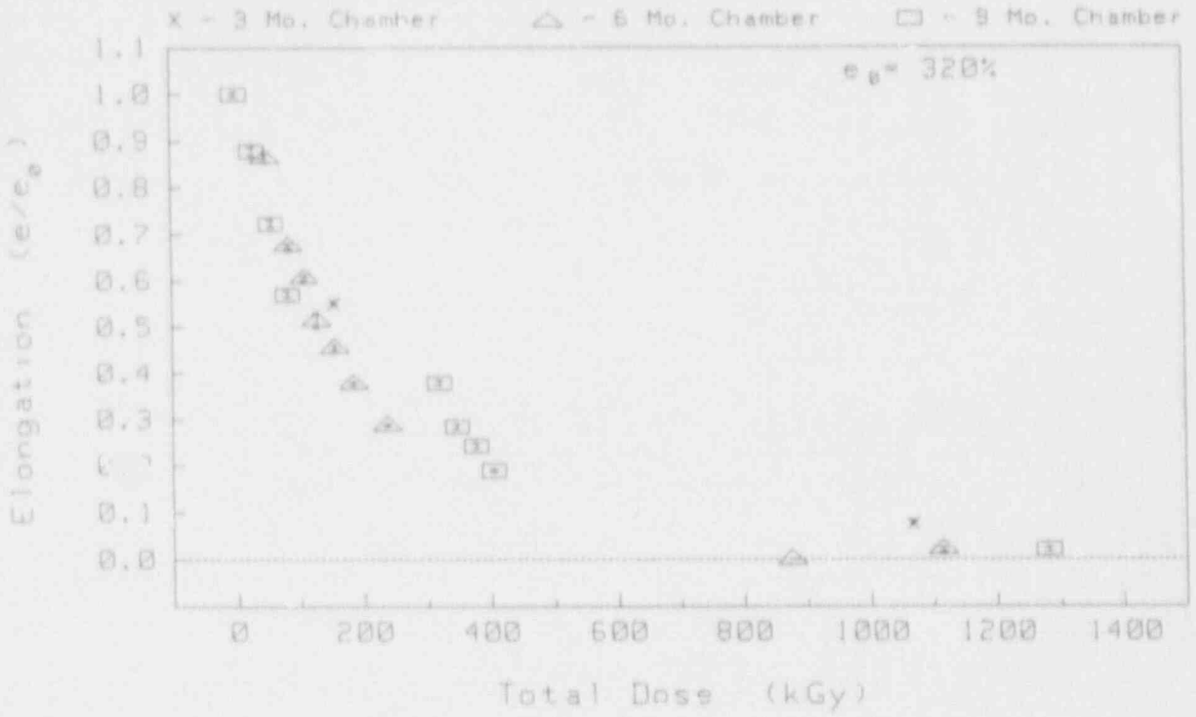

Figure E-1 Elongation of Brand Rex Insulation

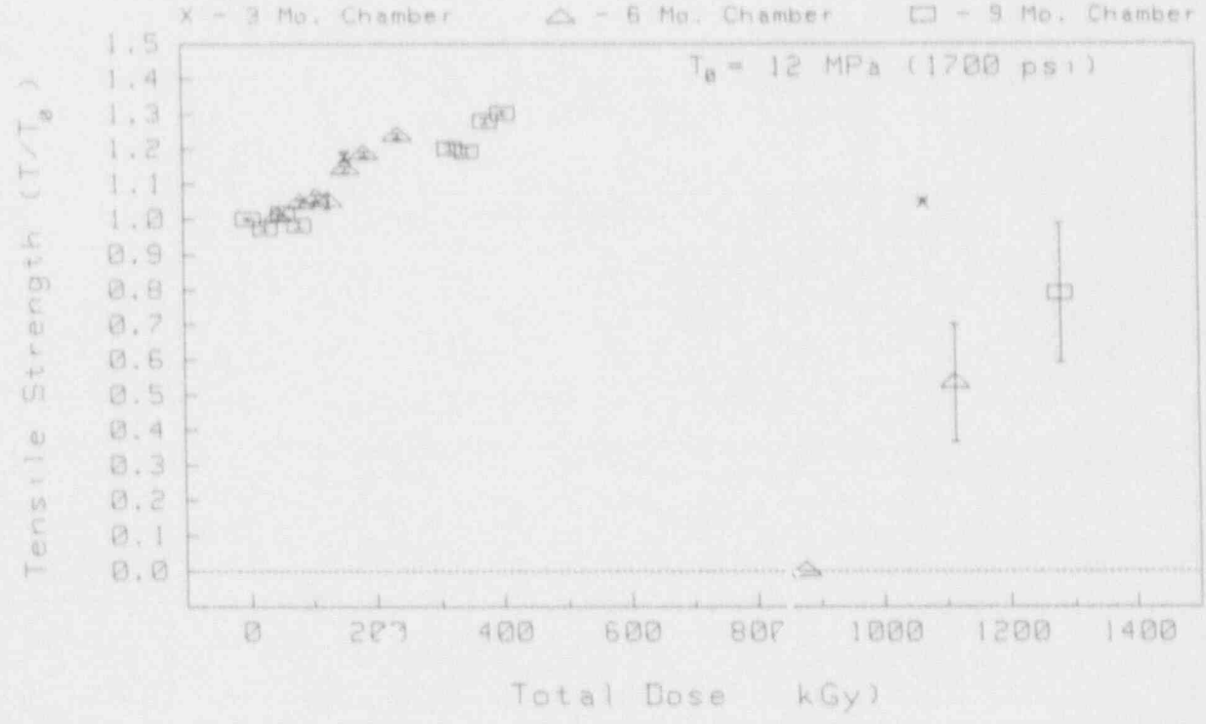

Figure E-2 Tensile Strength of Brand Rex Insulation

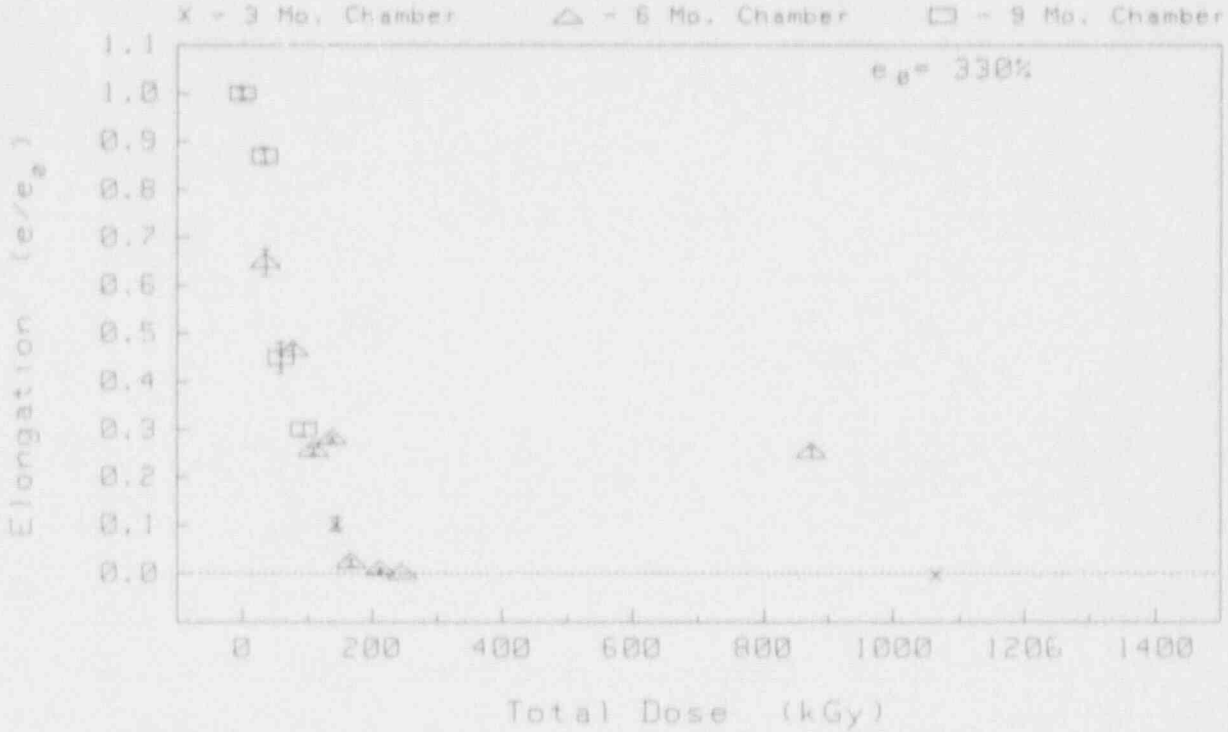

Figure E-3 Elongation of Brand Rex Jacket

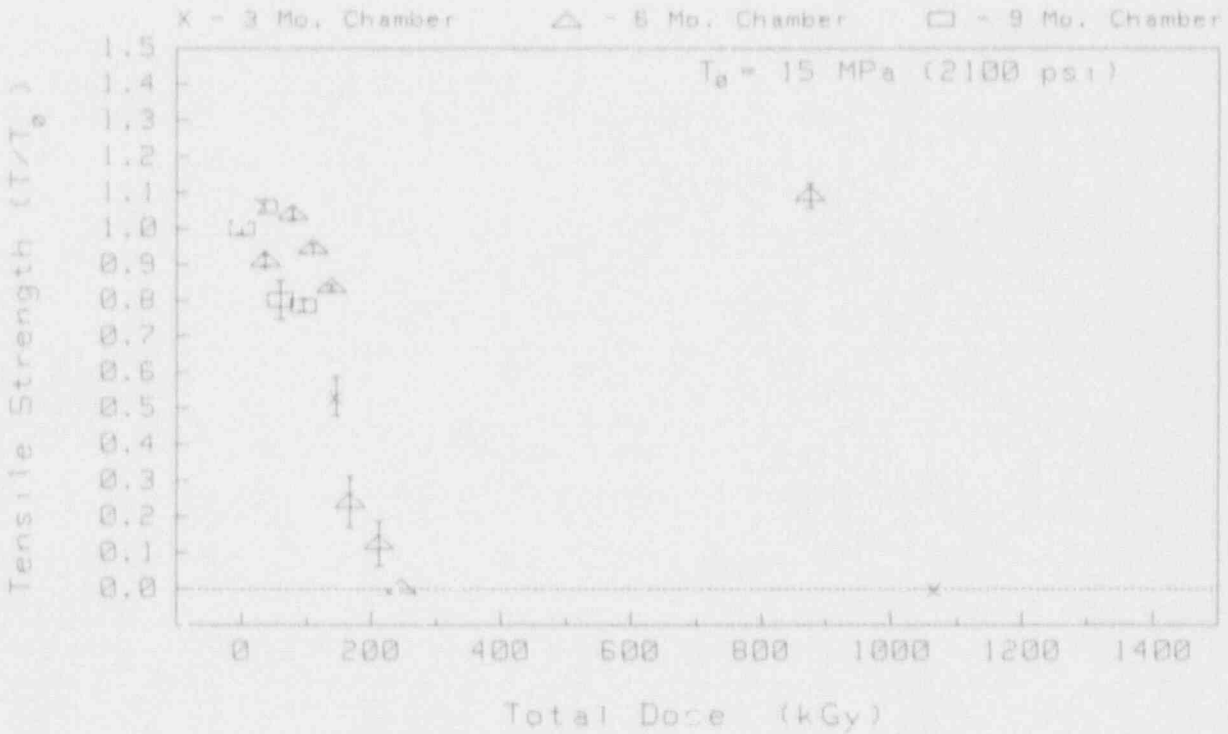

Figure E-4 Tensile Strength of Brand Rex Jacket

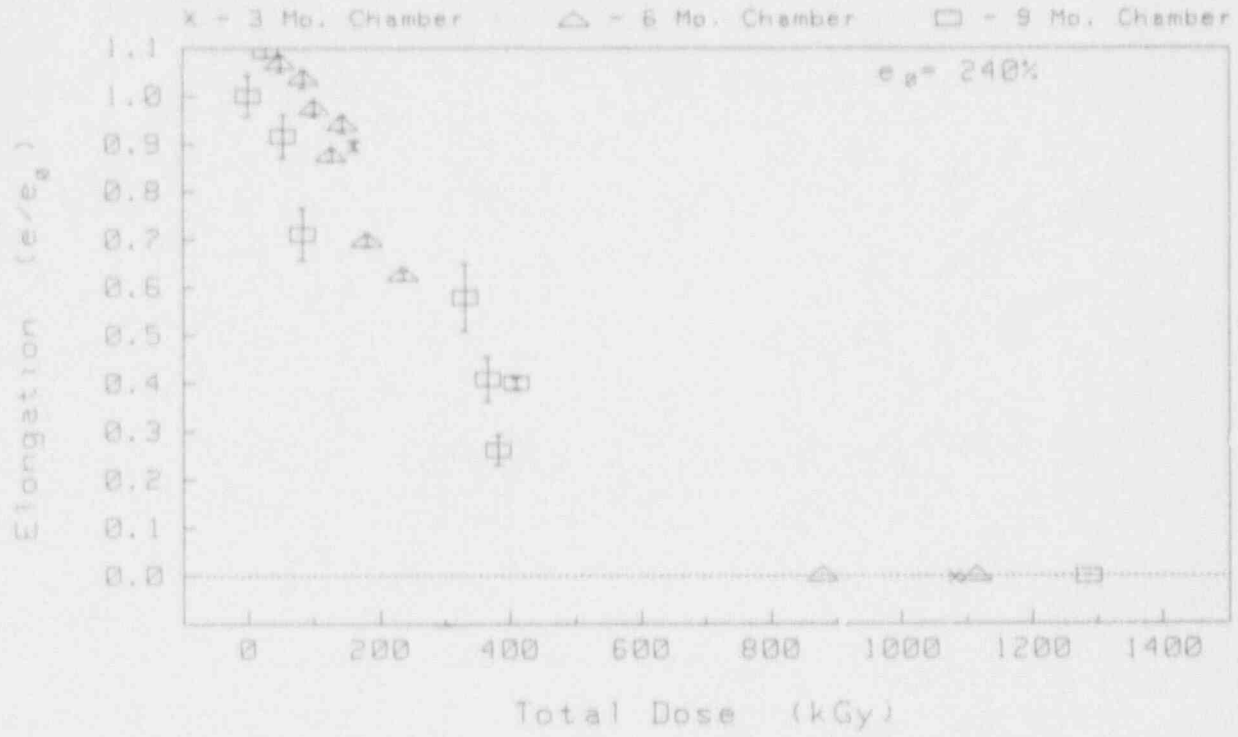

Figure E-5 Elongation of Rockbestos Insulation

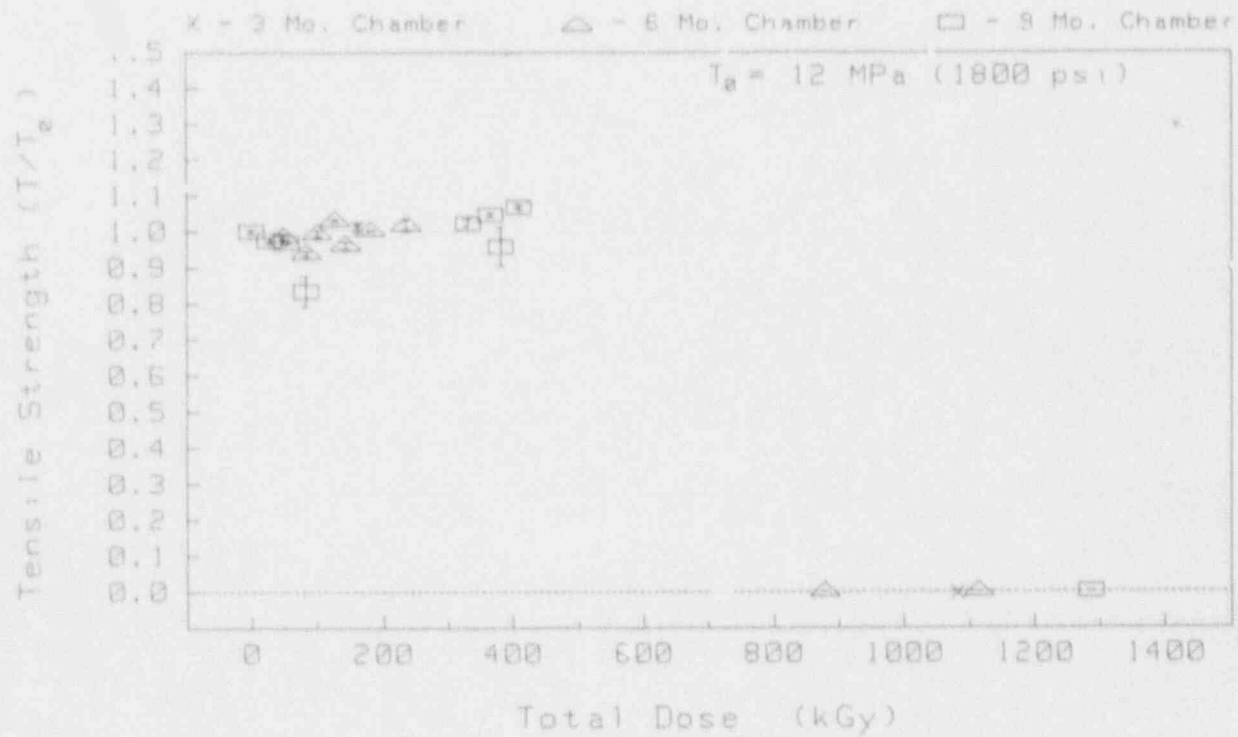

Figure E-6 Tensile Strength of Rockbestos Insulation

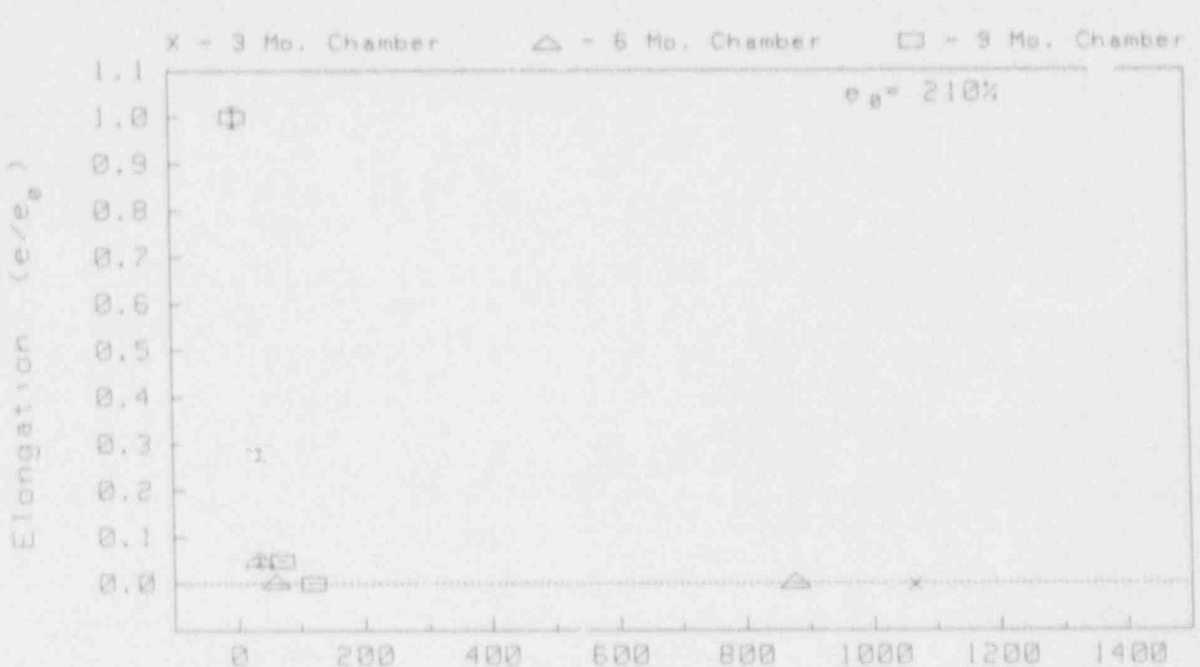

Figure E-7 Elongation of Rockbestos Jacket

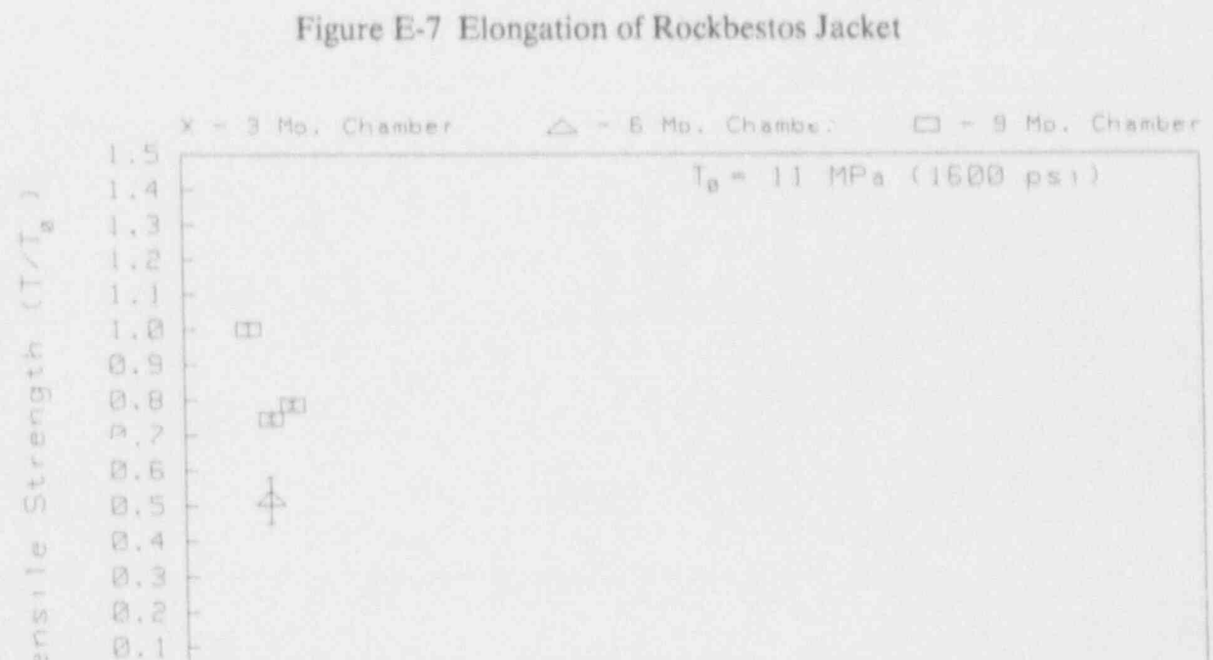

Figure E-8 Tensile Strength of Rockbestos Jacket

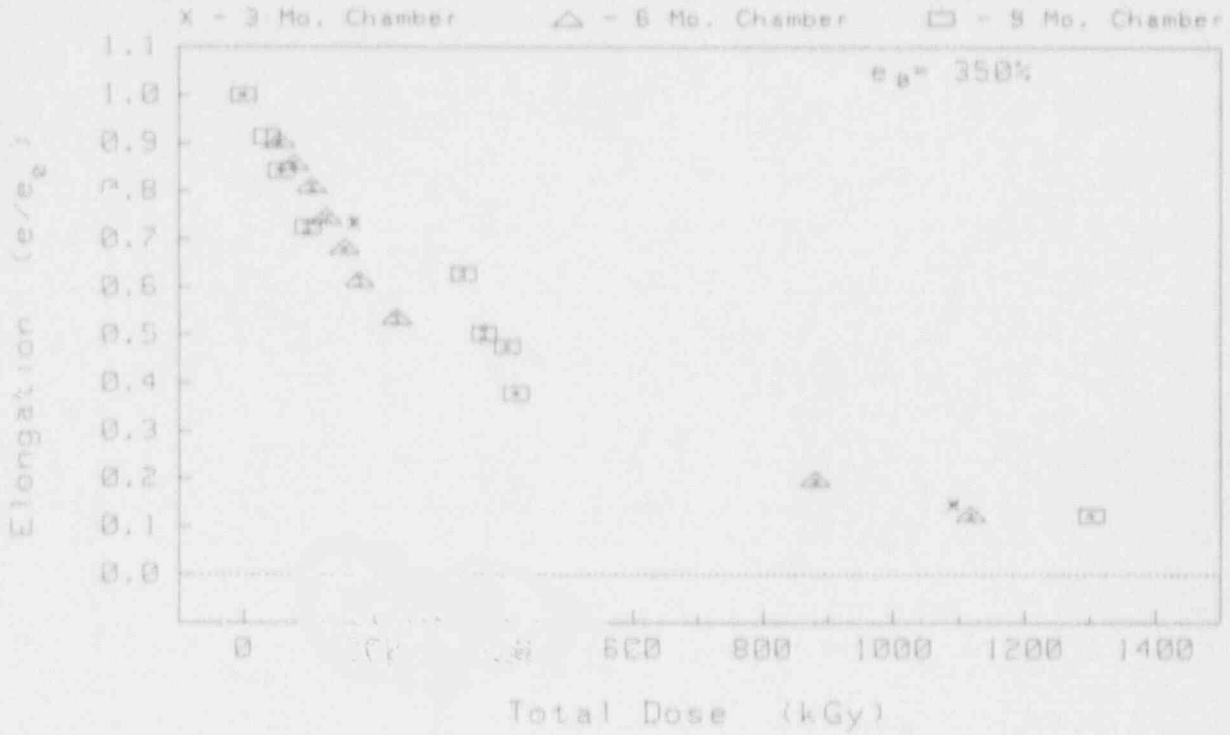

Figure E-9 Elongation of Dekoron Polyset Insulation

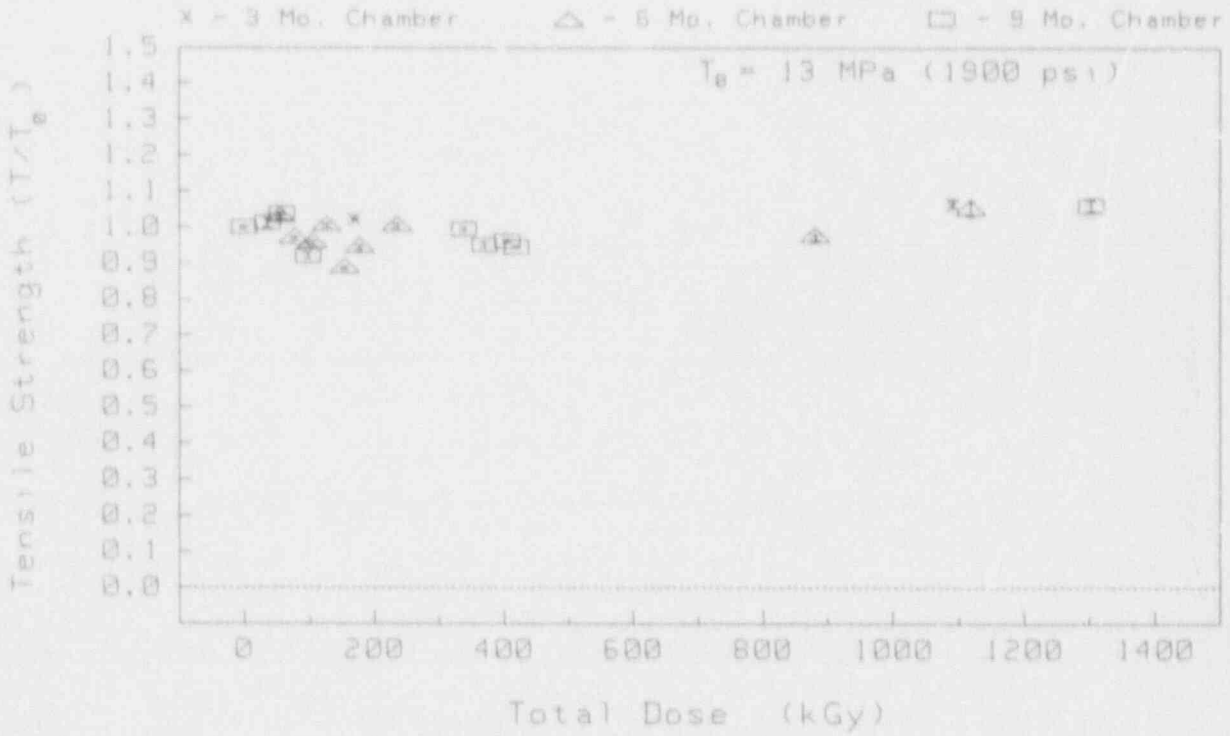

Figure E-10 Tensile Strength of Dekoron Polyset Insulation

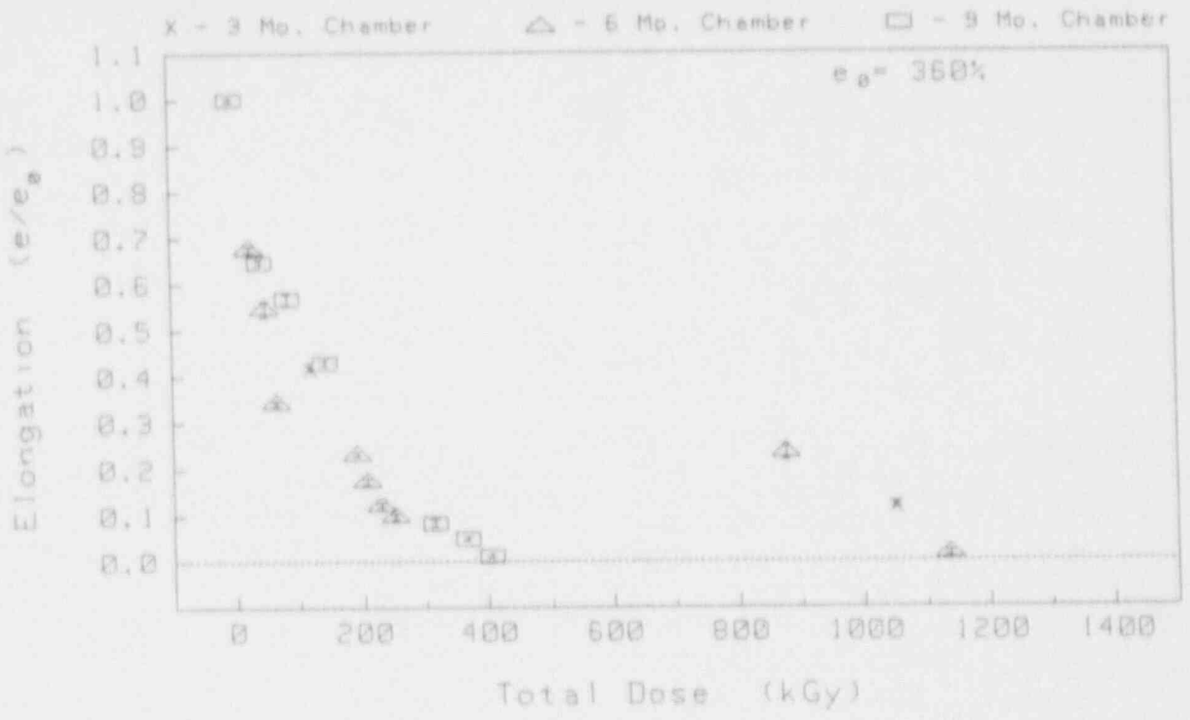

Figure E-11 Elongation of Dekoron Polyset Jacket

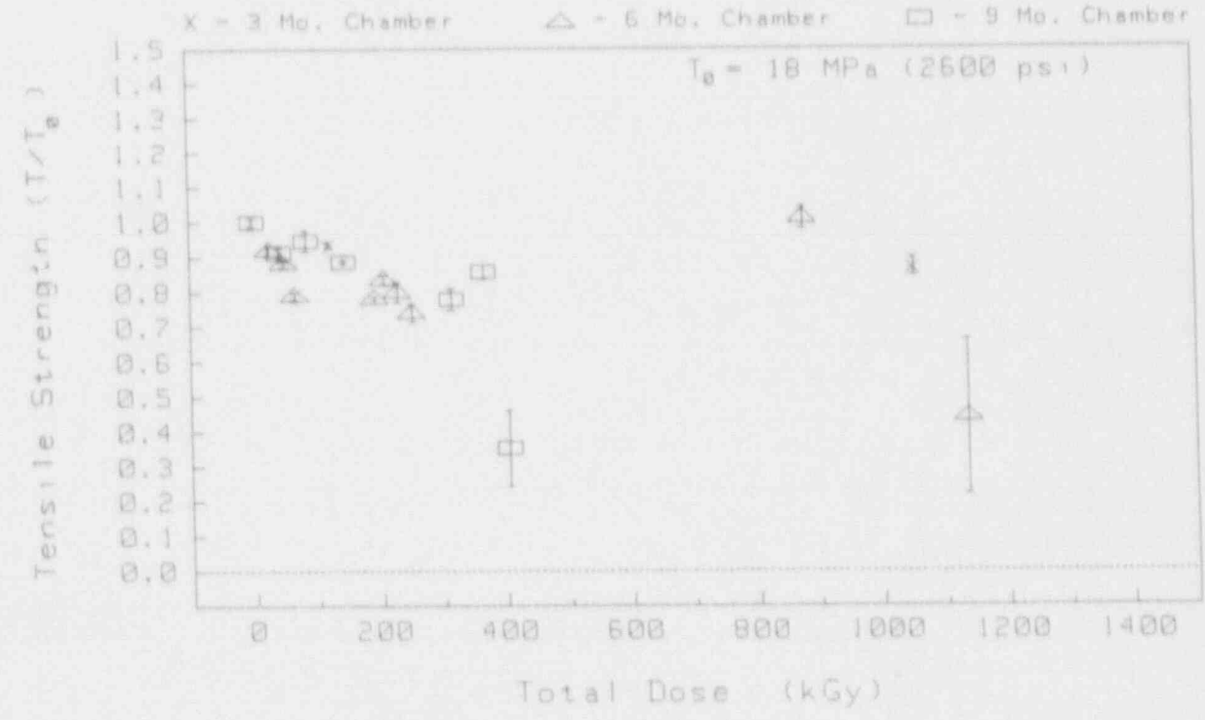

Figure E-12 Tensile Strength of Dekoron Polyset Jacket

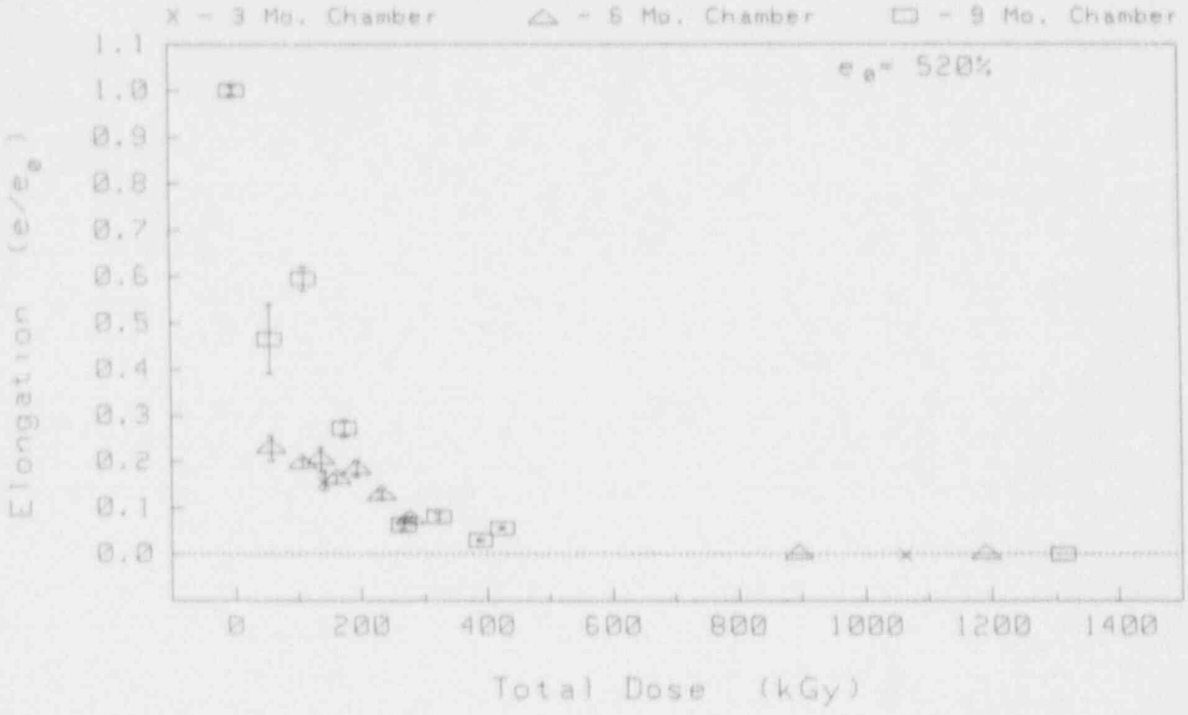

Figure E-13 Elongation of Raychem Insulation

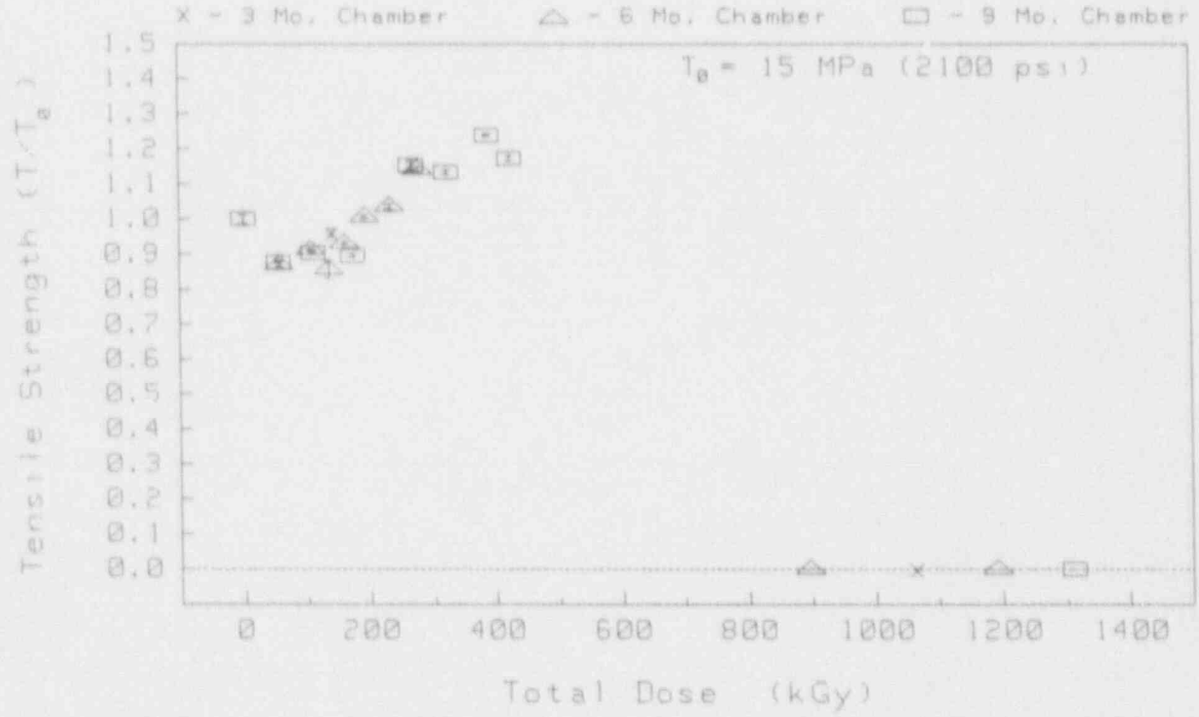

Figure E-14 Tensile Strength of Raychem Insulation

Appendix F Data from EPRI/Franklin Cable Indenter and Hardness Data

In this appendix, relative modulus and hardness are presented for each cable type. Error bars around each data point symbol represent one sample standard deviation of the data. The data point at 0 kGy total dose on each plot is from virgin cable specimens. The data points between 0 and 600 kGy are from samples exposed to aging only. The data points at 800-1000 kGy are from samples that were exposed only to accident radiation. (These samples were placed in the 6-month chamber after aging, but prior to the accident radiation exposure.) Finally, the data points beyond 1000 kGy are from samples exposed to both aging (either 3, 6, or 9 months) and accident radiation.

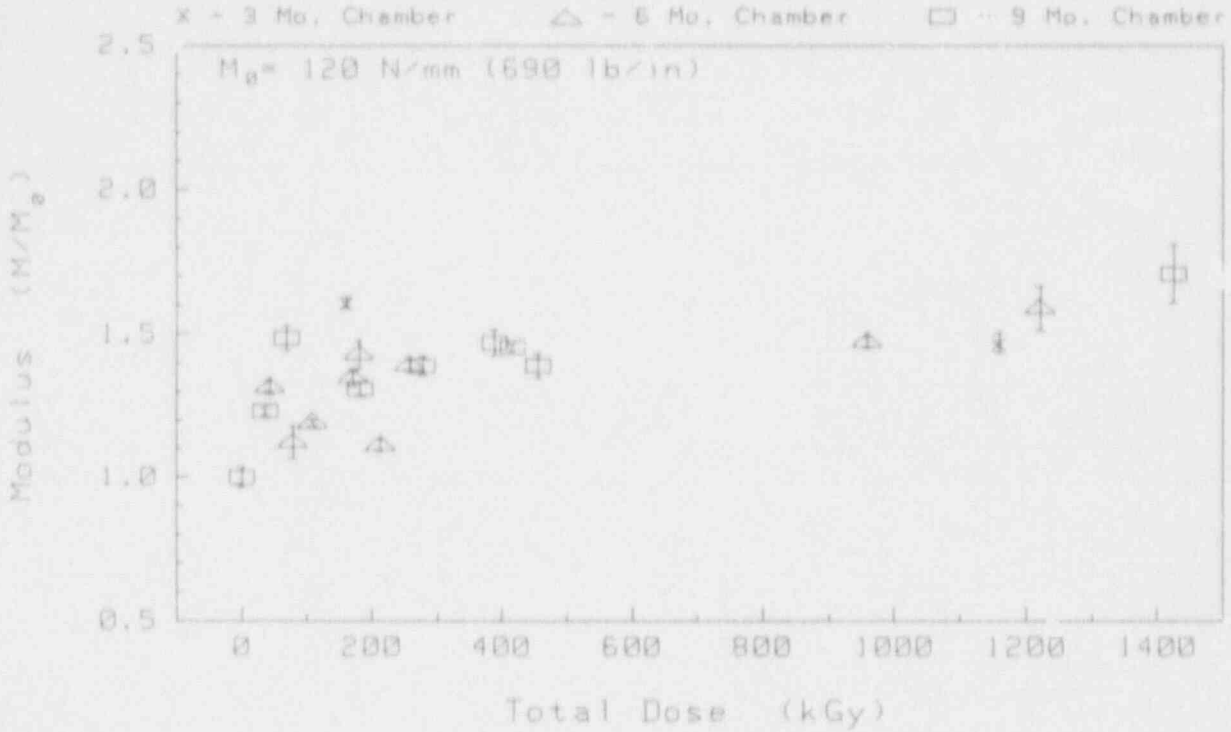

Figure F-1 Indenter Modulus of Brand Rex Insulation

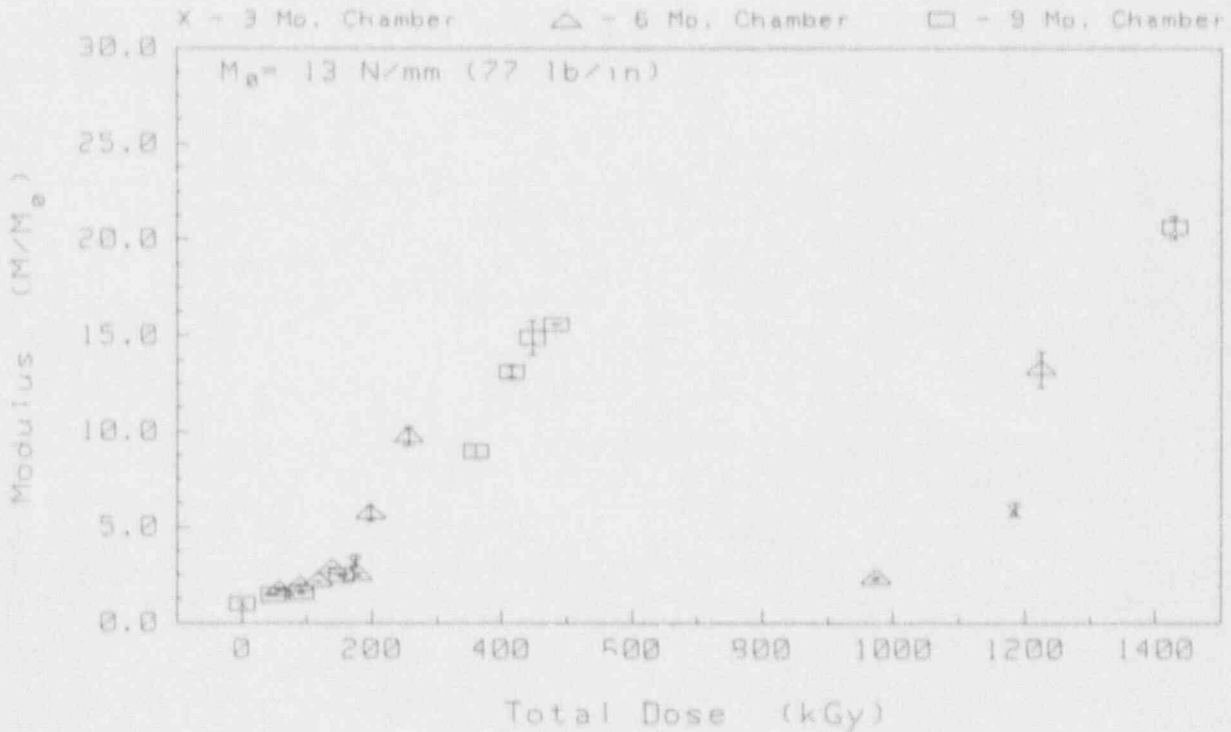

Figure F-2 Indenter Modulus of Brand Rex Jacket

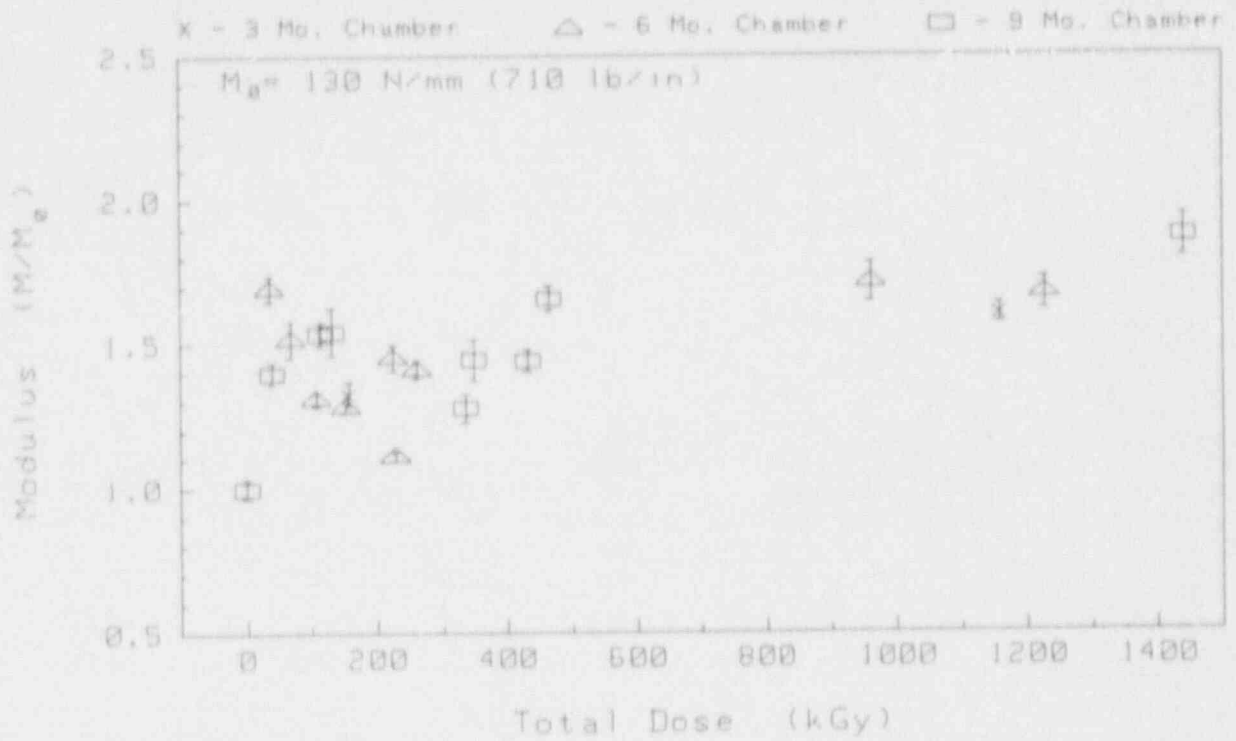

Figure F-3 Indenter Modulus of Rockbestos Insulation

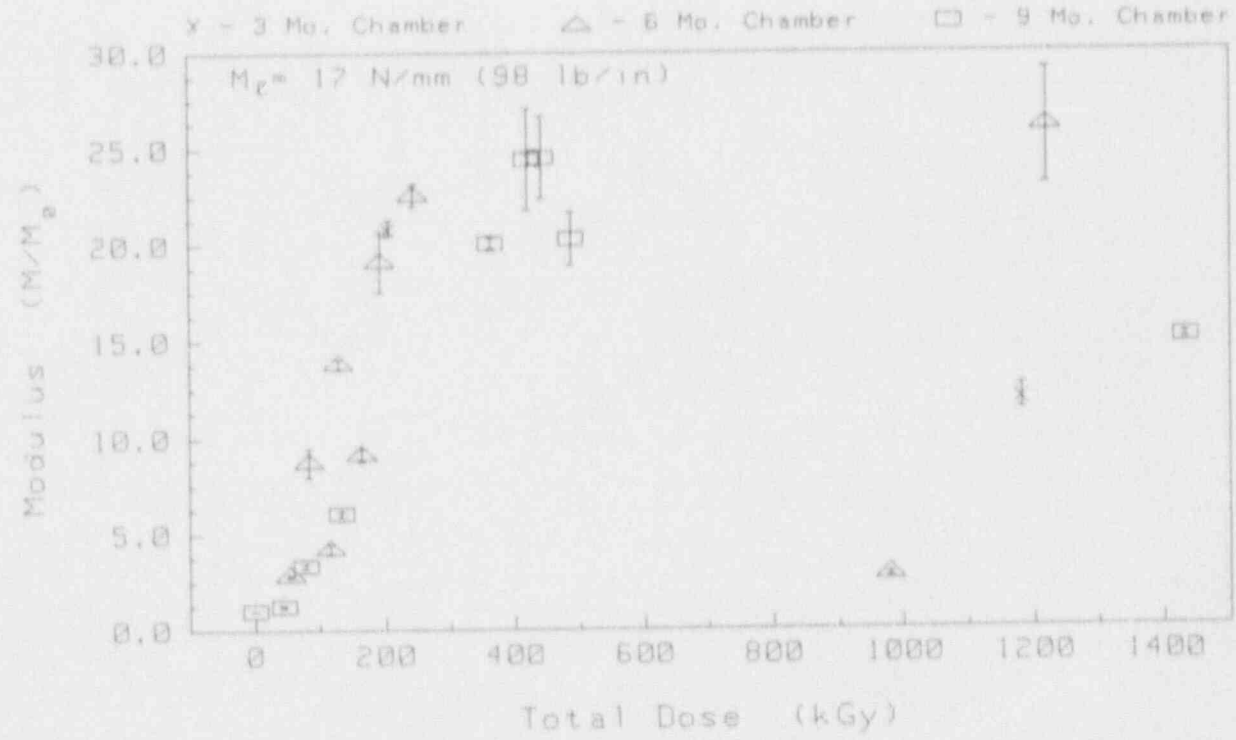

Figure F-4 Indenter Modulus of Rockbestos Jacket

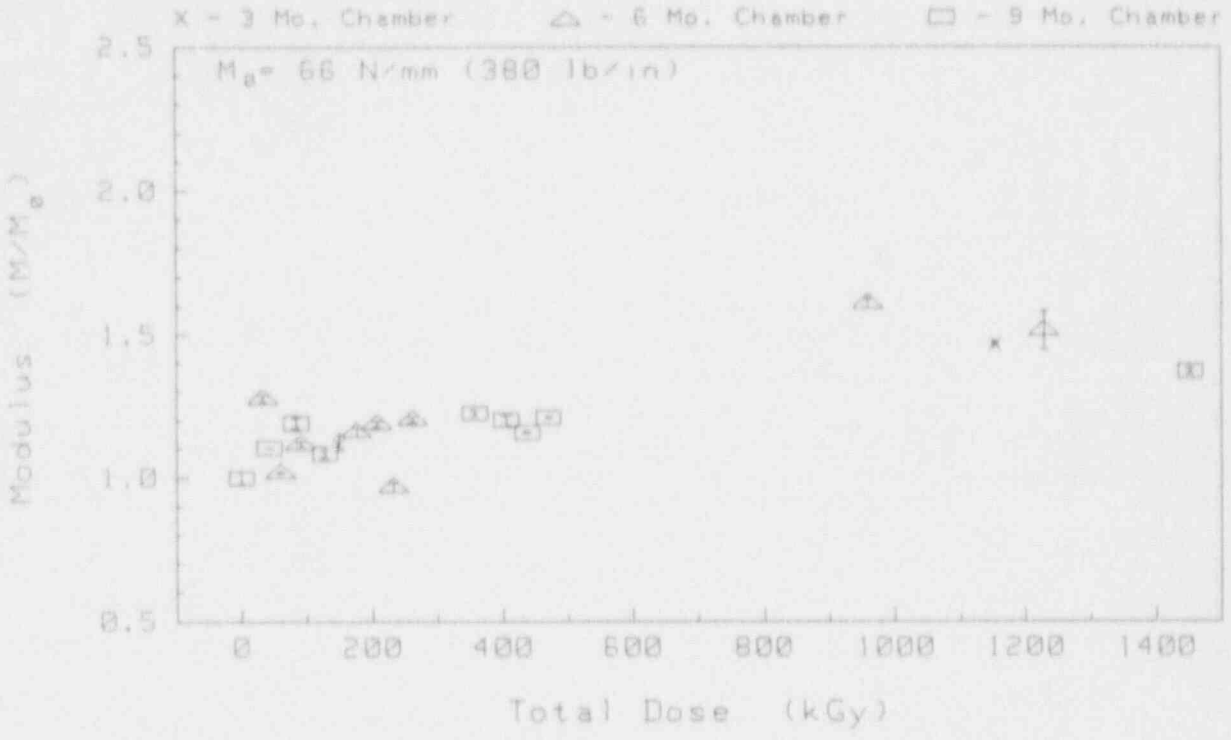

Figure F-5 Indenter Modulus of Dekoron Polyset Insulation

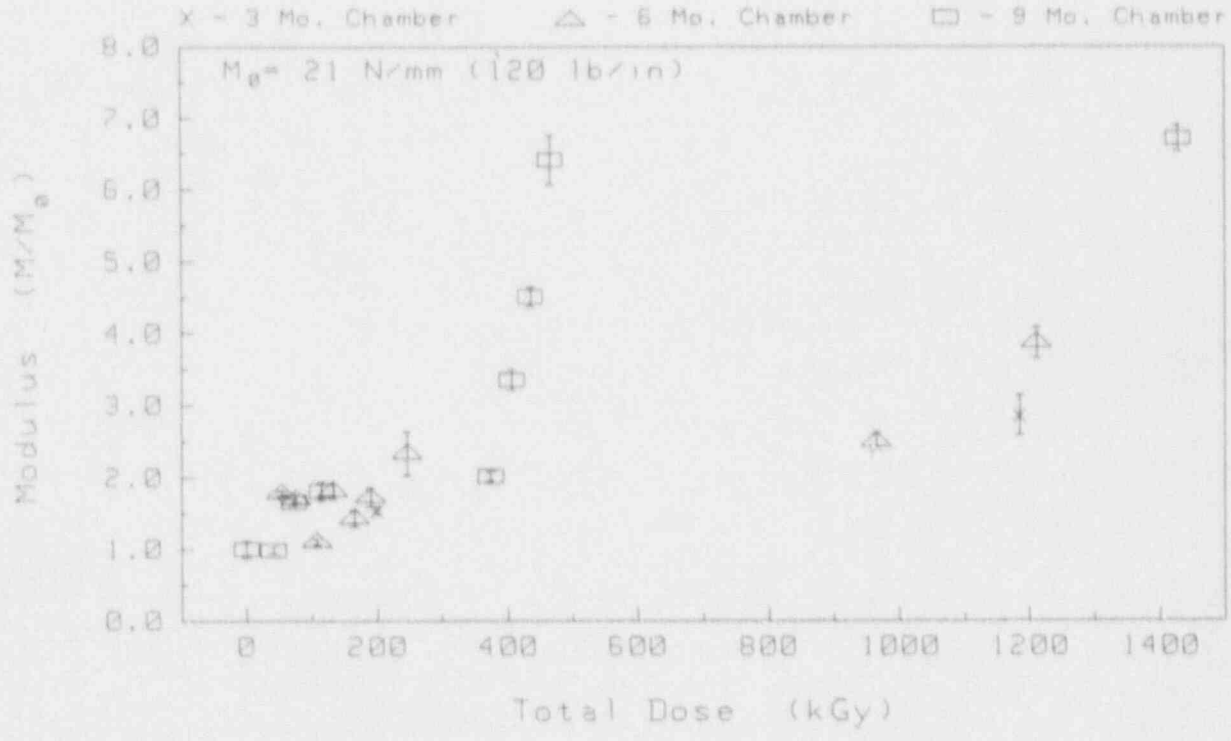

Figure F-6 Indenter Modulus of Dekoron Polyset Jacket

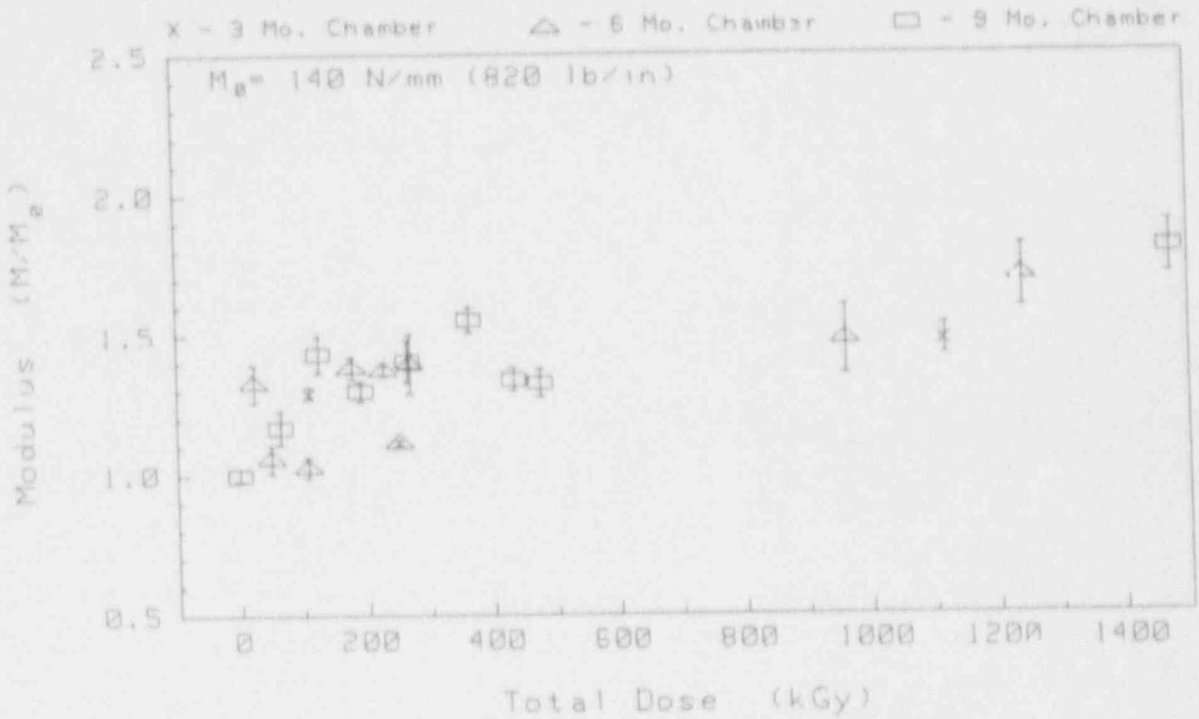

Figure F-7 Indenter Modulus of Raychem Insulation

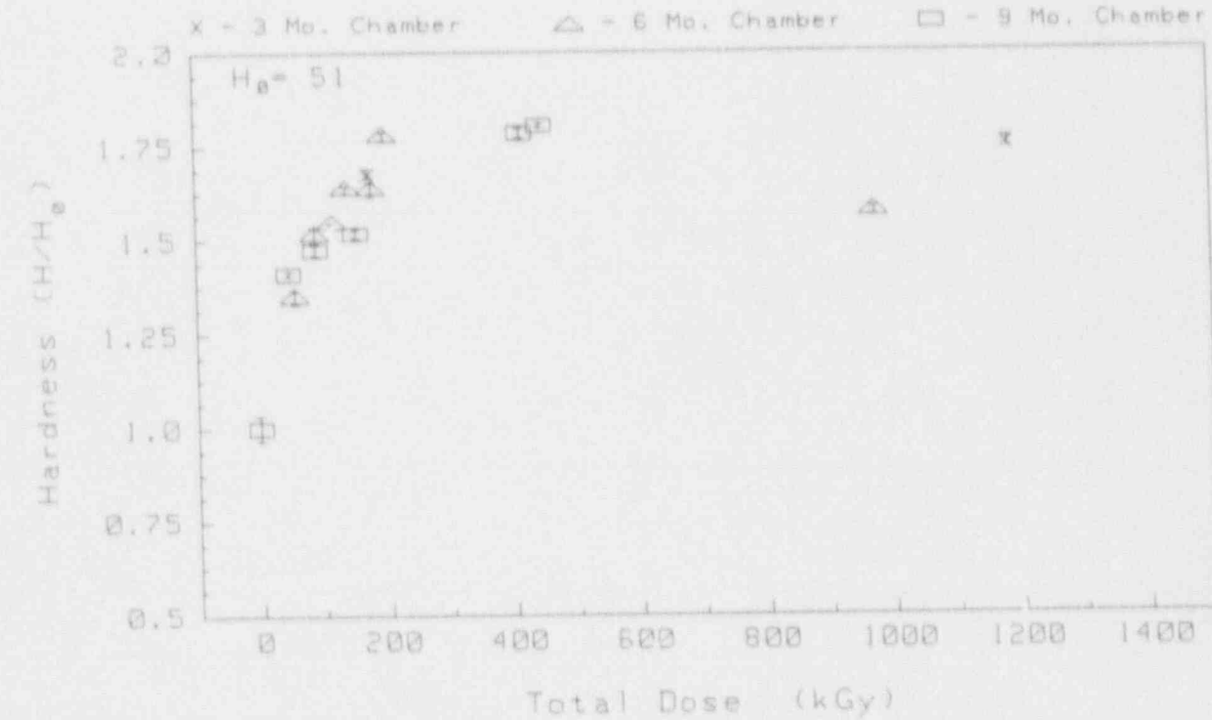

Figure F-8 Hardness of Brand Rex Jacket

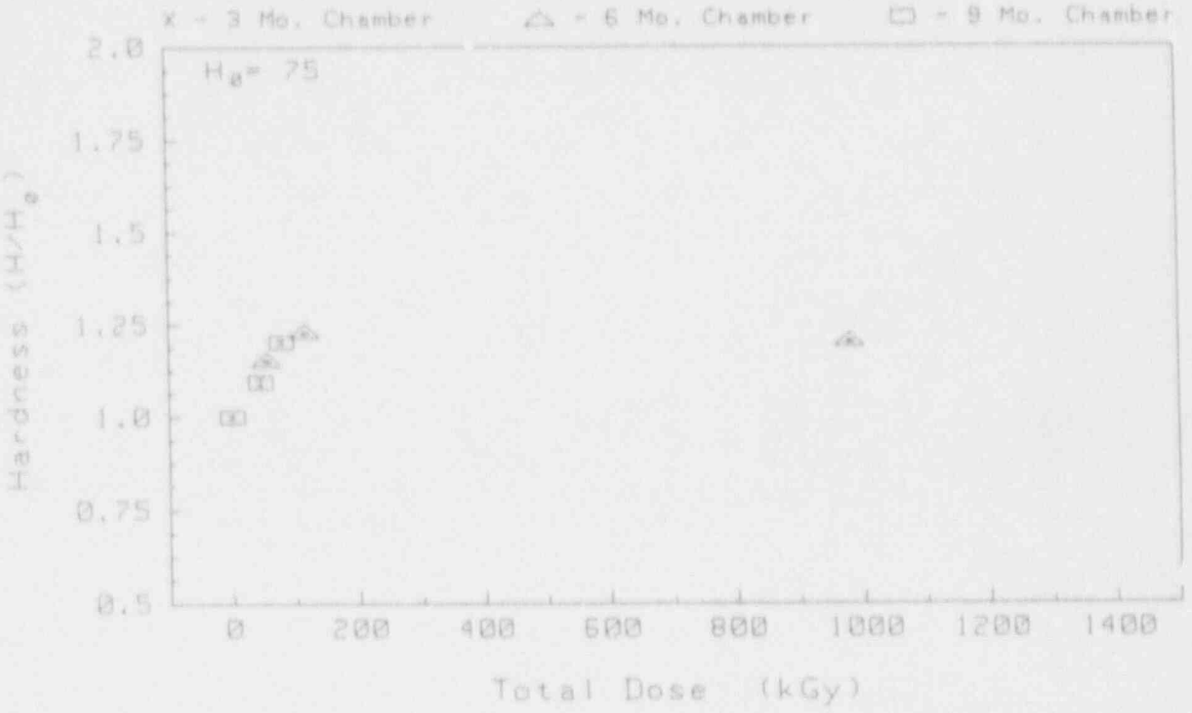

Figure F-9 Hardness of Rockbestos Jacket

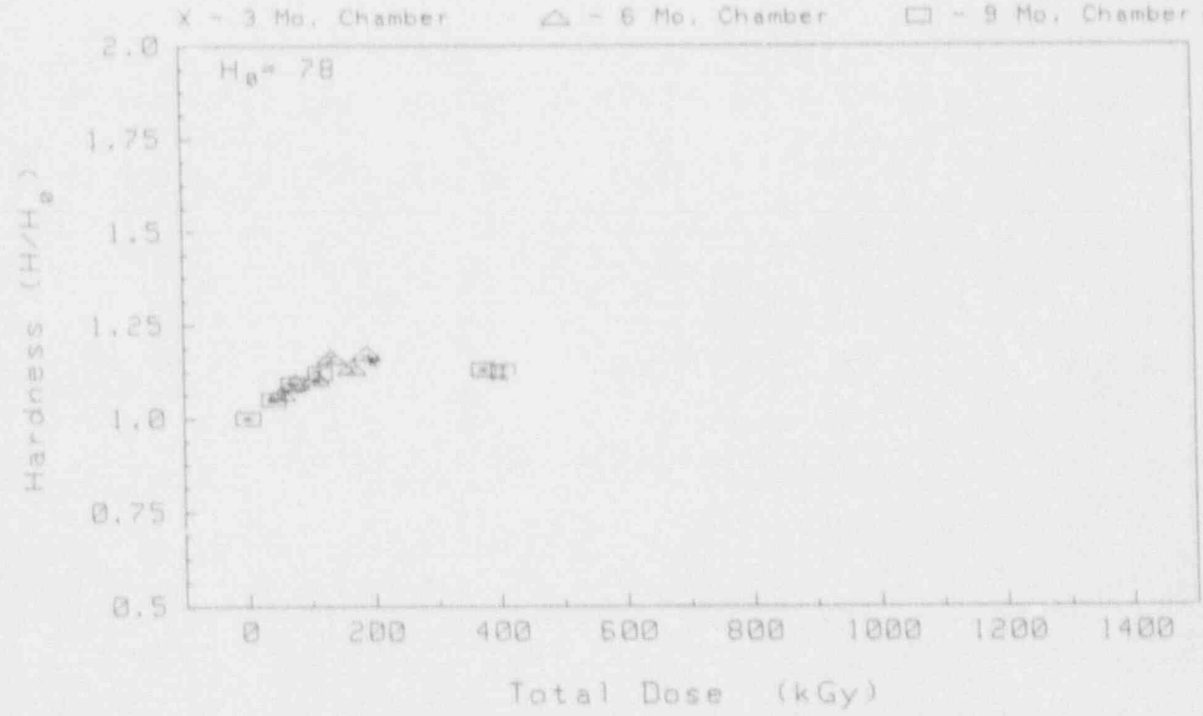

Figure F-10 Hardness of Dekoron Polyset Jacket

Appendix G Density Data

In this appendix, relative density is presented for each cable type. Error bars around each data point symbol represent one sample standard deviation of the data. The data point at 0 kGy total dose on each plot is from virgin cable specimens. The data points between 0 and 600 kGy are from samples exposed to aging only. The data points at 800-1000 kGy are from samples that were exposed only to accident radiation. (These samples were placed in the 6-month chamber after aging, but prior to the accident radiation exposure.) Finally, the data points beyond 1000 kGy are from samples exposed to both aging (either 3, 6, or 9 months) and accident radiation.

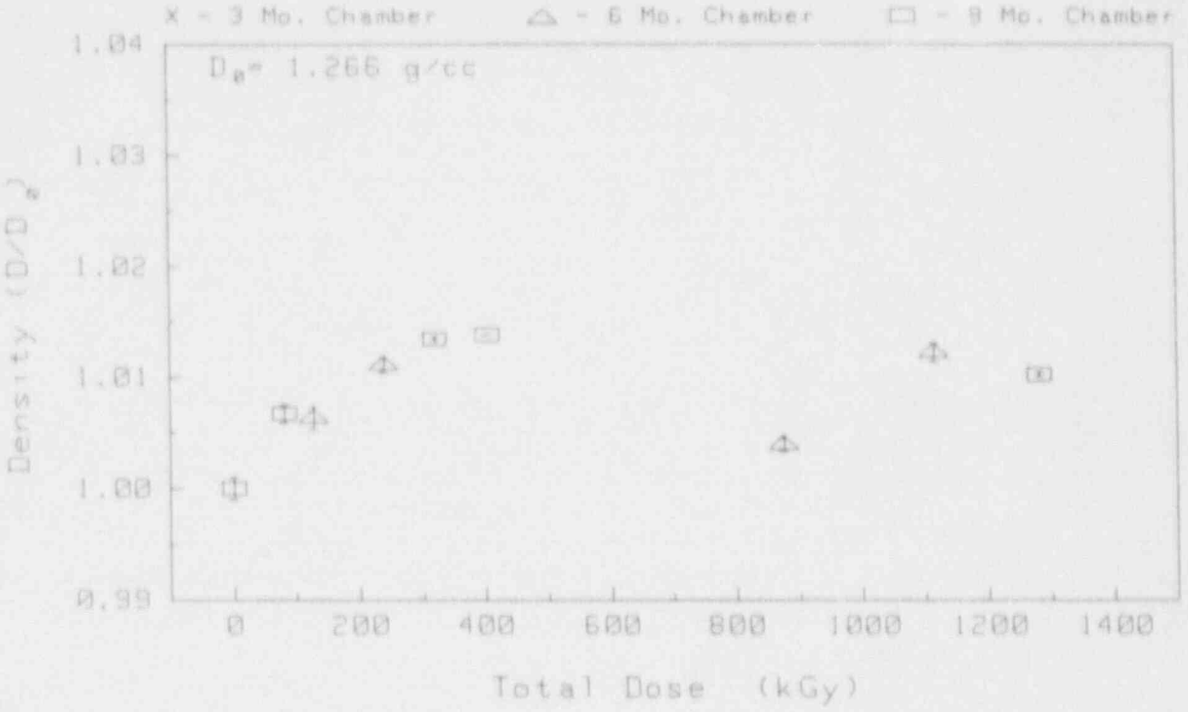

Figure G-1 Density of Brand Rex Insulation

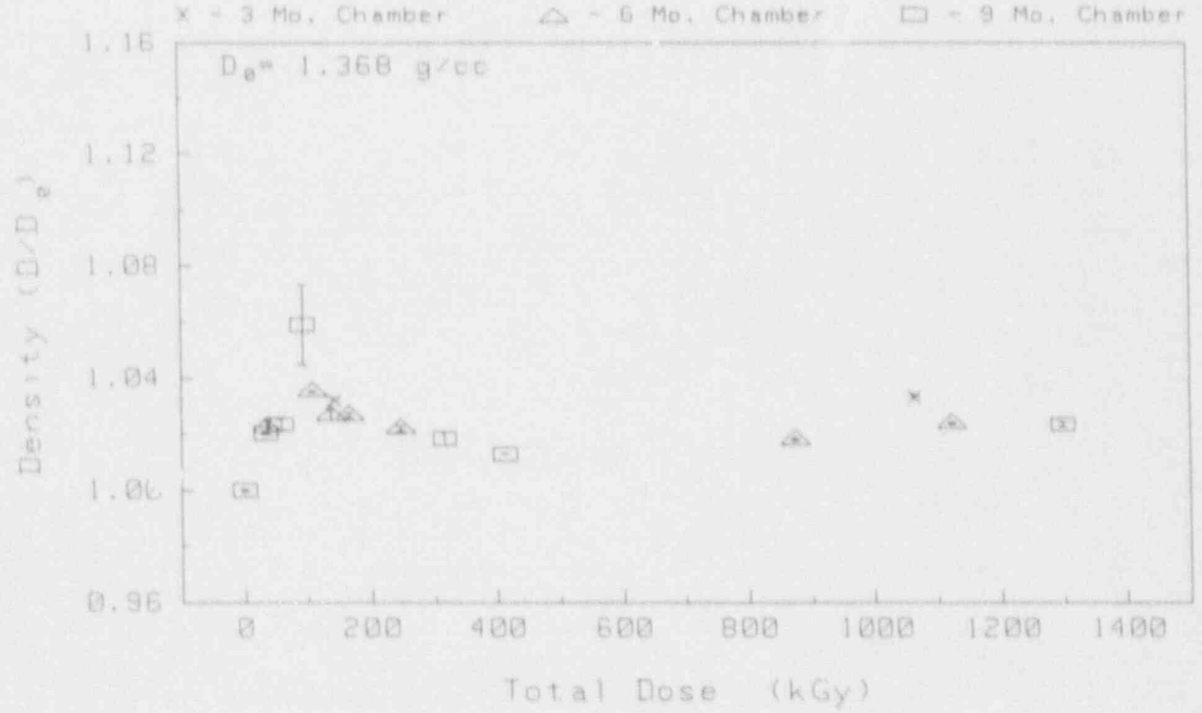

Figure G-2 Density of Brand Rex Jacket

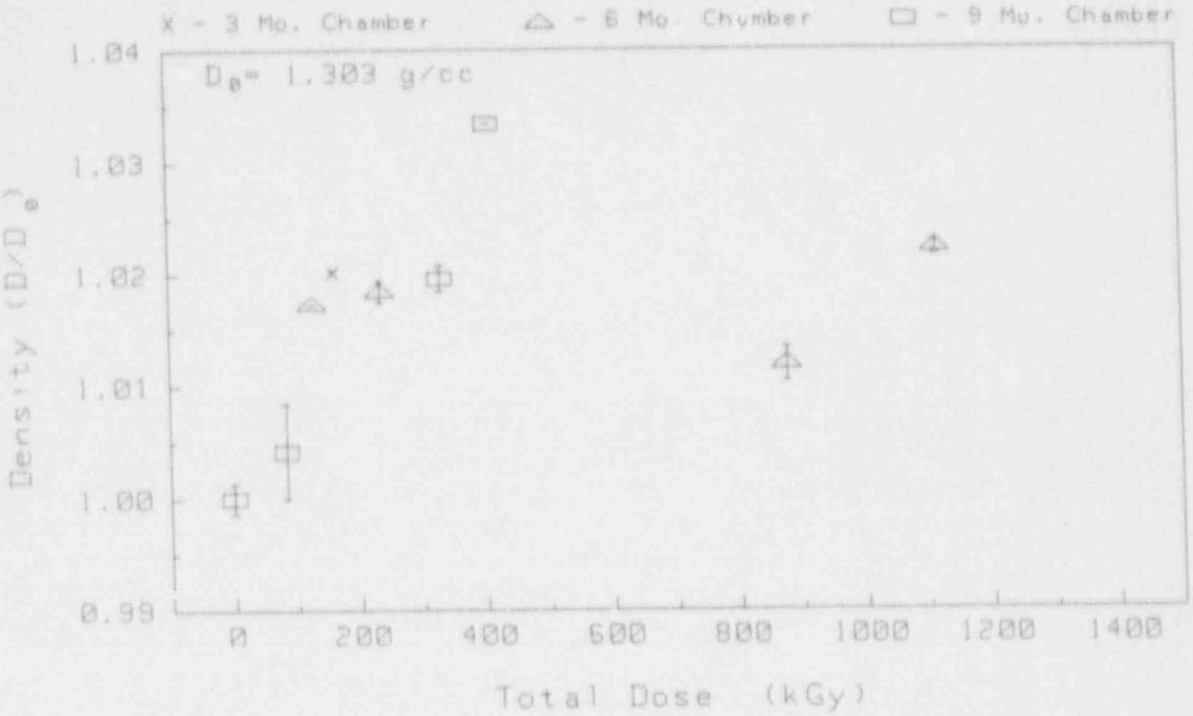

Figure G-3 Density of Rockbestos Insulation

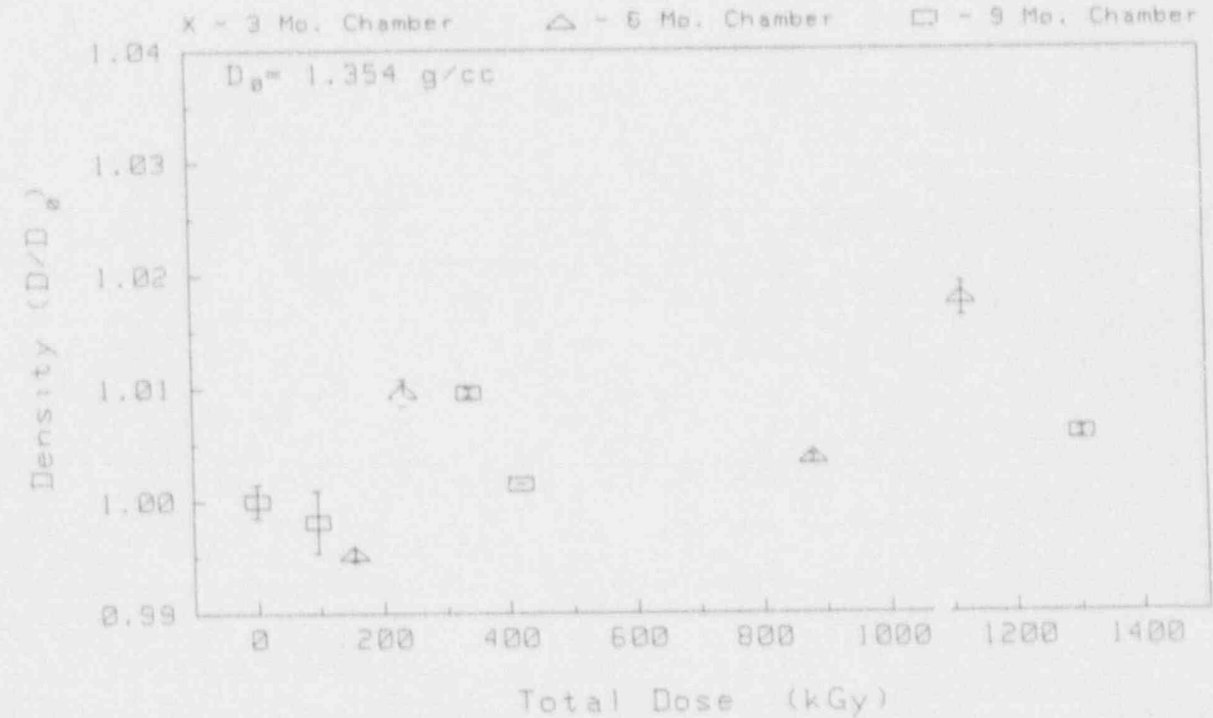

Figure G-4 Density of Dekoron Polyset Insulation

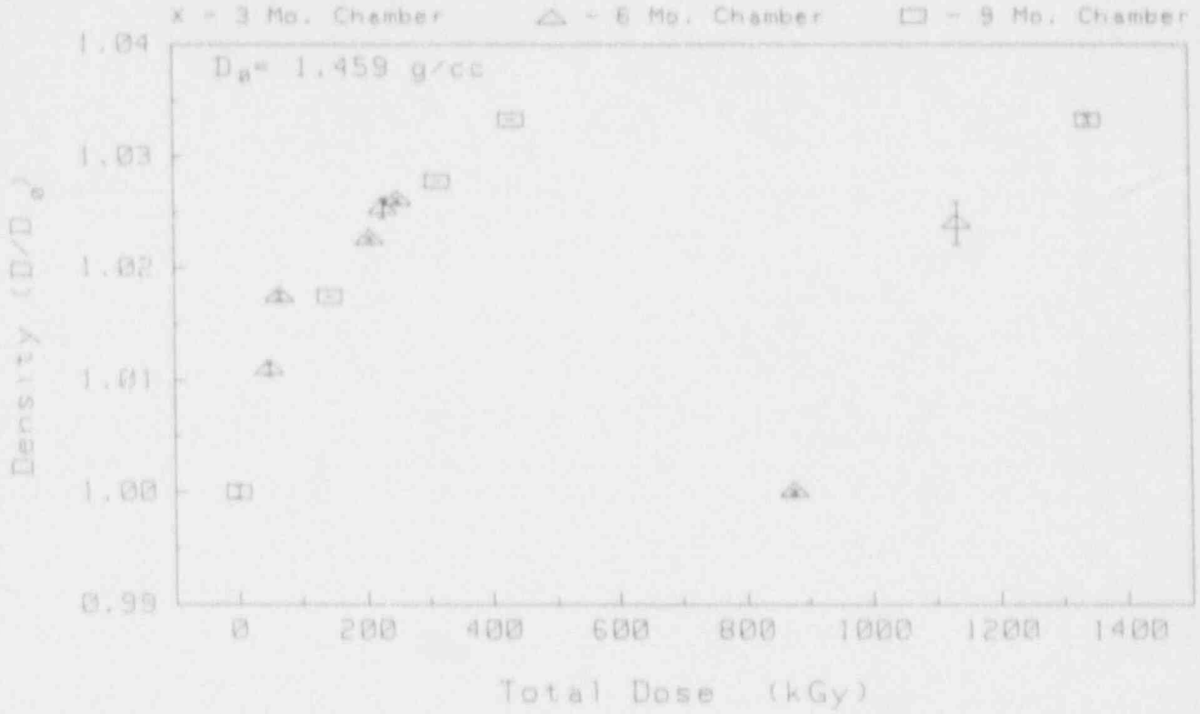

Figure G-5 Density of Dekoron Polyset Jacket

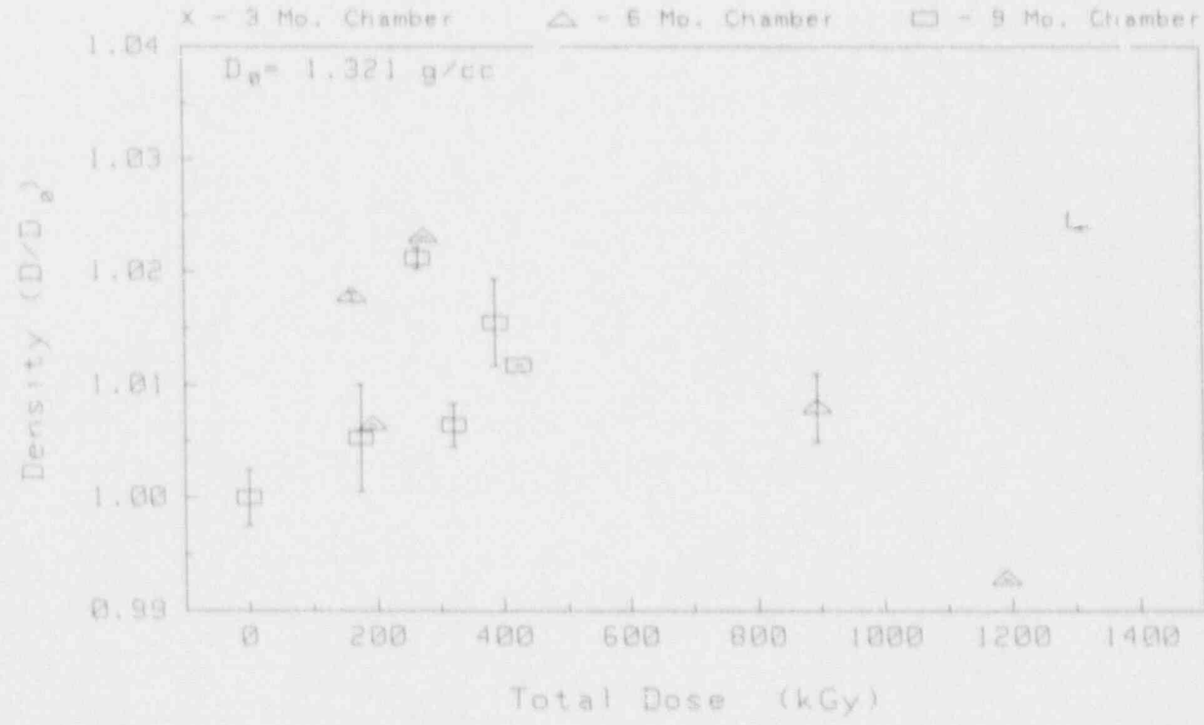

Figure G-6 Density of Raychem Insulation

Appendix H Modulus Profiles

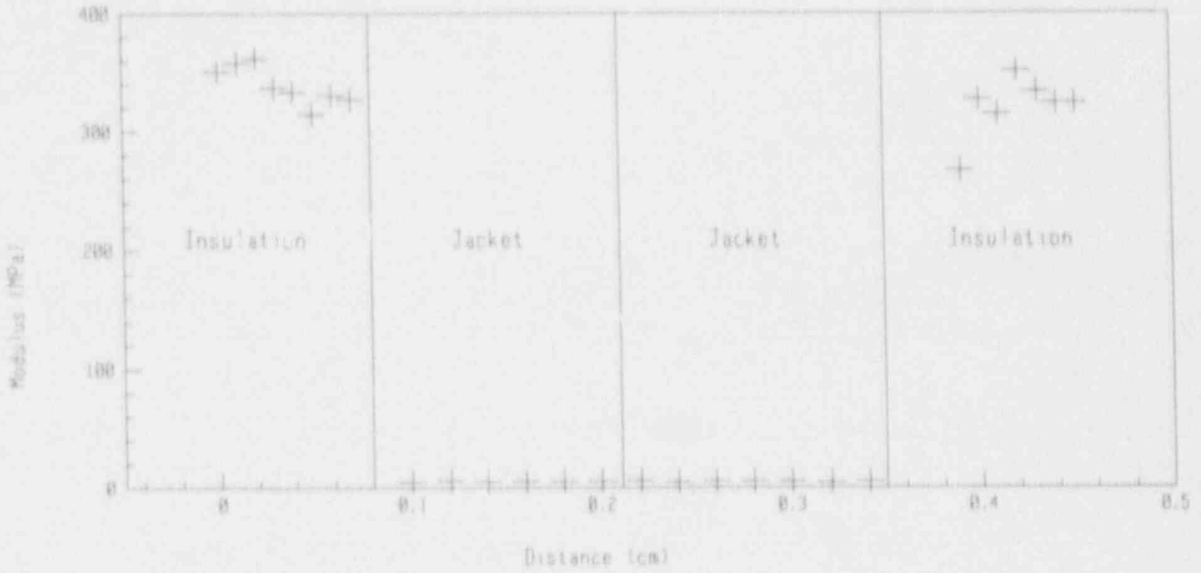

Figure H-1 Modulus Profile of Unaged Brand Rex Cables

Figure H-2 Modulus Profile of Brand Rex Cables Aged for 3 Months (89.7 kGy)

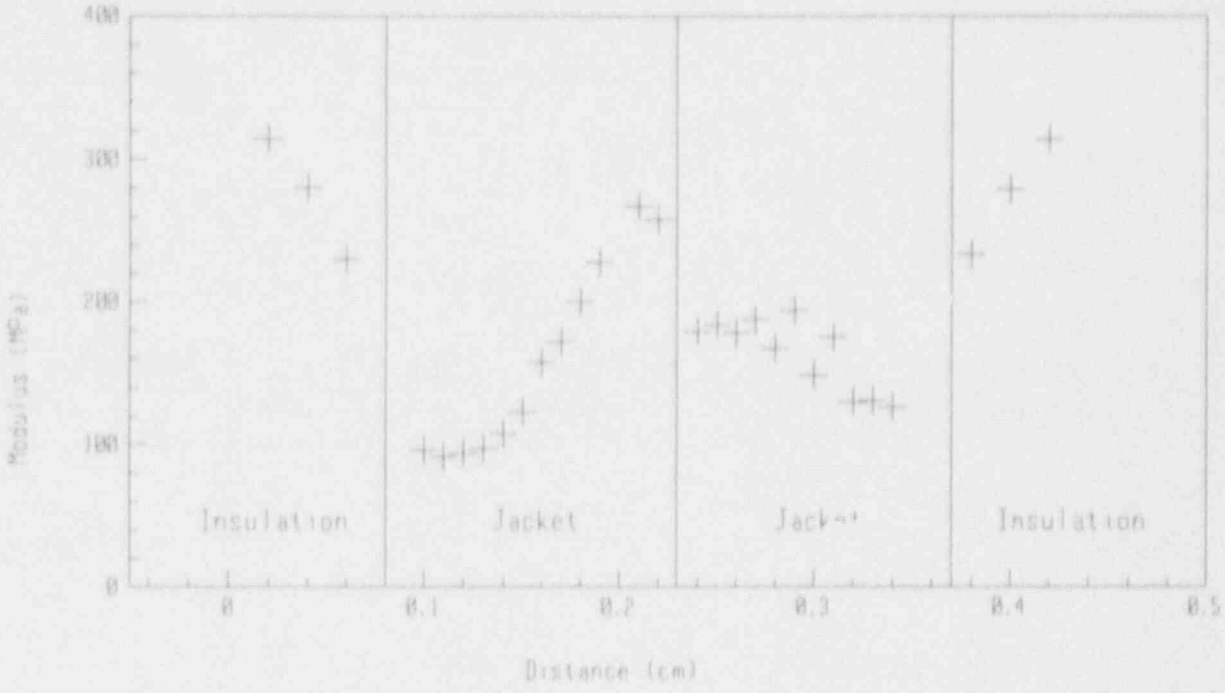

Figure H-3 Modulus Profile of Brand Rex Cables Aged for 6 Months (359 kGy)

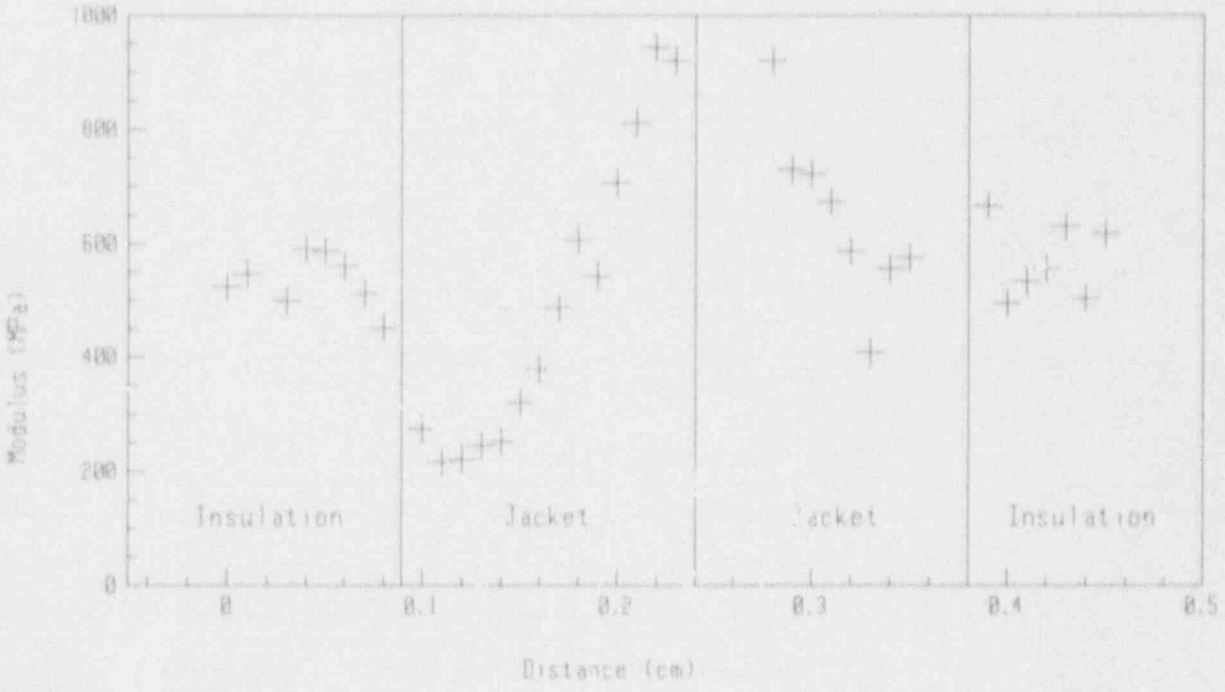

Figure H-4 Modulus Profile of Brand Rex Cables Aged for 9 Months (484 kGy)

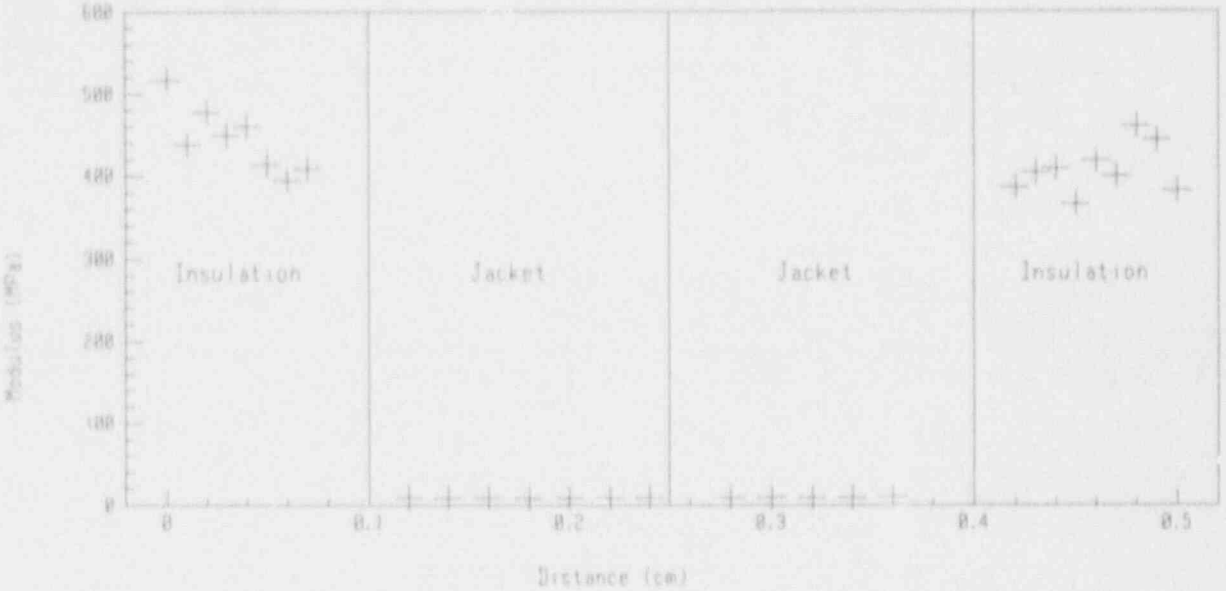

Figure H-5 Modulus Profile of Unaged Rockbestos Rex Cables

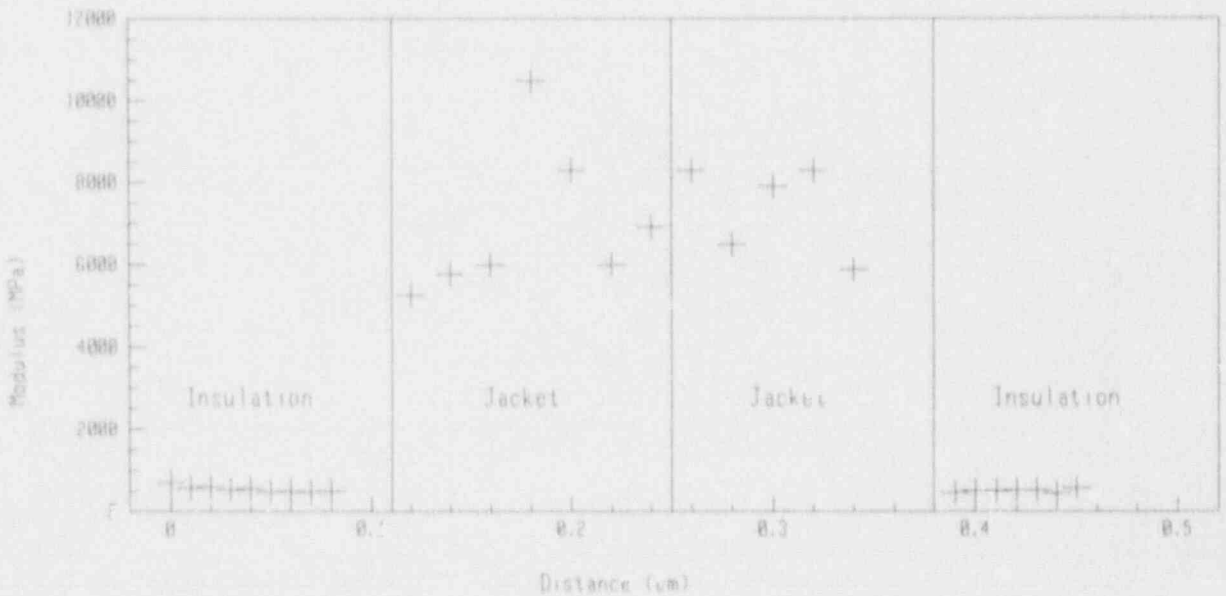

Figure H-6 Modulus Profile of Rockbestos Cables Aged for 9 Months (487 kGy)

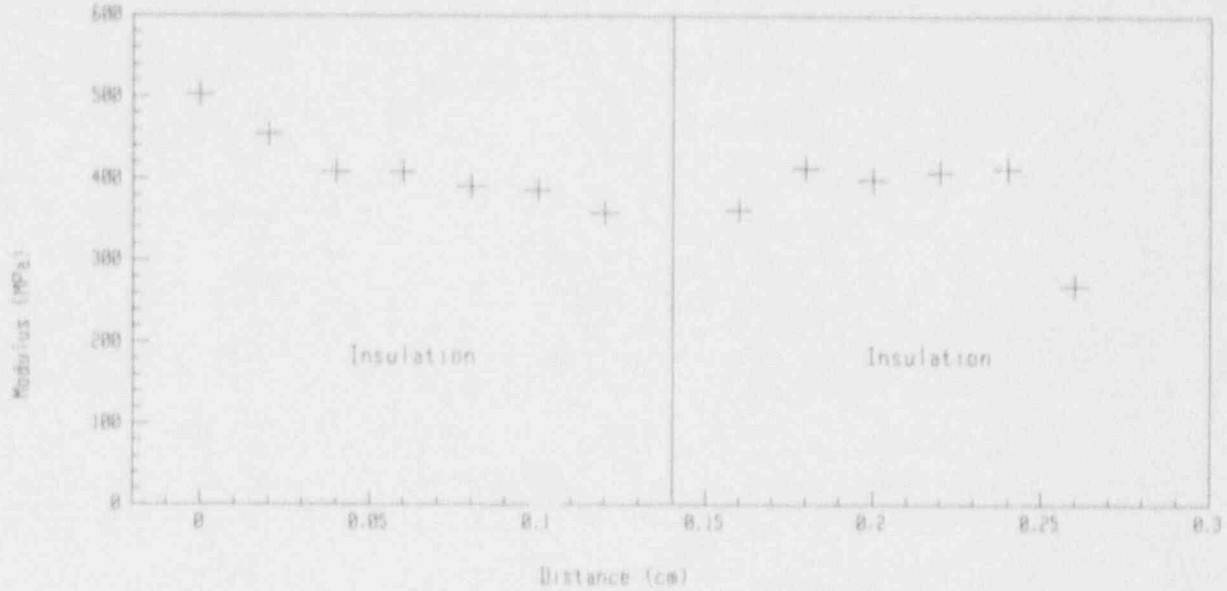

Figure H-7 Modulus Profile of Unaged Raychem Cables

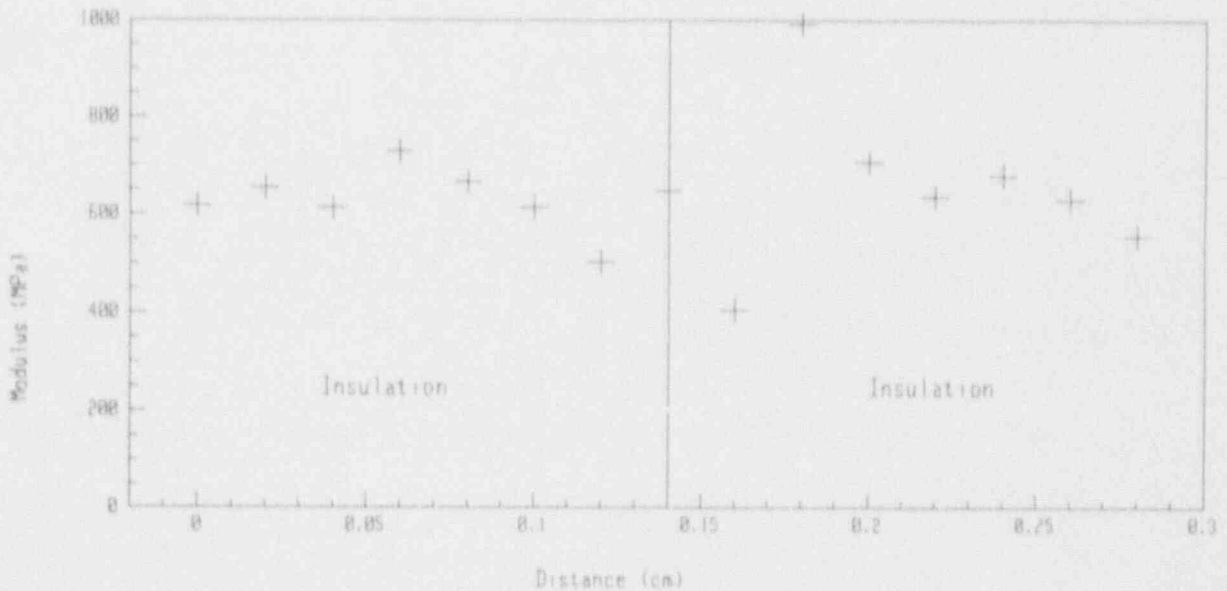

Figure H-8 Modulus Profile of Raychem Cables Aged for 9 Months (477 kGy)

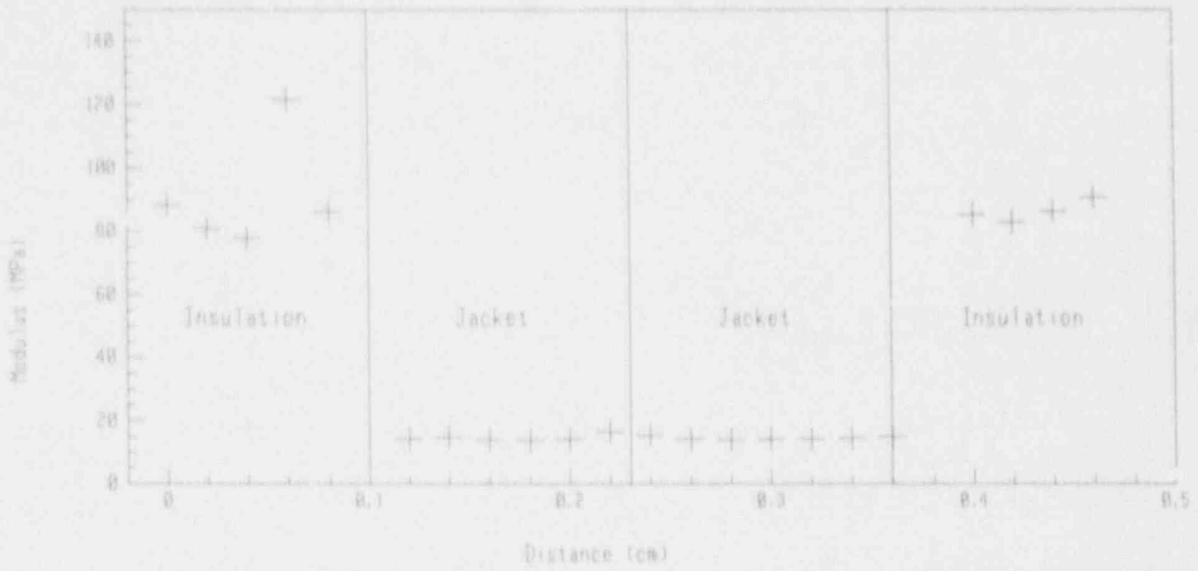

Figure H-9 Modulus Profile of Unaged Polyset Cables

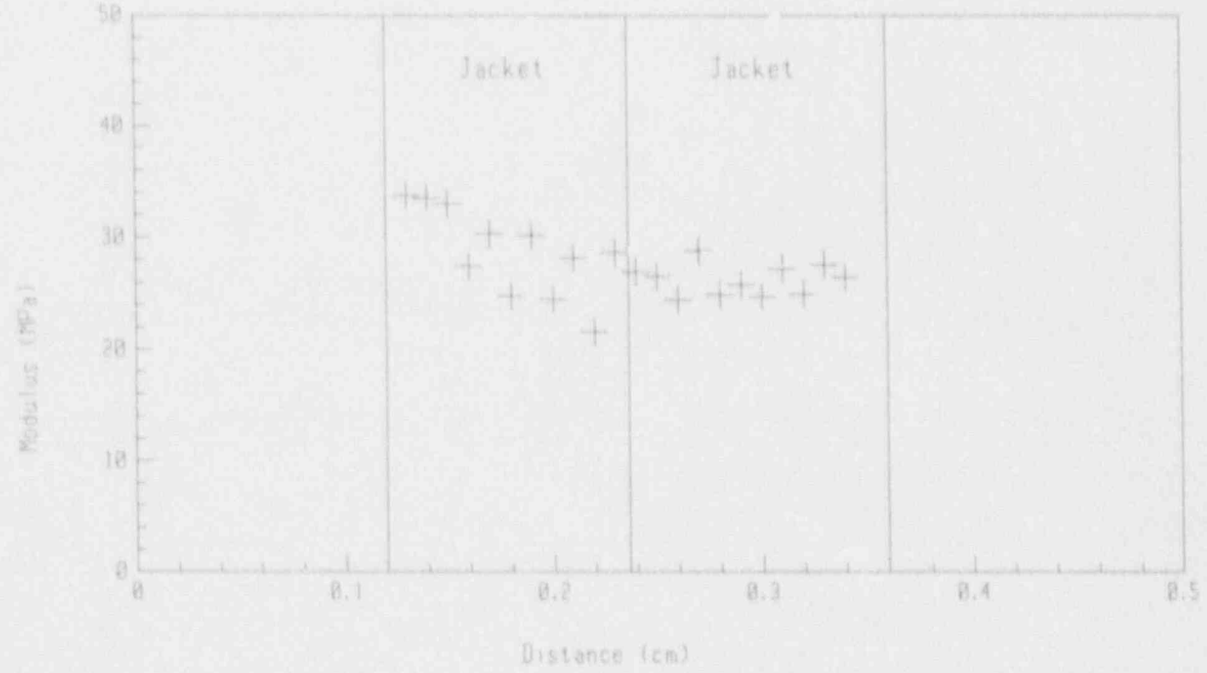

Figure H-10 Modulus Profile of Polyset Cables Aged for 6 Months (246 kGy)

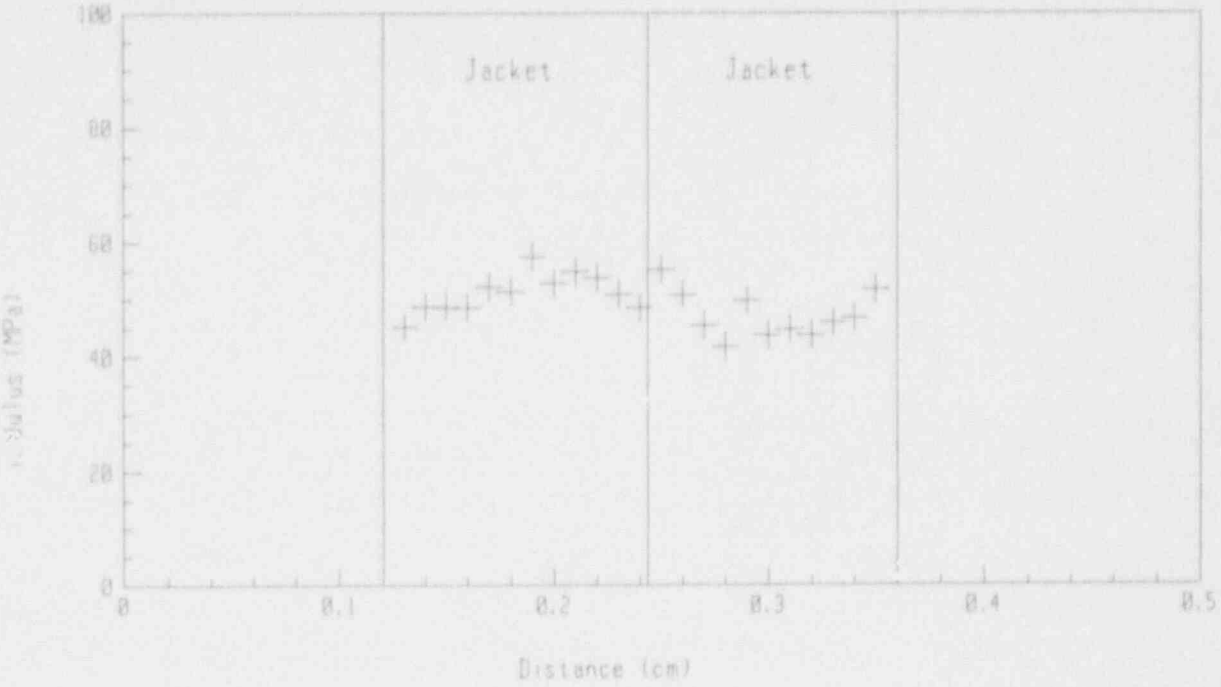

Figure H-11 Modulus Profile of Polyset Cables Aged for 7 Months (406 kGy)

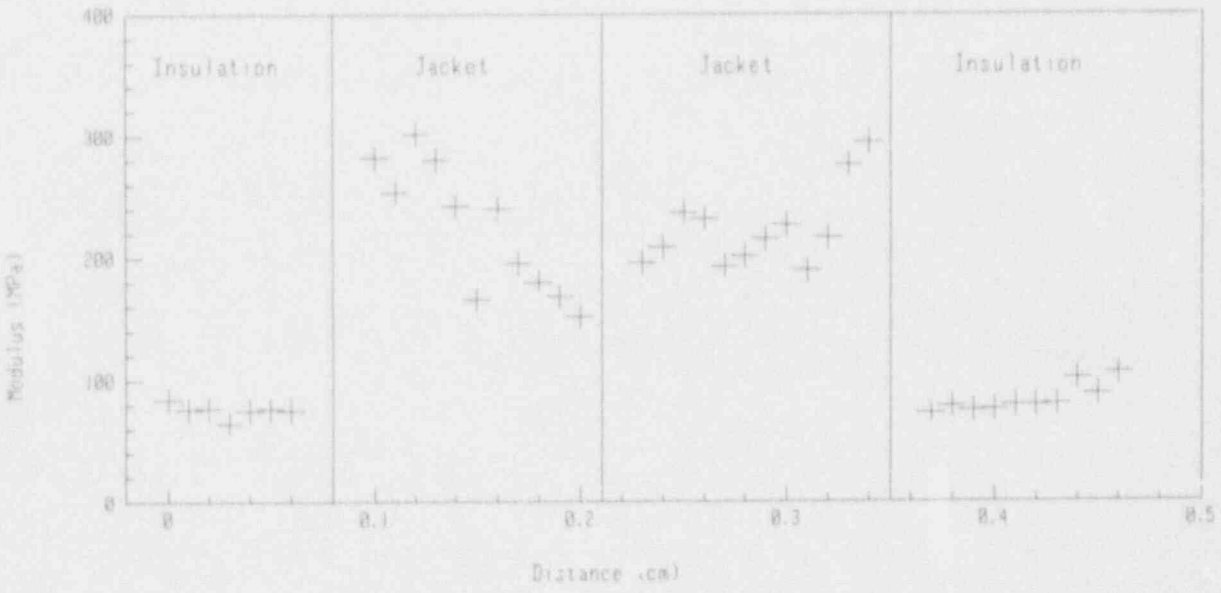

Figure H-12 Modulus Profile of Polyset Cables Aged for 9 Months (466 kGy)

Appendix I IR of Each Conductor During Accident Testing

In this appendix, conductor identification numbers are given by the chamber number (20, 40, or 60 based on the nominal life simulated during the aging in that chamber), followed by a conductor number from Table 2. Some of the plots only show the data from the Keithley because those conductors were connected to ground during the on-line measurements (see Figures 8-9). In each of the figures, one plot shows the data for the first 20 hours of the test and a second plot shows data for the entire test. The discrete measurements shown on the plots are identified as Keithley measurements at 50, 100, or 250 Vdc (see Appendix A). Note that the upper limit for reasonably accurate continuous measurement is somewhere above 1 MΩ-100 m (see Appendix A).

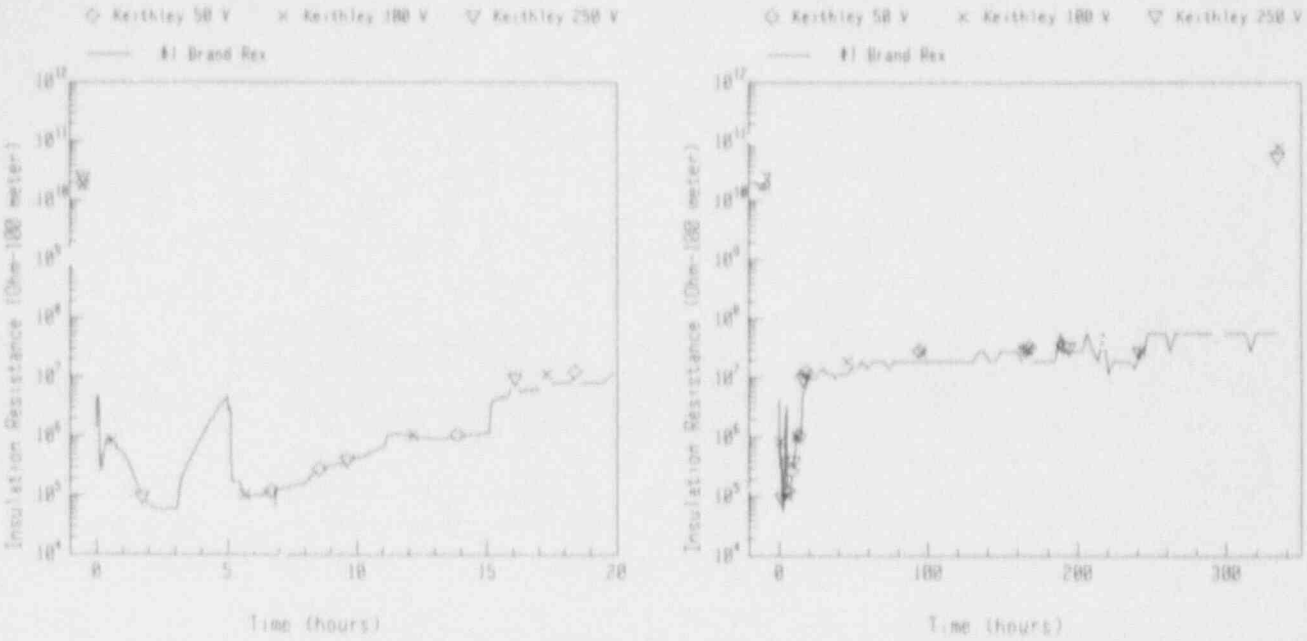

Figure I-1 IR of Brand Rex Conductor 20-1

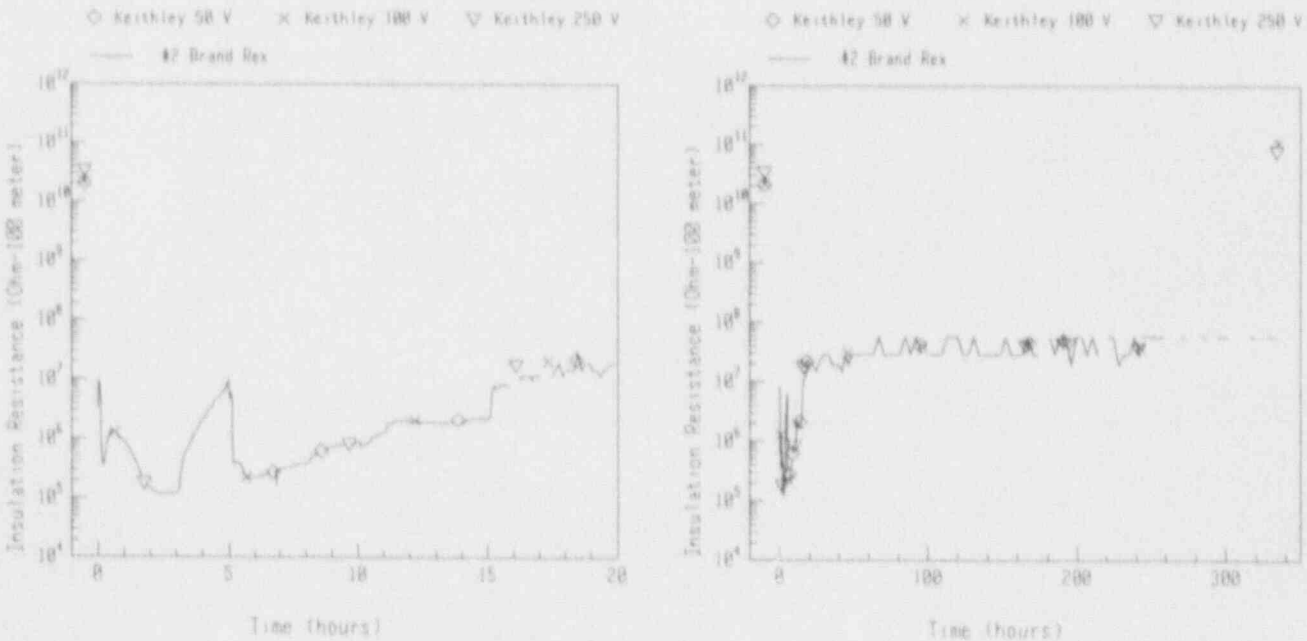

Figure I-2 IR of Brand Rex Conductor 20-2

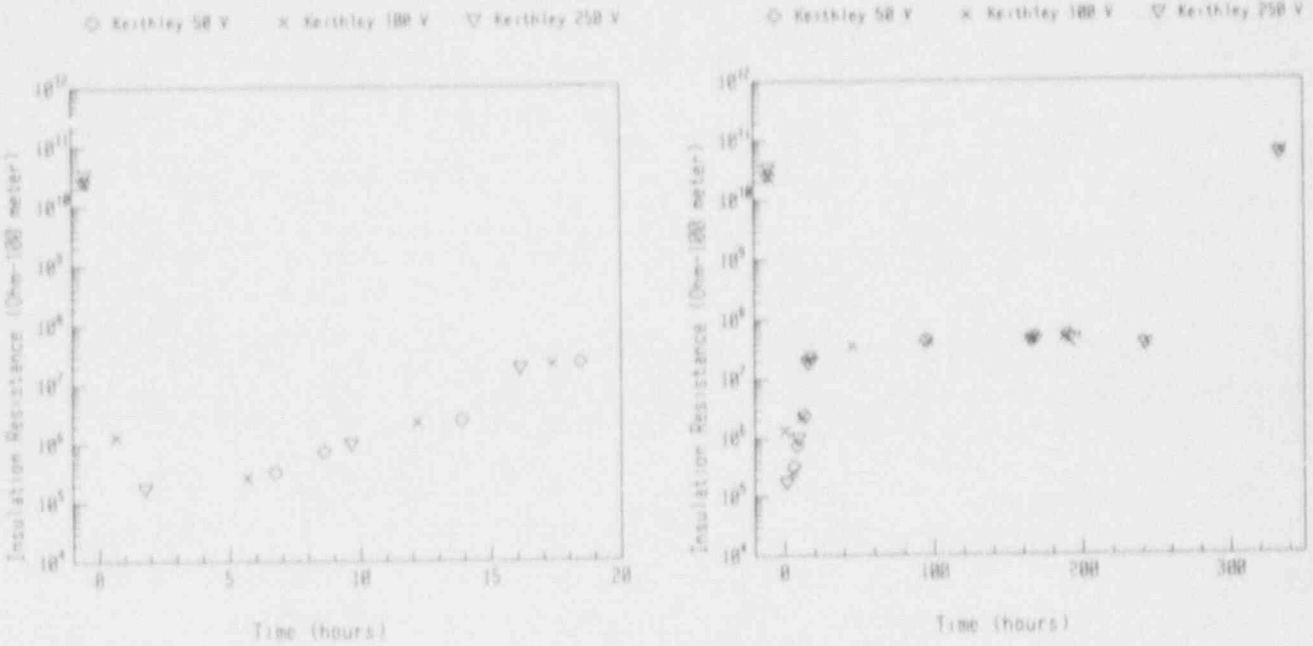

Figure I-3 IR of Brand Rex Conductor 20-3

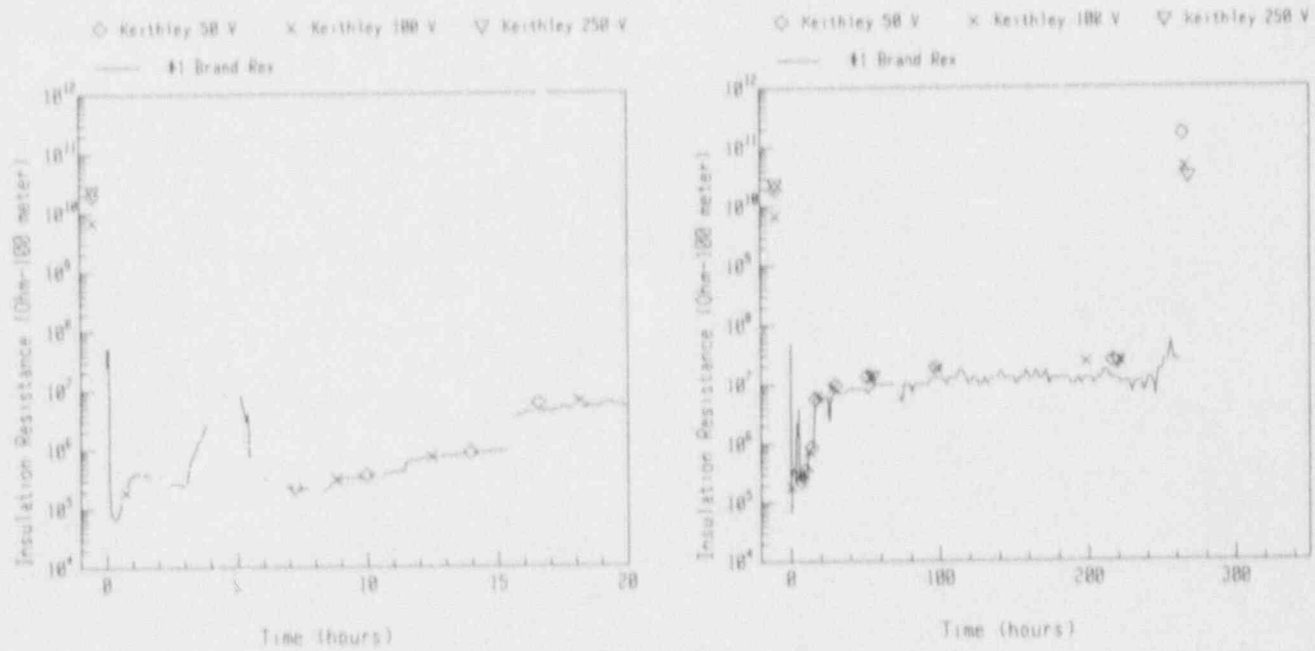

Figure I-4 IR of Brand Rex Conductor 40-1

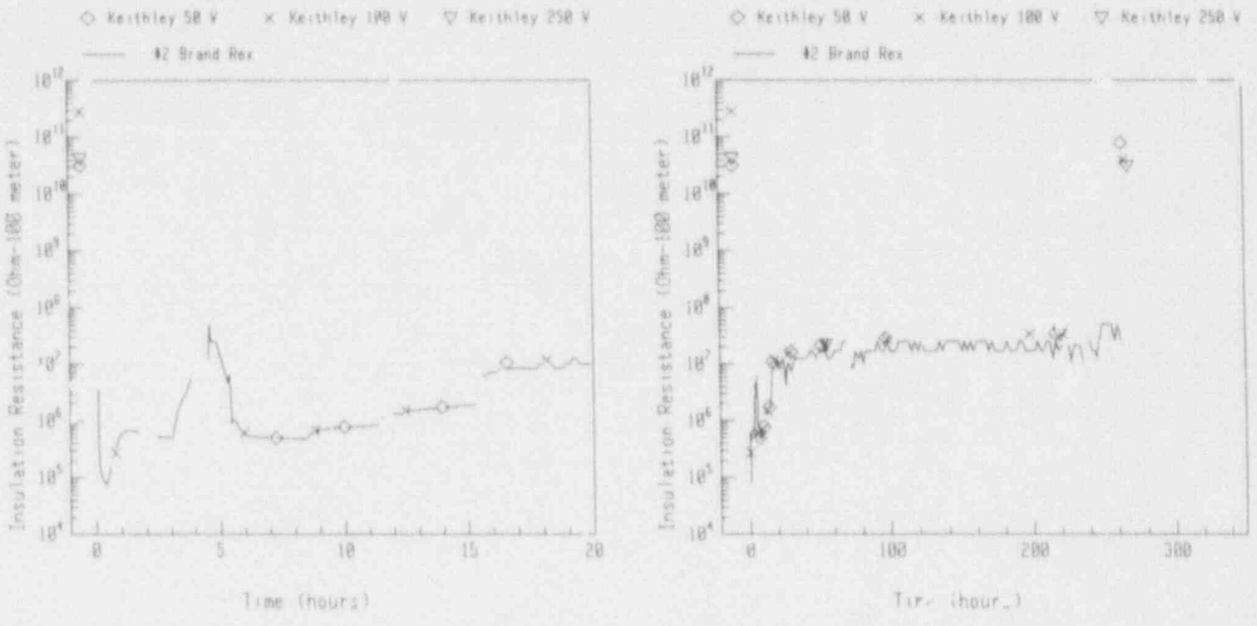

Figure I-5 IR of Brand Rex Conductor 40-2

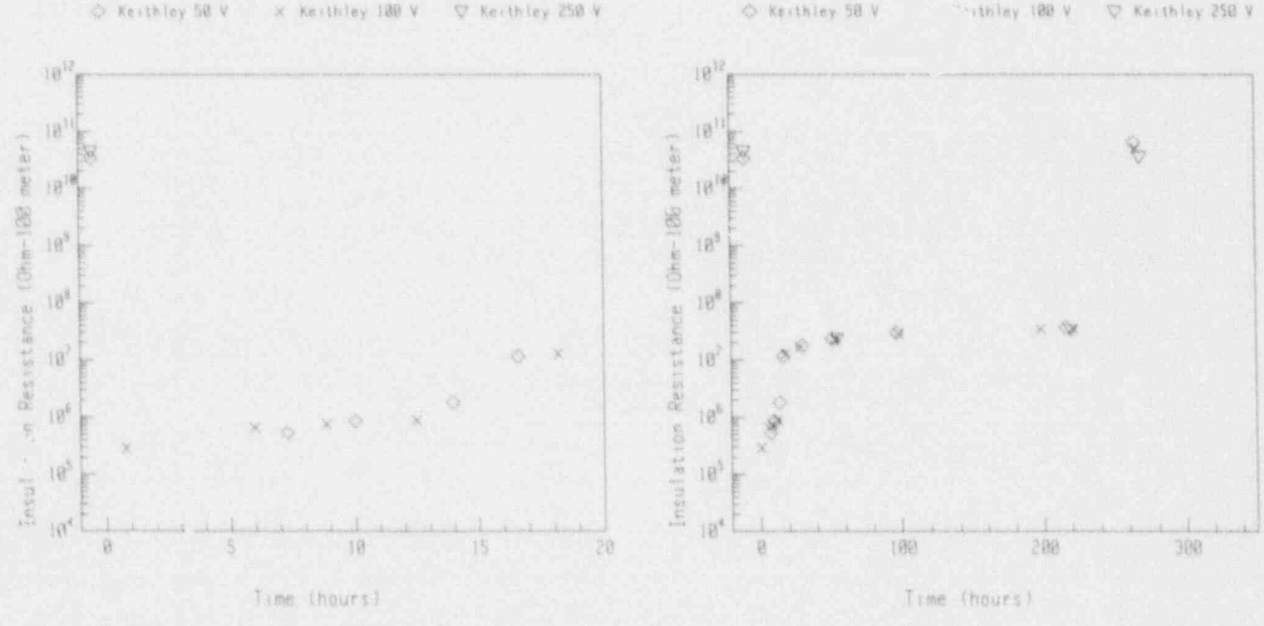

Figure I-6 IR of Brand Rex Conductor 40-3

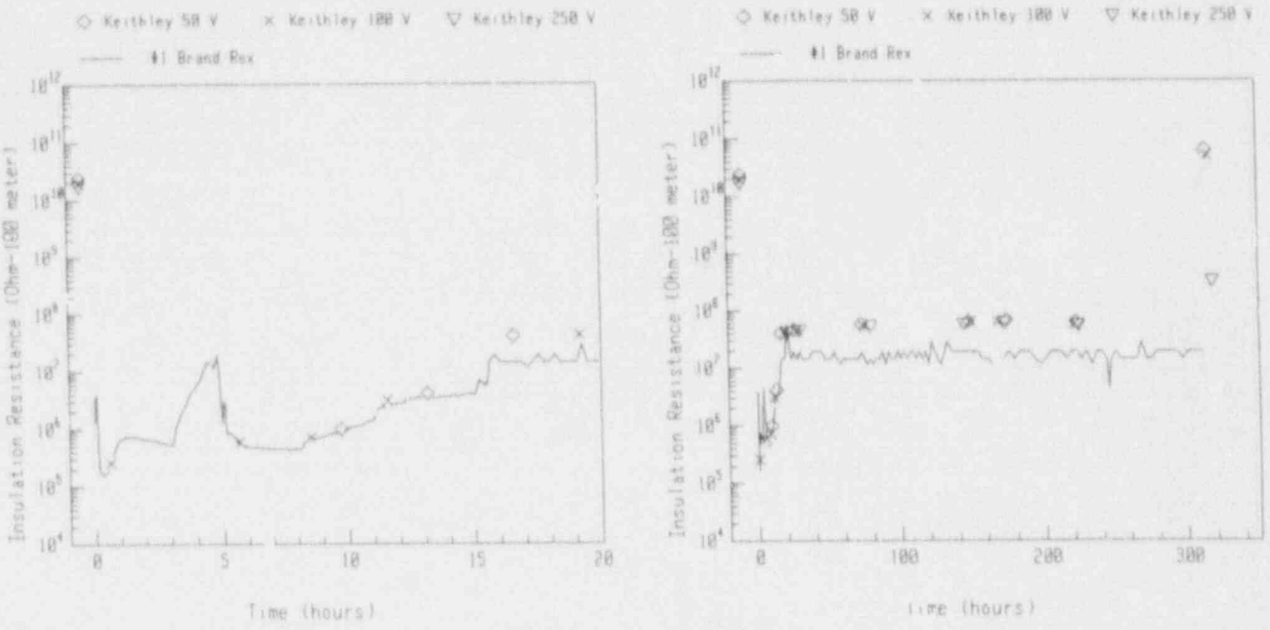

Figure I-7 IR of Brand Rex Conductor 60-1

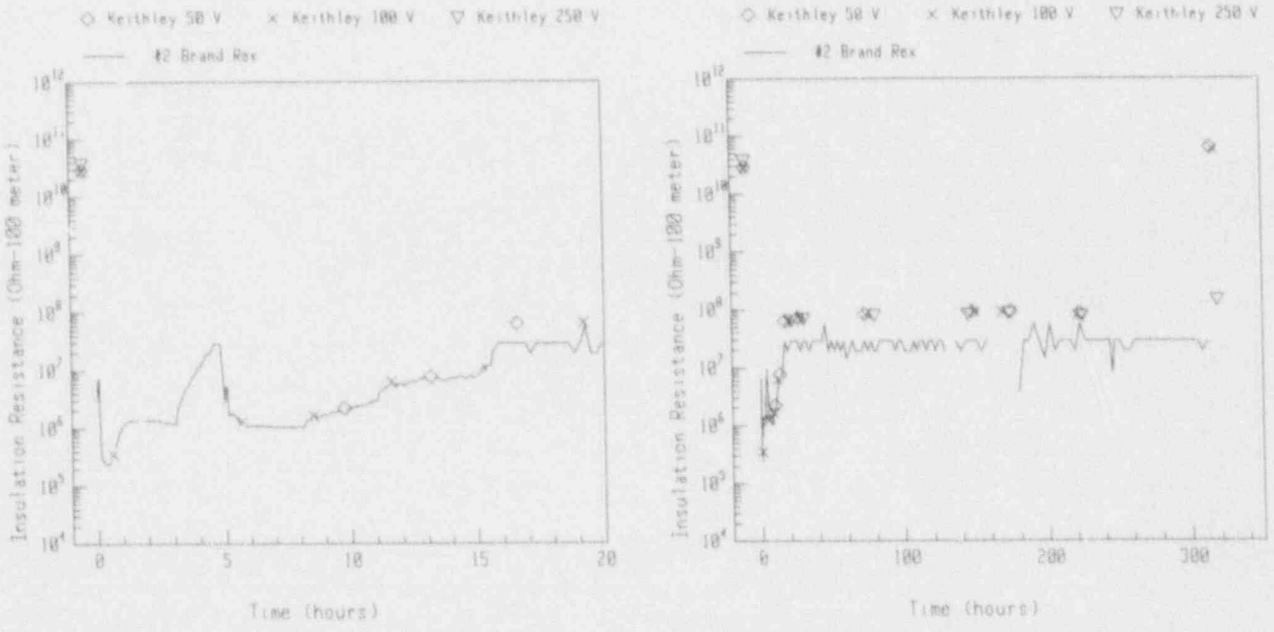

Figure I-8 IR of Brand Rex Conductor 60-2

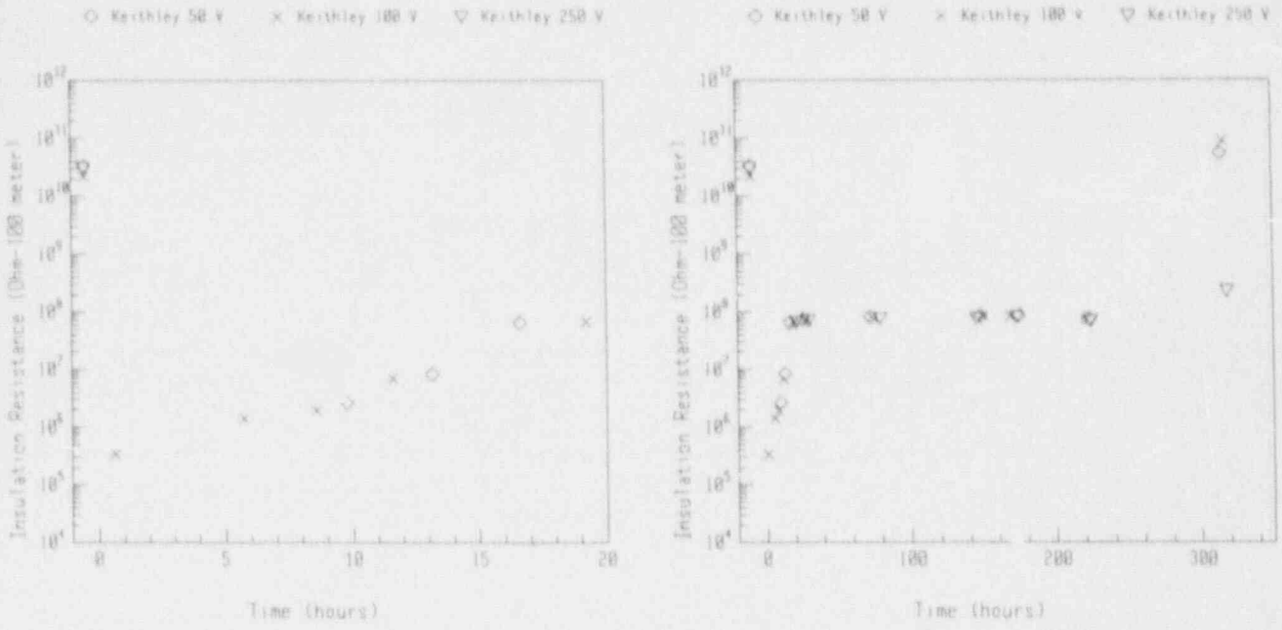

Figure I-9 IR of Brand Rex Conductor 60-3

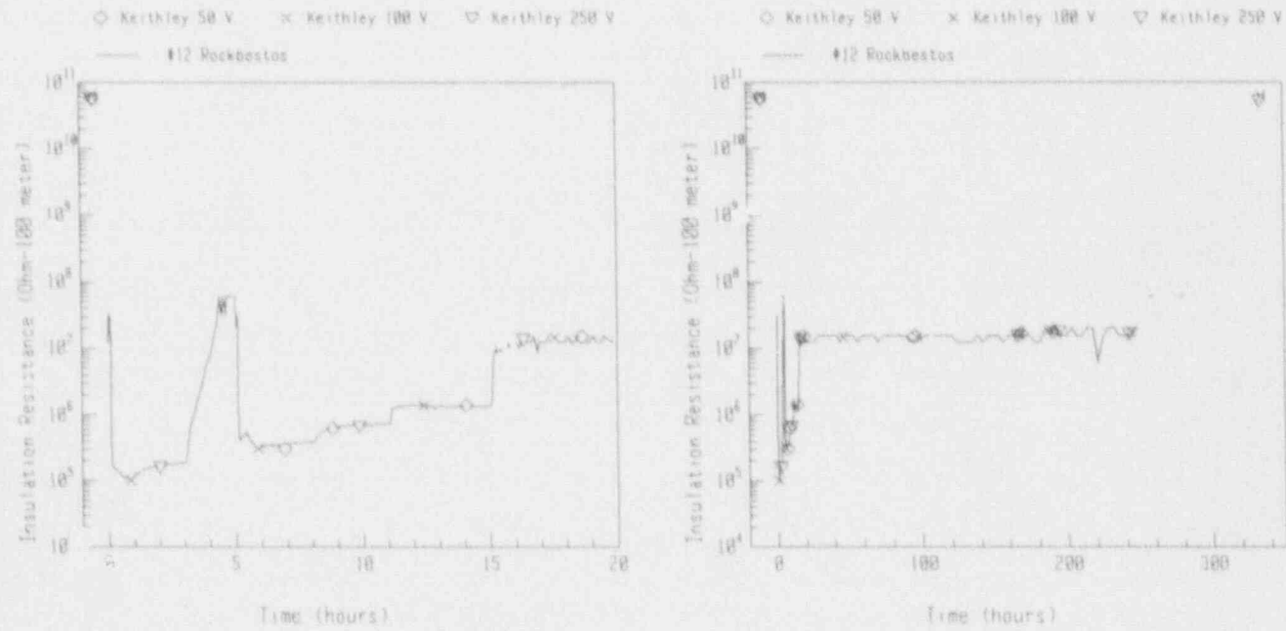

Figure I-10 IR of Rockbestos Conductor 20-12

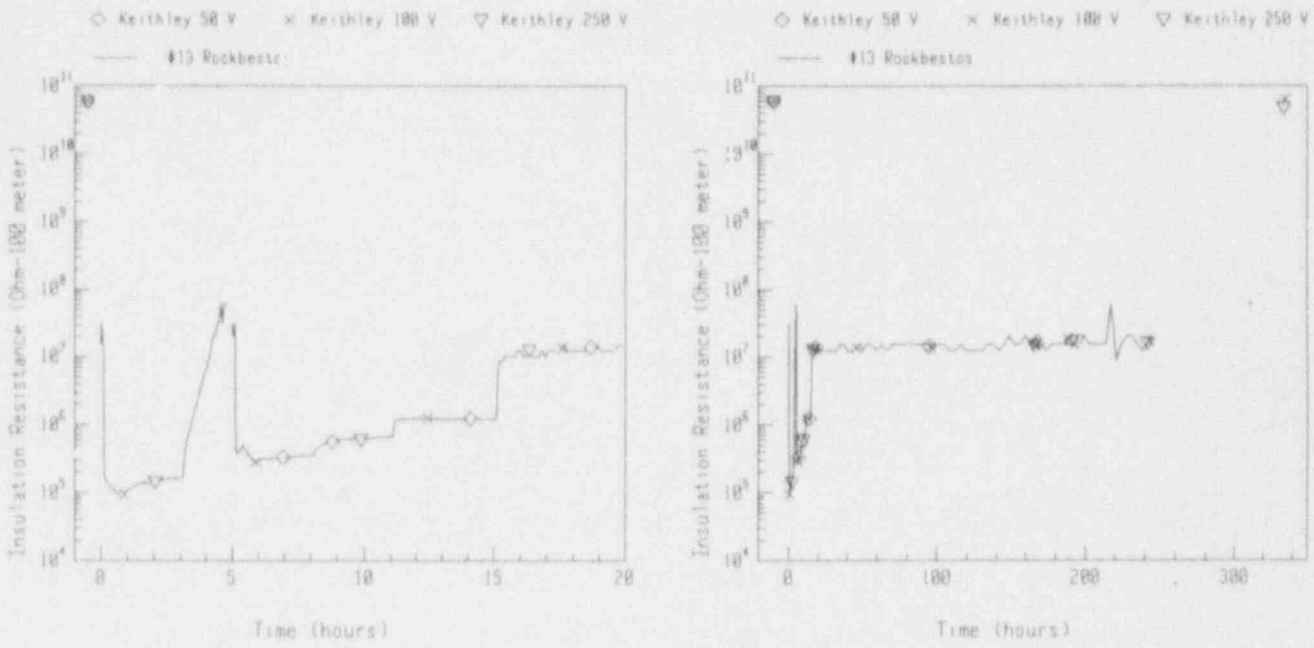

Figure I-11 IR of Rockbestos Conductor 20-13

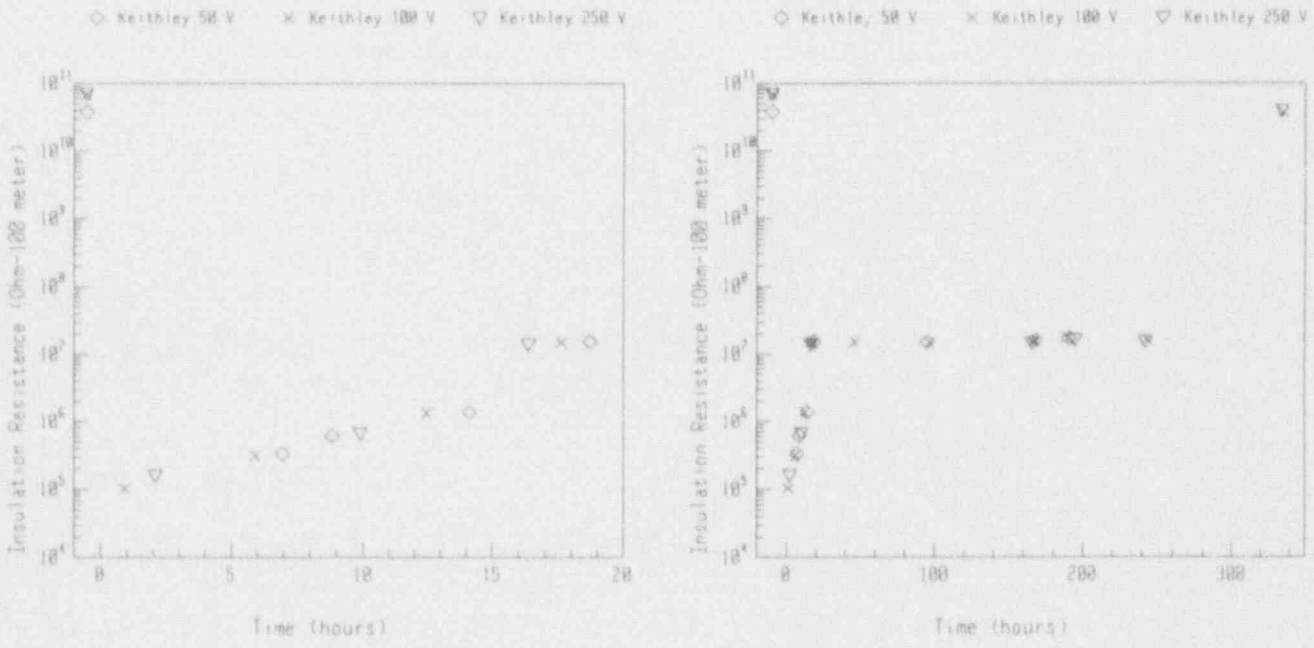

Figure I-12 IR of Rockbestos Conductor 20-14

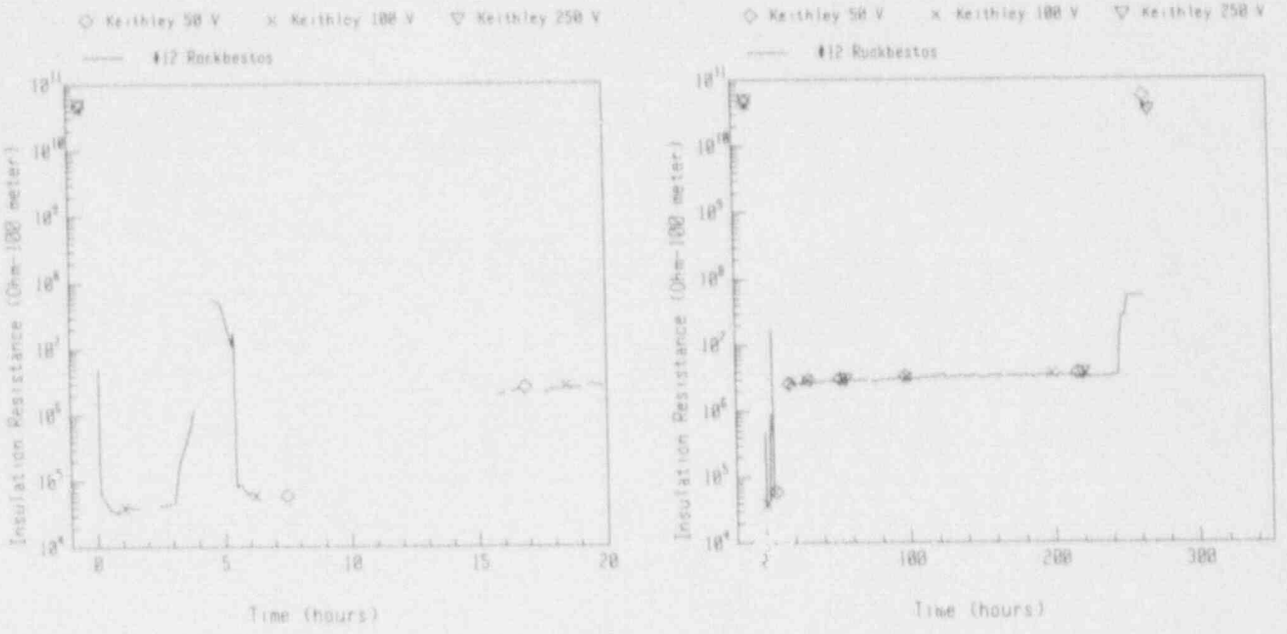

Figure I-13 IR of Rockbestos Conductor 40-12

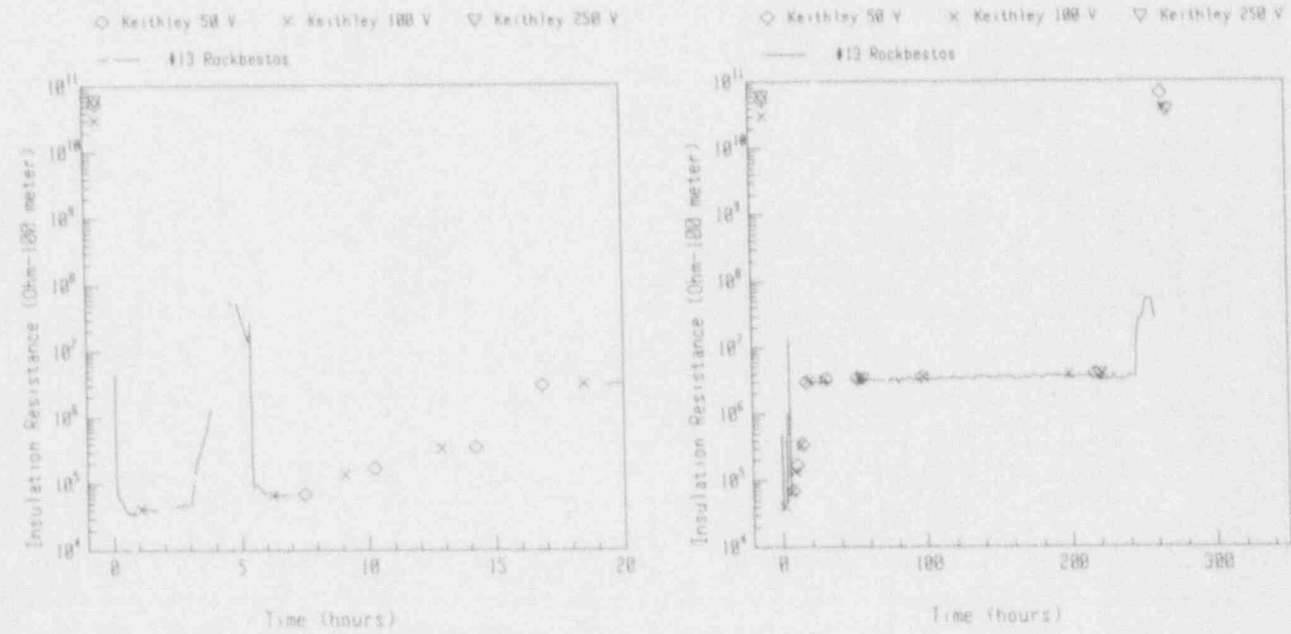

Figure I-14 IR of Rockbestos Conductor 40-13

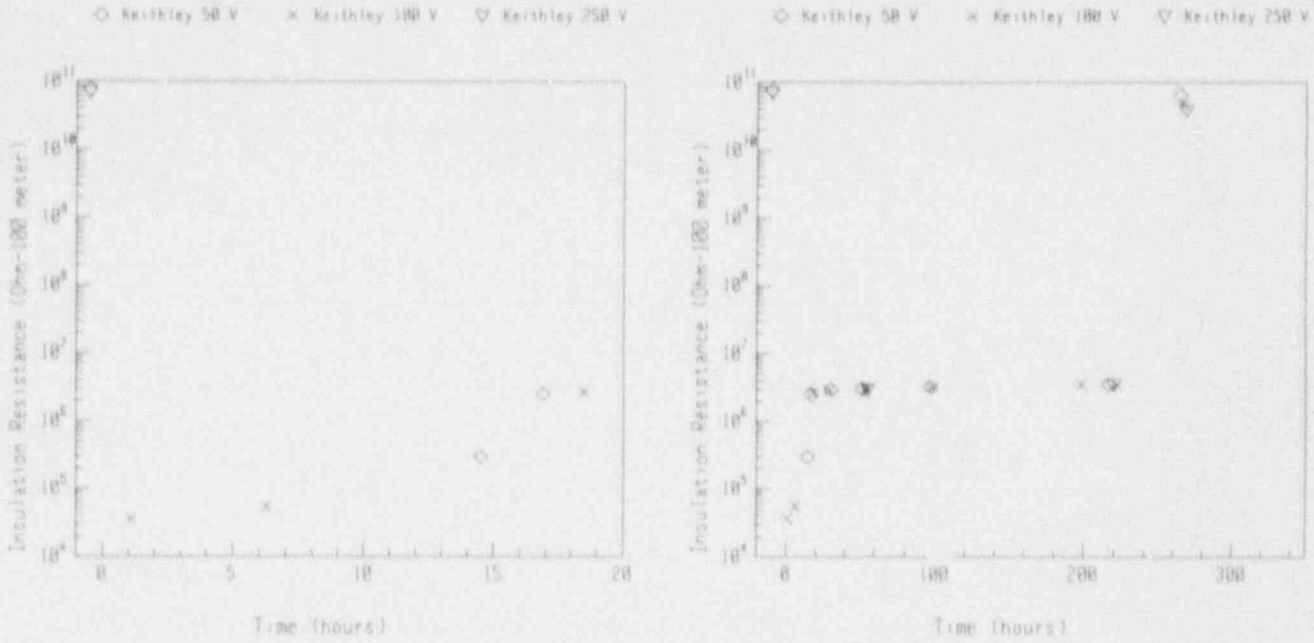

Figure I-15 IR of Rockbestos Conductor 40-14

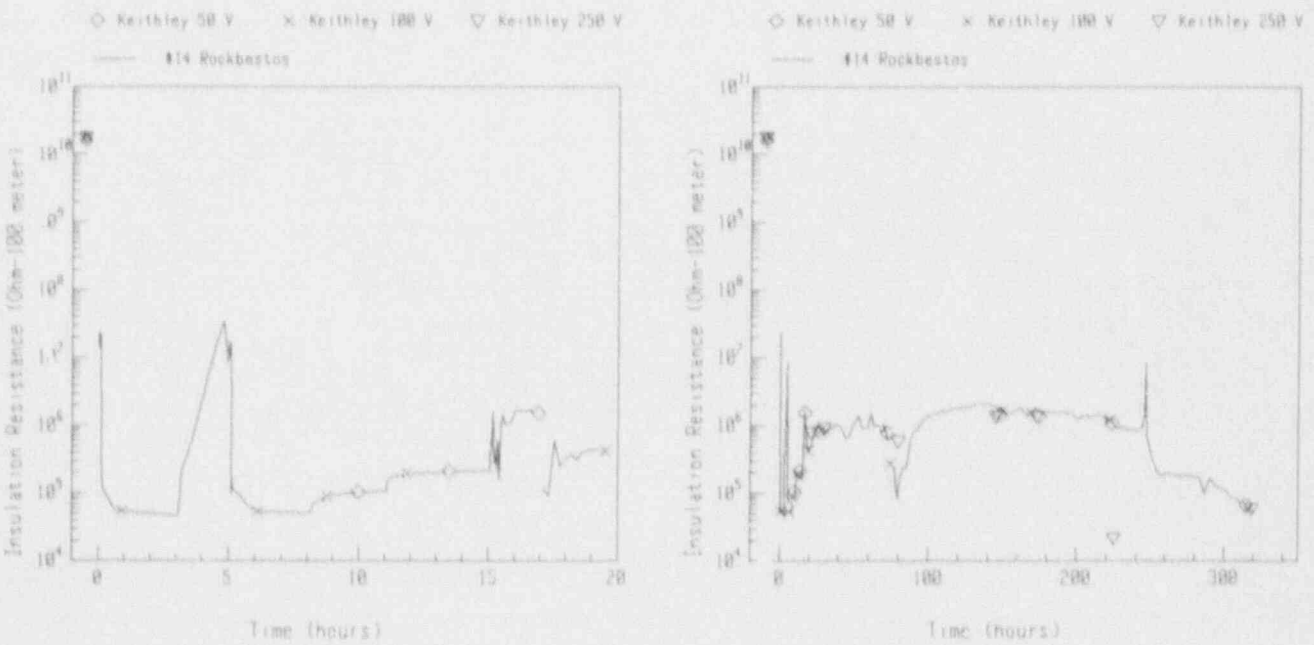

Figure I-16 IR of Rockbestos Conductor 60-14

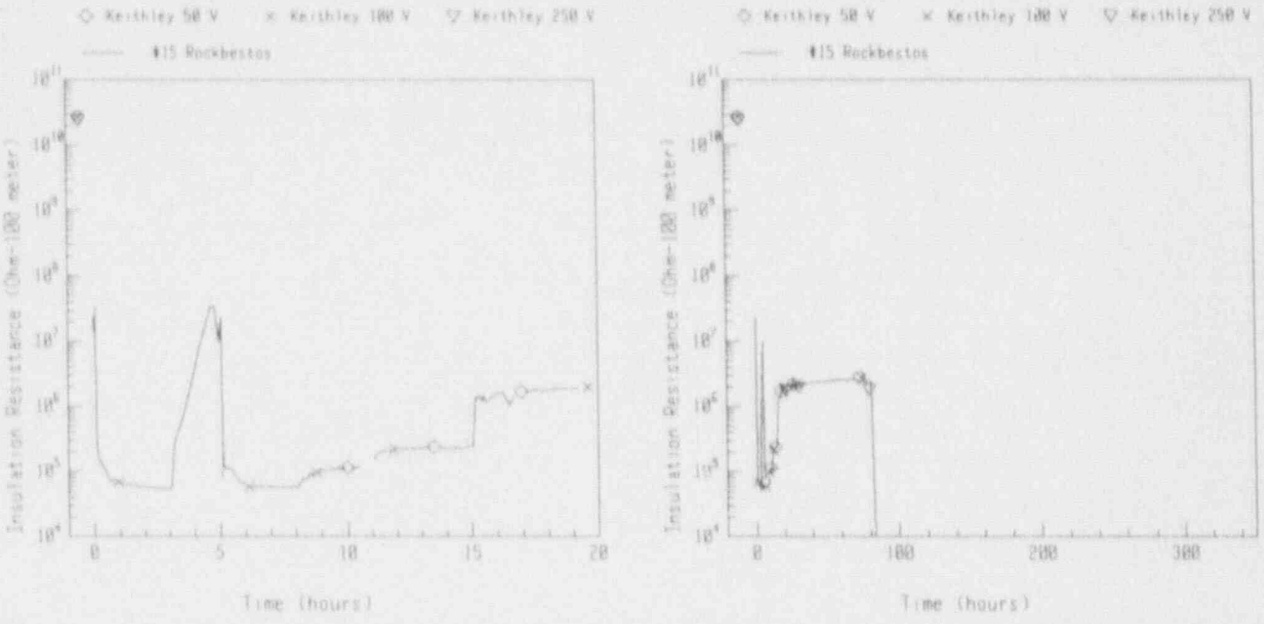

Figure I-17 IR of Rockbestos Conductor 60-15

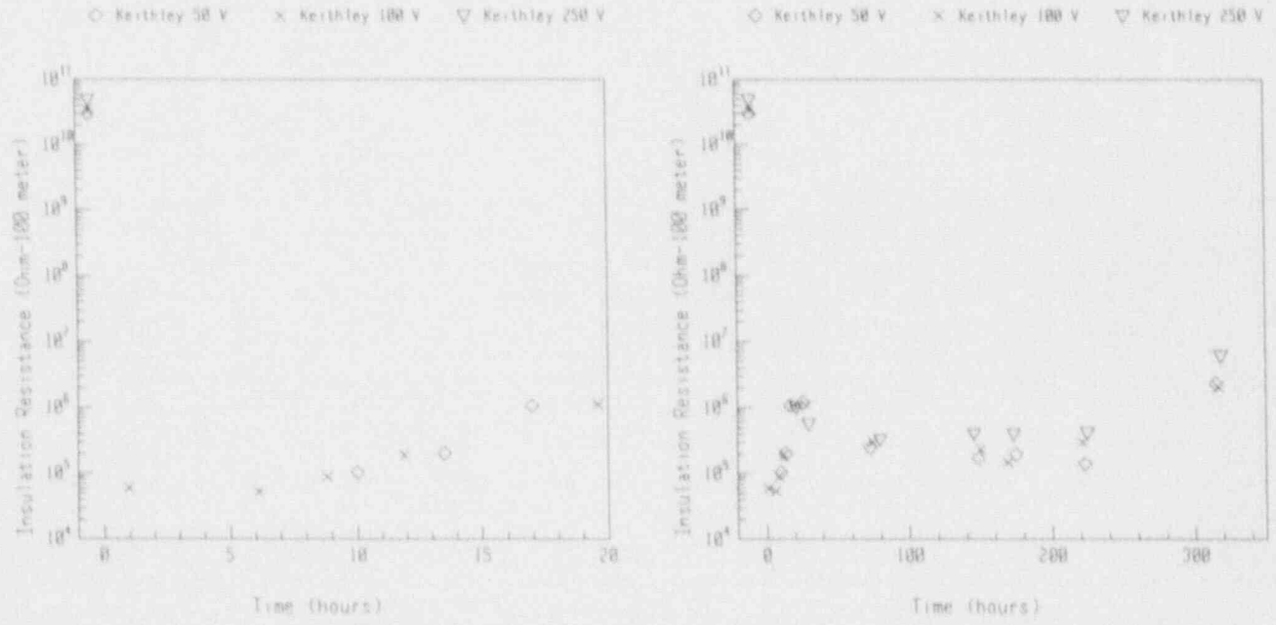

Figure I-18 IR of Rockbestos Conductor 60-16

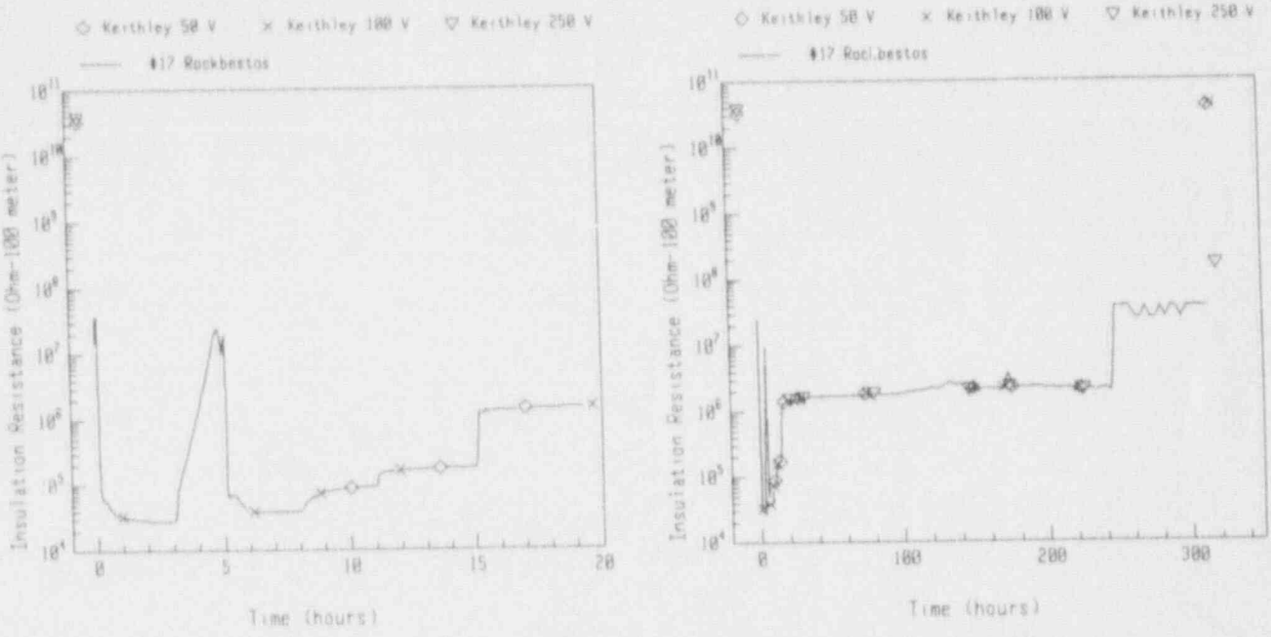

Figure I-19 IR of Rockbestos Conductor 60-17

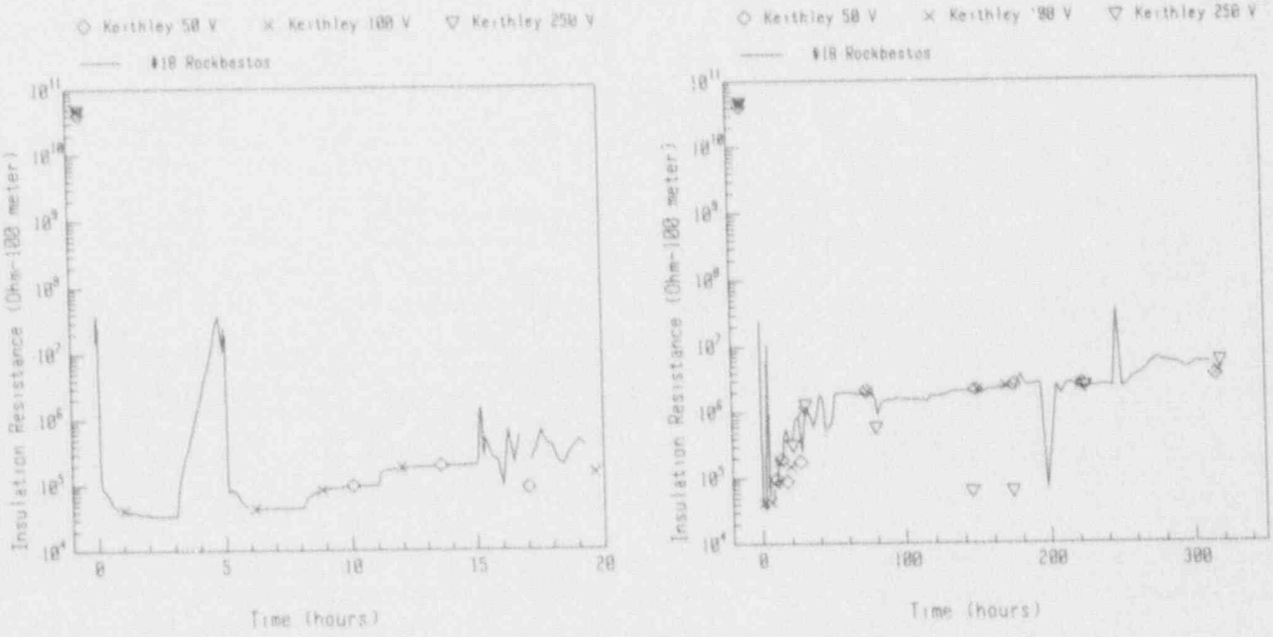

Figure I-20 IR of Rockbestos Conductor 60-18

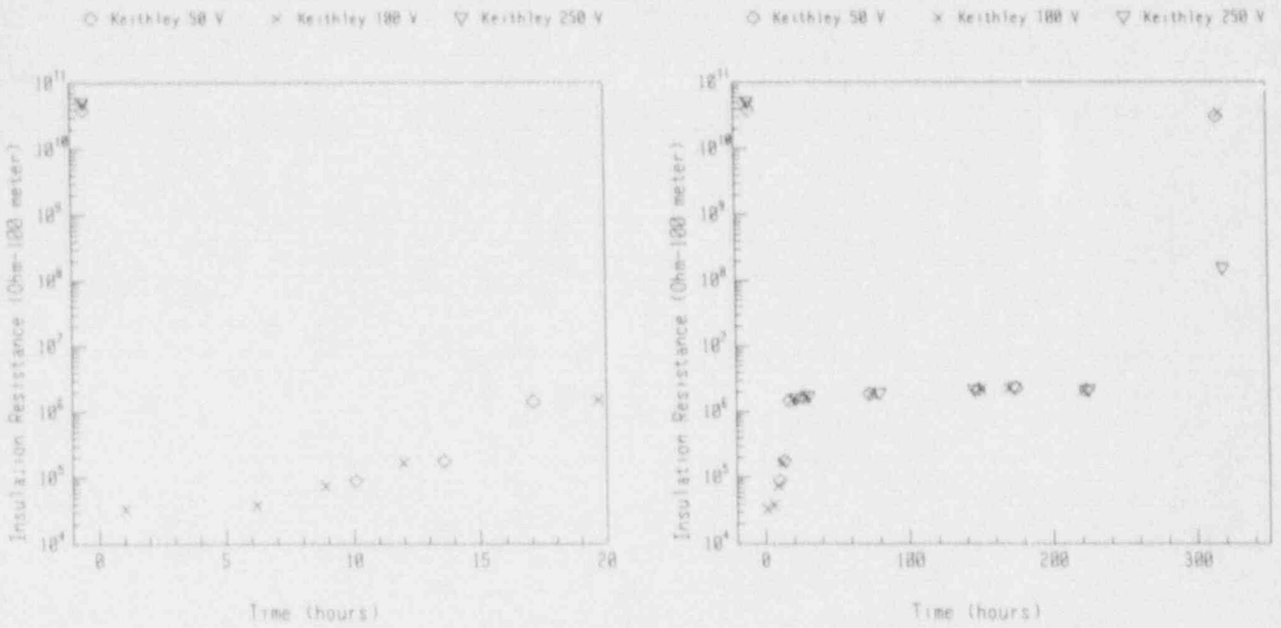

Figure I-21 IR of Rockbestos Conductor 60-19

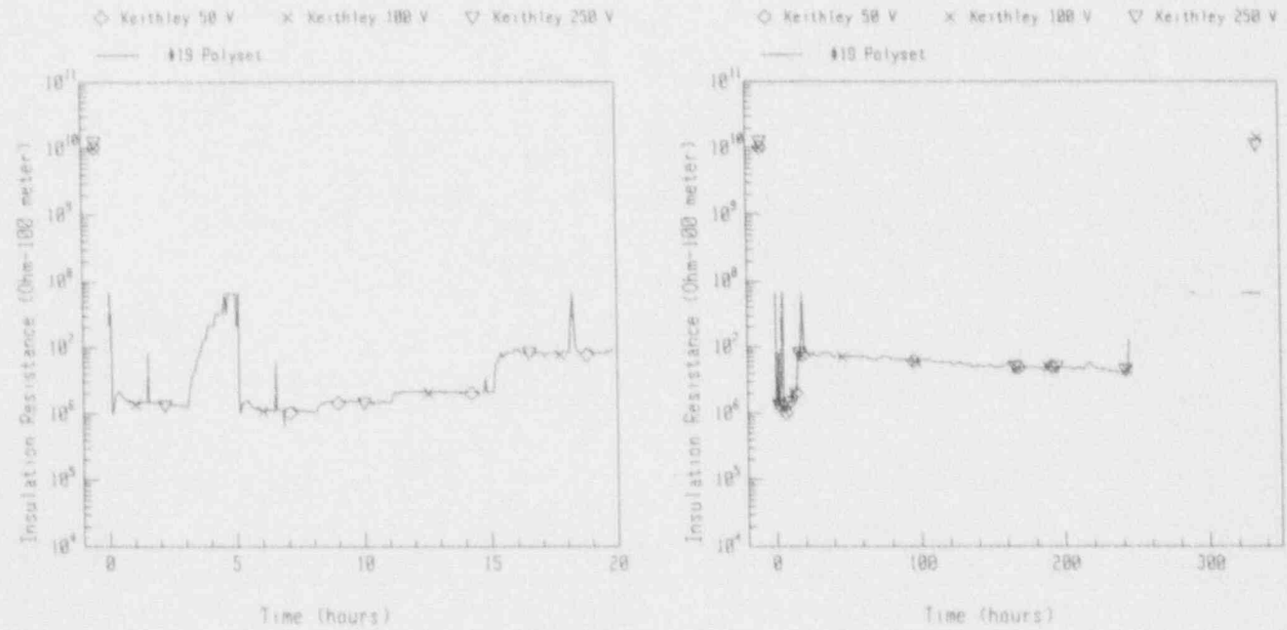

Figure I-22 IR of Dekoron Polyset Conductor 20-19

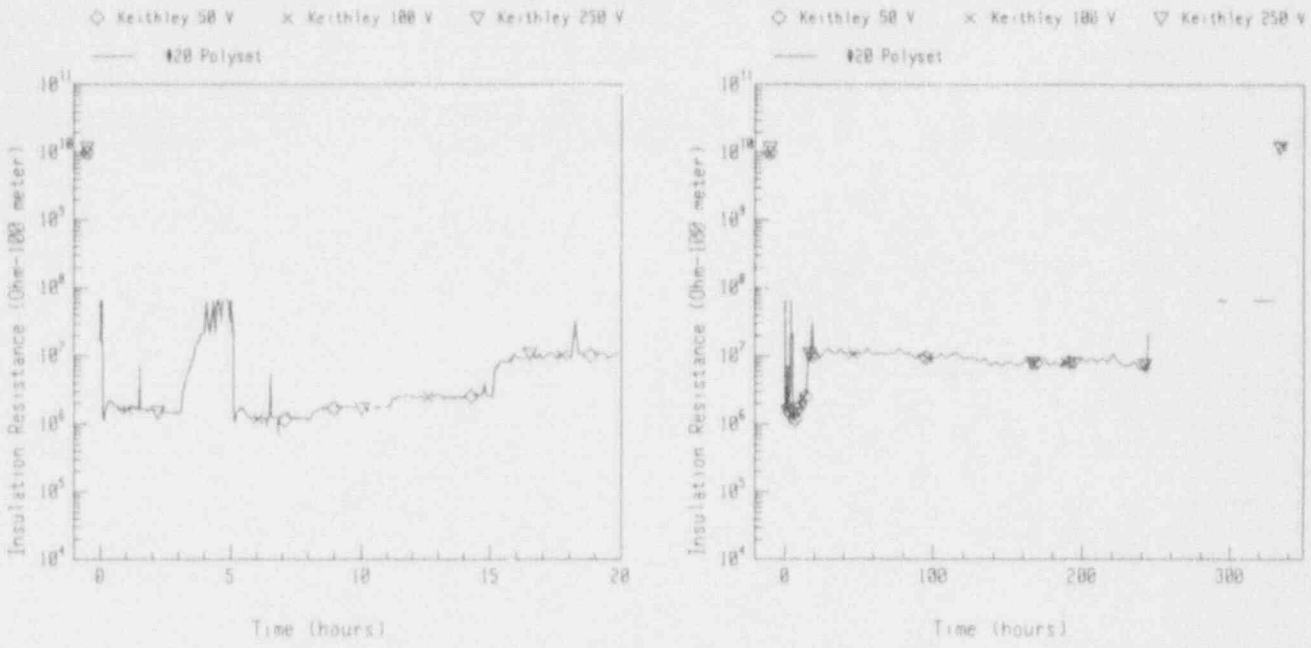

Figure I-23 IR of Dekoron Polyset Conductor 20-20

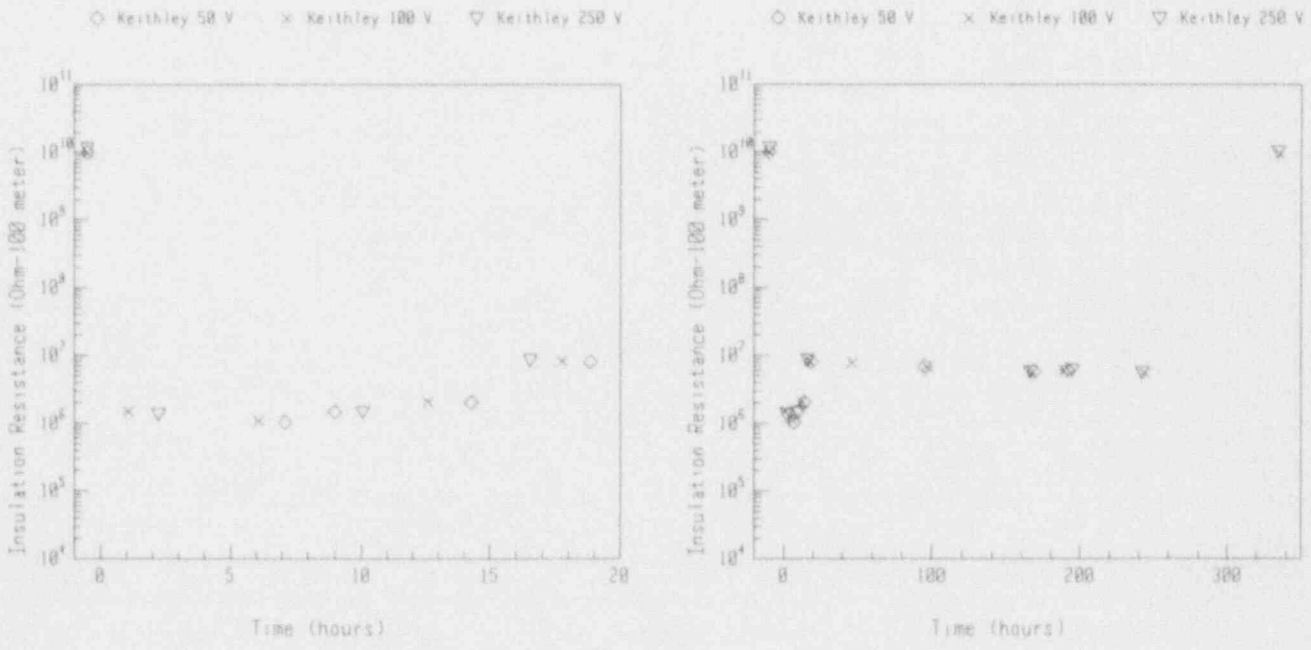

Figure I-24 IR of Dekoron Polyset Conductor 20-21

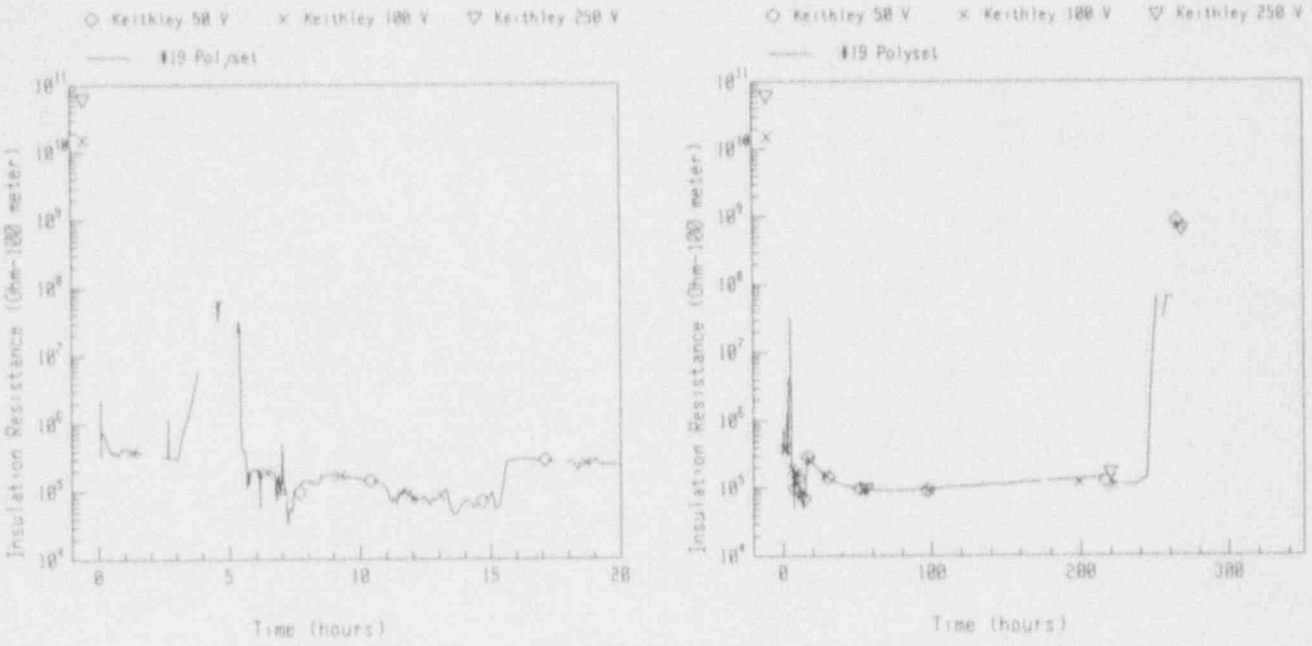

Figure I-25 IR of Dekoron Polyset Conductor 40-19

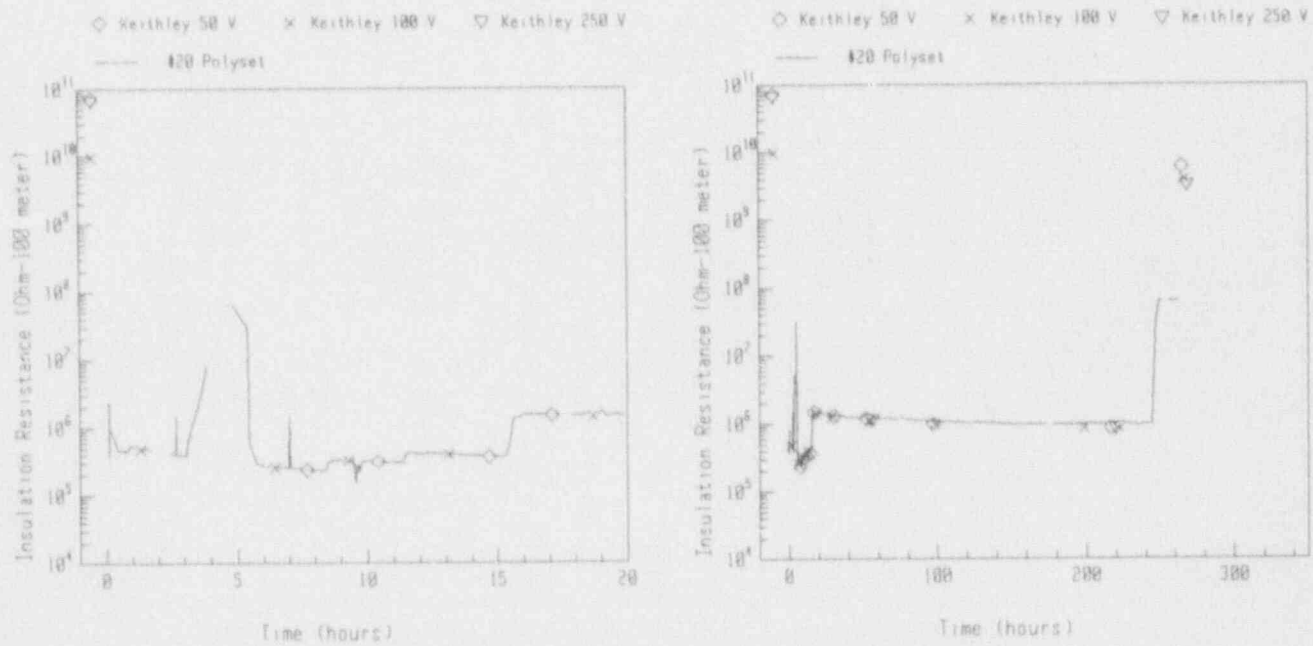

Figure I-26 IR of Dekoron Polyset Conductor 40-20

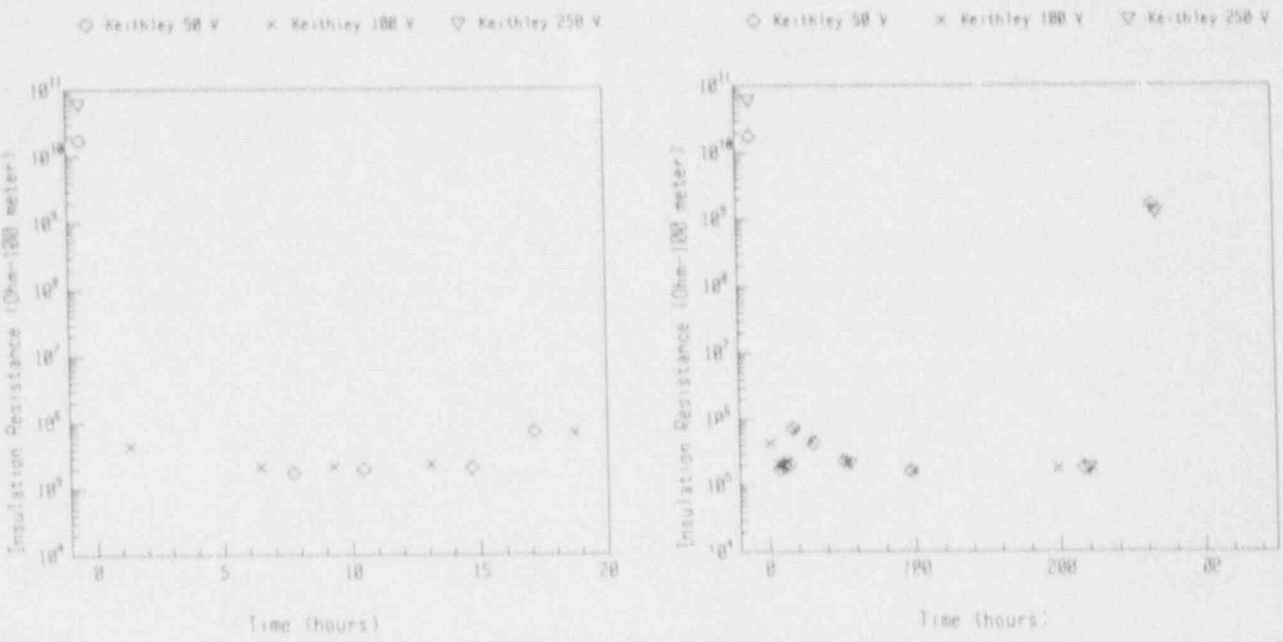

Figure I-27 IR of Dekoron Polyset Conductor 40-21

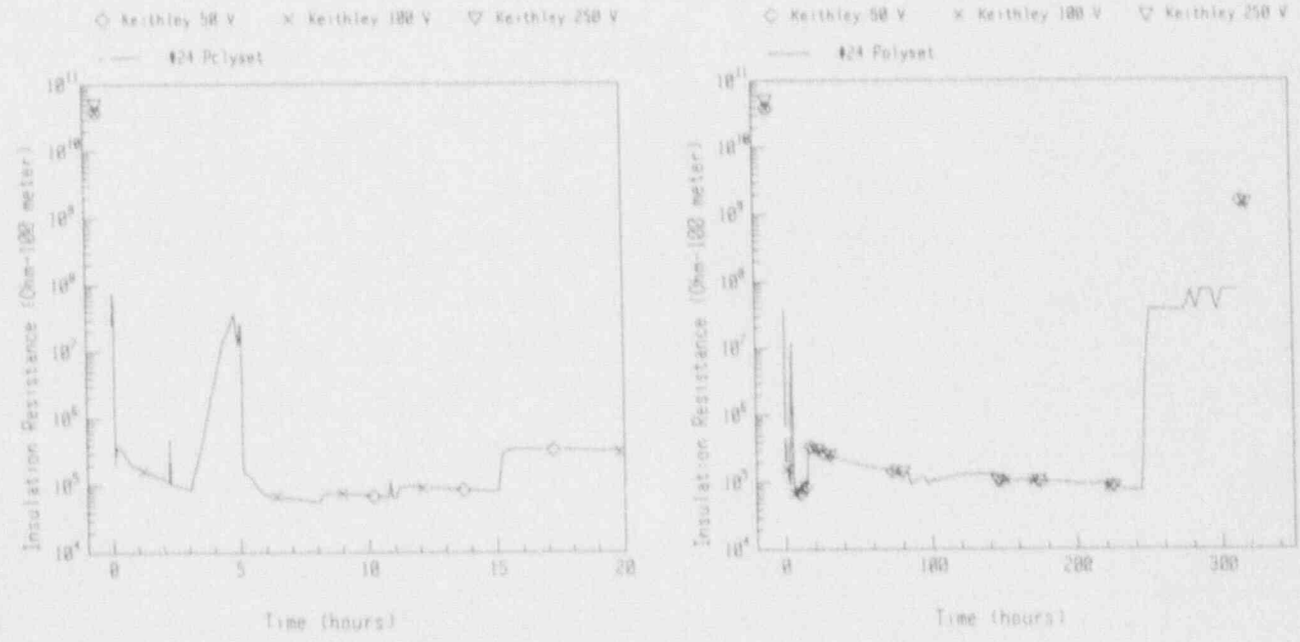

Figure I-28 IR of Dekoron Polyset Conductor 60-24

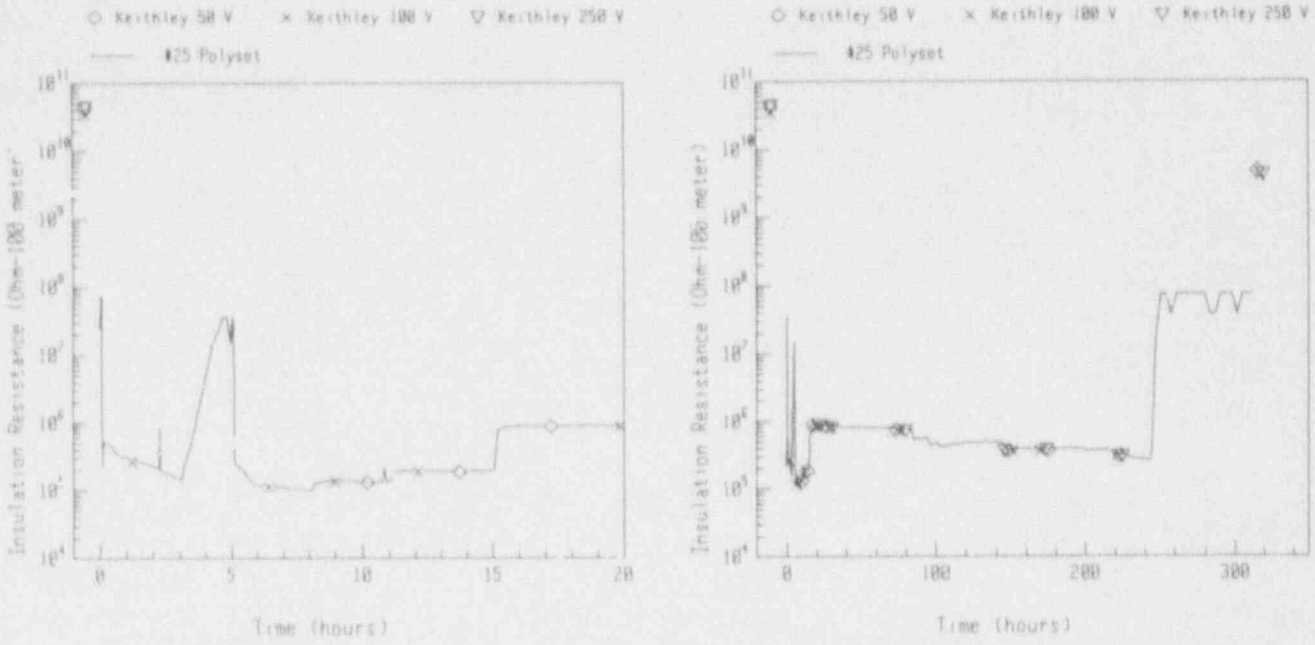

Figure I-29 IR of Dekoron Polyset Conductor 60-25

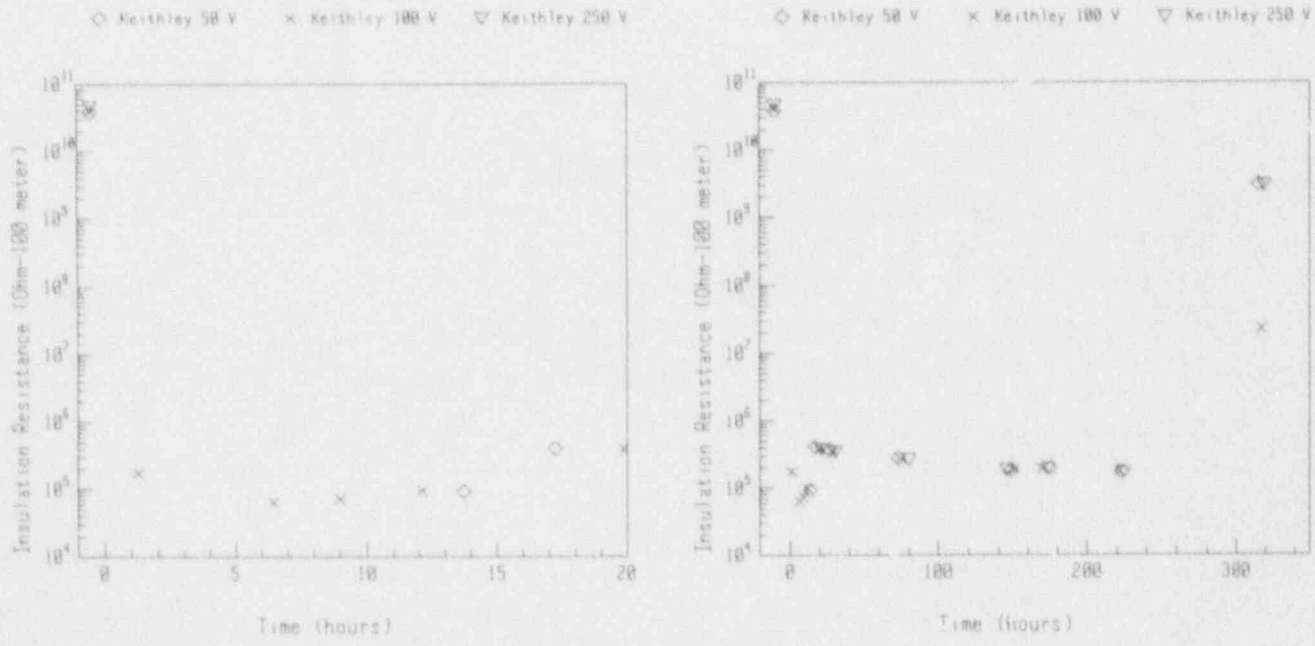

Figure I-30 IR of Dekoron Polyset Conductor 60-26

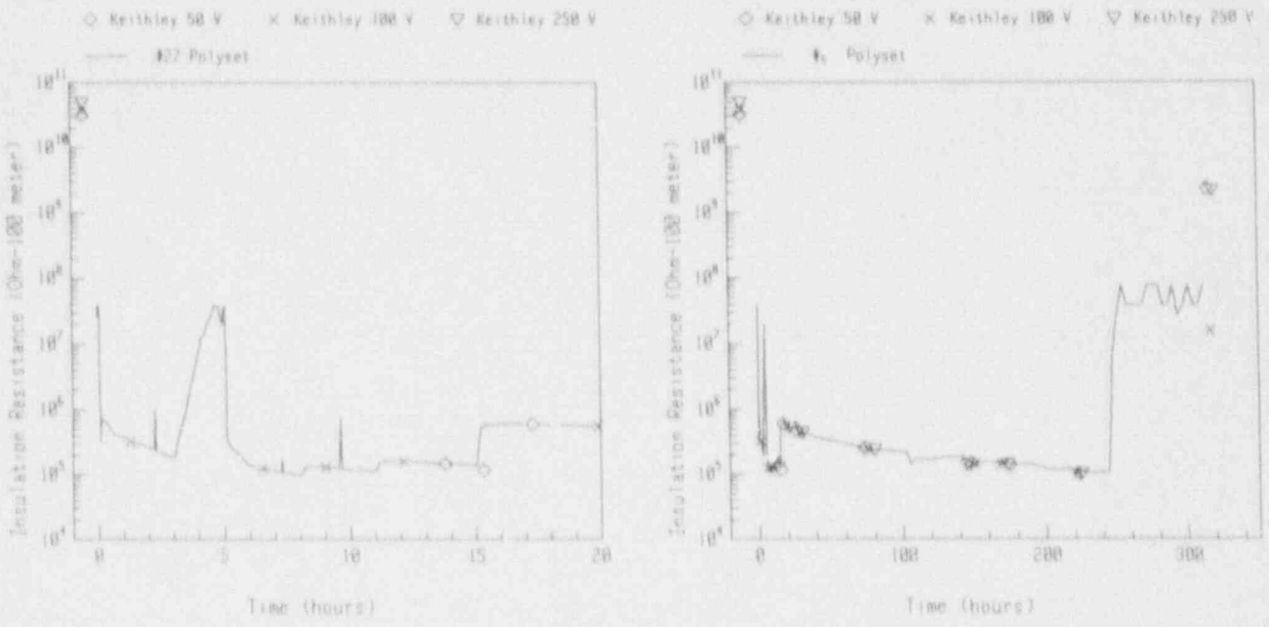

Figure I-31 IR of Dekoron Polyset Conductor 60-27

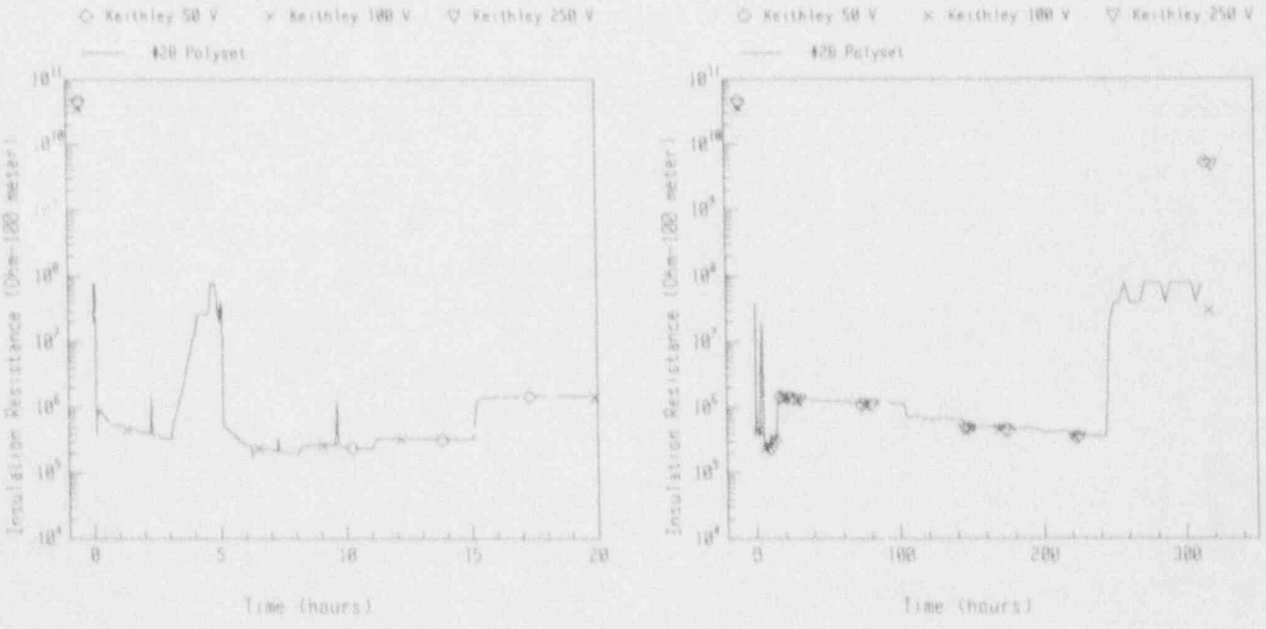

Figure I-32 IR of Dekoron Polyset Conductor 60-28

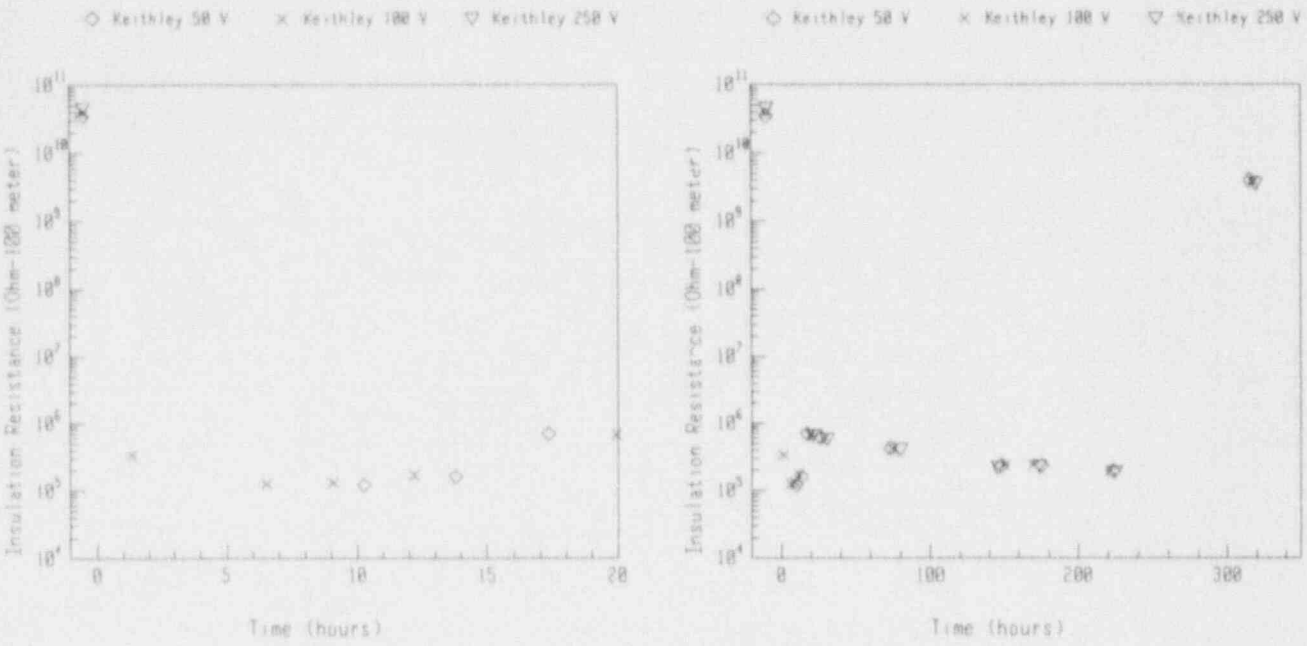

Figure I-33 IR of Dekoron Polyset Conductor 60-29

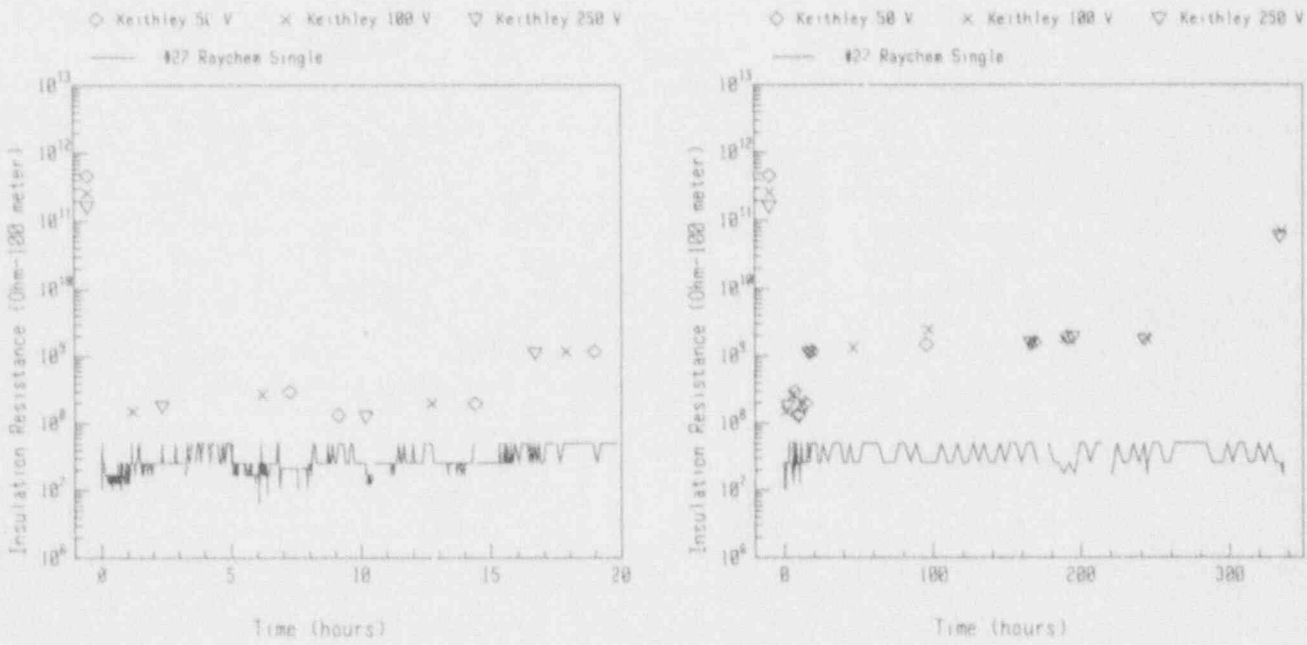

Figure I-34 IR of Raychem Conductor 20-27

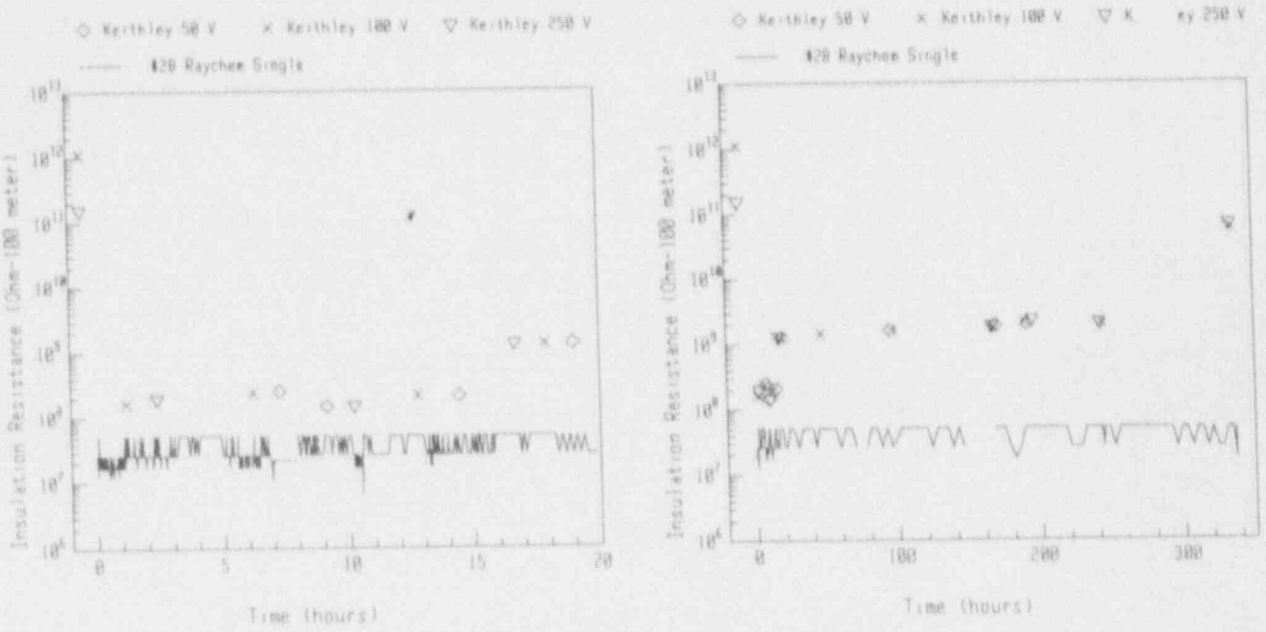

Figure I-35 IR of Raychem Conductor 20-28

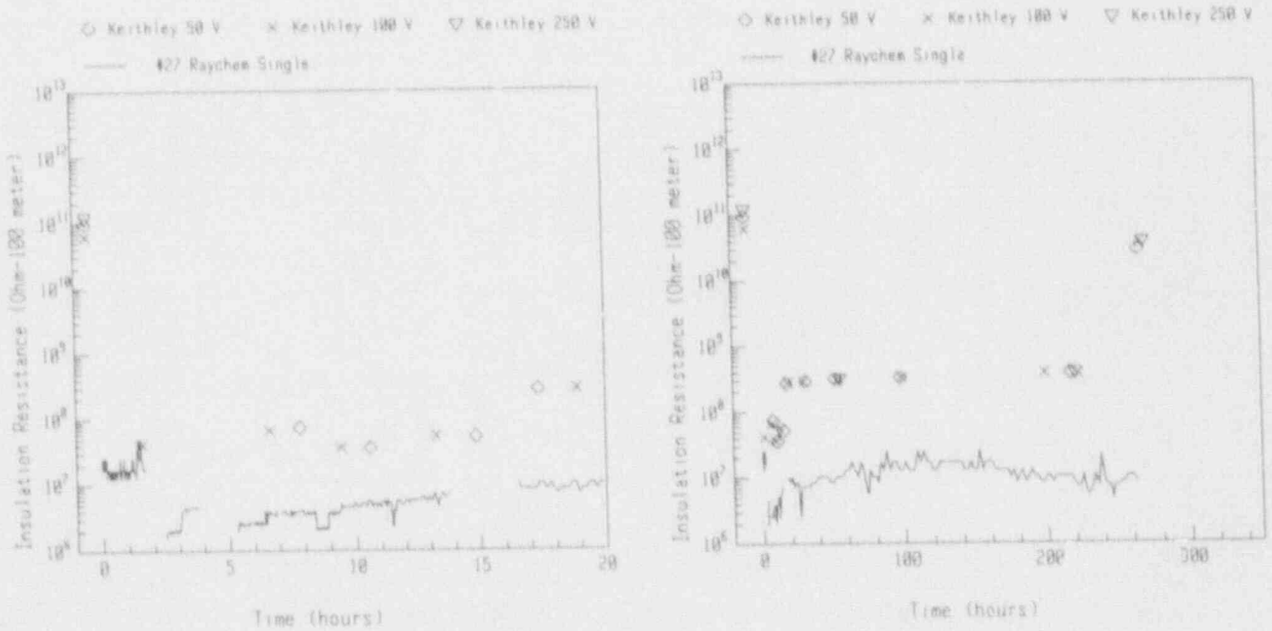

Figure I-36 IR of Raychem Conductor 40-27

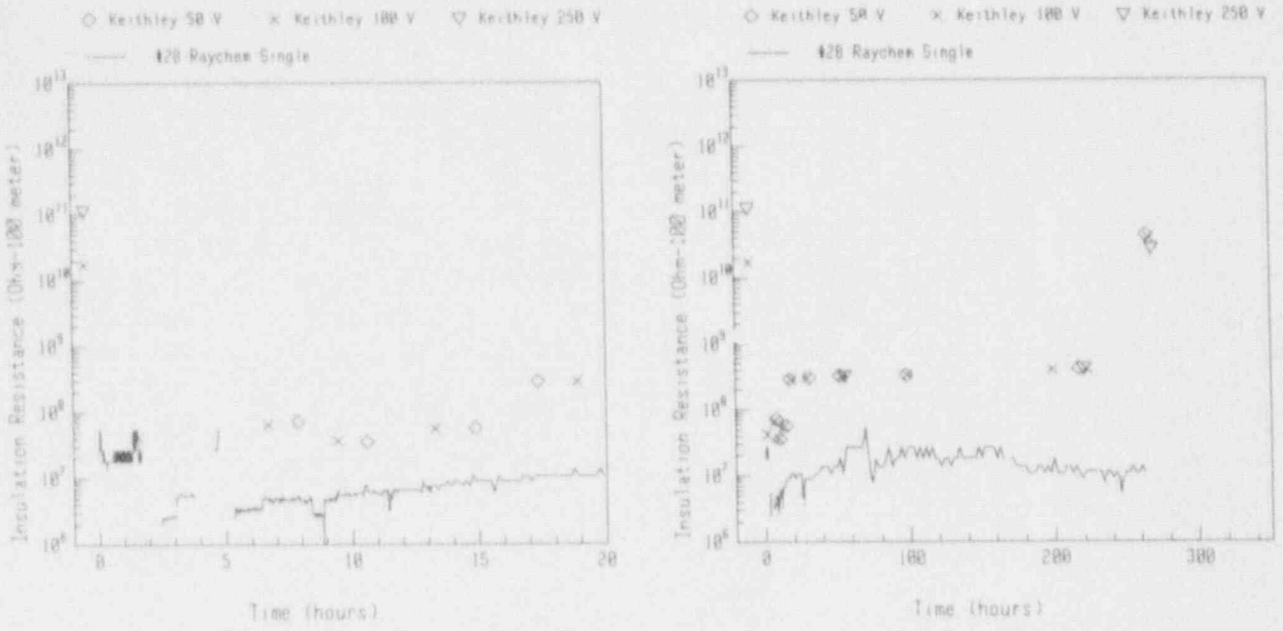

Figure I-37 IR of Raychem Conductor 40-28

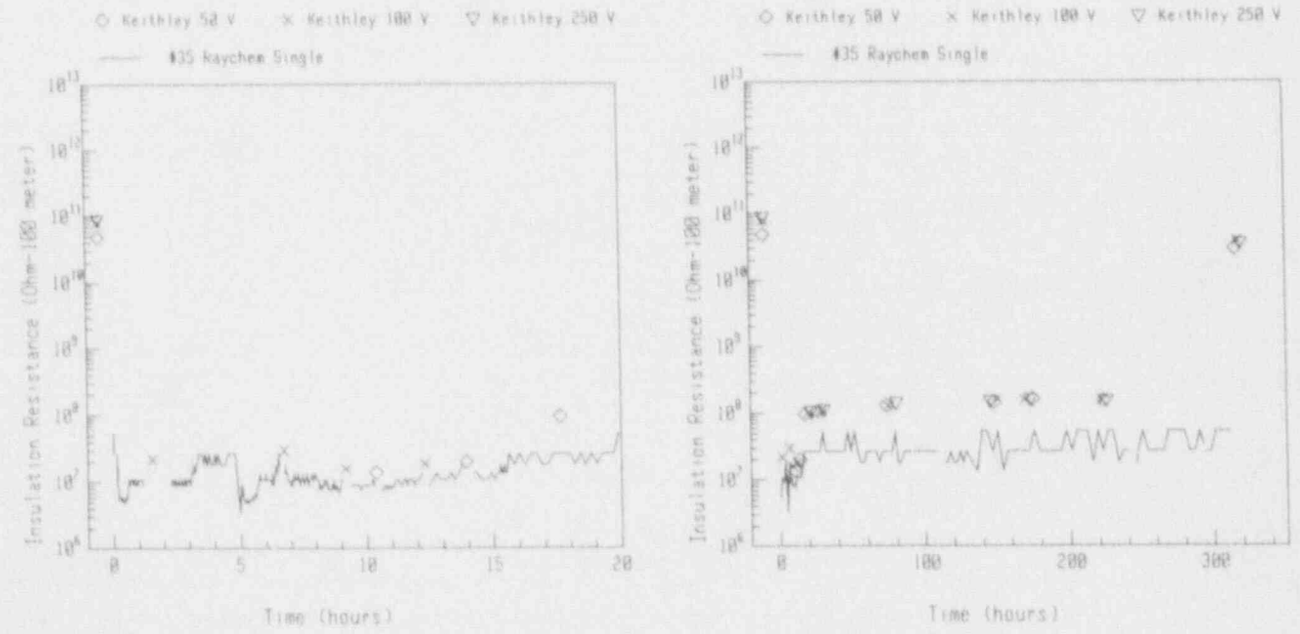

Figure I-38 IR of Raychem Conductor 60-3.

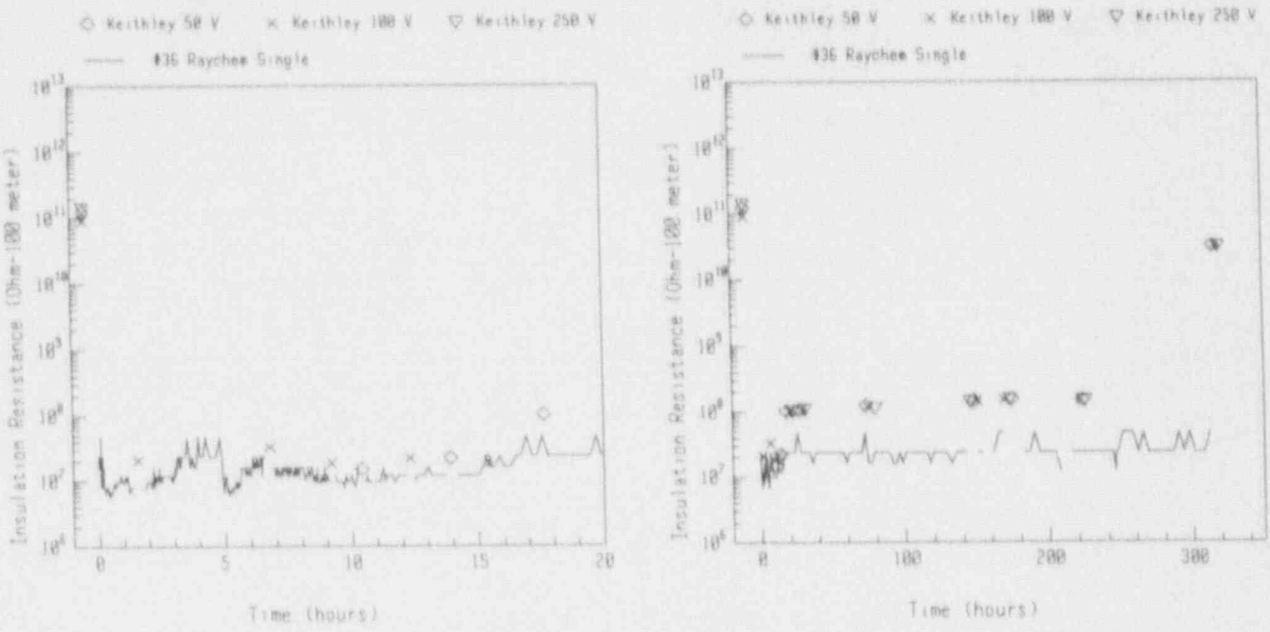

Figure I-39 IR of Raychem Conductor 60-36

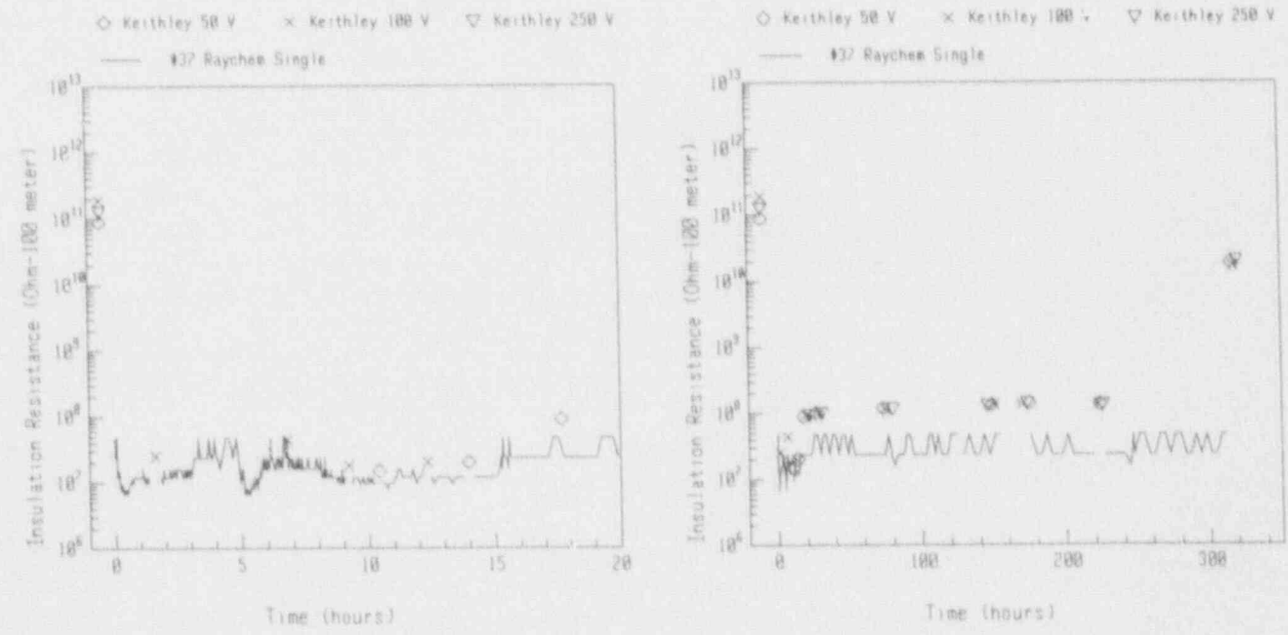

Figure I-40 IR of Raychem Conductor 60-37

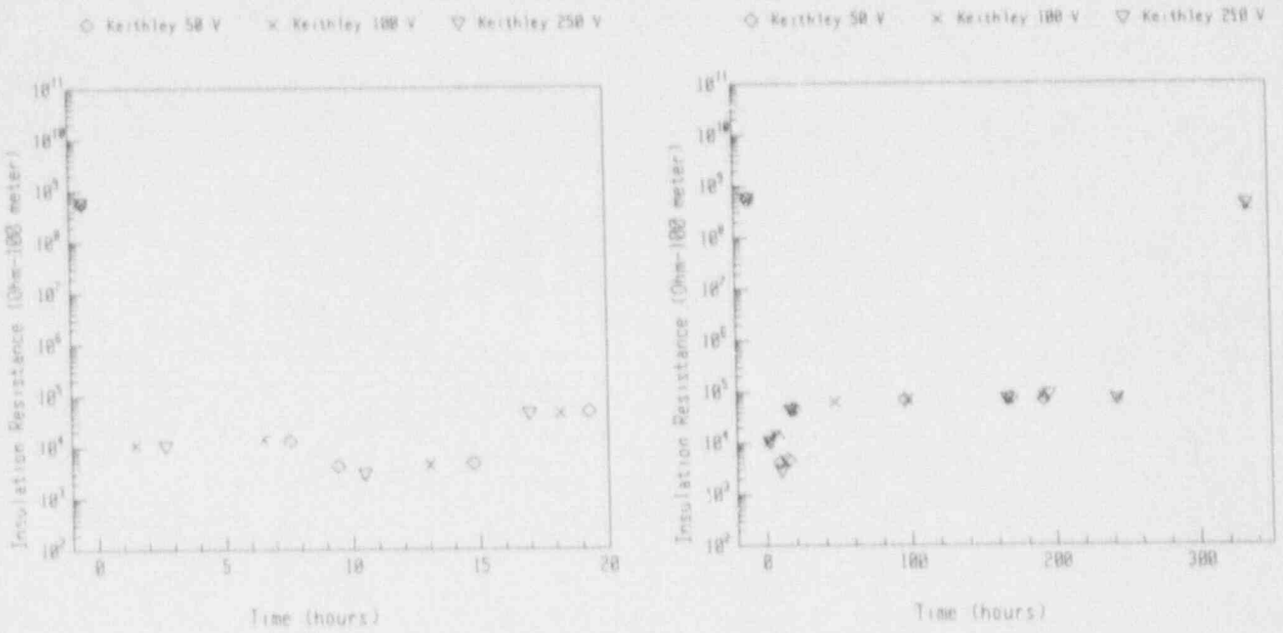

Figure I-41 IR of Dekoron Polyset Jacket Conductor 20-41

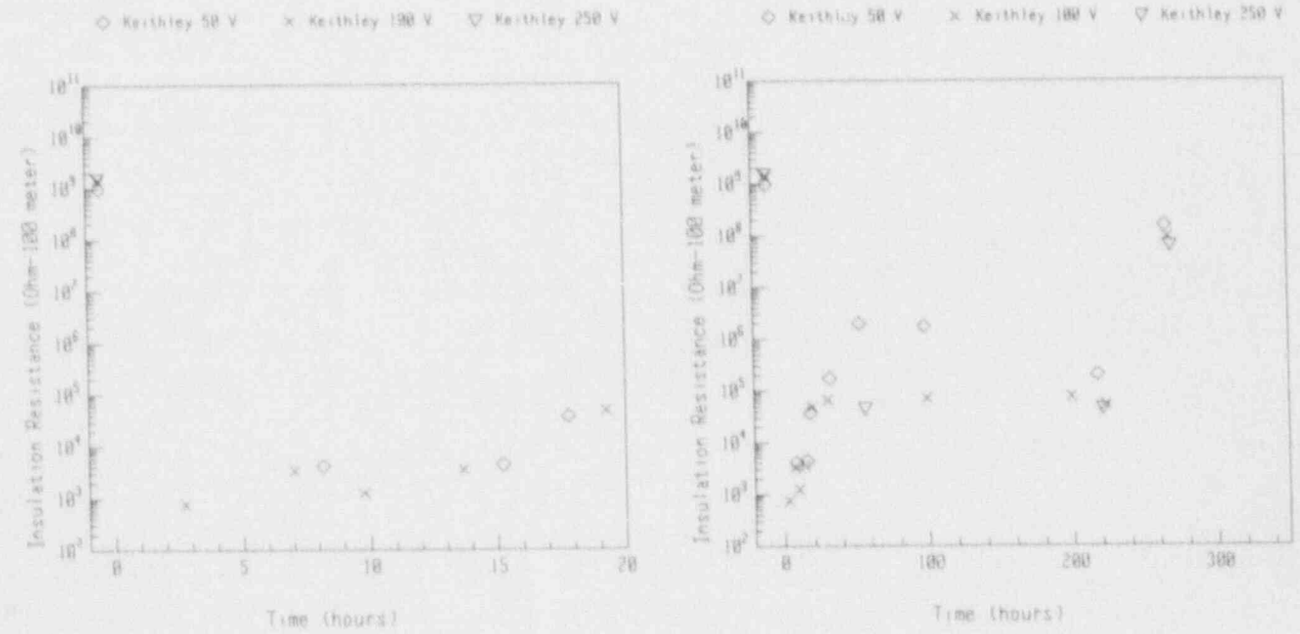

Figure I-42 IR of Dekoron Polyset Jacket Conductor 40-41

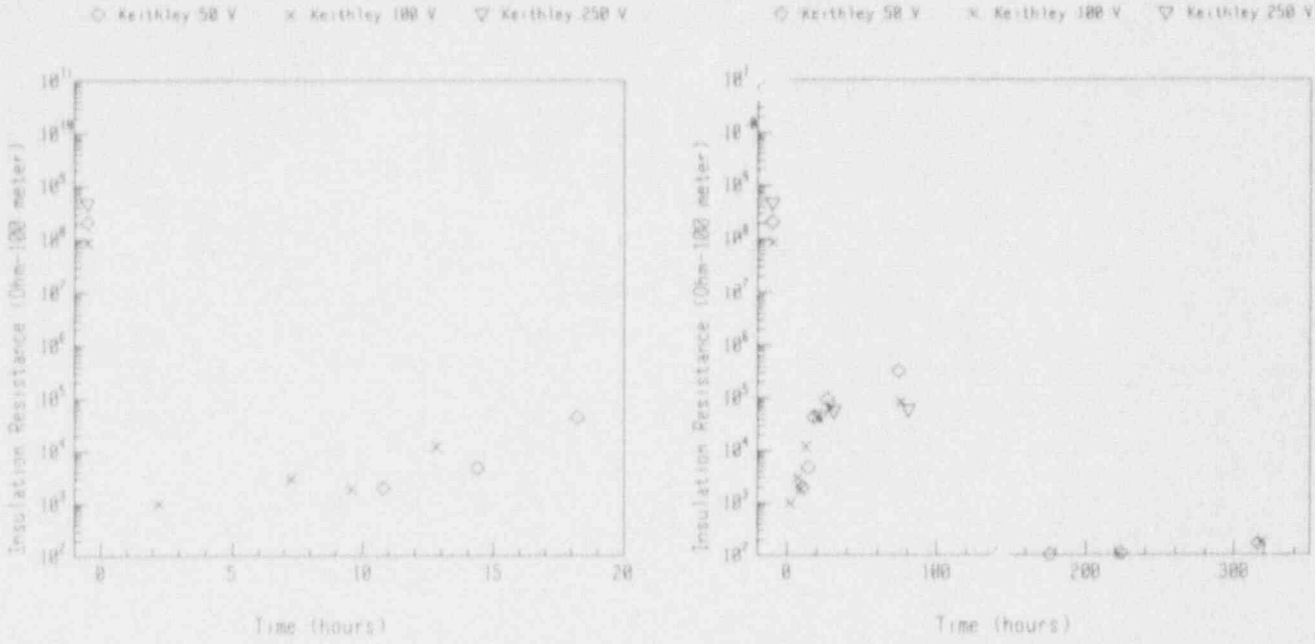

Figure I-43 IR of Dekoron Polyset Jacket Conductor 60-55

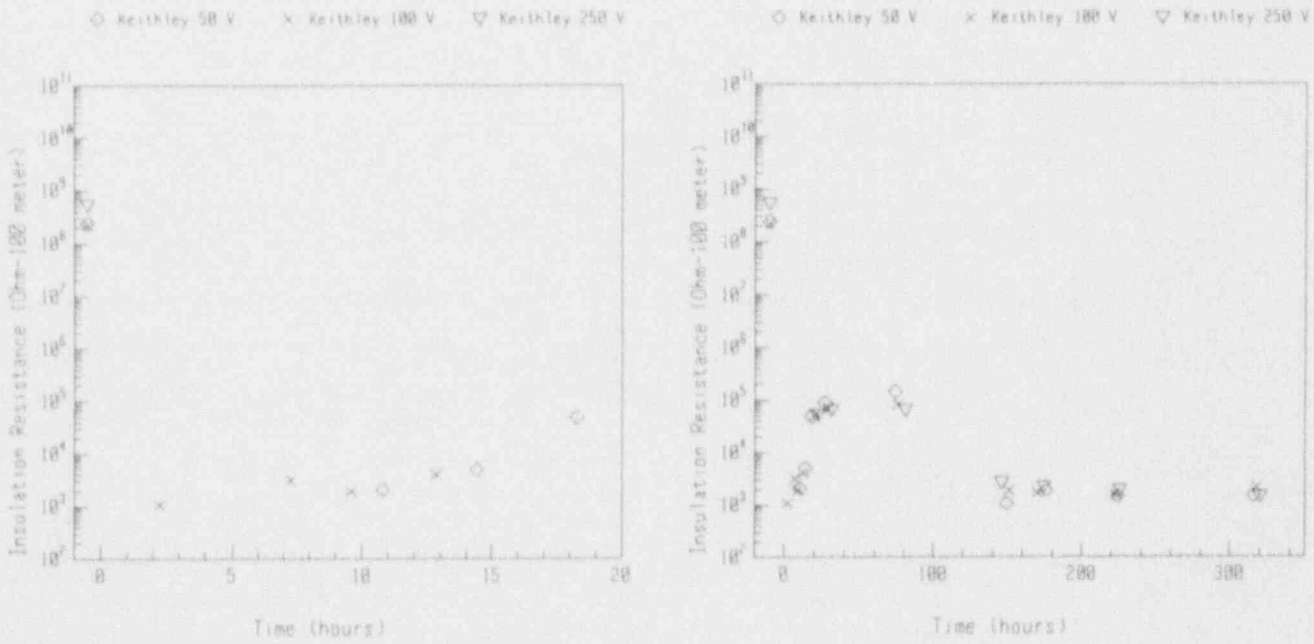

Figure I-44 IR of Dekoron Polyset Jacket Conductor 60-56

Appendix J--Anomalies

Appendix J--Significant Test Anomalies

The following list discusses a number of test anomalies that occurred during the test program. A detailed discussion of minor anomalies, such as power outages, is not included.

1. Loss of data during aging--As a result of problems with a disk used to store the aging data, several segments of data were lost for the 6- and 9-month chambers. Backup printouts and logs kept during aging were used to verify that the temperature in the chamber did not deviate significantly from the desired conditions. Thus, there was no adverse effect from the loss of data.

2. Loss of data loggers during AT6--Between about 1.8 and 2.3 hours into AT6 (during the first dwell at the peak temperature) and again between about 4.0 and 4.5 hours into AT6 (during the cooldown after the first transient), data logger readings were lost as a result of a problem with the data logger input boards. The problem was corrected and the test was continued uninterrupted. The only adverse effect of the problem was the loss of IR data during the time when the data logger was malfunctioning.

3. Moisture out ends of cables during accident tests--During all of the accident tests, moisture dripped from the ends of some of the cables outside the test chamber. During AT6 (the first accident test run), a few of the conductors leaked enough to potentially disrupt the leakage current monitoring system by leakage on a connection panel. The most leakage occurred from Kapton and silicone rubber insulated cables and monitoring of these cables was somewhat affected by the leakage. The redundant IR monitoring system (using the Keithley electrometer) was not affected by the water dripping. The IR data during the LOCA that was potentially affected by the water dripping has been deleted from the continuous IR data plots. An improved connection panel in the remaining accident tests precluded any adverse effects of the water dripping.

4. Damage to thermocouples as a result of accident tests--Following AT6 and AT9, the stainless steel thermocouple sheaths were found damaged. In several cases, the bare conductors were visible through the mineral insulation. Because of the consistency of the thermocouple data (and its relation to pressure) during the accident tests, there was no significant temperature error as a result of the damage. However, it is possible that the thermocouples acquired false junctions and that the actual measured temperature was at a different location than the end of the thermocouple. Since the chamber temperature was very uniform during the accident tests, this anomaly had no adverse effects on the test results. The most likely cause of the damaged thermocouples is from chloride attack originating in cable jacket materials. Inconel thermocouples eliminated this type of damage during subsequent testing.

DISTRIBUTION:

Atomic Energy of Canada, Ltd.
Attn: E. C. Davey
Instrument and Control Branch
Chalk River Nuclear Laboratories
Chalk River, Ontario K0J 1J0
CANADA

Atomic Energy of Canada, Ltd.
Attn: S. Nish
1600 Dorchester Boulevard West
Montreal, Quebec H3H 1P9
CANADA

Canada Wire and Cable Limited
Attn: Z. S. Paniri
Power & Control Products Division
22 Commercial Road
Toronto, Ontario
CANADA M4G 1Z4

Commissariat a l'Energie Atomique
CIS Biointernational LAPRI (3)
Attn: G. Gaussens
J. Chenion
F. Carlin
BP No 32
91192 Gif-Sur-Yvette CEDEX
FRANCE

Commissariat a l'Energie Atomique
Attn: J. Campan
CEN Cadarche DRE/STRE
BP No 1
13115 Saint Paul Lez Durance
FRANCE

Electricite de France (2)
Attn: G. Kauffman
C. Rey
(S.E.P.T.E.N.)
12, 14 Ave. Dubrieroz
69628 Villeurbanne
Paris, FRANCE

Electricite de France
Attn: F. Duchateau
Direction des Etudes et Recherches
1, Avenue du General de Gaulle
92141 CLAMART CEDEX
FRANCE

CEA/CEN-FAR (3)
Attn: M. Le Meur
J. Calmet
G. Gauthier
Departement de Surete Nucleaire
Service d'Analyse des Matériels
et Structures
B.P. 6
92260 Fontenay-aux-Roses
FRANCE

Electricite de France (2)
Attn: M. Pays
M. Dorison
Direction des Etudes et Recherches
Les Renardieres
Boite Postale No 1
77250 MORET SUR LORING
FRANCE

FRAMATOME (2)
Attn: G. Chauvin
E. Raimondo
Tour Fiat - Cedex 16
92084 Paris La Defense
FRANCE

ITT Cannon Electric Canada
Attn: B. D. Vallillee
Four Cannon Court
Whitby, Ontario L1N 5V8
CANADA

Ontario Hydro (2)
Attn: R. Wong
B. Kukreti
700 University Avenue
Toronto, Ontario M5G 1X6
CANADA

R. McCoy
Yankee Atomic Electric Company
1671 Worcester Road
Framingham, MA 01701

M. Shaw
Institute of Materials Science
University of Connecticut
Box U-136
97 N. Eagleville Rd.
Storrs, CT 06268

K. W. Brown
Tennessee Valley Authority
Electrical and Technical Services
W11C110
400 W. Summit Hill Drive
Knoxville, TN 37902

W. Farmer (5)
USNRC/RES
M/S NL-005

S. D. Alexander
USNRC/NRR
M/S OWFN 9D4

R. Moist
USNRC/NRR
M/S OWFN 9D4

U. Potapovs
USNRC/NRR
M/S OWFN 9D4

R. Wilson
USNRC/NRR
M/S OWFN 9D4

H. Garg
USNRC/NRR/OSP
M/S 7E23

A. Marinos
USNRC/NRR/OSP
M/S 7E23

H. Walker
USNRC/NRR/OSP
M/S 8D1

C. Anderson
USNRC Region I

R. Paolino
USNRC Region I

N. Merriweather
USNRC Region II

C. Paulk
USNRC Region IV

T. Stetka
USNRC Region IV

G. Hubbard
USNRC/NRR
M/S 8D1 OWFN

P. Shemanski
USNRC/NRR
M/S 11F23 OWFN

G. Toman
ERCE
2260 Butler Pike
Plymouth Meeting, 19462-1412

G. Littlehales
The Rockbestos Company
285 Nicoll St.
New Haven, CT 06511

M. Tabbey
Fluorocarbon Corp.
1199 Chillicothe Rd.
Aurora, OH 44202

G. Sliter
Electric Power Research Institute
3412 Hillview Ave.
Palo Alto, CA 94304

J. Gleason
Wyle Laboratories
P.O. Box 077777
Huntsville, AL 35807-7777

J. B. Gardner
29 Miller Road
Bethany, CT 06525

Thamir J. Al-Hussaini
Duke Power Company
P.O. Box 33189
Charlotte, NC 28242

Kenneth Baker
Raychem Corporation
300 Constitution Place
Menlo Park, CA 94025

Michael G. Bayer
Dow Chemical Company
Building B129
Freeport, TX 77541

Bruce Bernstein
EPRI
1019 19th St. NW
Washington, DC 20036

Premnath Bhatia
Baltimore Gas & Electric
P.O. Box 1475, FSRC
Baltimore, MD 21203

John Billing
ERA Technology Ltd.
Cleeve Road
Leatherhead KT22 75A
UNITED KINGDOM

William Z. Black
Georgia Tech
School of Mechanical Engineering
Atlanta, GA 30332

Bruce P. Bolbat
Pennsylvania Power & Light
2 North Ninth Street
Allentown, PA 18101

Paul Boucher
GPU
1 Upper Pond Road
Parsippany, NJ 07974

Robert J. Brunner
Pennsylvania Power & Light
2 N. Ninth Street
Allentown, PA 18101

Daniel O. Bye
Southern California Edison
P.O. Box 128
San Clemente, CA 92672

T. Champion
Georgia Power Company
62 Lake Mirror Road
Forest Park, GA 30050

Jim Civay
Washington Pub. Pow. Supply Sys.
P.O. Box 968
M/S 981C
Richland, WA 99352

Allen Davidson
Patel Engineers
408 Cedar Bluff Road
Suite 353
Knoxville, TN 37923

Barry Dooley
EPRI
3412 Hillview Avenue
Palo Alto, CA 94304

John R. Ferraro
Northeast Utilities Service Co.
P.O. Box 270
Hartford, CT 06141-0270

Edward E. Galloway
Detroit Edison
2000 Second Avenue
Detroit, MI 48226

Larry Gradin
ECOTECH
6702 Bergenline Avenue
West New York, NJ 07093

Ken Hancock
EBASCO Plant Services, Inc.
2 World Trade Center
90th Floor
New York, NY 10048

Izhar Haque
Ontario Hydro
700 University (A8H4)
Toronto, Ontario
CANADA M5G1X6

Bruce L. Harshe
Consumers Power Company
1945 Parnall Road
P-14-408
Jackson, MI 49201

Jerry Henley
Digital Engineering Inc.
658 Discovery Drive
Huntsville, AL 35806

John Hoffman
Raychem Corporation
300 Constitution Drive
Menlo Park, CA 94025

John J. Holmes
Bechtel Western Power Company
12440 E. Imperial Highway
Norwalk, CA 90650

Nels Johansson
INPO
Suite 1500
1100 Circle Parkway
Atlanta, GA 30339-3064

Suresh Kapur
Ontario Hydro
700 University
Toronto, Ontario
CANADA M5G1X6

Brent Karley
Nebraska Public Power District
1414 15th Street
P.O. Box 499
Columbus, NE 68601

S. Kasturi
MOS
25 Piedmont Drive
Melville, NY 11747

T. A. Kommers
The Okonite Co.
1601 Robin Whipple
Belmont, CA 94002

Yasuo Kusama
Japan Atomic Energy Research Inst.
1233 Watanuki-machi
Takasaki, Gunma-ken
JAPAN 37102

Vince Lamb
Westinghouse
P.O. Box 355
Pittsburgh, PA 15230

M. Lebow
Consolidated Edison Co. of New York
4 Irving Place
New York, NY 10003

Ting Ling
Cablec Industrial Cable Co.
East Eighth St.
Marion, IN 46952

Stuart Litchfield
Cleveland Electric Illuminating Co.
P.O. Box 97-E-290
Perry, OH 44081

Sam Marquez
Public Service Co. of Colorado
2420 W. 26th Avenue
Denver, CO 80211

B. G. McCollum
EBASCO Plant Services, Inc.
400 N. Olive
L.B. 80
Dallas, TX 75201-4007

Richard D. Meininger
ECAD Services
P.O. Box 229
Middletown, PA 17057

T. Narang
Texas Utilities Electric Company
P.O. Box 1002
Glen Rose, TX 76043

Richard Dulski
Conax Buffalo Corp.
2300 Walden Avenue
Buffalo, NY 14225

David K. Olson
Northern States Power
P.O. Box 600
Monticello, MN 55441

Keith A. Petty
Stone & Webster
P.O. Box 2325
Boston, MA 02107

Paul Phillips
Kansas Gas & Electric
201 N. Market
Wichita, KS 67202

Paul J. Phillips
University of Tennessee
434 Dougherty Eng.
Knoxville, TN 37996-2200

Ben E. Preusser
Arizona Public Service Co.
Arizona Nuclear Power Project
P.O. Box 52034; Station 6078
Phoenix, AZ 85072-2034

Larry Raisanen
Detroit Edison
6400 N. Dixie Highway
Fermi 2, M/C 205EF2TAC
Newport, MI 48166

Albert B. Reynolds
University of Virginia
Reactor Facility
Charlottesville, VA 22901

Ted Rose
Electro-Test, Inc.
P.O. Box 159
San Ramon, CA 94583

Marcia Smith
Pacific Gas & Electric
P.O. Box 56
Avila Beach, CA 93424

J. Solano
Illinois Power
V-928D
Route 54 East
Clinton, IL 61727

Richard St. Onge
Southern California Edison
P.O. Box 128
San Clemente, CA 92672

Clint Steele
Washington Pub. Pow. Supply Sys.
P.O. Box 968
M/X 981C
Richland, WA 99352

Jan Stein
EPRI
3412 Hillview Avenue
Palo Alto, CA 94304

Greg Stone
Ontario Hydro
800 Kipling Avenue
KR151
Toronto, Ontario, CANADA

Don Sonkus
Ontario Hydro
800 Kipling Avenue
Toronto, Ontario
CANADA M8Z 5S4

Harvey Sutton
Virginia Power
P.O. Box 26666
Richmond, VA 23261

Mike Sweat
Georgia Power Company
333 Piedmont Avenue
Atlanta, GA 30302

Steve Swingler
Central Electricity Research Labs.
Kelvin Avenue
Leatherhead, Surrey
UNITED KINGDOM KT 22 7SE

Aki Tanaka
Ontario Hydro
700 University Avenue, A7-F1
Toronto, Ontario
CANADA M5G 1X6

Doug Van Tassell
Florida Power & Light
P.O. Box 14000
700 Universe Beach
Juno Beach, FL 33408

Joseph Weiss
EPRI
3412 Hillview Avenue
Palo Alto, CA 94304

Robert N. Woldstad
GE Nuclear Energy
175 Curtner Avenue
San Jose, CA 95125

Asok Biswas
Southern California Edison Co.
San Onofre Nuclear Generating Station
5000 Pacific Coast Highway
San Clemente, CA 92672

Phil Holzman
STAR
195 High Street
Winchester, MA 01890

Vince Bacanskas
Gilbert Commonwealth
P.O. Box 1498
Reading, PA 19603

Alfred Torri
Risk and Safety Engineering
1421 Hymettus Ave.
Leucadia, CA 92024

George Daniels
Rochester Gas and Electric
89 East Ave.
Rochester, NY 14649-0001

Kurt Cozens
Nuclear Management and Resources Council
1776 Eye St. NW, Suite 300
Washington, DC 20006-2496

Fred Mogolesko
Nuclear Engineering Department
Boston Edison Company
25 Braintree Hill Office Park
Braintree, MA 02184

Gil Zigler
Science and Engineering Associates
P.O. Box 3722
Albuquerque, NM 87190

Edward H. Aberbach
Brand Rex Company
1600 West Main Street
Willimantic, CT 06226-1128

1811 R. L. Clough
1812 K. T. Gillen
7141 S. A. Landenberger (5)
7151 G. C. Claycomb
6400 N. R. Ortiz
6403 W. A. von Riesemann
6404 D. A. Powers
6405 D. A. Dahlgren
6449 M. P. Bohn
6449 G. F. Fuehrer
6449 E. E. Baynes
6449 D. M. Ramirez
6449 C. F. Nelson
6449 S. P. Nowlen
6449 M. J. Jacobus (25)
6624 L. D. Bustard
6471 A. J. Moonka
8523-2 Central Technical Files

NRC FORM 335 (2-89) NRCM 1102, 3201, 3202

U.S. NUCLEAR REGULATORY COMMISSION

BIBLIOGRAPHIC DATA SHEET

(See instructions on the reverse)

1. REPORT NUMBER (Assigned by NRC, Add Vol., Supp., Rev., and Addendum Numbers, If any.)
NUREG/CR-5772
SAND91-1766/1
Vol. 1

2. TITLE AND SUBTITLE
Aging, Condition Monitoring, and Loss-of-Coolant Accident (LOCA) Tests of Class 1E Electrical Cables

Crosslinked Polyolefin Cables

3. DATE REPORT PUBLISHED
MONTH: August
YEAR: 1992

4. FIN OR GRANT NUMBER
A1318

5. AUTHOR(S)
M.J. Jacobus

6. TYPE OF REPORT
Technical

7. PERIOD COVERED (Inclusive Dates)

8. PERFORMING ORGANIZATION - NAME AND ADDRESS (If NRC, provide Division, Office or Region, U.S. Nuclear Regulatory Commission, and mailing address; if contractor, provide name and mailing address.)
Sandia National Laboratories
Albuquerque, NM 87185

9. SPONSORING ORGANIZATION - NAME AND ADDRESS (If NRC, type "Same as above"; if contractor, provide NRC Division, Office or Region, U.S. Nuclear Regulatory Commission, and mailing address.)
Division of Engineering
Office of Nuclear Regulatory Research
U.S. Nuclear Regulatory Commission
Washington, DC 20555

10. SUPPLEMENTARY NOTES

11. ABSTRACT (200 words or less)

This report describes the results of aging, condition monitoring, and accident testing of crosslinked polyolefin (XLPO) cables. Three sets of cables were aged for up to 9 months under simultaneous thermal (≈100°C) and radiation (≈0.10 kGy/hr) conditions. A sequential accident consisting of high dose rate irradiation (≈6 kGy/hr) and high temperature steam followed the aging. The test results indicate that most properly installed XLPO cables should be able to survive an accident after 60 years for total aging doses up to 400 kGy and for moderate ambient temperatures on the order of 50-55°C (potentially higher or lower, depending on material specific activation energies). Mechanical measurements (primarily elongation, modulus, and density) were more effective than electrical measurements for monitoring age-related degradation.

12. KEY WORDS/DESCRIPTORS (List words or phrases that will assist researchers in locating the report.)
aging, condition monitoring, loss-of-coolant accident (LOCA), LOCA test data, Class 1E cables, cable properties, dielectric tests, crosslinked polyolefin cables

13. AVAILABILITY STATEMENT
unlimited

14. SECURITY CLASSIFICATION
(This Page)
unclassified
(This Report)
unclassified

15. NUMBER OF PAGES

16. PRICE

NRC FORM 335 (2-89)

UNITED STATES
NUCLEAR REGULATORY COMMISSION
WASHINGTON, D.C. 20555-0001

OFFICIAL BUSINESS
PENALTY FOR PRIVATE USE, $300

SPECIAL FOURTH-CLASS RATE
POSTAGE AND FEES PAID
USNRC
PERMIT NO. G-67

UNITED STATES
NUCLEAR REGULATORY COMMISSION
WASHINGTON, D.C. 20555-0001

OFFICIAL BUSINESS
PENALTY FOR PRIVATE USE, $300

SPECIAL FOURTH-CLASS RATE
POSTAGE AND FEES PAID
USNRC
PERMIT NO. G-67

120555139531 I 1AN1RV
US NRC-OADM
DIV FOIA & PUBLICATIONS SVCS
TPS-PDR-NUREG
P-211
WASHINGTON DC 20555